Final Project Report

Cummins Active Noice Control

Sponsor: Cummins Inc.

EML4552

4/13/09

Group 7 Members:

Quennan Davis
Marshall Goerg
Joshua Hogue
Michael Priebe
Chris Schultz

Table of Contents

1 Abstract

The design project discussed herein implements both active and passive materials to reduce the noise and vibrations of a gear cover of a mid-size diesel engine. The design problem was proposed by Cummins Inc. to help aid in their efforts to make a more acoustically friendly engine component. The overall design is constrained by the available space and harsh conditions of a physical diesel engine. The project focuses primarily on active materials using both open and closed loop controls to attenuate structure born vibrations. Macro Fiber Composite piezoelectric actuators are implemented to essentially vary the stiffness of the gear cover and to reduce the vibration propagation through the structure. A secondary method to further reduce the overall radiated sound power utilizes passive materials to compliment the active materials. This is accomplished by adding a sound barrier panel with soundproof foam in front of the gear cover to reduce any remaining noise transmitted to the environment. A compliant seal is placed between the barrier and the gear cover to eliminate metal-to-metal contact and to keep the vibrations from propagating through the periphery of the gear cover to the barrier. Testing of the design is implemented by using a scaled model which makes the design's analysis more economically and analytically feasible. Characterization of the MFC actuators and their associated control scheme is provided by the use of a cantilever beam apparatus. A lead lag filter control scheme adapted from a PI controller proved extremely effective at reducing the perturbations to the cantilever beam for high and low magnitudes of disturbances. However, due to the methods used to build the control scheme and its basis of the characterization of the cantilever beam, it could not be tuned appropriately to provide an overall reduction in sound emitted from the scale mode gear cover. Dynamic characteristics of the gear cover proved to be more complex than the ability of the controller to adapt. The addition of passive components, especially the sound barrier panel, was very effective at reducing radiated sound. The MFCs were also tested passively by using the actuator's ability to increase the system's stiffness and proved as effective as marketed gear covers that utilize ribs to add stiffness. Due to the MFC actuator's high price, the patch actuators were not concluded to be cost effective in comparison to much more inexpensive passive materials.

2 Project Scope

2.1 Problem Statement

Vibrations have presented problems for engineers for many years, especially in modern times when dealing with oscillatory systems like internal combustion engines. These vibrations lead to an increase in audible noise, damage to hardware, and a reduction in performance. One area that has been considered for improvement lies in the propagation of vibrations in the valve and gear covers of mid sized diesel engines.

The design challenge is to research methods to actively and passively control radiated noise of an engine panel and to develop an effective means to reduce the acoustic emissions of the engine panels using these controls. The vibration reduction system must accommodate the existing diesel engine in terms of the operating temperature range, hi and low frequency range, engine compartment space limitations, and long lasting durability. The aim of the design is to control the propagation of the surface velocity activity and to be complimented passively. The design is then to be compared with existing noise reduction systems and study its effectiveness.

2.2 Background

The design project for vibration and noise control was proposed by Cummins Incorporated. Cummins is a leading provider in the design and manufacture of a wide range of engines and their related components. One can find Cummins' products located in various mechanical applications ranging from large machinery and tractor-trailers to common mid-sized trucks (About Cummins…). Cummins encompasses an international market in many diverse environments.

Over the years, noise reduction has become a very popular area of interest. In diesel-powered vehicles, noise vibration and sound harshness properties are being focused on due to cylinder and injection pressures increasing. It can be seen that one key area of improvement lies in the engine covers like the valve and gear covers. These engine covers are usually comprised of lightweight thin metal panels. The covers are connected to the main engine components on their outer edge, where inertia and impact forces are transmitted from the operating engine. The thin panel surfaces act much like a speaker cone in the way that sound is radiated due to surface vibrations.

One method currently used to dampen and lessen the radiated sound is to use a passive, rather than an active, system. A passive system can be comprised of some type of noise absorbing material such as acoustic foam. Other passive systems incorporate a double-wall shell structure for the panels instead of a single-wall design. These passive systems help to muffle the noise but do not eliminate the vibrations that cause the radiated sound. Foams and other sound absorbing materials also have very selective higher frequency ranges and cannot address lower frequencies that are major contributors to overall noise. An active system that is aimed to control and cancel surface vibrations is a better means to reduce overall noise. Current trends in vibration control research have focused on active systems utilizing active materials like piezoceramics, polyvinylindine fluoride film, and ferro-foams (Green, Edward Ray…). Active systems boast a wider range of frequency control but are more costly in terms of material cost and power requirements.

Specifically, the design proposed is based on the gear and valve covers located on Cummins' mid-sized diesel engines. The mid-sized diesel engine to be considered at this time is the Cummins ISC diesel engine. The ISC platform is very popular in mid to large diesel trucks and tractor rigs. The gear cover is found vertically mounted to the front of the diesel engine, and the valve covers are located horizontally oriented on top of the engine. Diesel engine's are known for their harsh working environments. Temperatures can easily rise into the hundreds of degrees and space is always a factor when considering the internal structure of an engine bay and other engine components that neighbor space.

Research conducted in the field of active vibration control in recent years has become a keystone for design ideas in the noise reduction field. In the past decade, many new developments in the smart structures and actuators field have been made available due to smart materials such as piezocermanics, shape memory alloys, and piezoelectric patch actuators. Piezoceramic stack actuators come in various sizes, are known to be low-cost, and are lightweight. These stack actuators boast high control force properties with micron accuracy and can be directly embedded into composite structures for active control (Song, G…). Piezoelectric actuators have also been used to absorb and dissipate structural vibration energy by extracting the mechanical energy from the device structure and diffusing it into an electric voltage (Moheimani, S. O. Reza...). Piezoelectric patch actuators, also known as macro-fiber composite actuators, provide a wide range of applications due to their thin size and high strain capabilities. These patch actuators can be surface bonded to materials with little to no modifications to the original surface (Song, G…). These actuators can be easily controled via electrical voltage signal provided by a signal generator or computer amplification system. These smart materials not only offer a means of dissipating mechanical energy, but also the ability to be controlled with precision control codes.

Passive systems, on the other hand, have been quite effective relative to the amount of noise reduction versus additional expense of weight, space, and material cost. Gear covers have been improved in their noise levels in recent years due to the addition of multiple layers. Dual layer covers act as a vibration dampener and can even be combined in layers with foam for enhanced noise reduction. Innovations in acoustic dampening foams have also posed a solution. These porous materials are used to reduce sound and vibration by dissipating and converting the vibroacoustic energy into heat as the vibration and acoustic waves travel through the foam (Goransson, Peter). Sound damping foams have been used in the automotive and aerospace fields for many years mostly targeted at reducing acoustic and vibration noise. Foams such as melamine foam provide an excellent sound dampening material for high heat situations. Melamine foam can withstand heat up to 375° F and exhibits fire retardant characteristics. These passive devices tend to target higher frequencies, but they are easy to incorporate into many designs at low costs.

Both active and passive systems have been used to reduce unwanted surface vibrations and noise propagation. However, they have never been used together efficiently in combustion engine applications for vibration control of specific engine components. The main questions that arise when considering the use of these materials are usually based off the topic of effectiveness. It has been shown in previous research that active materials can reduce the vibration levels through metal structures by essentially altering the stiffness of the material. The problem at hand is just how effective are these active materials in correlation with the overall cost that is compiled from purchase, assembly, and widespread manufacturing. By comparison of both original single and dual layer covers with the proposed design and its specific components, this problem can be answered.

2.3 Objective

The goal of the design project is to research and minimize the vibrations and forces originating from an engine gear cover mounted on a midsize diesel engine. As the automotive industry advances, engine size and combustion capacity has increased which is directly related to the increase in existing noise levels. The project's main aim is to successfully characterize the effects of surface deformations and vibrations of a gear cover and housing system and implement an active means to either minimize or eliminate the surface velocity. The design is comprised of an altered scale model of the original gear cover to test for design feasibility and material use.

The first step of characterization is to design a scale model representation of our desired theoretical design for testing. The model utilizes techniques and simpler models common to dynamic systems such as an initial cantilever beam for motion and controls analysis. The research conducted in the initial steps of the design provides data for the application of the active materials on a physical model that represents the actual gear cover more closely for a practical comparison of the design's effectiveness. The next step of characterization is to research the existing gear cover and attachments to collect data of an experimental control for later comparison. Both gear covers provided by Cummins Inc. are tested; a single layer gear cover and a dual-layer gear cover. From the models and tested controls, a comparison is produced to assess the effectiveness of the active materials along with their accompanied passive counterparts to reduce propagated noise versus relative cost and size requirements.

Ideally, eliminating all noise originating from the gear cover by cancelling out any surface vibrations with active and passive noise control technologies is the main objective. Realistically, reducing the vibrations by a noticeable amount and gaining valuable knowledge and research in this area will satisfy the design problem. The end product not only presents a working solution for vibration control, but also provides data and ideas from the results and testing to supply a base for more research. From the design model constructed and the data collected in testing, sufficient research is made available to implement the design on an actual existing gear cover.

The first semester of the project was used primarily to research existing or new methods for active and passive noise control as well as modeling the gear cover in different software programs for additional testing and planning. A theoretical model of the active and passive system was designed so that a working prototype could be machined, tested, and edited. The second semester of the project was to build a physical working solution to the design problem and project description. Once the working model is tested and optimized, a concise comparison between the prototype and unaltered system is presented.

2.4 Methodology

In order to cancel or reduce sound emission a very clear picture of the origin of that sound must be obtained. As stated in our project description, the gear cover tested acts like a speaker cone, rapidly vibrating and emitting sound through very small oscillatory displacements. While characterizing the cover, it is important to identify several characteristics including the locations of maximum displacements, the forces involved in aforementioned displacements, as well as the range of frequencies. Finite element analysis of the nodal locations allows for an accurate means to locate the maximum displacement locations. The forces involved with the system are more difficult to attain directly, but an idea of how much force is required to reduce the propagation of vibrations can be concluded from the results in how effective are the active materials. The range of frequencies are based on the frequency range of the data provided by Cummins. This is the range that is replicated in the testing of the original and scale model gear covers. Specific frequencies and frequency ranges that result in resonance peaks are researched in more depth. Even though the noise emitted from the gear cover is not directly related to the resonance frequencies of the gear cover, these ranges provide the best means of testing the effectiveness of the active and passive materials in reducing the noise. The data collected from experimental testing is then used to determine specific material selection and the orientation and arrangement of the active and passive components.

The displacement along the surface of the cover is not constant, and the locations at which it is the highest needs to be determined. Cummins provided finite element modal analysis of the existing single layer gear cover. Finite element modal analysis of the scale model cover is conducted to compare the overall shapes and locations to determine if the scale model is a useful substitute in testing. To test the gear covers, operating conditions must be simulated. Since an entire engine is not a practical test bed for this stage and level of research, other testing equipment such as a mechanical shaker is required. The displacement and frequency measurements are to be taken with either a capacitor probe or some type of piezoelectric set-up that convert the mechanical motion to electrical signal. The audible noise due to the cover will be recorded by means of a common sound level meter to measure the output decibel level.

The actual arrangement of the individual materials in the design depend heavily on the data collected during testing. A cantilever beam model is to be utilized for active material characterization. By combining the piezoelectric actuators with the cantilever beam model, surface movement and nodal analysis can be studied to assure a mathematical means of providing the coordinates of the needed composite material locations. It is concluded that the active material should be positioned in the direction of the vibration source. This can be assumed due to prior research conducted by institutions and companies like Boeing with very similar vibration systems. This assumption is to be used unless experimental data results in conflicting evidence. These active materials are combined with preexisting passive materials to optimize overall noise reduction. Automotive acoustic foam and barrier paneling are already in use with other manufactured gear covers and are the probable choice for the passive component. The overall system is then tested against a non-modified cover as well as various arrangements of passive components. From these comparisons the value and feasibility of the of using active materials for noise reduction is determined.

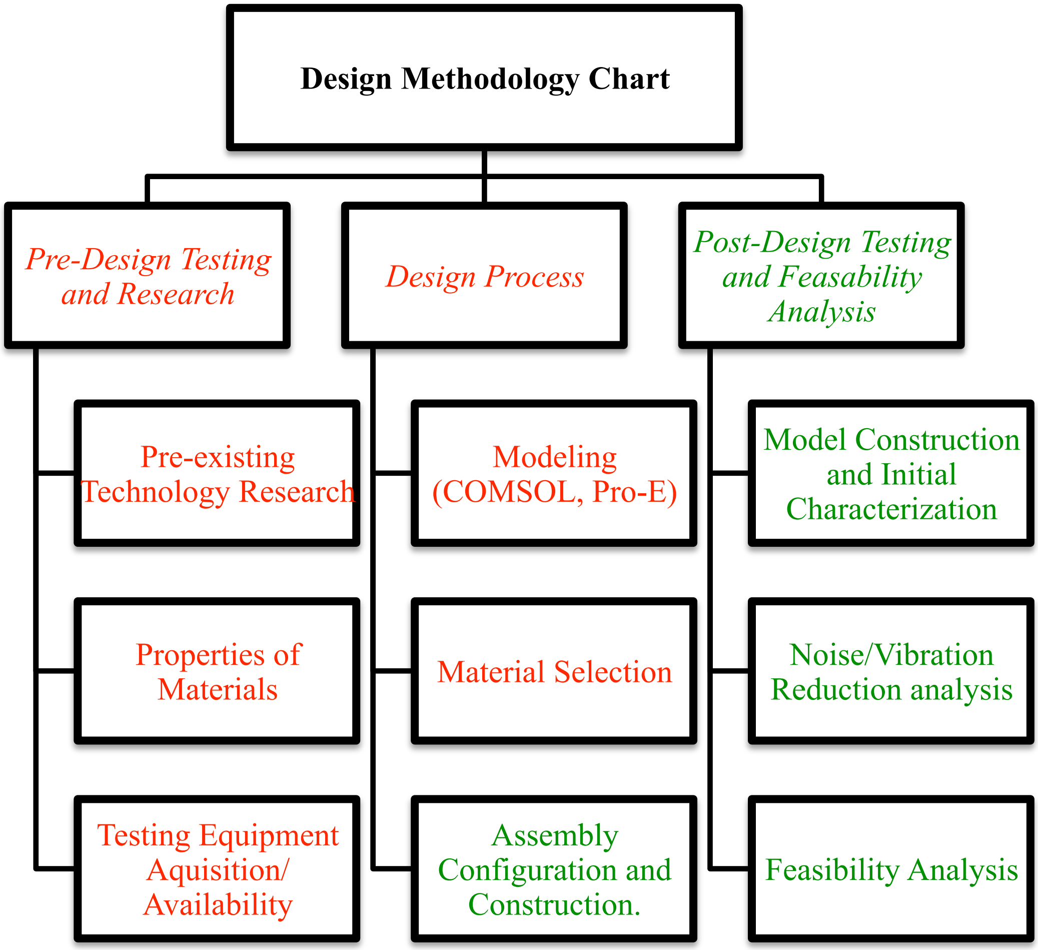

Figure 2-1: The Design Progression Chart.

Red indicates 1st semester tasks whereas Green indicates 2nd semester tasks.

2.5 *Product Specifications*

One key to successful designing lies within the inherit constraints and limitations set forth by the customer, supply, or engineering capabilities. It is these constraints that construct guidelines that can be followed to achieve a successful product. These product specifications aid in focusing the design's progress from initial ideation to project completion. For the active noise control device proposed, the project specifications provide a preliminary description of what the product must do.

The active noise control of an engine cover is to be accomplished by utilizing both active and passive materials. However, the design should incorporate a larger percentage of research in active material use than passive material use. The active material or materials selected should act as a vibration reducer rather than noise cancelation. The specific active material to be chosen is to be a result of the material's ability to be adapted to the cover's structure, its control over specific frequency and vibration ranges, and its size to actuation force ratio. The active material must also be able to withstand the harsh environment of a diesel engine and the exceptionally long life that diesel engine manufacturers boast. In particular, the material must be able to withstand high temperatures, be environmentally sealed due to electrical power and durability, and perform at different orientations that might arise due to the use of the engine. More specifically, the maximum temperature assumed is 275°F. The passive materials must also be able to withstand a typical diesel engine environment. The passive material or materials selected are to target a higher frequency range that the active material will most likely not be able to comply to. These two components of the overall noise control system are to work together to reduce or eliminate surface vibrations that act as the source of the propagated noise.

Due to the characteristics of the Cummin's diesel engine considered for the design, certain geometrical limitations must be met. The main cover being addressed in the project is the gear cover that is oriented vertically on the front side of the engine. The design must not increase the effective thickness of the cover by more than 15 mm, or beyond its outline when viewing the cover from the front. Despite the size limitations, the active material may be applied anywhere on the cover or its connection to the engine. The connection cannot compromise potential joint sealing between the cover and its periphery. If passive materials are used in conjunction with the gear cover's periphery, layering materials such as isolation gaskets must be accounted for in the design.

One area of particular concern that constrains the design pertains to overall safety. This safety is in direct relation to the active materials to be used on the cover. These active materials are known for their high levels of associated voltages. However, with these high voltages a low amount of amperage is characteristic. This does mean a level of safety must be incorporated into the design of the associated electrical network.

The design project does not require a fully sized working model on a gear cover. A scaled working prototype utilizing active control is a more practical and feasible means for this stage. However, the potential for a comparison of noise reduction relative to a plain cover must be assessable for characterization of the design system's performance and practicality. Due to the improbability of not being provided a physical diesel engine, a mechanical shaker can be used to replicate the actions of a working diesel engine. The prototype must also be completed on the initially set budget of $1500 within the time constraint of two college semesters.

3 Design and Analysis

3.1 Concept Generation and Selection

To reduce the overall noise emanating from the gear cover a passive and an active component are implemented into the design. The passive portion of the design is partially dependant upon the active material chosen due to the active material's size and abilities. However, the active portion varies dramatically depending on the chosen approach. In the initial ideation stages of the design, three basic approaches for applying the active components to the system were considered; one being to control the noise at the point of maximum deflection, one to control the deflection from a point away from maximum deflection in order to achieve higher displacement lower force if needed, and the other is to target the vibrations at the source of the noise. The first three concept ideas are listed below to get an understanding the direction the design group originally followed and to see how design progressed to its final version.

Each of the initial designs considered utilize two basic types of active materials. The first is the use of piezoelectric ceramics. These ceramic actuators come in an assortment of sizes and high strain capacities. For the design, the ceramic actuators to be considered are limited by the height limitations of the gear cover and by the necessary force required for control. These ceramic actuators are comprised of layers of piezo-ceramic material that expand when induced with an electric voltage. These stacks are capable of precision high frequency expansion and contraction. Despite the low magnitude expansion length, the strain or force provided is quite large.

The second type of active material is a piezo-composite patch actuator, also known as a Macro Fiber Composite, or simply MFC. MFCs are made up of piezo-ceramic rods interlaced within layers of polyimide film. These composite strips are thin and lightweight but do not offer the same high strain levels as ceramic stacks. Figure 3-1 displays a medium size MFC strip.

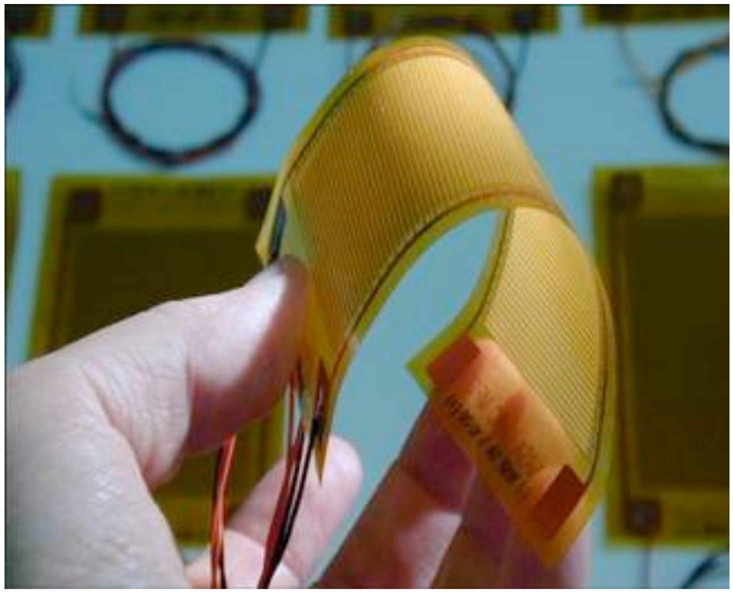

Figure 3-1: Macro Fiber Composite Strip
(http://smart-material.com)

3.1.1 Design Concept 1*: Control at the Point of Maximum Deflection*

One assumption to make when considering a structure like the gear cover is to assume that most of the sound and displacement of material occurs when the system reaches one of its resonance modes. Given the mode shapes for the first five modes one can approximate where most of the displacement and noise will occur. This approach utilizes a piezoelectric material directly at the points of maximum deflection. The piezo-material is used to directly oppose the motion of the cover. Figure 3-2 portrays two of the possible ways to put this approach into practice.

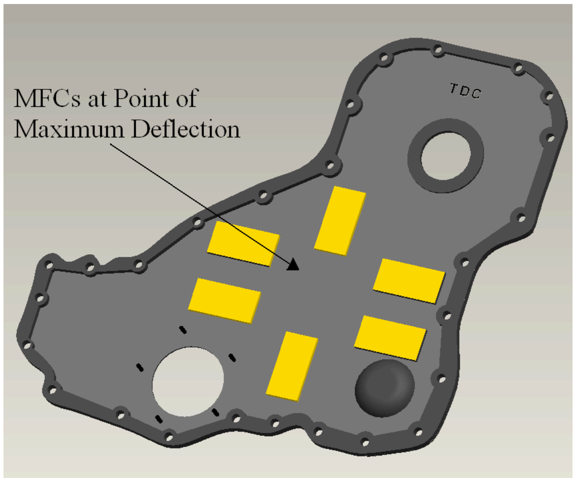

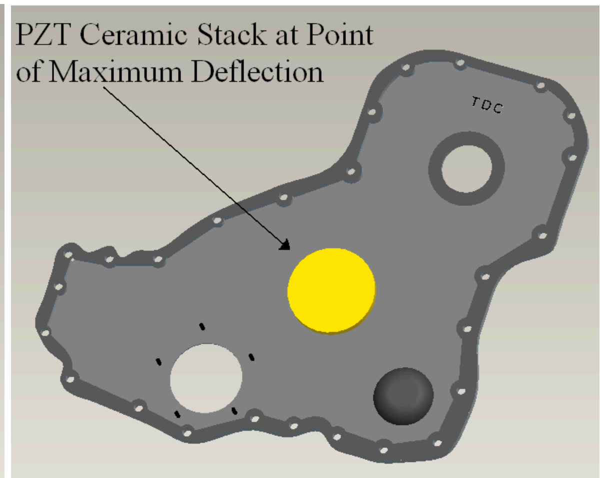

A) B)

Figure 3-2: A) Macro Fiber Composites Positioned on Actual Gear Cover
B) High Temperature Piezoelectric Ceramic Positioned at Center of Gear Cover

A)

Pros	**Cons**
• Low cost	• Low Force
• Easy attachment to cover	• Lower failure temperature
• Small size	• Force does not directly oppose motion

B)

Pros	**Cons**
• High Force	• Attachment may require secondary cover
• Directly opposes motion	• Brittle
• Higher Failure Temperature	• Higher cost than composite patch actuator

It should be noted that changing the mass of a system alters the resonance frequency and mode shapes of the system. Therefore it is logical to assume that if adding the piezoelectric material changes the location of maximum displacement too greatly this method becomes less effective.

3.1.2 Design Concept 2: *Amplified Control Away from Maximum Deflection*

The active system in some ways is limited by the properties of the active material. The materials have a fixed force that they can exert, as well as a maximum displacement. There is a possibility that if placed at the point of maximum displacement the materials will exert excessive force and will come up short for displacement. The solution for this potential problem is to move the materials to a location away from the maximum deflection point to allow the cover itself to act as a cantilever effectively decreasing the force and increasing the displacement at a desired location. Figure 3-3 demonstrates how this may be accomplished.

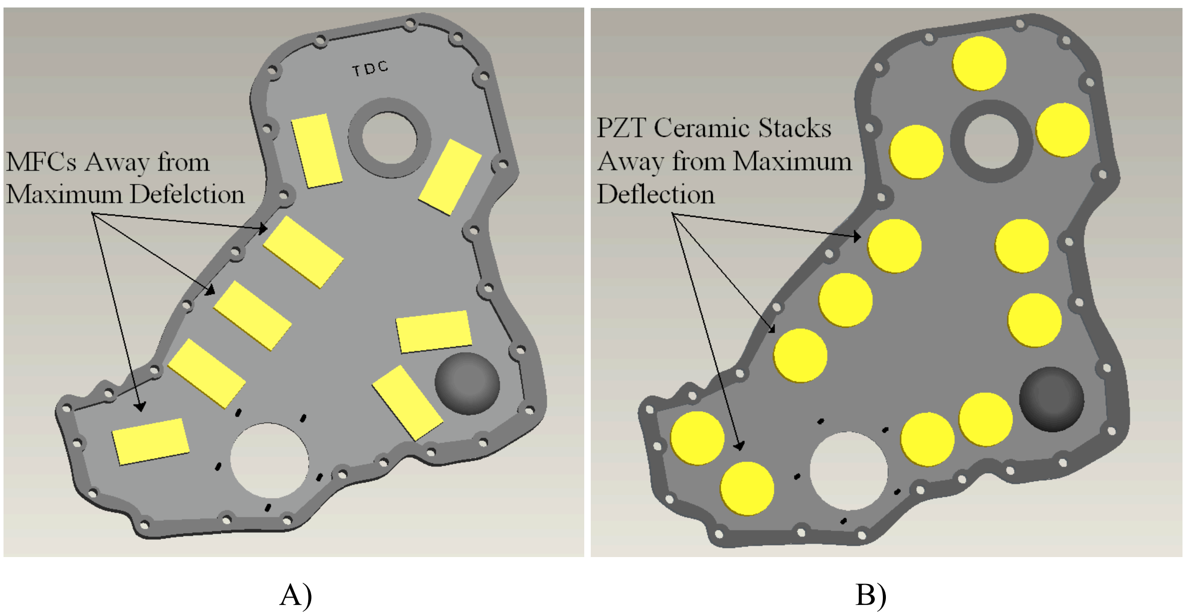

Figure 3-3: A) Levered Macro Fiber Composite Modeled On Gear Cover

B) High Temperature Piezoelectric Ceramics Positioned On Gear Cover

A)

Pros	**Cons**
• Low cost	•Very Low Force
• Easy attachment to cover	• Lower failure temperature
• Small size	• Force does not directly oppose motion

B)

Pros	**Cons**
• High Force	• Attachment may require secondary cover
• Directly opposes motion	• Brittle
• Higher Failure Temperature	• Higher cost than piezo strips

3.1.3 Design Concept 3: *Prevention of Resonance Modes*

The true purpose of incorporating active and passive materials together is that the combination allows for noise suppression over a larger range of frequencies than a strictly passive system. Simply passive systems are good for the suppression of higher frequency sound, but are less effective at lower frequencies. Most of the noise that emanates from the gear cover while it is not in resonance is high frequency and small displacements. The problem for a strictly passive system occurs when the system hits one of its resonance modes; the frequency becomes lower and the displacements become larger. This approach in theory keeps the system from reaching resonance by adding energy at the periphery, thereby allowing the passive system to remain effective. Figure 3-4 illustrates two possible ways to implement the approach.

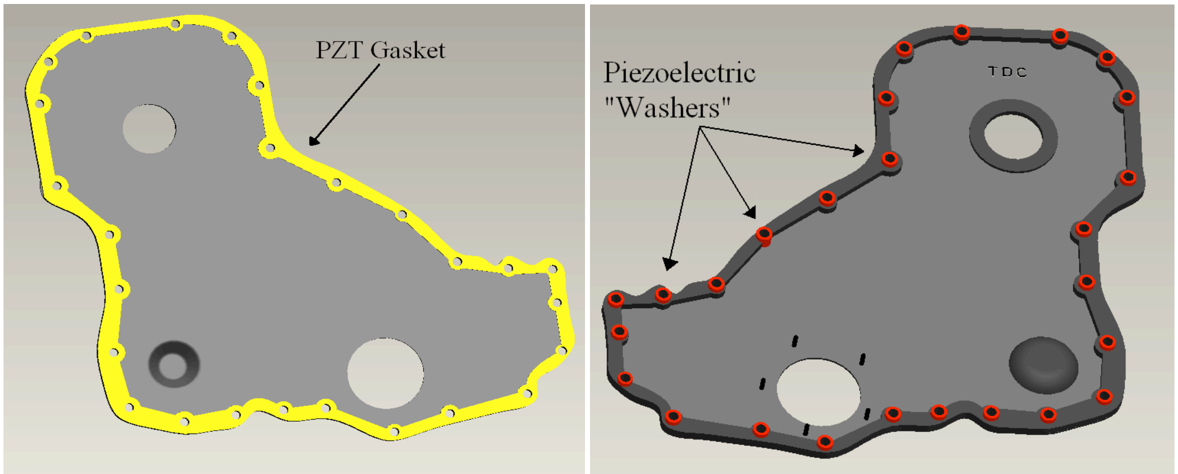

A) B)

Figure 3-4: A) Piezoelectric Ceramic Gasket Attached Around Gear Cover Periphery
B) Piezoelectric Stack Washers Attached at Bolt Locations

A)

Pros	**Cons**
• High Force	• Extremely expensive
• Can add energy around entire periphery	• Brittle
• Higher Failure Temperature	• Difficult characterization

B)

Pros	**Cons**
• High Force	• Less energy at periphery than gasket
• Cheaper than piezo gasket	• Brittle
• Higher Failure Temperature	• May require custom order

Figures 3-2 through 3-4 were created using Pro Engineering Wildfire and edited for labeling and clarification.

3.1.4 Passive Material Selection

Current passive techniques used in acoustic noise reduction include materials such as dual layer engine covers, foams, and sound absorbing elastic sheets. These noise reduction materials are applied to the overall design to compliment the active material design. These passive materials focus on absorbing higher frequencies compared to the lower frequency ranges targeted by the active materials. The following is a brief description of passive materials used in the final project design; other passive materials were considered by not used based on cost or functionality.

Delta dB

Delta dB is a sound damping coating for structural and mechanical noise generated through substrates and surfaces. This coating can be applied in coats with each additional coat resulting in additional vibration attenuation

Pros	**Cons**
• Paint on application	• Bulk order is necessary
• Very cost effective per unit volume	• Reapplication may become necessary
• Remains flexible upon drying	• Carbon steel requires primer

Carbon Fiber

Carbon fiber is used in applications like equipment racks that hold sensitive laboratory equipment in order to prevent outside vibrations from skewing testing results. With stiffness comparable to metal, carbon fiber will be able to be used in applications that require high durability while providing better vibration damping.

Pros	**Cons**
• Comparable stiffness to metal	• High material and machining cost
• Good vibration damping	• Difficult to machine
• Broad band attenuation	• Specialty order possibly required

Fiberglass

Fiberglass, like carbon fiber, is comprised of many layers sandwiched together. The fibers are often uniquely oriented and provide for a means of vibration dissipation. Fiberglass is a substitute for carbon fiber that is cheaper and easier to machine.

Pros	**Cons**
• Easy to machine/cut	• Not as stiff as carbon fiber
• Good vibration damping	• Low temperature range
• Broad band attenuation	• Numerous types

SSP Foam

SSP foam is a closed cell vinyl-nitrile noise control FOAM suitable as a sound barrier or a sound absorber. The foam is good for various uses including car, boat, and large machinery vibration reduction and is FAA approved for use on aircraft.

Pros	**Cons**
• Good sound barrier and absorber	• Adhesive backing may not withstand temp.
• Thickness is within design specs	•May be compressed when implemented
• Will not absorb moisture	• Cannot buy in small quantities

Vibra-Block

Vibra-Block is a high-performance vibration dampener designed for applications requiring reduction in structural & vibration based noise transmission. Vibra-Block is an easy-to-install, low profile, high-tech resin based noise stopper. Very effective in stopping a wide variety of vibration based noise transmissions.

Pros	**Cons**
• Eliminates sheet metal vibration	• Must be cut to the shape of the cover
• Low-profile visco-elastic polymer	• May be compressed when implemented
• Available in custom quantities	• At least 60% coverage of the surface

3.1.5 Preliminary Design

From the previous initial concept designs mentioned, decisions matrices and group consensuses were used to determine a preliminary design. The proposed design, similar to the design presented in Figure 3-3 A), was to use the piezoelectric stack actuators as washers between the gear housing and gear cover. Sound absorbing foam along with other passive materials were to be added to the open areas of the gear cover to incorporate a cheep and effective way to reduce higher frequency noise and vibration. Gasket material normally used between the gear housing and gear cover will be slightly modified to allow for the active and passive materials but still retain its ability to keep the connection tight to retain motor fluids. Controls would be added to the design to target and impede the gear cover form actually reaching resonance and thus reduce high surface deformation and vibrations.

However, when this design was presented to the Cummins Incorporated representatives, the group was informed that despite the attractiveness of the design in terms of its ability to reduce resonance modes it would probably not be the best choice for the group. From provided data, see Figure 3-5, it can be concluded that targeting the resonance of the gear cover would not be an overall efficient method to reduce broadband noise. It was suggested that a better approach to reducing overall vibration noise is to focus on the entire broadband frequency range. It was also recommended to not only use the passive materials on top of the gear cover but to incorporate the use of a sound barrier to decrease resonating noise emanating from the gear cover. This sound barrier idea is common to existing engine components like the dual-layer gear cover utilized by Cummins. To comply with these ideas, the preliminary design was altered and re-presented to Cummins. The main change to the initial concept design was to not focus on the locations of the nodes of the cover since they change throughout the large frequency range of the engine and to also take the proven effectiveness of a sound barrier and apply to the final design.

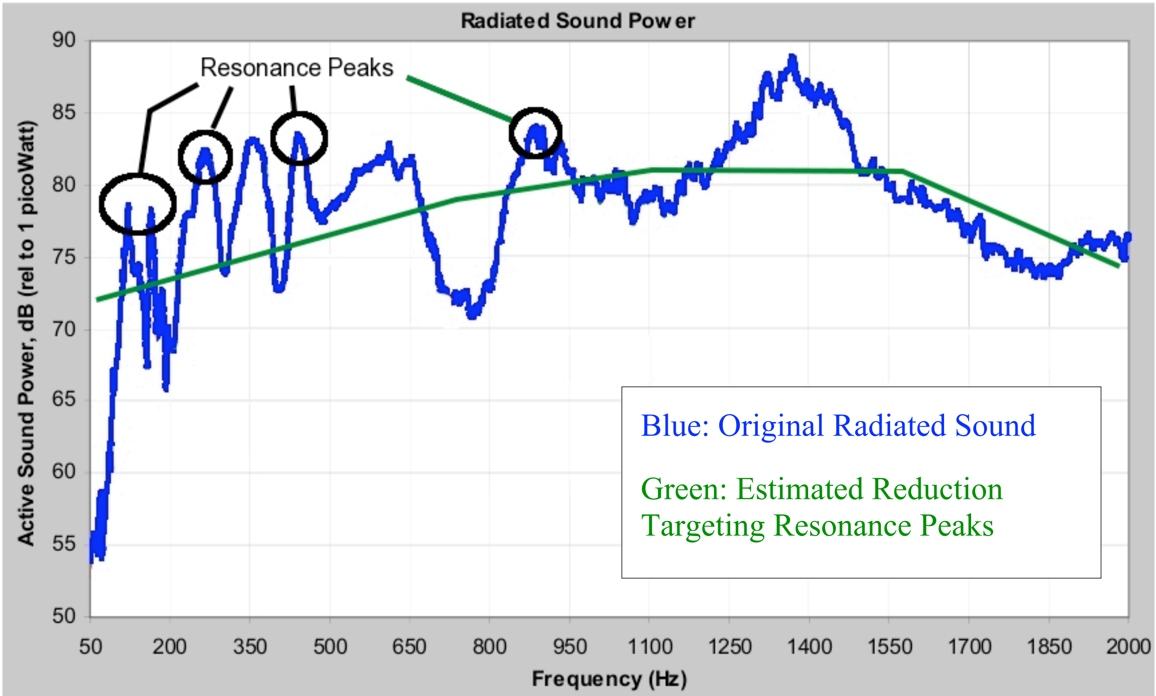

Figure 3-5: Radiated Sound Power of Single Layer Gear Cover

Original Graph is Included in Appendix B

3.1.6 Final Design

3.1.6.1 Hypothetical Design

The final design proposed consists of two main components; active material placed directly on the gear cover and a passive sound barrier. The active portion of the design implements piezoelectric patch actuators known as Macro Fiber Composite actuators, or MFCs. The passive sound barrier utilizes three components to block noise emissions from exiting past the gear cover. See Figure 3-6 for a portrayal of the design.

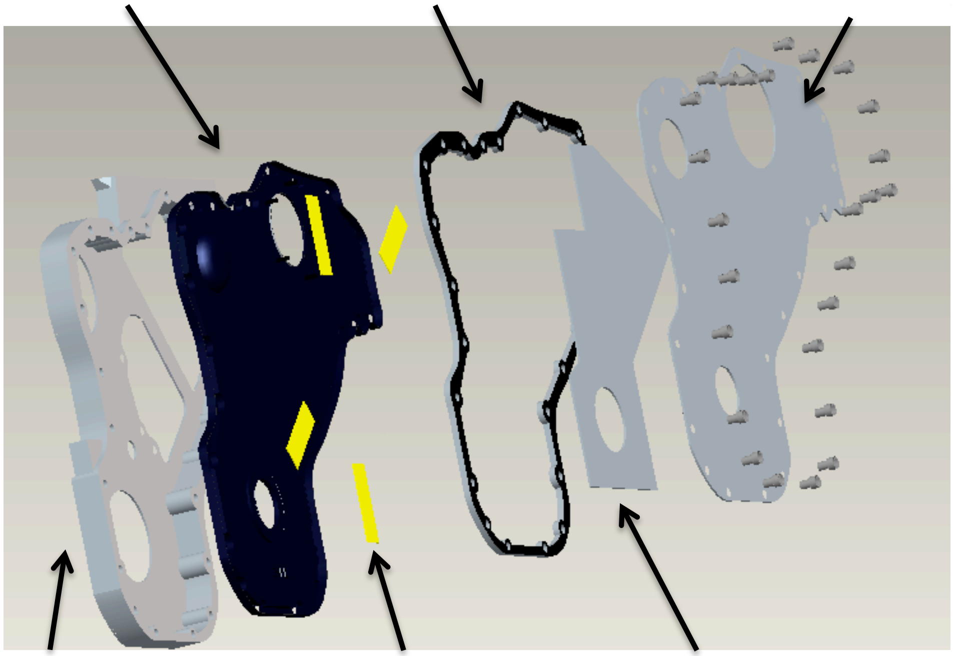

Figure 3-5: Pro-E Illustration of Hypothetical Design Including Component Identification.

The piezoelectric patch actuators are attached directly on the existing gear cover. The MFCs essentially affect the stiffness of the gear cover. The exact orientation and number of actuators needed is determined during preliminary active material characterization. The orientation of MFCs is assumed to be in the overall direction of the vibrations being propagated. An example of this is taken from research conducted by the Boeing Company where patch actuators were placed in the direction of propagated vibrations on the underbelly panel of a F-15 (Wu, Shu-yau. "Piezoelectric…). Above the gear cover, a sound barrier is attached consisting of a compliant seal, passive foam, and the sound barrier panel. The compliant seal is used to prevent the transmission of vibrations from the outer parts of the gear cover to the barrier panel. The seal only comes into contact with the barrier panel and gear cover at the outer edges relatively in the same shape at the gasket that exists between the gear cover and gear housing. The sound barrier panel is placed directly over the compliant seal. A piece of passive foam is attached on the underside of the barrier panel between the sound barrier and gear cover. The passive foam does not come into contact with the patch actuators or the gear cover. The same bolt holes of the gear housing and cover are utilized for attaching passive materials. As an added noise reduction effort, a sound damping coating is to be applied to the exterior of the device. Please refer to Section 3.3 for specific material characteristics and applications.

This design was deemed "hypothetical" for one main reason. The fabrication, testing, and cost of this design are very unrealistic and unpractical for this portion of the design stage. The finances required for the design would easily exceed the mandated budget and the complicated shape and structure of the gear cover would present a considerable problem in analysis. Thus, a more appealing design in terms of its shape and size must be used for fabrication and testing.

3.1.6.2 Scale Model Design

A "scaled" model design is used for ease of testing, fabrication, and analysis. The scale design utilizes the same components as the hypothetical design, but in a more feasible size and shape. An approximate two to one scale ratio was decided upon based off material availability, testing equipment, and simplicity of later analysis. A symmetric shape was chosen that is very similar to the overall shape of the original gear cover. The symmetrical characteristics of the shape will also simplify orientation of the active materials and the machining of parts. The scale also incorporates enough of a similarity to make a viable comparison to the original gear covers to determine the effectiveness of the design. Figure 3-6 portrays the original and scaled designs side by side. Please refer to Appendix E for detailed drawings of each component of the scale model.

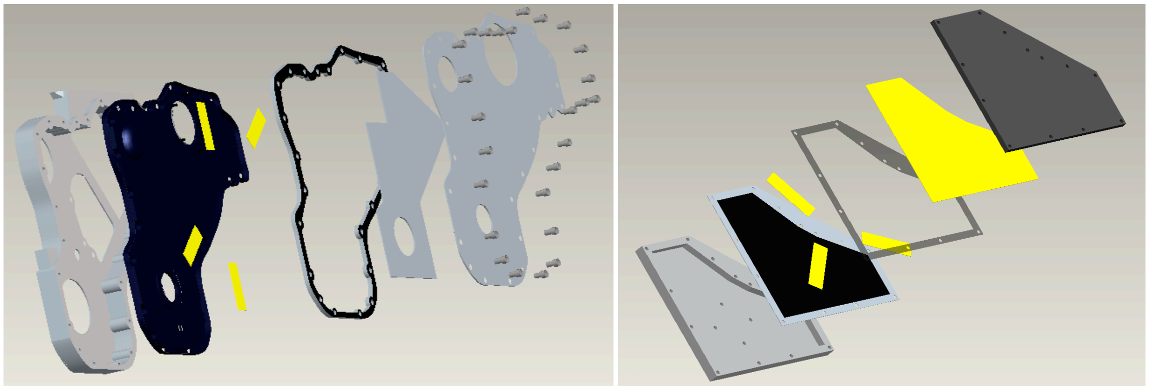

Figure 3-6: Side-by-Side Comparison of the Hypothetical and Scaled Model Designs.

3.2 Controls Design

The design project does not only incorporate the physical structure of the device, but also the means of controlling the active materials. The piezoelectric patch actuators display impedance dependant damping and stiffness characteristics when connected with an electrical network (Cunefare, Kenneth A. "Negative…). The electrical impedance operates as a process of removing the mechanical energy from the physical structure (Moheimani, S. O. Reza. "A Survey…). The piezoelectric patches use their ability to strain and convert a portion of the vibration energy into electrical energy to either passively or, for the purpose of actively controlling the gear cover structure, semi-actively control the surface via shunt damping or brute force actuation. These patch actuators also have been researched to exhibit "negative stiffness" which is very useful for active vibration control (Cunefare, Kenneth A. "Negative…).

Shunt damping is a research proven method of dissipating mechanical energy. However, shunt damping can be considered a predominately passive means despite the use of electrical networks and computer controls. Shunt damping provides a very important starting point to reduce vibrations in the gear cover and any improvements to the controls design will be based off initial testing using this open and closed circuit method. Initially, the controls system is made up of simple open loop control and shunt damping. The control scheme is tested using a cantilever beam setup. The cantilever beam is a simpler model, and the controls can be implemented without the complexities of multiple actuators or non-symmetric shapes. The goal of the controls design is to utilize a closed loop controls system. The close loop system is based off of a PID feedback code.

3.2.1 Open Loop Control

The basic order of operations of open loop control starts with the computer software requesting a voltage to be applied to the piezoelectric material. This request is sent through hardware into a power amplifier where the electrical voltage is sent into the piezoelectric material and thus expand the piezoelectric actuator. Matlab in conjunction with Simulink is the standard command prompt used for most scientific testing and the basis for the design's control system. Simulink is very useful when dealing with data collection software such as dSapce. A simple open loop control system in Simulink can be seen in Figure 3-7. The displacement or strain of the active material or structure can then be monitored using a feedback device for data collection and analysis.

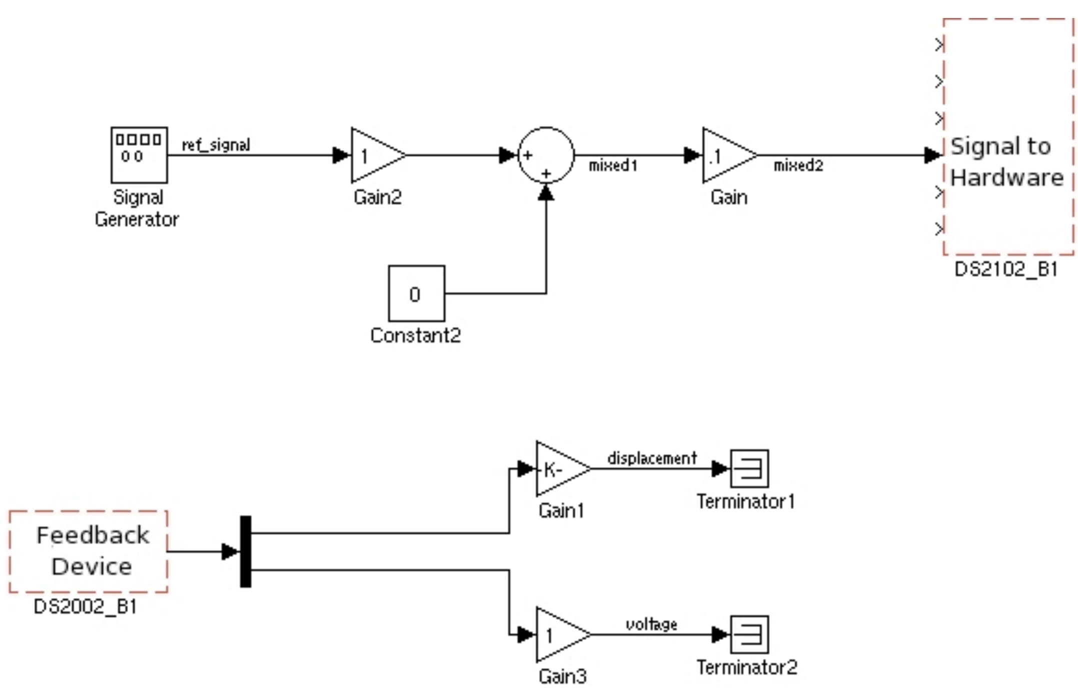

Figure 3-7: Open Loop Control Code Displayed in Simulink.

3.2.2 Closed Loop Control

Closed loop control uses a feedback device to achieve the desired motion of the structure by incorporating the current displacement or strain of the structure into the code. A simple PID control, Proportional Integral Derivative control, or narrowband control is an effective active means to reduce overall vibrations through the gear cover. An example of a PID control scheme can be seen in Figure 3-8.

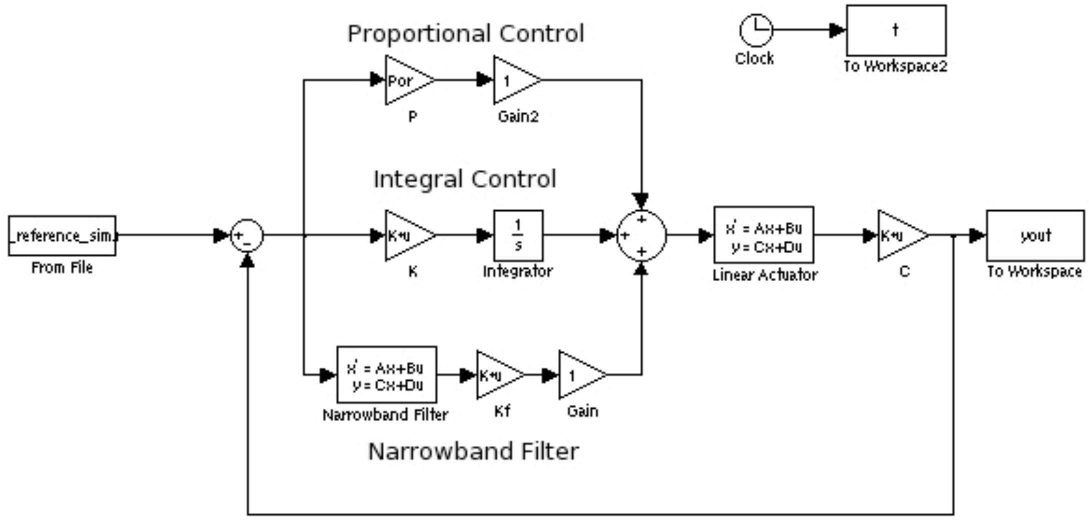

Figure 3-8: Closed Loop Control Utilizing Narrowband Control Displayed in Simulink.

The control code necessary for the design is dependant on the active material being used and also on the feedback device being used. The design constraints do not allow for the use of microphones. Thus, for the active gear cover design, feedback sensors are to be used. Certain active materials can be used for both control and sensing which eliminate the need for an extra feedback device. MFCs have this active material characteristic. However, using the piezoelectric patch as both actuators and sensors adds a level of complexity to the circuitry and data acquisition hardware that might prove to be cumbersome and problematic. So, a better option is to use devices such as capacitor probes, LVDTs, laser vibromaters, or strain gauges. Capacitor probes, LVDTs, and laser vibromaters are mainly used in scientific research data acquisition and are potentially expensive. To characterize the active materials with the cantilever beam model, devices such as these are very useful. However, for the scale model design or real world design these types of feedback sensors are difficult to incorporate into such a design and make the final product price unfeasible. Strain gauges provide a solution to this problem. Strain gauges are easily applied to the structure surface and relatively low cost.

The actual controls used with the active noise control device are mentioned in Section 7.2

3.3 Material and Equipment Selection

3.3.1 Material Selection

Active Material:

The active materials used on the final design are Macro Fiber Composite actuators. The patch actuators are a technology licensed by the National Aeronautics and Space Administration, NASA, and distributed by Smart Material Corporation (www.smart-material.com…). These MFCs boast high performance and surface conformability at a reasonable and cost competitive price. The patch actuators use small piezoelectric ceramic rods held together between electroded polyimide film. When a voltage is applied to the MFC, the piezoelectric material expands inducing a positive or negative moment pending on a positive or negative voltage. Also, the opposite happens when a moment is applied to the patch actuator; a voltage is created. The voltage can be used for sensing applications or for energy harvesting. The composite actuators can conform to almost any surface, are durable and efficient, and are damage tolerant. One very important characteristic that the product presents is how the MFC comes environmentally sealed and ready to be connected via wiring hardware. This allows the design safety when dealing with engine oils and lubricants. Engine temperatures are also lower than the material's curie temperature. Specifically, the design is uses Smart Material's d33 85mm by 28 mm MFC.

Patch actuators such as MFCs have been used in many other vibration reducing applications. As mentioned earlier, patch actuators were used on the underbody panel of a F-15 to reduce propagated vibrations (Wu, Shu-yau. “Peizoeletric…). Reductions of more than 10 dB were shown experimentally at peak amplitudes in the lower frequency range. The stiffness effect of piezoceramic patch actuators used with feedback control was researched by the Institute of Sound and Vibration Research (Aoki, Y. P Gardonino. S J Elliott. “Modeling…). Reductions of about 20 dB were modeled throughout a very broadband frequency range.

The method of attaching the MFCs to a structure involves the use of simple adhesives. Smart Material Corporation recommends using two component adhesives such as 3M’s DP 460 Epoxy. The two part adhesive is applied using a mixing applicator also supplied by 3M. The epoxy should then be cured at about 50° to 60° C for two hours while the patch actuator is being pressed against the structure. The adhesive also complies with the temperature constraints of the problem specifications.

Passive Materials:

Four passive materials are used together which make up the design’s sound barrier. The compliant seal that is sandwiched between the gear cover and sound barrier panel is to be made out of Vibra-Block, a high-density low profile polymer. The Vibra-Block seal isolates structure born vibrations and is easy to cut and install. The seal aim is to reduce the vibrations that are transmitted from the model gear cover to the sound barrier panel. The Vibra-Block material is manufactured and distributed by American Micro Industries Incorporated. The sound barrier panel is then placed directly on top of the compliant seal. A carbon fiber and fiberglass barrier panel are tested as panel materials. Each material exhibits good stiffness properties, but carbon fiber and fiberglass also have good vibration damping for middle to high frequencies unlike normal metals. Carbon fiber and fiberglass are not new to vibration reduction applications. One example is the use of carbon fiber and fiberglass for equipment anti-vibration equipment racks (www.composite.com…). Figure 3-9 is data collected by Composite Products displaying the reduction in sound for different shelves of an equipment rack made of carbon fiber and fiberglass.

Dynamic Response vs. Frequency

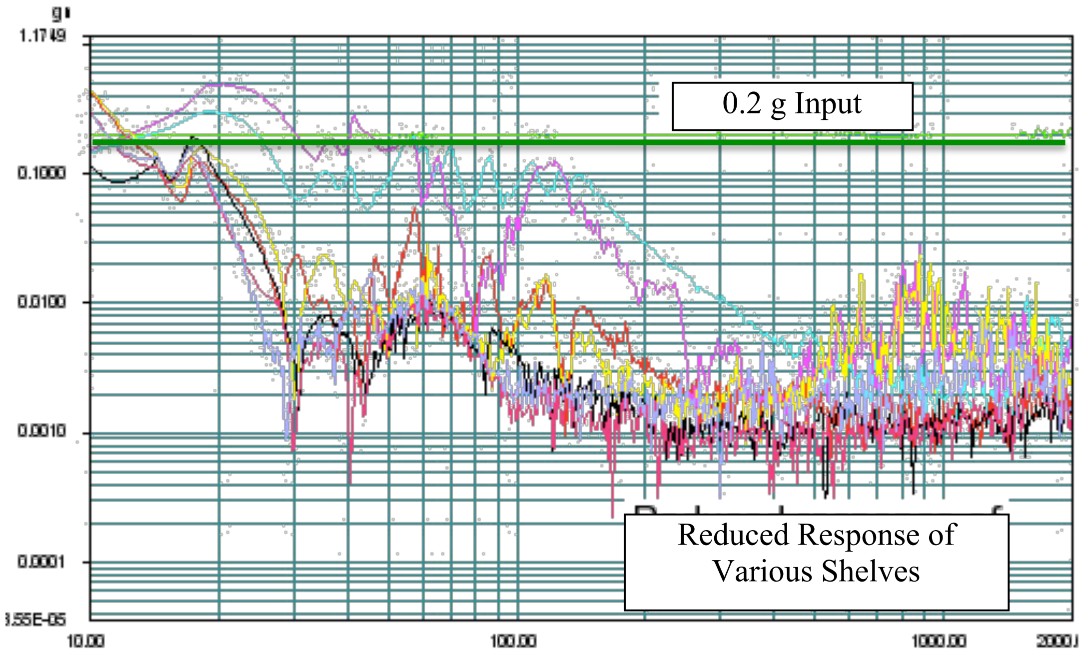

Frequency

Figure 3-9: Sound Reduction of Multiple Layers of Equipment Rack
(www.composite.com/technology.htm)

Directly underneath the barrier panel in the unused space between the model gear cover and barrier panel, passive foam is attached for added noise reduction. The passive foam to be used is the SSP Foam, and it is to be purchased from Super Soundproof Company in a thickness of 1/8 inch. The SSP foam is a closed cell vinyl-nitrile foam used for sound absorption and is approved by the FAA for aircraft. The last portion of the sound barrier is the layer added to the extremities of the sound barrier panel. This layer is composed of an acrylic based paint coat known as Delta dB Coat Gel. The coating is provided by Hagemeyer in as a free sample. The coating is easily installed via brush application and is also a class 1A fire retardant (www.mascoat.com…). Reductions of approximately 10 dB can be seen for a very broad frequency range; see Figure 3-10. The sound barrier is portrayed in Figure 3-11 for clarification.

SOUND DAMPING EFFECTS USING COATINGS

Decrease in Decibels vs. Frequency

Frequency Hz	188	366	585	881	1000	3000	5000
60 mils Delta~dB	9.3	11.5	10.7	11.6	10.8	10.9	11
40 mils Delta~dB	4.0	5.8	5.3	5.7	5.7	5.7	5.8
Delta~dB + Delta T Marine	10.2	11.8	11.7	12.9	12.9	12.9	12.9
Plain panel (no coating)	0.0	0.0	0.0	0.0	0.0	0.0	0.0

Figure 3-10: Sound Damping Effects Using Coatings of Delta dB (www.mascoat.com)

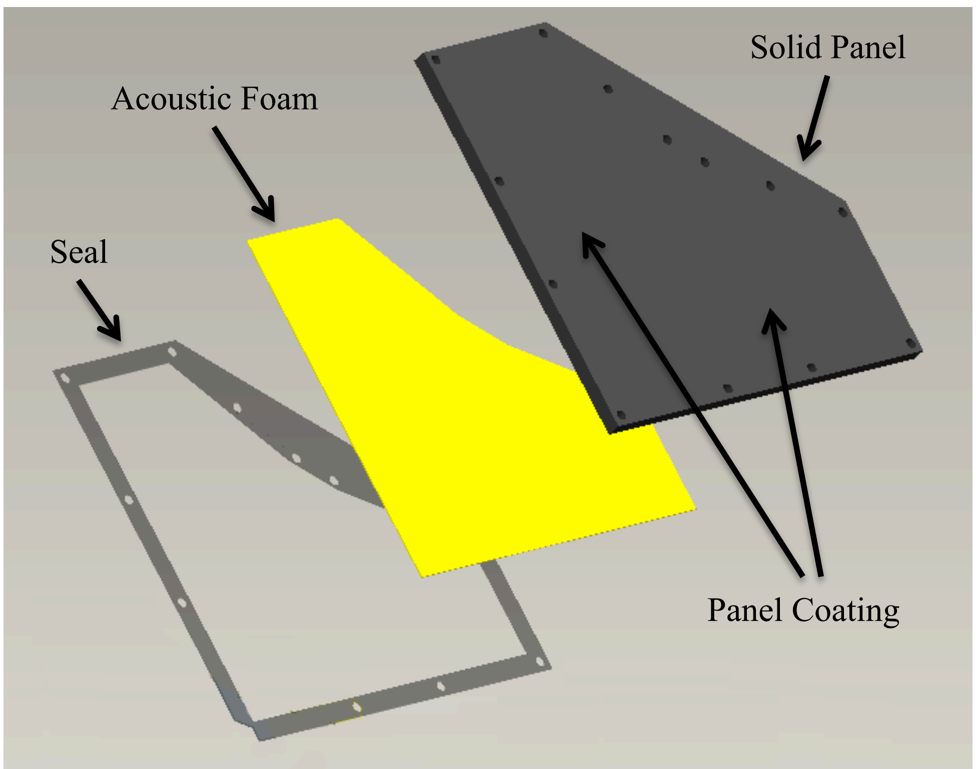

Figure 3-11: Sound Barrier Components

Scale Model Gear Housing and Cover Materials:

The model gear housing is machined out of 6061 aluminum purchased from McMaster-Carr. The original gear housing was determined to be the same type of aluminum. The model gear cover is cut out of 0.036 inch thick piece of steel sheet metal. This sheet metal is also to be ordered from McMaster-Carr and complies with the original material of the single-layer gear cover provided by Cummins Incorporated.

Cantilever Beam Materials:

The cantilever beam model used for active material characterization is made up of three pieces; a base plate to connect the testing apparatus to the shaker table, a connection block to mate the base plate and the cantilever beam, and the sheet metal cantilever beam. The base plate and connection block are to be milled out of 6061 aluminum stock and the cantilever beam is to be cut from the same steel sheet metal being used for the scale model gear cover. One MFC is attached directly to the top of the sheet metal beam as close to the permanent fixed end as possible. Figure 3-12 is a schematic of the cantilever beam set up for both one free end and two fixed ends.

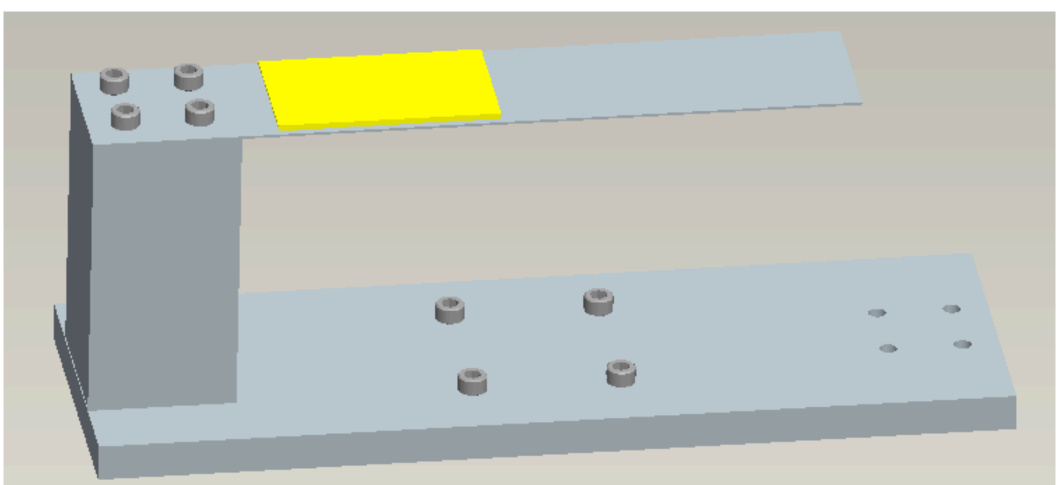

Figure 3-12: Cantilever Beam Apparatus for Testing

3.3.2 Equipment Selection

Due to the fact it is unlikely and unfeasible to be supplied with a full size diesel engine for testing and analysis, another devise must be utilized to simulate the vibrations produced by such a system. Luckily, the College of Engineering is equipped with a large mechanical shaker in Dr. Collins' lab. The mechanical shaker is a Gearing & Watson Electronics Ltd. V300 powered by a DSA1 power amplifier. The hardware is connected to a Data Physics computer data acquisition system. The shaker was actually unused at the time, and the system had yet to be installed or implemented until the design project requested its services. Also, an adapter piece is necessary for the top plate of the shaker to connect the actual gear housing Cummins provided. The adapter piece is made out of the same material of the actual gear housing, 6061 aluminum stock.

The other required equipment for the design pertains to the active material controls. The piezoelectric material requires high voltages in the range of about a kilovolt. The specific setup used at the Advanced Aero Propulsion Laboratory for active material controls is used for this design project. To power the piezoelectric actuators, a PiezoMechanik power amplifier is connected to a large capacitance source for sustained voltage. A dSpace data acquisition system is used inline with the power amplifier and the computer, which is used as the control code source. Figure 3-13 shows the power amplifier used for testing. For the proposed scale model design and also the final design that could pertain to a real world production model, this large power amplifier is very unpractical due to its size and associated cost. A solution to this space and cost issue lies within products such as an EMCO miniature DC to AC converter, shown in Figure 3-14. For feedback and displacement readings, a capacitor probe is used due to its high level of accuracy and data sampling rates. The capacitor probe has been used with patch actuators before and has been proven quite effective for open and closed loop control. Another option more suited for the design project for feedback is using strain gauges for a feedback device. The use of strain gauges is addressed in later sections.

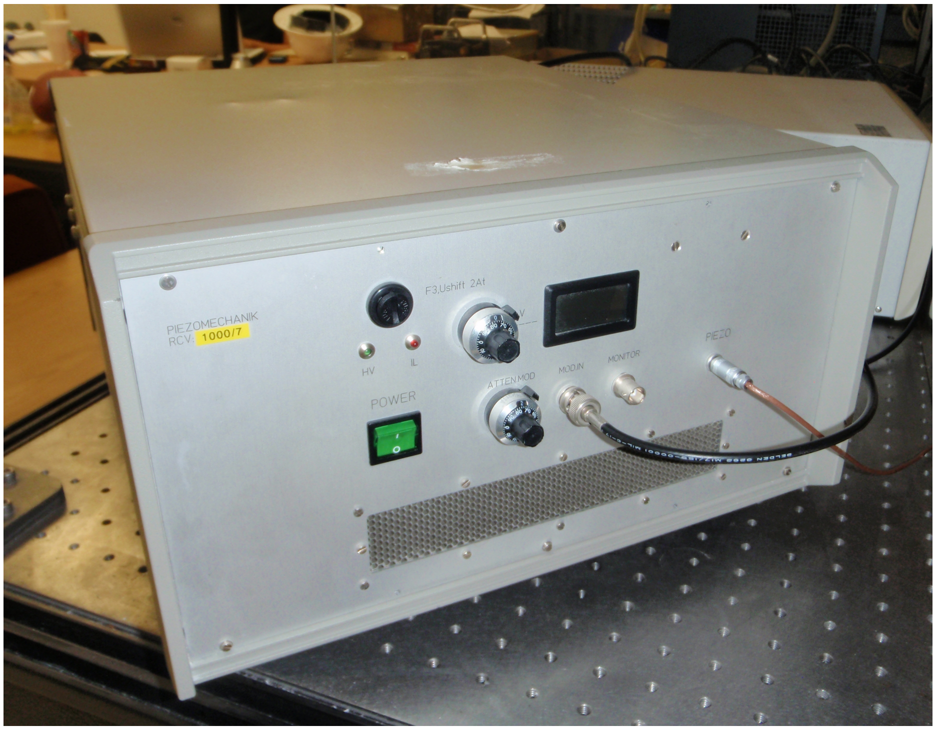

Figure 3-13: PiezoMechanik Power Amplifier Utilized at the AAPL

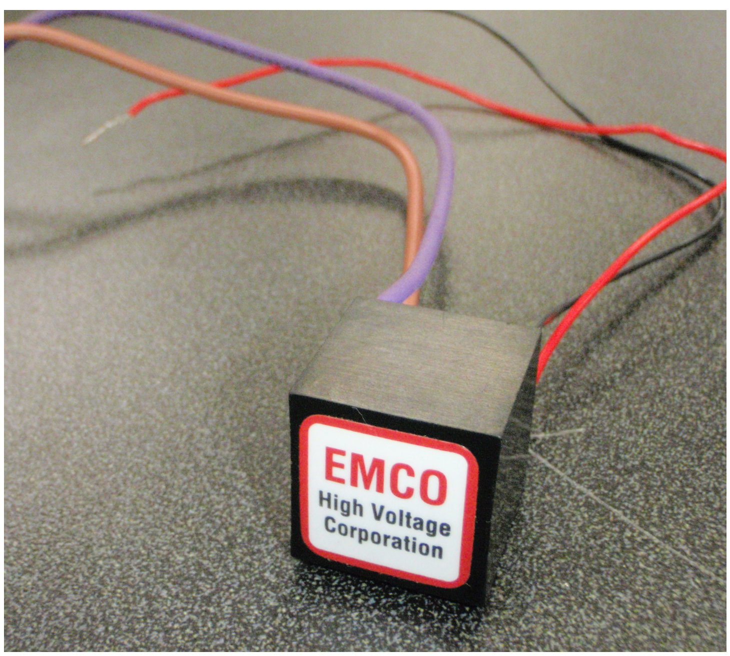

Figure 3-14: EMCO Miniature DC to AC Converter

The only other piece of equipment that is required is a device to record the radiated sound power of the devices throughout the testing phase of the design. This is accomplished by using a sound level meter connected to the data acquisition system. Specifically, the Extech 407730 sound level meter is used for testing. In this manner, the motion, input frequency, and sound can be measured and compared to each other at the same time.

Figure 3-15: Extech Sound Level Meter

3.4 2D Modeling and Analysis

3.4.1 Cantilever Beam

Successful vibration control of any system depends on whether the actuator is capable of manipulating the vibrating system in question. The system illustrated in Figure 3-16 shows a MFC actuator that has been fixed onto a thin piece of low carbon steel.

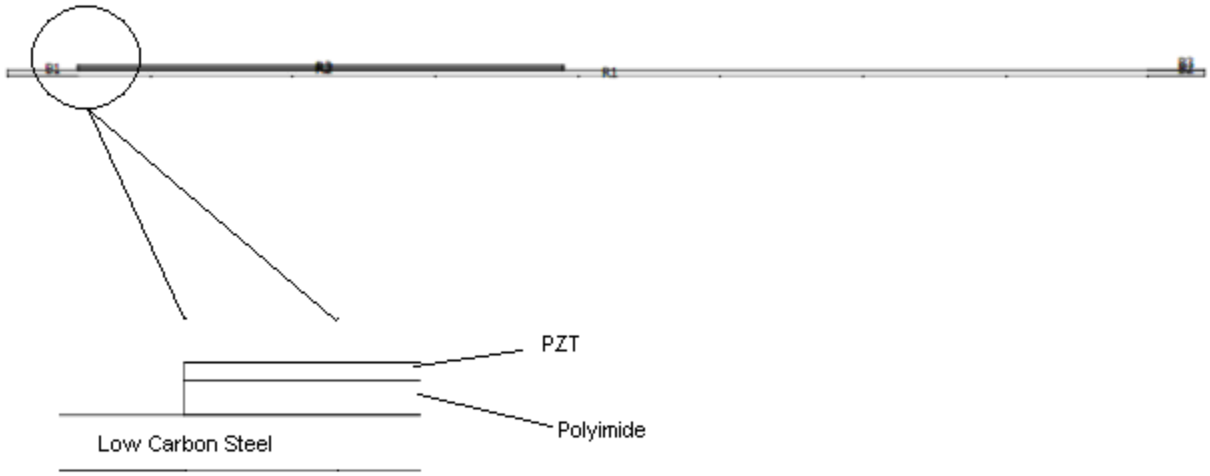

Figure 3-16: MFC Actuator on Low Carbon Steel

Piezoelectric properties dictate that when a voltage is applied to a piezoelectric material the material will undergo a change in shape. In this instance the top piezoelectric layer will be expanding or contracting, depending on the voltage, on top of a mostly rigid polyimide layer resulting in a shape change. First, it must be determined if the actuator can manipulate the system and how. The overall system reaction as a result of an applied voltage can be analyzed with one and both ends of the steel beam fixed. A second analysis is then performed in order to determine the actuators influence on the overall vibration properties of the system. The first three resonance modes of each experimental set up will be evaluated to determine how that actuator is affecting the system.

3.4.2 Theoretical Analysis of Cantilever Beam

The basic equations that govern the overall system are:

$$\sigma := E \cdot \varepsilon \quad (1) \qquad \varepsilon = du/dx \quad (2) \qquad 0 = d\sigma/dx \quad (3)$$

where sigma is the stress, E is young's modulus, epsilon is the strain, u is the displacement and x is the position along the system. Equations 1, 2, and 3 are valid for the non-piezoelectric materials in the system such as polyimide and steel. The equations for the piezo-material as seen in equations 4 and 5 are very similar with the exception being there added stress and strain as a result of the voltage and the piezoelectric constant

$$\sigma = E \cdot \varepsilon - e_p \cdot E_v \quad (4) \qquad\qquad \varepsilon = du/dx + d_p \cdot E_v \quad (5)$$

where e_p is the piezoelectric stress constant, E_v is the negative change in voltage per change in position in a given direction, and d_p is the piezoelectric strain constant. When these equations are expanded out to encompass a two dimensional model the equations become (6) through (11)

$$\sigma_x = C_{11} \cdot \varepsilon_x + C_{12} \cdot \varepsilon_y - e_{31} \cdot E_y \quad (6) \qquad\qquad \sigma_y = C_{12} \cdot \varepsilon_x + C_{22} \cdot \varepsilon_y - e_{33} \cdot E_y \quad (7)$$

$$\sigma_{xy} = G \cdot \varepsilon_{xy} - G \cdot e_{16} \cdot E_x \quad (8) \qquad\qquad \varepsilon_x = \sigma_x / E_1 - \upsilon_{12} \cdot \sigma_y / E_1 + d_{31} \cdot E_y \quad (9)$$

$$\varepsilon_y = \sigma_y / E_2 - \upsilon_{21} \cdot \sigma_y / E_2 + d_{33} \cdot E_y \quad (10) \qquad\qquad \varepsilon_{xy} = \sigma_{xy} / G + d_{16} \cdot E_x \quad (11)$$

where v_{12} and v_{21} are the Poisson ratio, G is the shear modulus, C_{11}=C_{22}= E/(1-v_{12}*v_{21}), and C_{12}=v_{12}* C_{11}. This form is necessary since the piezoelectric material displaces more in 33 direction than in the 31 as a result of the piezoelectric constants for each direction being different. It is important to recognize that for this system the Poisson ratio is the same in the x-direction as it is in the y direction (v_{12}= v_{21}) for each of the materials, and that E_1 = E_2 within each individual material.

While there is no external force acting directly on the system, the piezoelectric material due to its change in shape will exert some stress and strain on the non-piezoelectric parts of the system. By examination of the above equations a qualitative estimation of system response is possible. Both the one fixed end and two fixed end solutions are examined; see Figure 3-17 through 3-19.

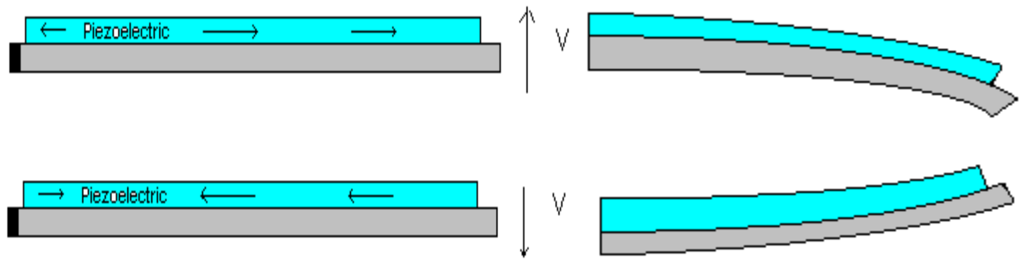

Figure 3-17: One Fixed End Cantilever Beam

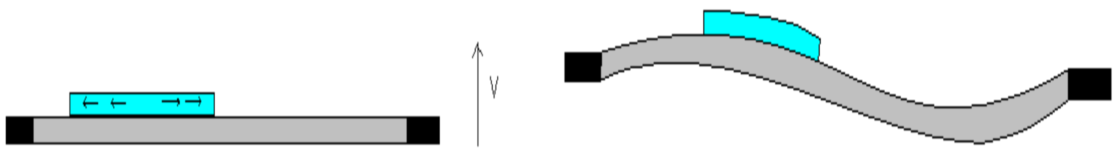

Figure 3-18: Two Fixed Ends Beam in Expansion

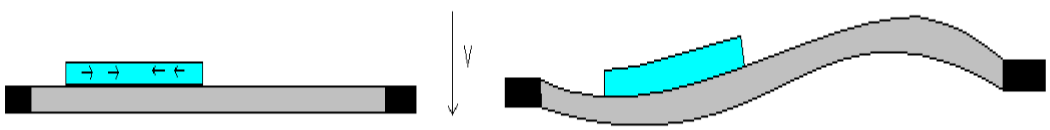

Figure 3-19: Two Fixed Ends Beam in Contraction

3.4.2 Finite Element Model of Cantilever Beam

The system is composed of a thin piece of low carbon steel 8.4 inches long with the MFC actuator 3.4 inches in length off set 0.5 inches from the left most end as shown in Figure 3-20. In order to properly assess what the effect of the actuator are, certain constants and material properties must be known. Table 3-A shows some of the needed material properties for each component. Table 3-B and 3-C lists the piezoelectric constants that relate applied voltage to mechanical stress along different directions.

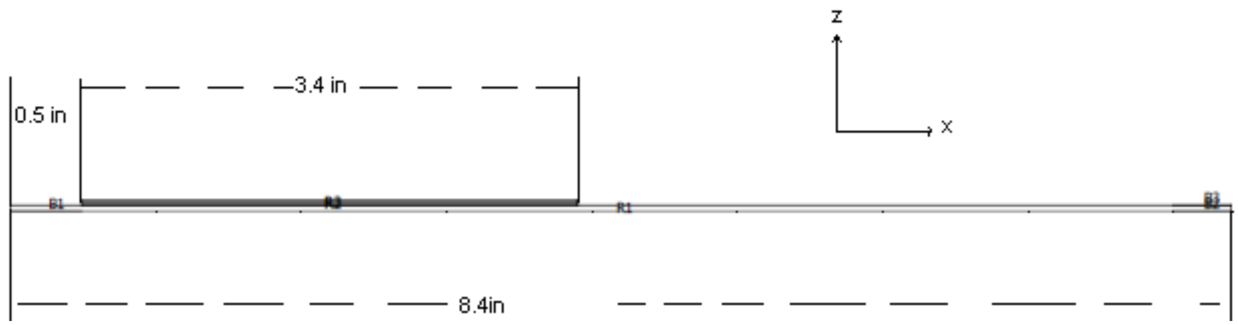

Figure 3-20: System Layout

Table 3-B: Material Properties

Material	*Thickness (in)*	*Modulus (GPa)*	*Shear Modulus (Gpa)*	*Poisson Ratio*	*Density (kg/m³)*
Piezo Material	0.01181	71 open / 62 short	5.15	0.35	7600
Low Carbon Steel	0.036	207	79.9	0.3	7861.093
Polyimide	0.023	2.3	5.15	0.35	1430

Table 3-C: Piezoelectric Constants

Piezoelectric Stress Constants (C/m^2)		
(e33) y	(e31) x	(e16) z
-5.2	15.1	12.7

The above model and material properties were input to COMSOL multi-physics program. The following solutions where obtained for each given condition. Please refer to Appendix B for model figures.

It is evident from Figures B-14 through B-17, located in Appendix B, that the COMSOL model qualitatively agrees with the theoretical predictions in terms of how the actuator affects the system. The overall displacement depends directly on the applied voltage, shown as 100V. Referring back to equations (4) and (5) it can be determined that the displacement is linearly related to the applied voltage by the piezoelectric constants. However, the scale at which these movements are taking place is very small; in the range of about 1E-6 meters.

Given that the system's intended use is vibration attenuation, the first three resonance modes have also been examined to find what if any effect the actuator has on the system during resonance. Figures B-18 through B-20, located in Appendix B, show the first three modes of the one fixed end model. The mentioned figures show that the actuator has an effect on the vibration properties. There is an observable difference in the stress concentrations at the locations near the actuator when the actuator is in closed circuit, ie. a positive or negative potential difference. The location and magnitude of the stress concentrations move depending on the voltage and resonance mode.

3.4.3 Finite Element Modal Analysis

To analyze the locations of the largest displacement at a wide range of frequencies, one can consider the finite element analysis of nodal locations for different modes. In Figure 3-21 the first five resonance modes are illustrated of the original single layer gear cover. The red areas are the locations of maximum displacement and the blue areas represent regions with little to no displacement.

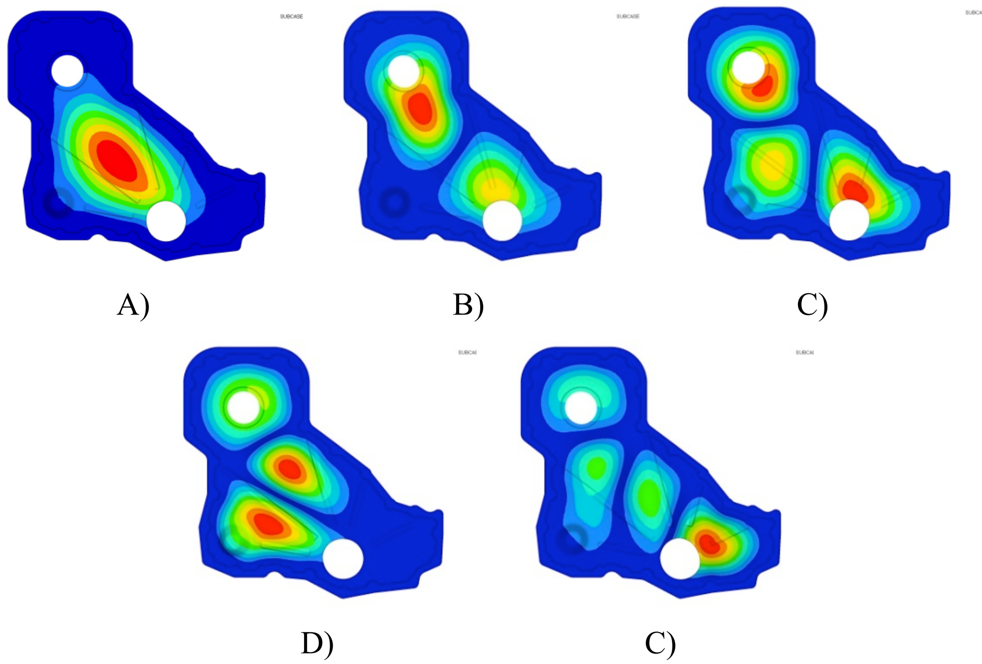

Figure 3-21: FEA of Single Layer Gear Cover

A) First Mode B) Second Mode C) Third Mode D) Fourth Mode E) Fifth Mode

(FEA diagrams provided by Cummins Incorporated)

The FEA of the gear cover is useful when comparing the original design of the gear cover versus the scale model design. Figure 3-22 illustrates the first five modes of the scale model cover. The nodal analysis of the original gear cover and the final design can be seen in detail in Appendix B. The shape of the scale model cover was determined by testing various shapes similar to the original cover. It was found that a square without a corner produced nodal shapes that resembled the nodal shapes of the original cover. However, the nodes did not split in shapes similar to the original cover, so the angled side was modified into a three-segmented side that is convex into the corner. This segmented side produced the best nodal shapes and also maintained symmetry. The original gear cover is not flat and incorporates raised ribs, which add to the cover's stiffness. This has an effect on the nodal locations but is very difficult to reproduce without adding more complexity to the design.

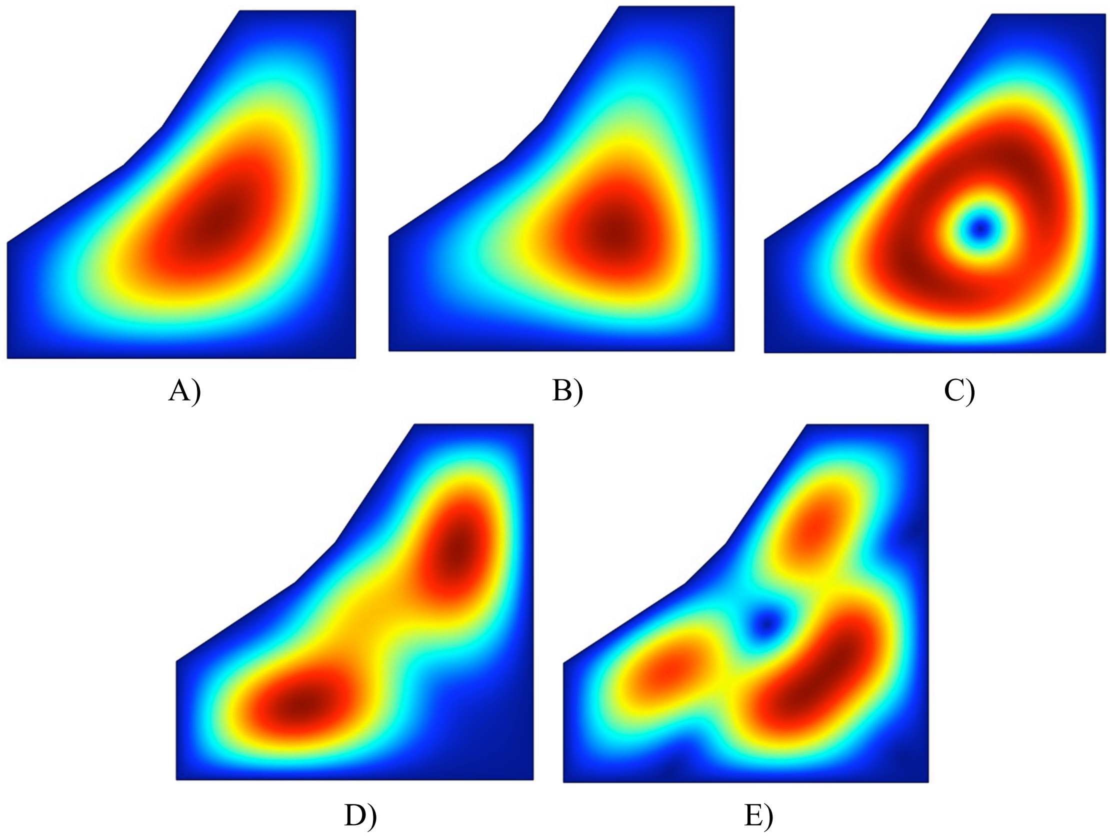

Figure 3-22: FEA of Scale Model Gear Cover
A) First Mode B) Second Mode C) Third Mode D) Fourth Mode E) Fifth Mode
(FEA Diagrams Created with COMSOL)

Despite the differences of the exact shape and location of the nodal points between the original and scale model gear covers, it can be seen that similar trends are associated that can lead to conclusion that the scale model cover is an acceptable simplified version of the original. A more complex geometry of the gear cover can be designed to produce more similar nodal trends. However, as the complexity of the geometry increases, the difficulties associated with the analysis and orientation of the MFCs increase. Also, a more complex geometry produces a larger risk of testing issues and time is the major constraint of this design project.

To orient the MFCs, it is research suggested to place the patch actuators in the same direction of the vibrations. For a structure that is constrained by the outside perimeter and vibrations that are transmitted around the periphery of the perimeter, it can be concluded that the source location of the vibrations is the outside perimeter. Thus, the vibrations propagate from the outside of the structure to the inside. The first mode of the scale model cover provides information on where the vibrations originate from and their destination. Figure 3-23 portrays the direction of the vibrations towards the center nodal point.

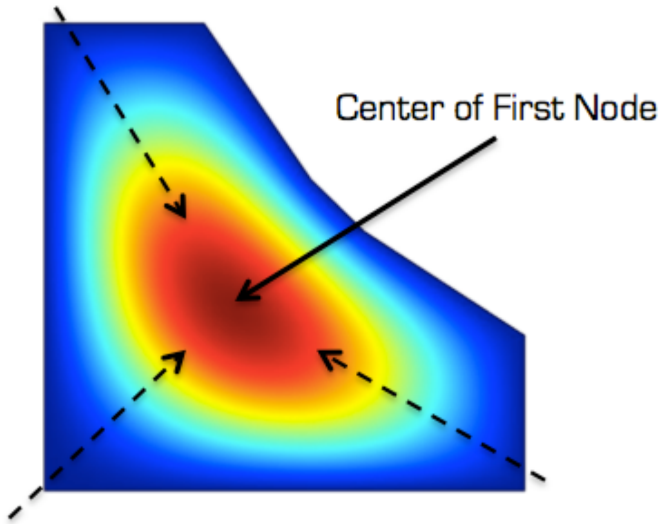

Figure 3-23: First Mode and Nodal Location for the Scale Model Cover

The nodal locations change as the frequency of the system increase. However, due to the stiffness of the scale model and the relatively low frequency range associated with the project design, it is unlikely that the system will ever reach the point when the nodes split into two nodes during the third mode. This provides enough supporting evidence to conclude that the patch actuators should be oriented toward the first central nodal point. This also complies with the available surface area of the scale model gear cover that is required to attach three MFCs.

3.4.5 Conclusion

The overall systems behaved at least qualitatively the same in the COMSOL model as in the theoretical predictions. This implies that the actuator is capable of manipulating the overall system, which bodes positively for the desired application. The scale of these movements generated by the actuator as previously discussed is very small on the order of 1E-6 meters. The vibration properties of the system were also clearly affected by the actuator. The increased stress concentrations clearly imply that the actuator is resisting the motion of the steel. There is also some evidence that the motion of the steel is made less chaotic by the force of the actuator. This particular control method only tests open and short circuit configurations, the actuator is either on or it is off. Although it is unclear to the extent of which the vibrations can be attenuated it is evident that the current set up can achieve some level of vibration control. Through some more advanced control methods a higher level of attenuation may be obtained.

The modal analysis of the original gear cover and the scale model gear cover are similar enough to allow for a proper evaluation of the effectiveness of the patch actuators. Thus, if the MFCs are capable of reducing the magnitude of surface vibrations of the scale model cover, the MFCs are capable of reducing the magnitude of surface vibrations of the original gear cover with proper scaling of the required force and adjustment of active system controls. Also, the patch actuators should target the first nodal point unless data collected from the characterization of the cantilever beam concludes otherwise.

3.5 Prototypes

Three main devices where modeled in Pro-E and Solid Works for machining and assembly. The following prototype views are the final versions tested. The main device to be fabricated is the scale model. Figures 3-22 and 3-23 show the assembly of the scale model and its components.

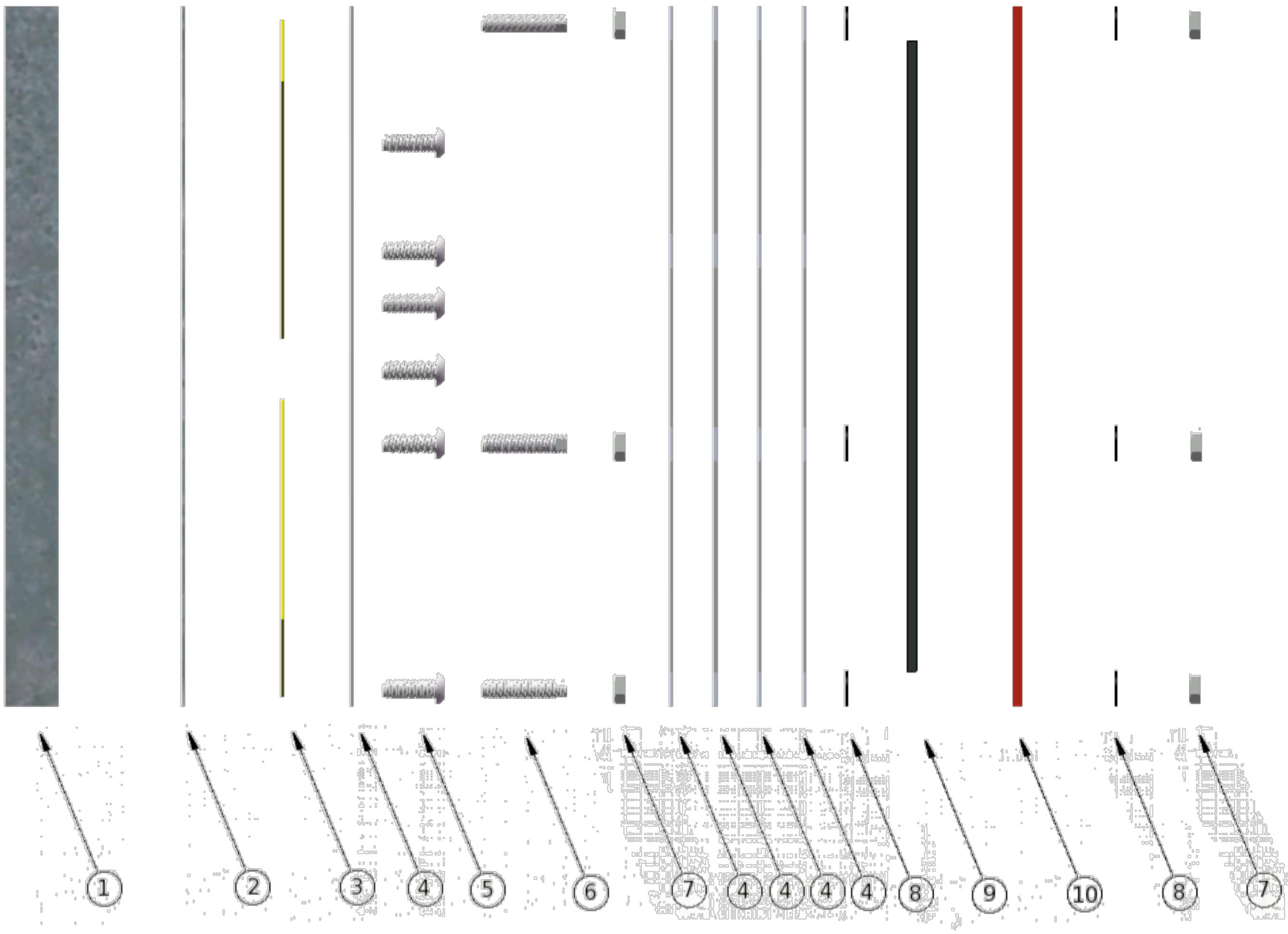

Figure 3-22: Exploded View of Scale Model Design

Table 3-D: Bill of Materials of Scale Model

PART #	PART	MATERIAL	QUANTITY
1	MODEL HOUSING	STEEL SHEET METAL	1
2	MODEL COVER	ALUMINUM 6061	1
3	MFC	PIEZOCERMAIC PATCH ACTUATOR	3
4	COMPLIANT SEAL	VIBRA BLOCK	5
5	¼-20 7/8” SCREW	STAINLESS STEEL SOCKET CAP SCREW	13
6	¼-20 KEYED ROD	STAINLESS STELL THREADED ROD	5
7	¼-20 HEX NUT	STAINLESS STELL	10
8	¼ ID WASHER	RUBBER WASHER	10
9	FOAM	SSP FOAM	1
10	BARRIER	CARBON FIBER or FIBERGLASS	1

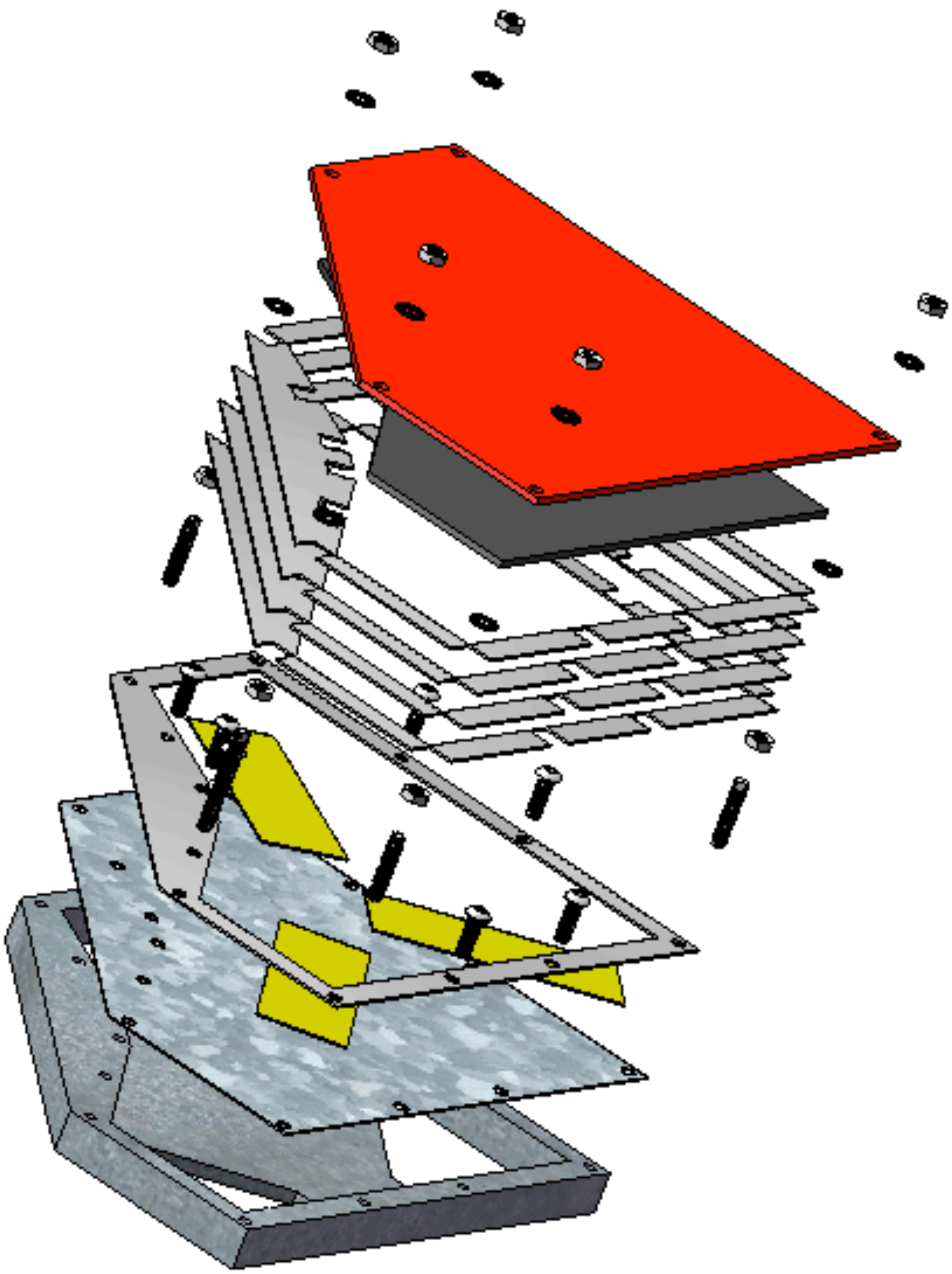

Figure 3-23: Side View of Scale Model Components

The second device to be machined is the cantilever beam testing apparatus. The different components of both one fixed end and two fixed in cantilever beam apparatuses can be seen in Figures 3-24 through 3-25.

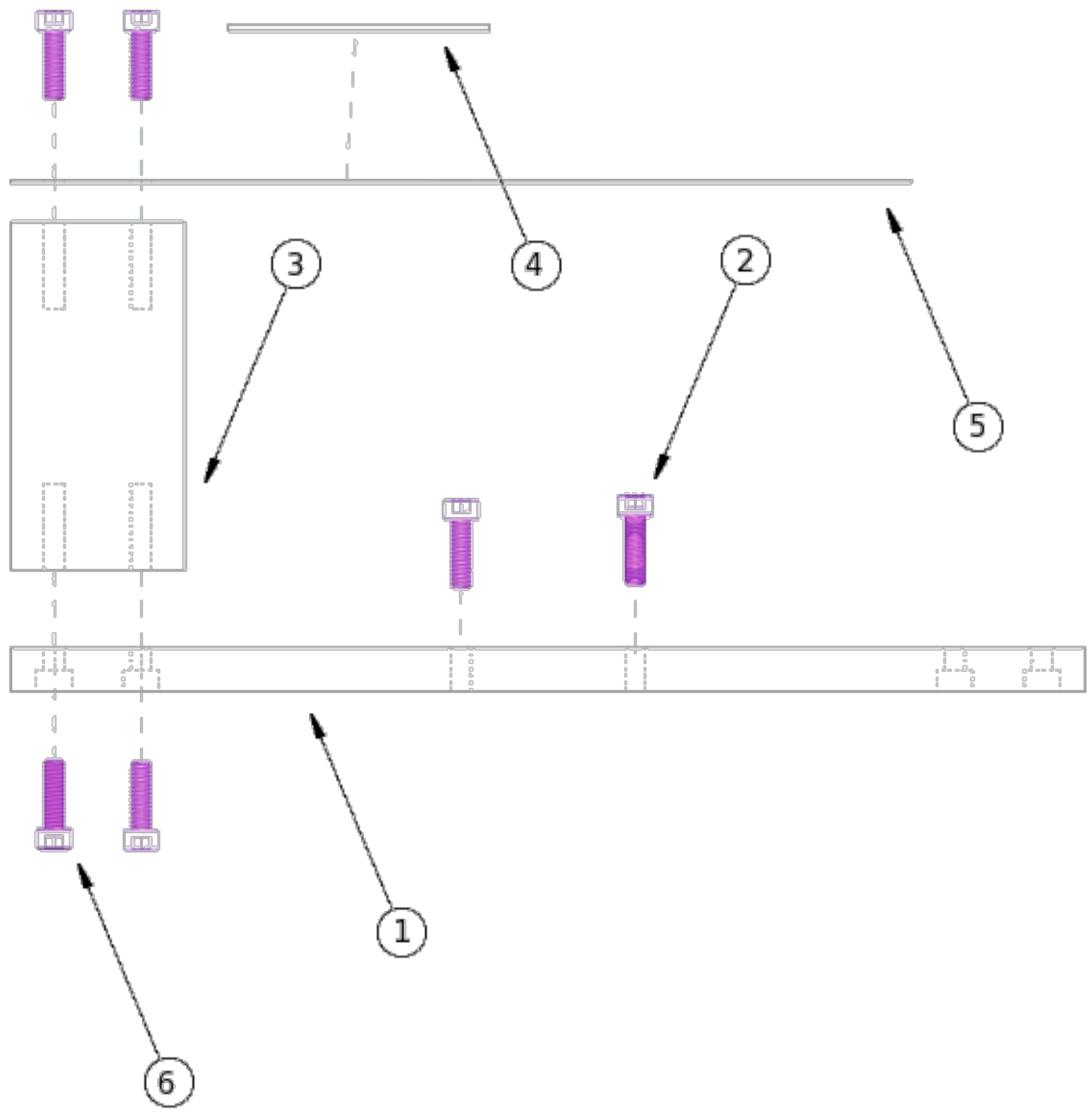

Figure 3-24: Exploded View of One Fixed End Cantilever Beam

Table 3-E: Bill of Materials for One Fixed End Cantilever Beam

PART #	PART	MATERIAL	QUANTITY
1	BASE PLATE	ALUMINUM 6061	1
2	M6 SCREW	STAINLESS STEEL SOCKET CAP SCREW	4
3	SUPPORT BLOCK	ALUMINUM 6061	1
4	MFC	PIEZOCERMAIC PATCH ACTUATOR	1
5	BEAM	STEEL SHEET METAL	1
6	¼-20 1/2” SCREW	STAINLESS STEEL SOCKET CAP SCREW	8

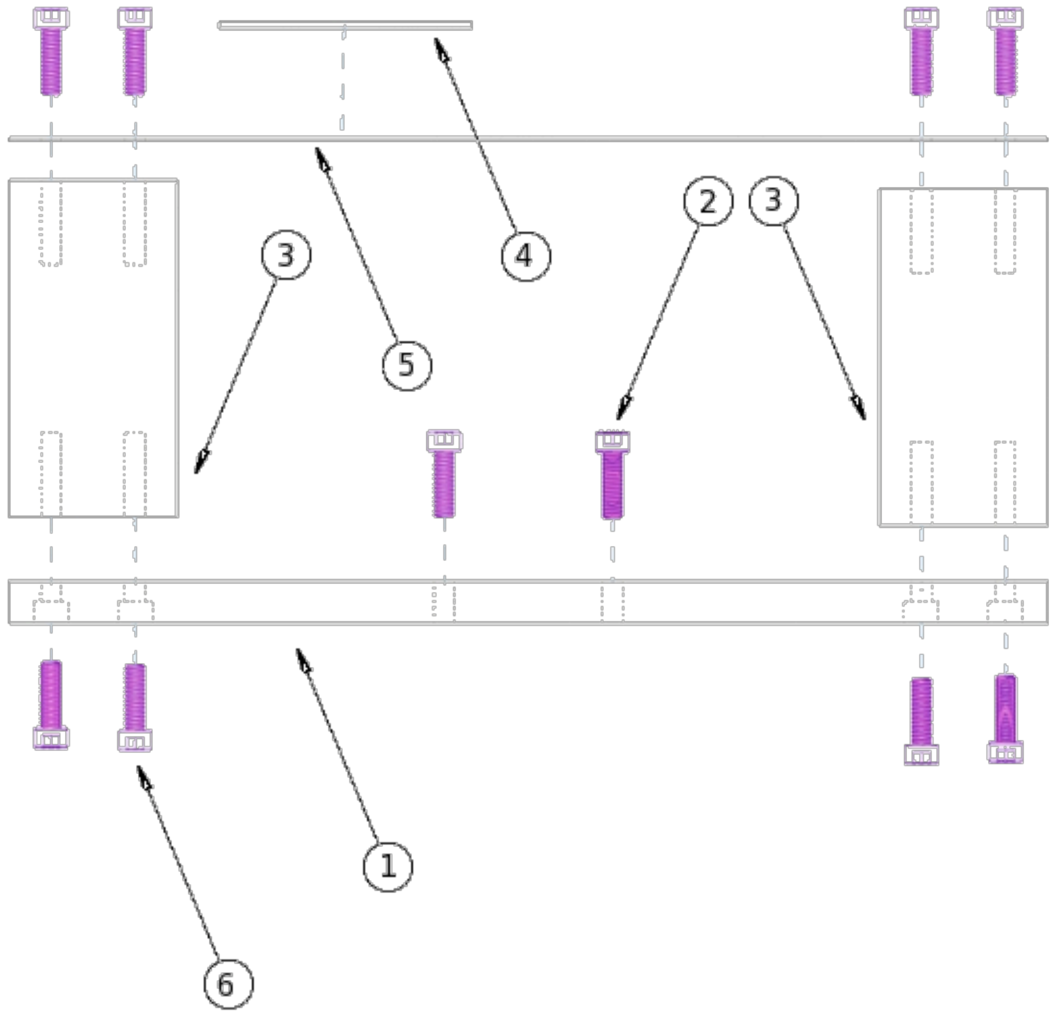

Figure 3-25: Exploded View of Two Fixed Ends Beam

Table 3-F: Bill of Materials for Two Fixed Ends Beam

PART #	PART	MATERIAL	QUANTITY
1	BASE PLATE	ALUMINUM 6061	1
2	M6 SCREW	STAINLESS STEEL SOCKET CAP SCREW	4
3	SUPPORT BLOCK	ALUMINUM 6061	2
4	MFC	PIEZOCERMAIC PATCH ACTUATOR	1
5	BEAM	STEEL SHEET METAL	1
6	¼-20 1/2” SCREW	STAINLESS STEEL SOCKET CAP SCREW	16

The third device that is crucial to testing the existing gear cover of the diesel engine is the adapter piece that connects the cover to the mechanical shaker. Figure 3-26 portrays the associated components of the adapter.

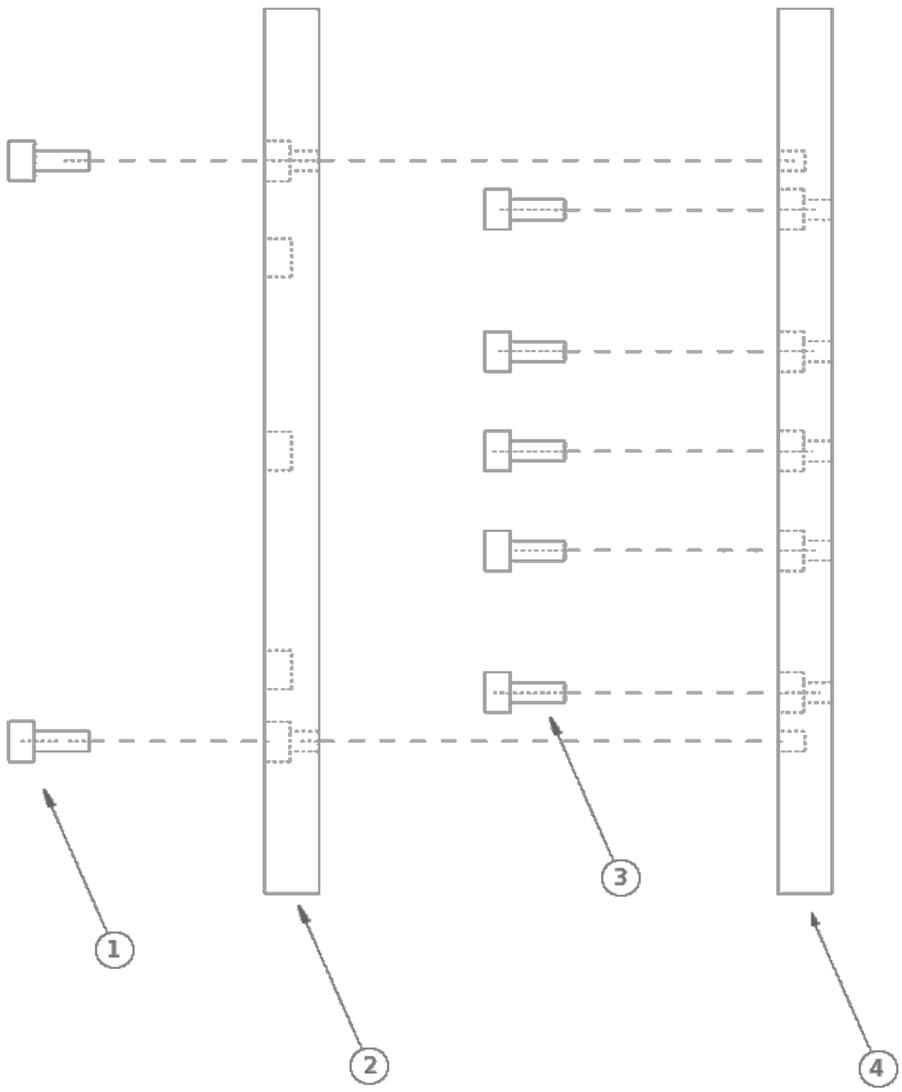

Figure 3-26: Exploded View of the Adapter Piece

Table 3-G: Bill of Materials for Adapter Piece

PART #	PART	MATERIAL	QUANTITY
1	¼-20 1/2" SCREW	STAINLESS STEEL SOCKET CAP SCREW	4
2	TOP PIECE	ALUMINUM 6061	1
3	M6 SCREW	STAINLESS STEEL SOCKET CAP SCREW	9
4	BOTTOM PIECE	ALUMINUM 6061	1

Please refer to Appendix E for detailed drawings of each component for each device.

4 Design Changes

Since the design proposed in December, no major changes have affected the project's final design. The only changes that arose were due to customer input or equipment availability due to time constraints. It was recommended by Cummins to modify the attachment configuration that was proposed in the December design. Originally, the design indicated that the sound barrier panel would be bolted down at the same locations the scale model gear cover connected to the scale model gear housing; this method used 13 screw holes. Cummins suggested to use fewer attachment points to reduce the vibrations propagating into the sound barrier panel. This was a simple fix to the design and it was decided to test various attachment points to identify which resulted in the least amount of propagated audible noise. This was done experimentally using c-clamps in various configurations at screw hole locations. Figure 4-1 indicates the attachment locations and the screw hole configurations tested. More detail about how the c-clamp testing is performed is mentioned in Section 7.3.

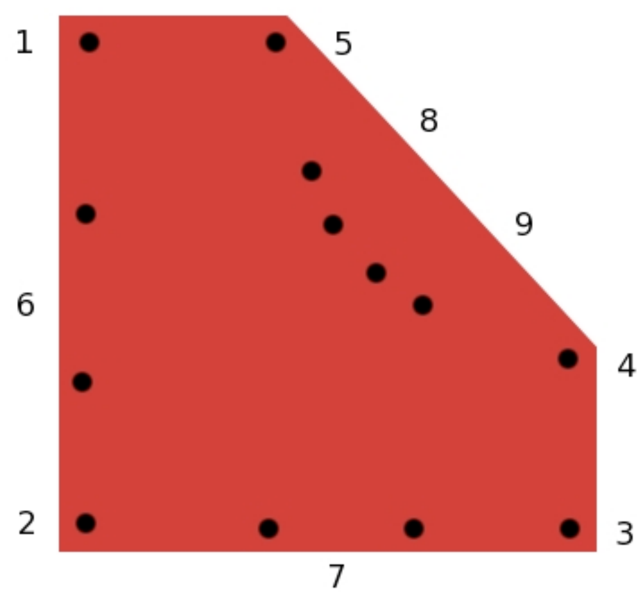

Testing Configurations:

1,2,3,4,5

1,2,3,4,5,6,7,8,9

2,4,5

6,7,8,9

4,5,6,7

1,2,3,8,9

Figure 4-1: Attachment Point Testing of Scale Model Cover

The best means of attachment was determined to be for holes 1,2,3,4, and 5 if referring to Figure 4-1. To accommodate only five screw holes being used in the housing for the sound barrier cover, ¼”-20 threaded rod segments replaced the five ¼”-20 socket cap screws. Figure 4-2 portrays the new means of attachment using threaded rod links that are keyed on one end for tool grasping. Rubber washers were added to both sides of the sound barrier panel to reduce the fiberglass to metal contact between the fiberglass barrier panel and the ¼”-20 hex nuts. It can be seen from Figure 4-2 how the ¼”-20 socket cap screws are not being used to constrain the sound barrier panel to the gear housing. The socket cap screws are used to attach the scale model cover to the scale model housing. The hex nuts are used at the five other locations to attach the scale model cover to the housing.

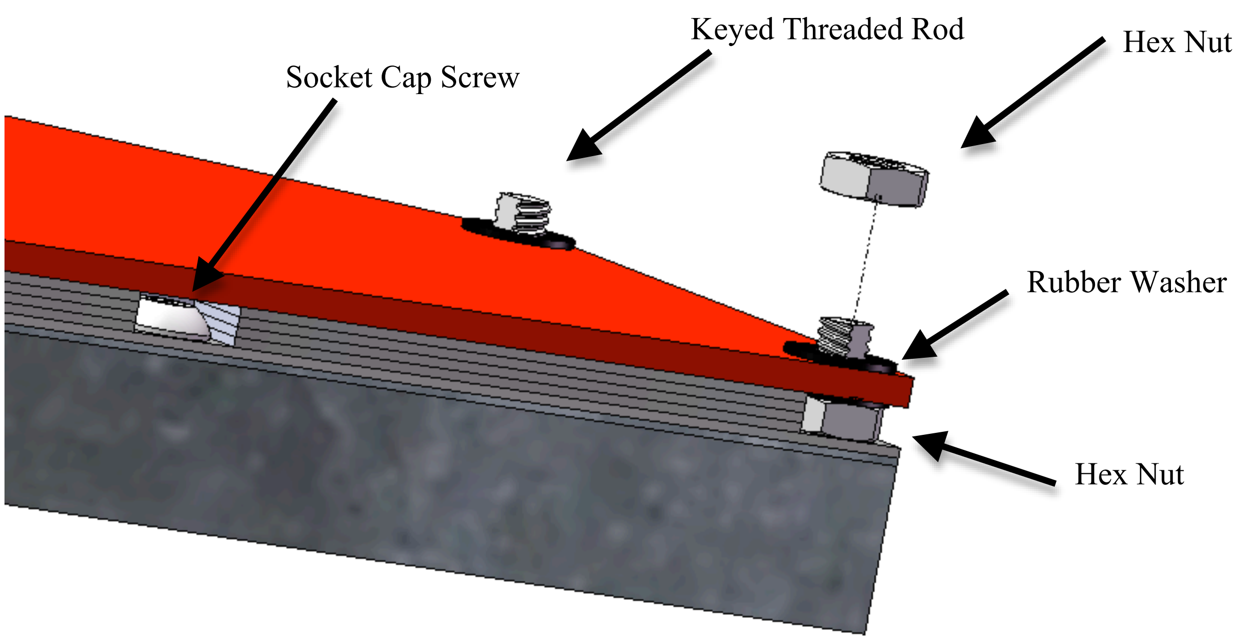

Figure 4-2: Close Up View of Attachment Alterations

The only other changes to the design are manifest in the controls portion of the design. However, these changes are more of a progression and refinement of the controls and are not mentioned in this section.

5 Manufacturing and Assembly

Due to the nature of the design project, the manufacturing and assembly phase did not encompass a large portion of overall project. A larger percentage of the project was reserved for data collecting and analysis of the scale model. Manufacturing of the scale model housing, adapter pieces, and cantilever beam apparatus took place at the machine shop located at the AAPL located on FSU's main campus. Group member Christopher Shultz, whom previously worked for the aforementioned machine shop, completed most of the machining with the exception of the scale model housing which required CNC tool paths to be completed properly. Bobby Avant, head machinist at the AAPL, thankfully provided his expertise and help on the scale model housing. Figure 5-1 illustrates the complex geometries of the housing and the end result. The scale model cover and cantilever beams were simply cut using a metal press. The holes for the duplicate scale model covers and cantilever beams were drilled using a mill by Christopher Schultz. The fiberglass sound barrier panel was cut using a laser cutter provided by Dr. Clark's Stride Lab. Stride Lab assistant Christopher Kulinka aided with this portion of machining. The carbon fiber sound barrier panel was intended to also be cut using the laser cutter. However, after procuring the carbon fiber sheet, it became evident that the material would burn when cut by the laser and deemed unsafe to attempt machining in this fashion. Since the carbon fiber could also not be machined using standard end mills due to its harsh machining characteristics, it was decided to not test the carbon fiber sound barrier panel unless more time became available and an excess portion of the project budget could be granted for a third-party company to cut the material.

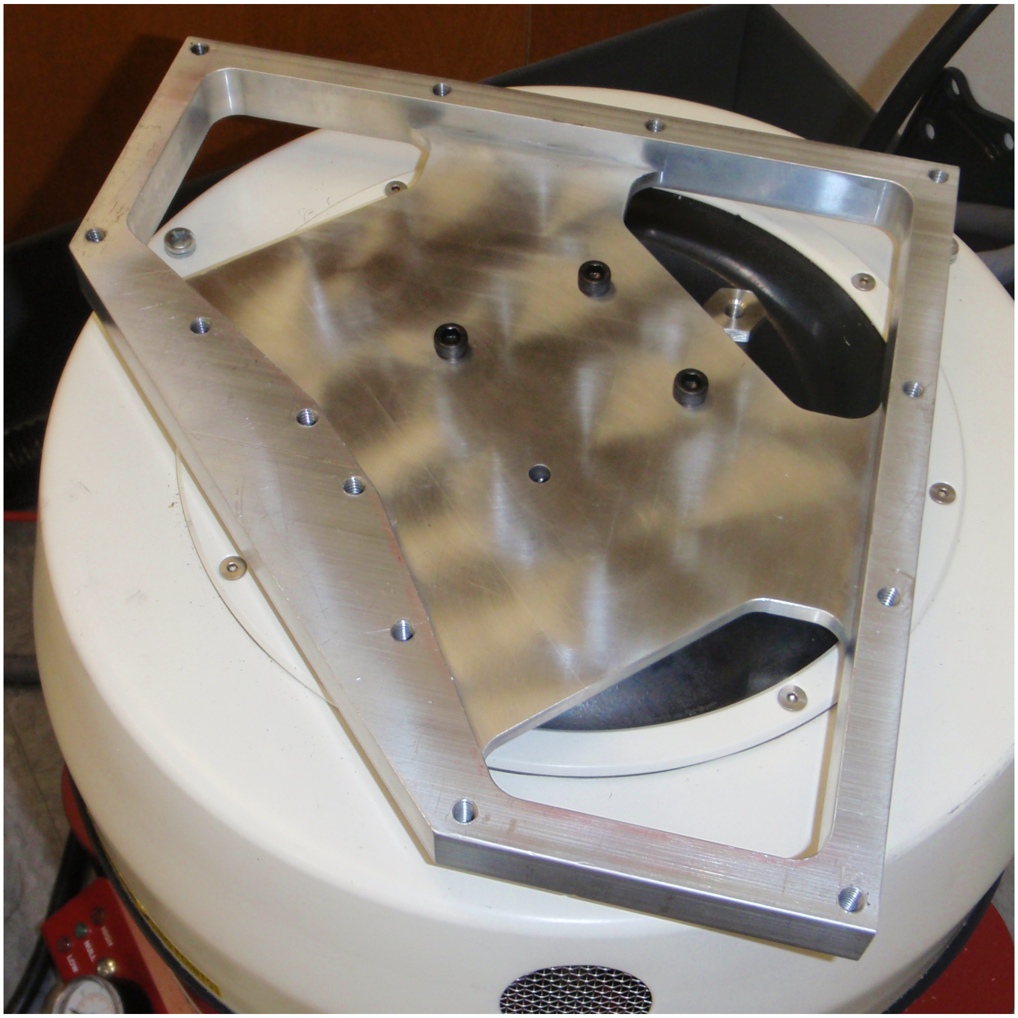

Figure 5-1: Scale Model Housing

Assembly of the scale model took place throughout the testing phase of the project. Since each component of the scale model was tested as it was added to the assembly, the scale model cover was put together and taken apart numerous times. Specific information regarding the assembly process of the scale model cover, including the application process of the MFCs, is located in the *Operations Manual* associated with this project.

6 Testing Setup

The following is description of how each portion of testing was conducted. For more specific information regarding the equipment selection, please refer to Section 3.3.2 or the *Operations Manual* associated with this project.

6.1 Sound Testing Setup

To test the sound radiated from the various components of the design, a sound level meter connected with the Abacus data acquisition system was used to collect decibel readings of the propagated noise. The sound level meter was positioned directly above the center of the shaker table, approximately two feet above the top of the shaker. The sound level meter was used with the wind screen and kept in the same location and position for every test performed with the shaker equipment. The room was not ideal for sound testing due to its shape, surroundings, and nearby walls that reflect noise. A more suitable environment would encompass the use of sound absorbing foam lined walls, much like a sound proof room specifically designed for its acoustics. However, since the testing environment was kept constant for all of the sound testing, the data collected is assumed to still be comparable with all data collected in this fashion.

The sound data was recorded for each test and scaled appropriately for each test. The scaling of the sound data was based off information provided by the manufacturers of the sound level meter and calibration data collected during each test. Prior to testing, the sound level meter was calibrated using a 94dB sound emitter, and it was also compared to two other sound meters; one sound meter was provided by the FSU Environmental Health and Safety department. It is also noted that since frequency sweeps were the main type of testing performed, selected frequencies were also tested for comparison to make sure the frequency sweeps were scaled correctly and conducted in such a manner to produce extremely similar decibel readings as if performed for individual frequencies. The testing setup is shown in Figure 6-1.

Figure 6-1: Sound Testing Setup

6.2 Active Material Testing Setup

The active materials, specifically the MFC actuators, were tested using the PiezoMechanik power amplifier and controlled using Simulink. The data was acquired using dSpace and analyzed in Matlab. Open and closed loop control codes were implemented using Simulink. Feedback data was supplied using a capacitor probe. The capacitor probe was positioned directly above the object being testing, within its range. The probe's position varied pending on the test for the cantilever beam apparatus. When testing the scale model cover, the probe was position directly above the center nodal location described in Section 3.4.3 and Section 7. The capacitor probe was always used on its lower sensitivity setting for the largest range available; a range of 2000 microns vs. 20 microns. The capacitor probe was secured in such a manner to make ambient vibrations negligible. The testing setup is shown in Figure 6-2 and Figure 6-3.

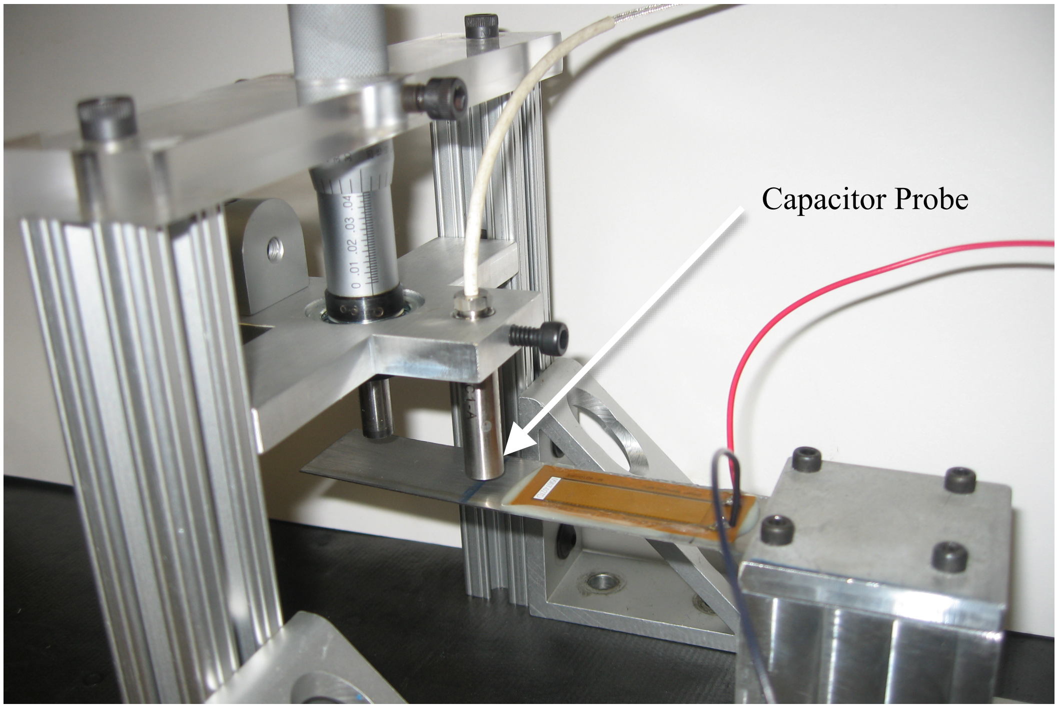

Figure 6-2: Testing Setup for Capacitor Probe and Cantilever Beam

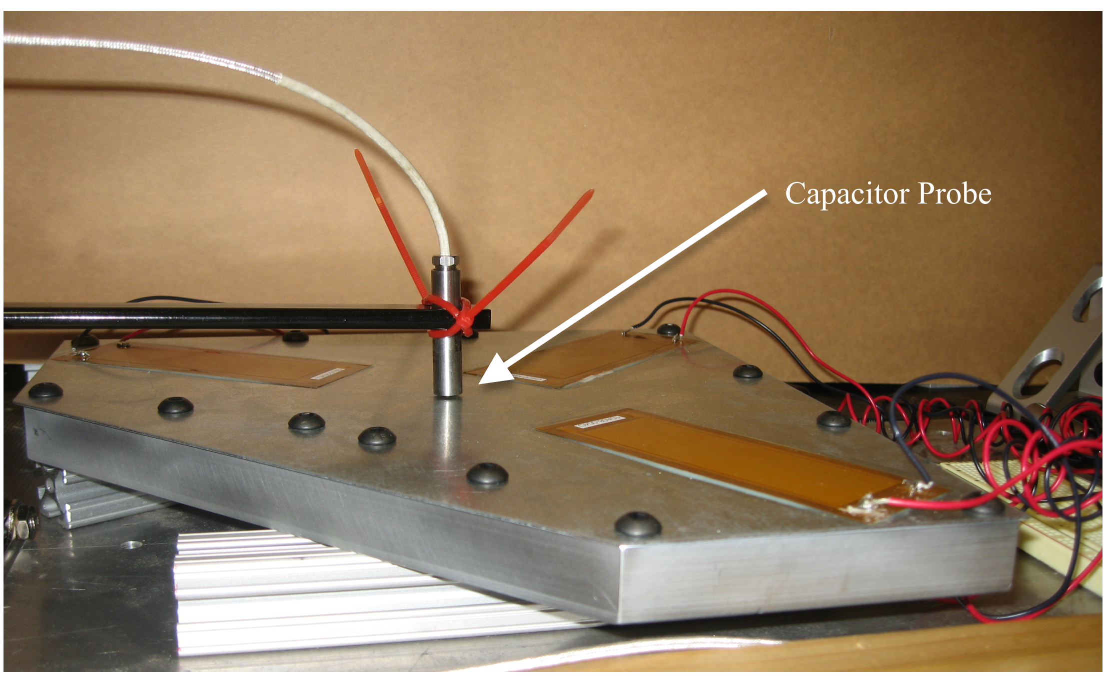

Figure 6-3: Testing Setup with Scale Model Cover and Capacitor Probe

When testing the MFCs in closed loop control, certain equipment limitations constrain the abilities of the MFCs. The MFCs have a full operation range of 2000 volts. This includes +1500 volts expansion and -500 volts contraction of the piezo-material. However, the power amplifier used during testing cannot produce a negative voltage and has a safe operating voltage range of 0 to +1000 volts. This means that only a half of the MFCs force and deflection potential can be acquired during testing. Also, since the MFCs cannot be driven negatively, the cantilever beam is constrained to one directional bending. This is not desirable for closed loop feedback control, which depends on two directional bending for successful reduction of system error. This problem can be taken care of by biasing the system to approximately 500 volts. This "preloading" of the MFC allows for a 0-500 volt range for upward deflection and 500-1000 volt range for downward deflection. Figure 6-4 illustrates this method.

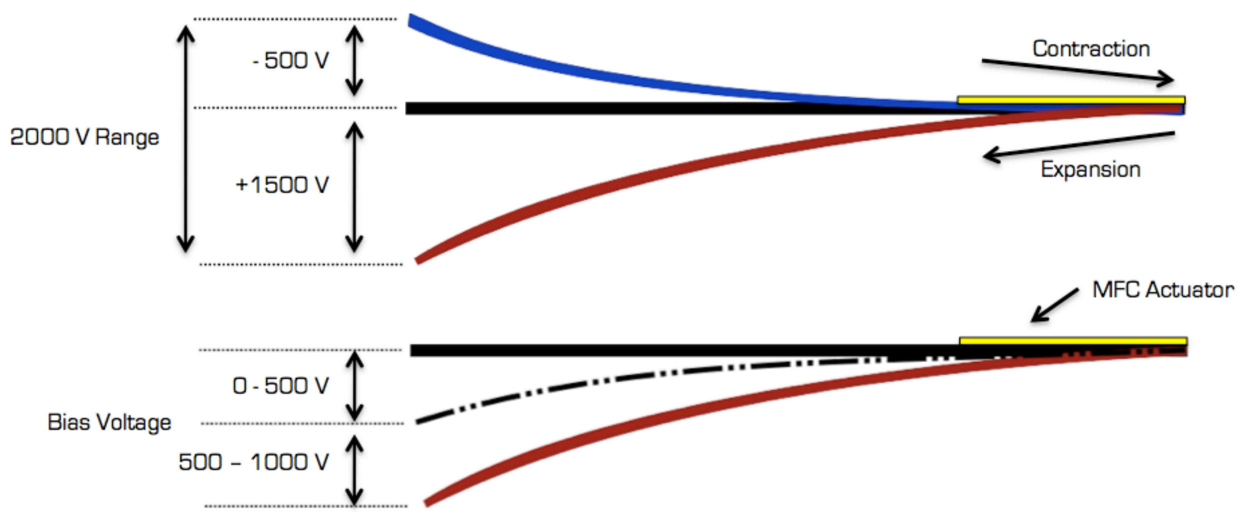

Figure 6-4: Cantilever Beam Schematic Portraying Constraints and "Bias" Method

During testing, a bias was directly or indirectly applied to the active system. The bias was either applied directly using the power amplifier or indirectly using the capacitor probe. To bias the system using the capacitor probe, the zero offset of the probe was manually adjusted. The probe's zero was raised above the zero of the control code and thus making the control code try to correct a "deflection" that was constant. This constant "deflection" cannot be corrected by the control code unless the beam is deflected using an applied voltage. The beam is then deflected by the voltage supplied due to the control code's effort to correct the manually inputted "deflection." However, due to the steady state error associated with this indirect method of biasing the system, a steady state oscillation is created. This steady state oscillation problem is a result of the control code and with more time could be corrected with additional programming and filters. For the purposes of the design, the steady state oscillations witnessed did not adversely affect the results and were regarded as a small problem that could be later addressed if deemed a nuisance.

6.3 Active Material and Sound Testing Setup

The MFCs attached to the scale model cover and the cantilever beam were also tested with the shaker table. Essentially, the two types of testing that had progressed in parallel were merged into one for final testing of the scale model and editing of the control code. The cantilever beam was set up in the same method mentioned previously in Section 6.2 but secured to the shaker. The testing setup is shown in Figure 6-5.

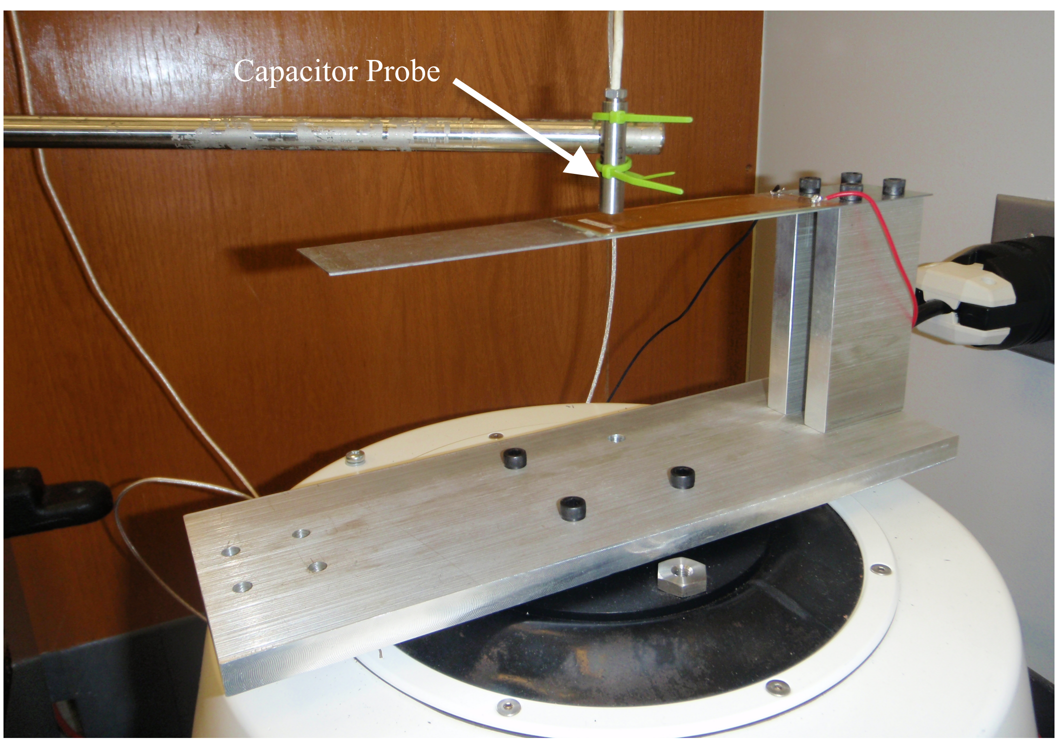

Figure 6-5: Test Setup for Cantilever Beam Attached to Shaker

The scale model cover with MFCs was attached to the shaker table for testing. Both sound data and deflection data were collected during tests. This method of testing allowed for the control code to be applied to the MFCs during steady state perturbation input from the shaker. Also frequency sweep tests were conducted while controls were applied to the scale model with MFCs. The setup used for testing the scale model cover with active control and input perturbations can be seen in Figure 6-6 and Figure 6-7.

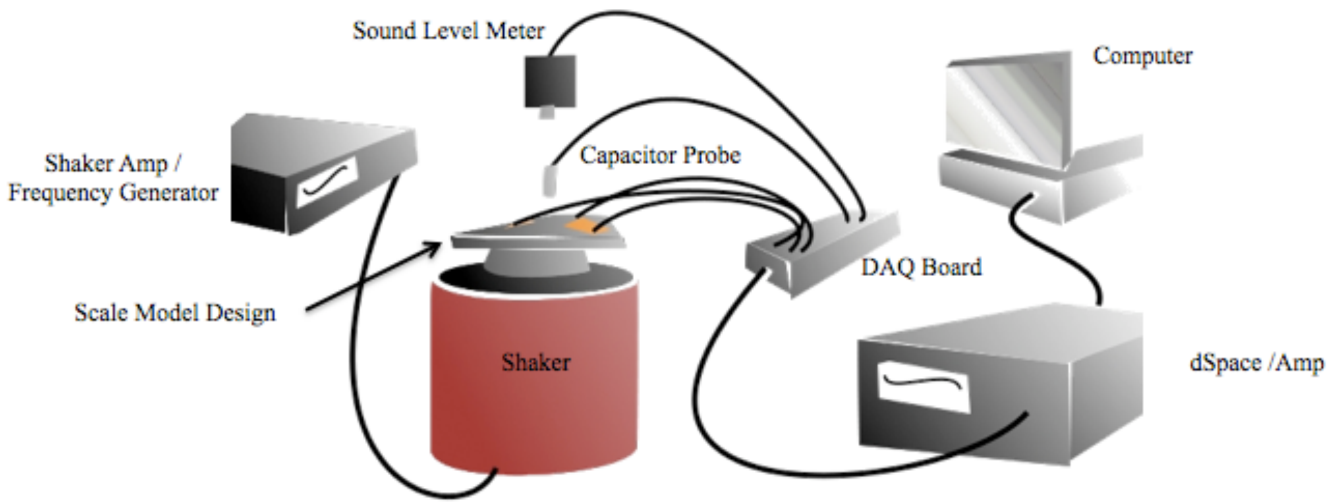

Figure 6-6: Schematic of Combined Testing Systems

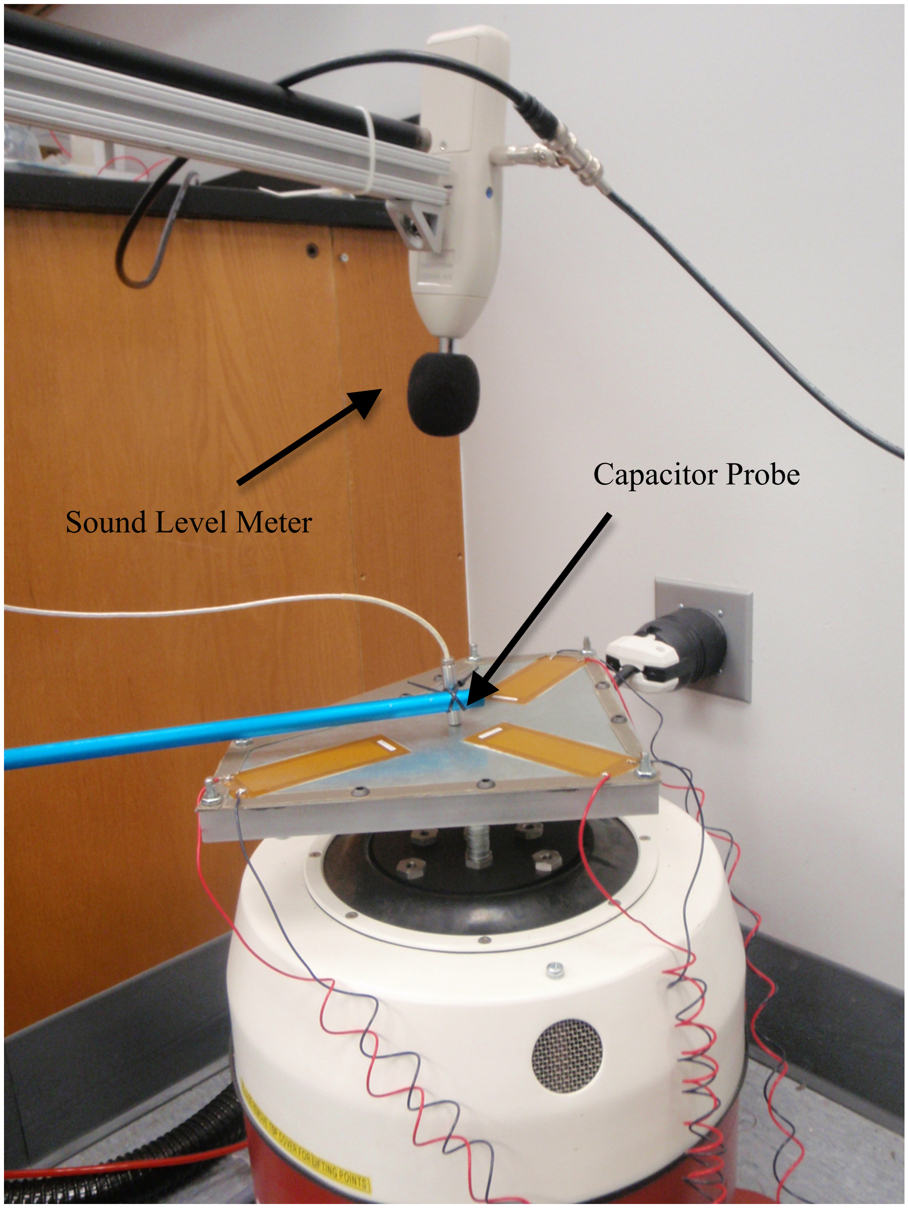

Figure 6-6: Combined Testing with Active Scale Model Cover

7 Data and Results

7.1 Active Material Characterization

To better understand the dynamics of the cantilever beam and the scale model cover, a closer look at the dynamic properties of the systems are required. Values such as the natural frequency are very useful when designing a closed loop control scheme. Also, having data on the locations of resonance peaks allows for comparison to be made about how the system dynamics are changing as various components of the system change.

The basic test conducted to provide this data is utilized in a frequency sweep. The frequency sweeps performed tested the same frequency range specified by the customer. The frequency sweep tests were conducted in two different manner; using the active materials themselves to excite the system or by using the shaker table to excite the system. If the active materials were used to excite the system, a sine wave with constant amplitude was used while the frequency varied. The shaker table also used a sine wave with constant amplitude.

The largest resonant frequency of the cantilever beam was calculated to be 17.01 Hz by analyzing the frequency sweep data. This can be seen in Figure 7-1 along with one other major resonant frequency close to 100 Hz. The frequency range is only 0 to 200 Hz in Figure 7-1 due to the little to no change in deflection after 200 Hz. The test conducted in Figure 7-1 used the MFCs to excite the beam. The same test was also performed on the shaker table and analysis of the data also concluded these same resonant frequencies. However, the second resonant frequency was found to be slightly greater than 100 Hz. The differences in the values are due to the stiffening effect that MFCs have on the beam as the voltage changes. Also, since the shaker equipment and testing equipment used with the active materials are not synched together, slight variations with time may exist.

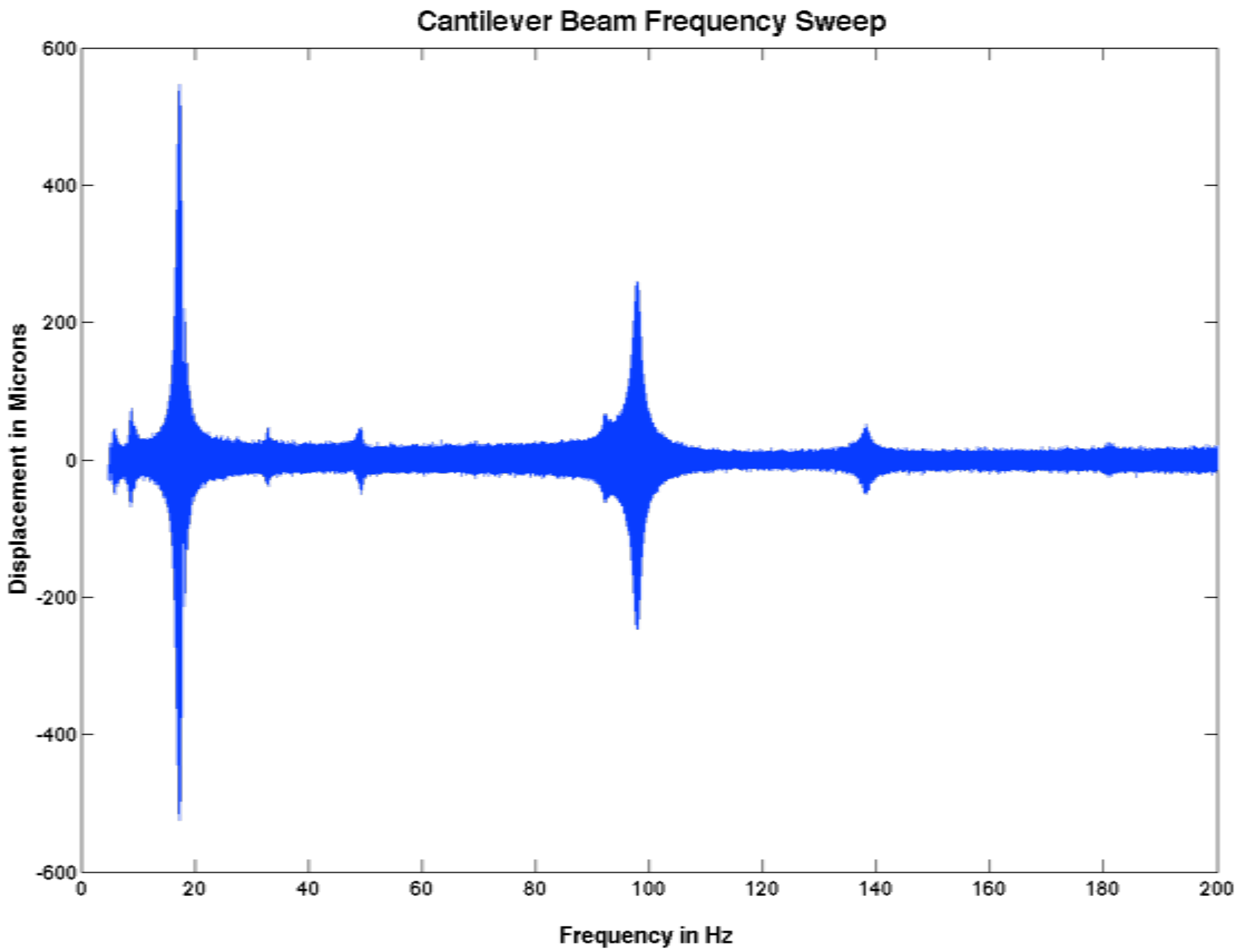

Figure 7-1: Frequency Sweep of the Cantilever Beam

The main resonant frequency calculated for the scale model cover is 210 Hz. The frequency sweep can be seen in Figure 7-2. The sweep tested in Figure 7-2 was conducted using the shaker table. Since the scale model cover is a more complex geometry than the cantilever beam and uses three MFCs versus one, it is assumed that the shaker table provides a more accurate means of performing a frequency sweep for the cover. Also, due to the stiffness of the scale model cover and the force capabilities of the MFCs, the deflection of the scale model cover is much less during the frequency sweeps performed using the active materials for excitation. The upward drift of data seen in Figure 7-2 is due to a drift in the capacitor probe and is evident due to the length of the test; each test was approximately seven to ten minutes in length. A longer test length provides for more accurate and precise data.

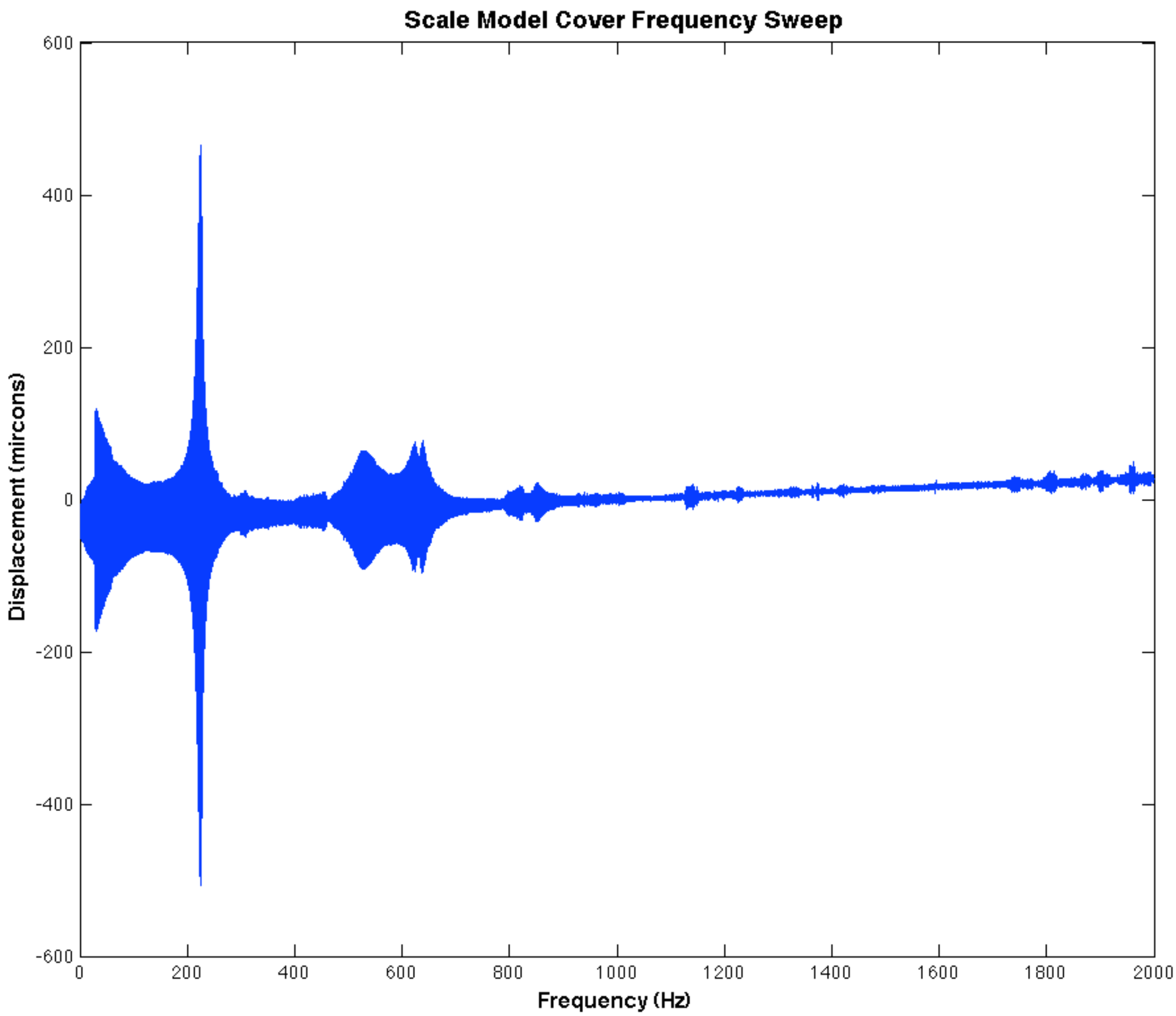

Figure 7-2: Frequency Sweep of the Scale Model Cover

7.2 Control Scheme Adaptation

7.2.1 Open Loop Control

Open loop control code is used for testing when no feedback device is utilized. When performing the frequency sweeps, open loop control code was used. Also, open loop control was the method for testing selected frequencies and direct voltage input. The open loop control code utilized in Simulink can be seen in Figure 7-3. The origin of the control is based on the signal generator used. This can either be a chirp or frequency sweep, constant voltage input, or a sine wave. It is evident that any feedback device is not incorporated into the controls going into the hardware. However, various metering devices can be used during testing for data acquisition.

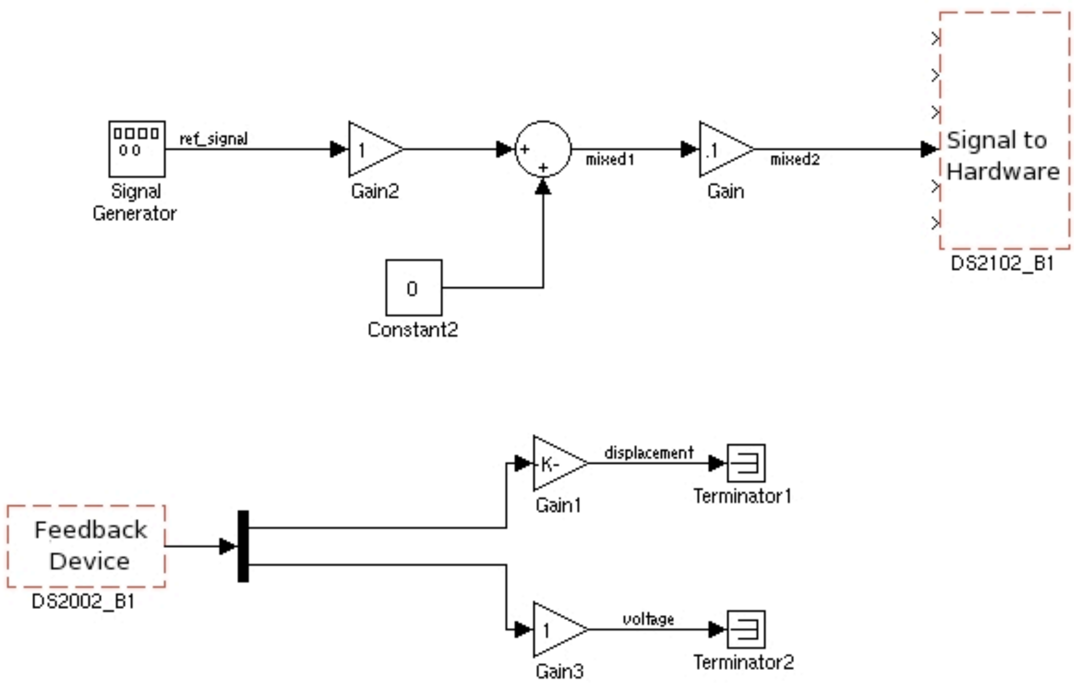

Figure 7-3: Simulink Block Diagram of Open Loop Controls

The open loop control was mainly used for frequency sweeps and material characterization. The open loop control code was also tested on the scale model cover to investigate the effects of constant voltage and shunting on the sound radiated. Using constant voltage and shunt techniques is a passive means to actively control the gear cover and was not the focus of the design. However, it is apparent that applying voltage and short circuiting the MFCs increase the stiffness of the system just as the COMSOL model's predicted. A simple test was conducted using maximum voltage, 1000 volts, versus no voltage open circuit. During the test, controlled perturbations were tested for these two cases. The perturbations were created by dropping a spherical ball of known mass and geometry from a specific height above the cantilever beam. Figure 7-4 displays the displacement data collected. A closer examination of the data also provides the conclusion that with the same small perturbation, there was an average increase in damping of 50 to 65% over an average of ten tests. It is noted that this conclusion requires the assumption that the system behaved like a second order ODE.

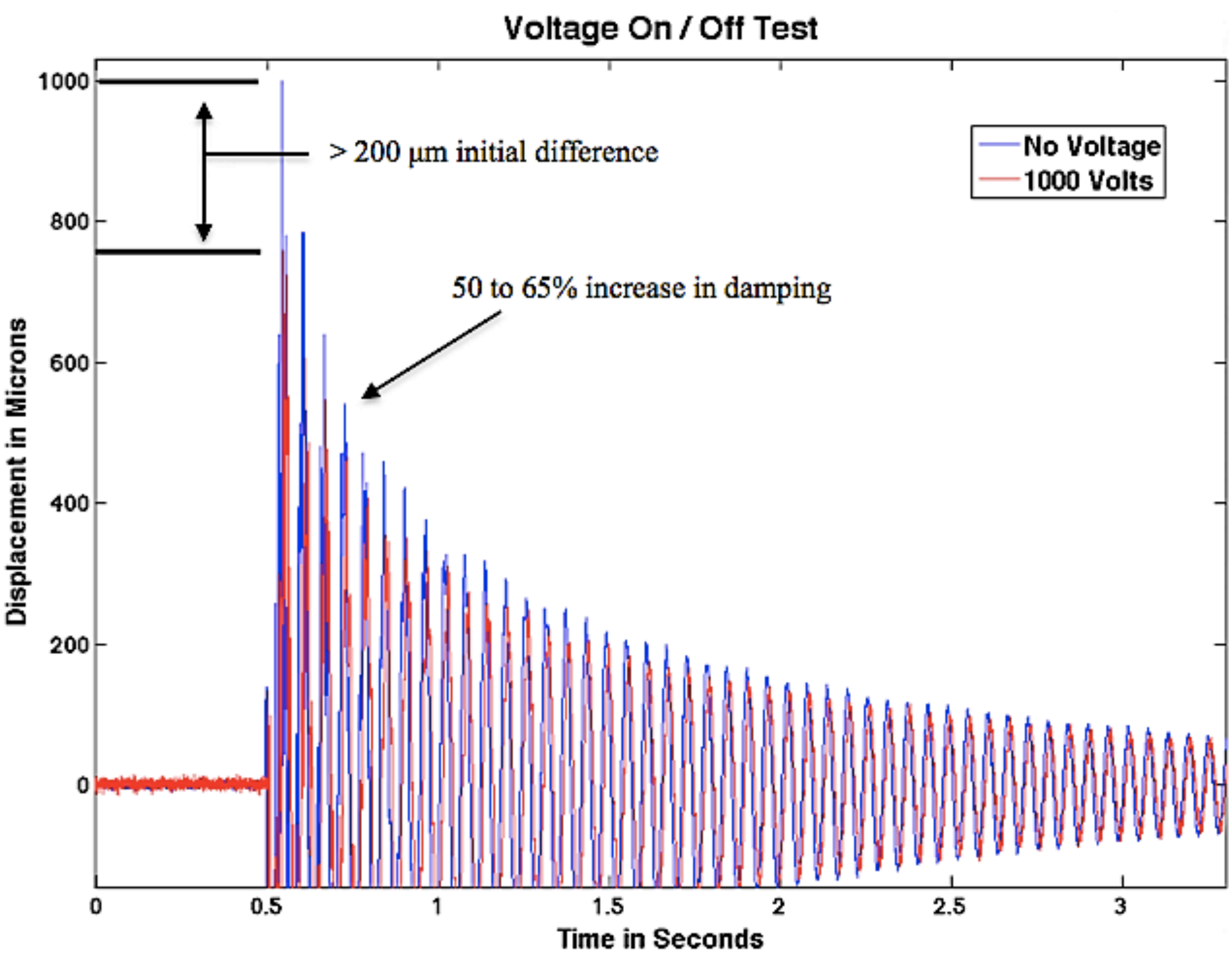

Figure 7-4: Maximum Voltage vs. No Voltage in Open Loop Testing

It is also interesting to mention that the natural frequency observed during these perturbation tests is calculated to be approximately 17 Hz. This natural frequency is seen in a variety of the testing whenever an oscillatory pattern is seen with the canilever beam.

During the characterization portion of testing, no evidence was found to refute the research that suggested to orient the MFCs in the direction of the propagation of vibrations. The scale model cover positioned the MFCs in the direction of the first nodal point, as mentioned previously.

7.2.2 Closed Loop Control

Closed loop control is used for feedback error tracking and error reduction. A feedback device is used inline with the controller. In the closed loop testing conducted, a capacitor probe was implemented. Strain gauges are also a type of feedback device that could be used for the design. Strain gauges are must cheaper and thinner than the MFCs used on the gear cover. However, despite the availability of a strain gauge amplifier and strain gauges chosen specifically for the project, time did not allow for proper testing and implementation of strain gauges for the closed loop control portion of testing.

The first type of closed loop control code used for testing was a Proportional Integral, or PI, controller. The PI controller used can be seen in Figure 7-5 as a Simulink block diagram. The main components of the PI controller were the gains associated with each. These gains are dependent upon the system's dynamic characteristics. Initially, these gains were computationally computed by researching the system's phase and gain bode plots. The K_P gain is determined by computing the phase angle when the phase shifts. The K_I gain is determined by computing the magnitude at the corresponding frequency to when the phase shifts in the phase plot. This magnitude is equal to K_P/K_I and thus K_I can be calculated (Oates, Phillip,…). The Bode diagram for the cantilever beam is shown in Figure 7-6. The natural frequency used in the Bode plot is 104 Hz.

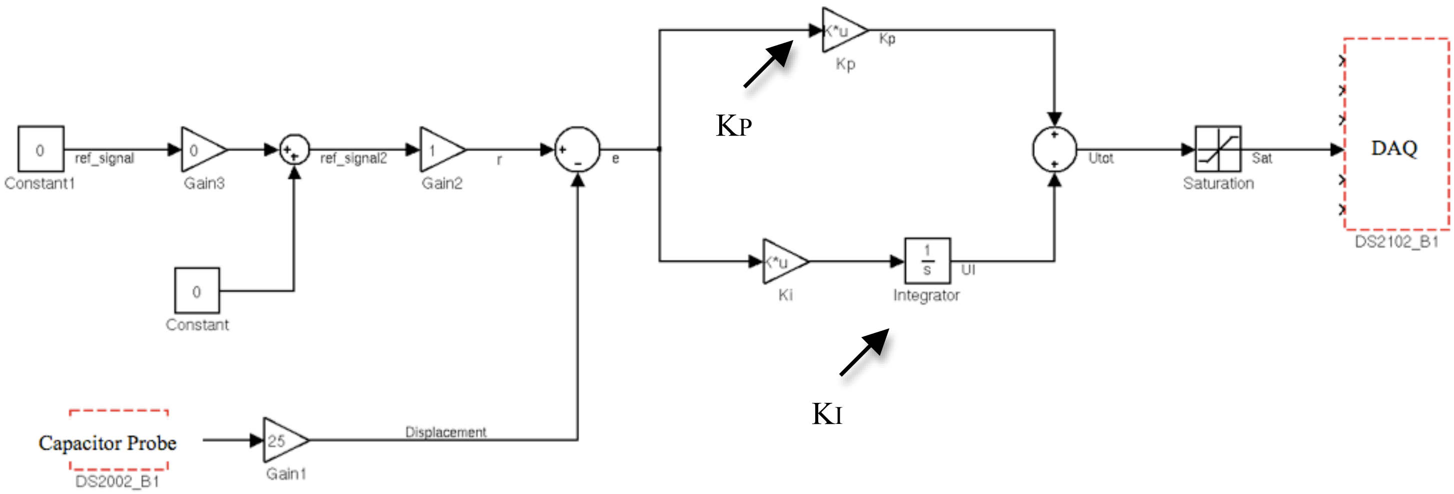

Figure 7-5: Simulink Block Diagram of PI Controller

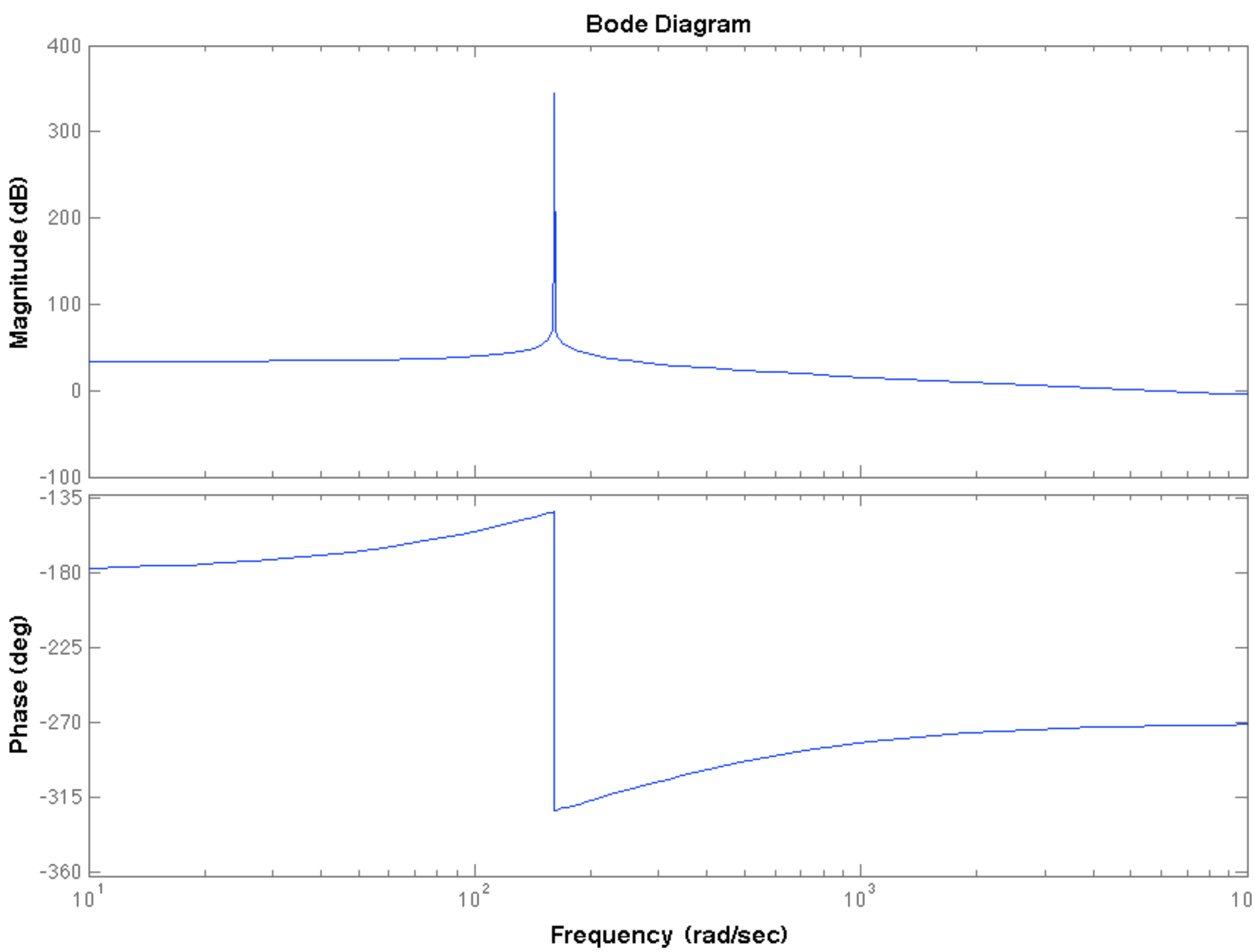

Figure 7-6: Bode Diagram for the Cantilever Beam Model

The PI controller, however useful it has proven itself in other research, did not work well with the active systems used in the design project. The gains were adjusted for various resonant frequencies and later by trial and error; a combination of K_I and K_P could not be found to allow for stable control. The problem that arose while using the PI controller was the presence of steady state error that was amplified in the K_P gain, which caused the system to go unstable. The source of this steady state error was determined to be the active system itself, including the amplifier and hardware. Figure 7-7 shows the very small steady state oscillations that take place when just the amplifier is on with no control. The steady state oscillations were found to occur at the natural frequency of the beam, and it is thus assumed that it is this system error that excited the natural frequency. Whenever the PI controller caused the active system to go unstable, the unstable oscillation of the system also occurred at the natural frequency of 17 Hz.

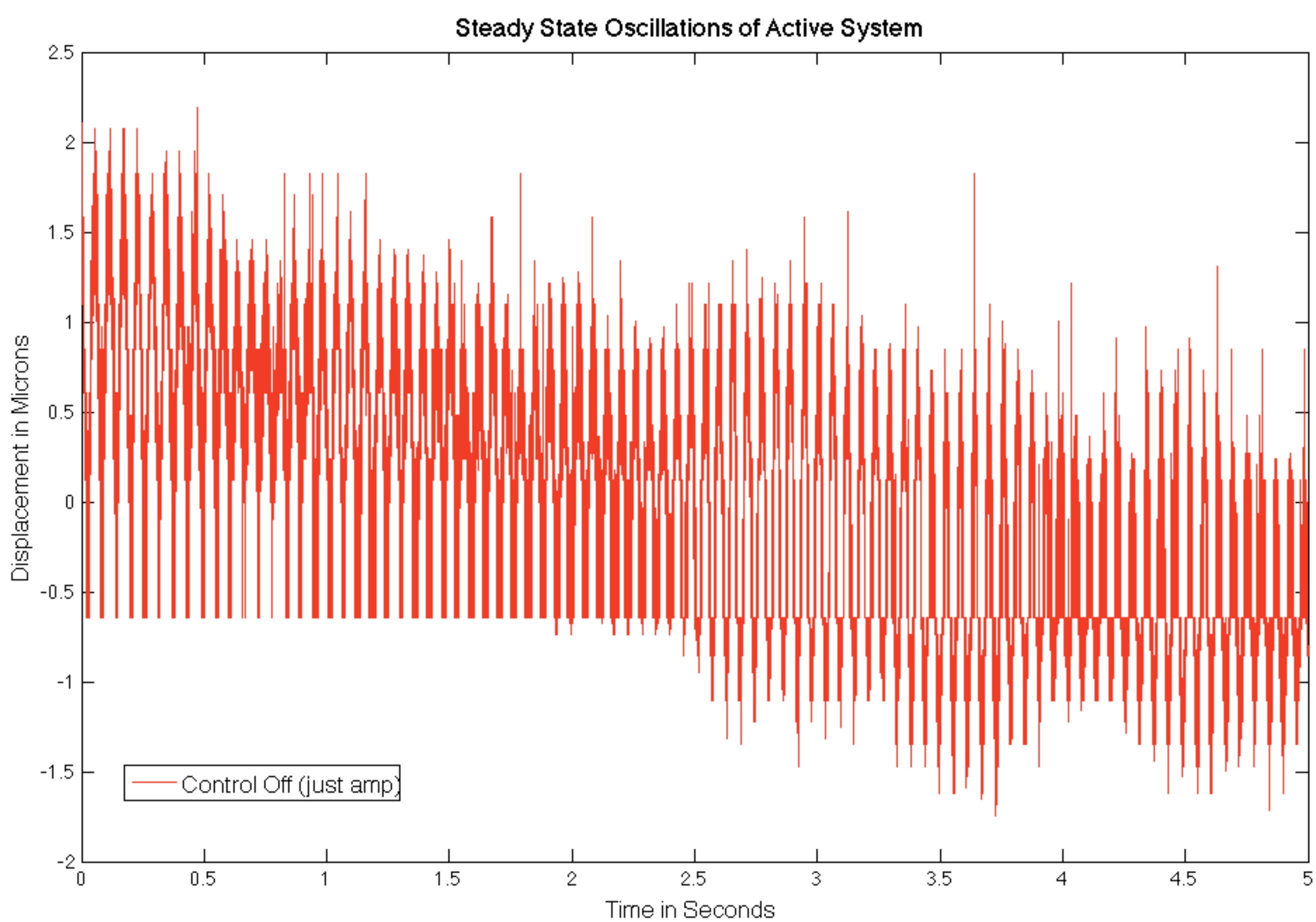

Figure 7-7: Steady State Oscillations Witnessed During Testing

The issue of steady state error was correctable. The answer to this issue was the application of a filter to the controller to add damping to the resonant frequencies observed during the prior tests. A lead lag filter in the form of (s+α)/(s+β) was used to replace the proportional control. The values of "α" and "β" were implemented as 2π and 200π to add damping to the frequency range of 1 Hz to 100Hz. The lead lag controller can be seen in Figure 7-8. The gains associated with the filter and the integral control were adjusted and fine-tuned during testing to maintain the system's stability and quick error correcting response time. It is also noted that a switch event is used in the controller to allow for a period of time prior to each test to adjust the "zero" of the capacitor probe and allow the system to arrive at a stable reference state.

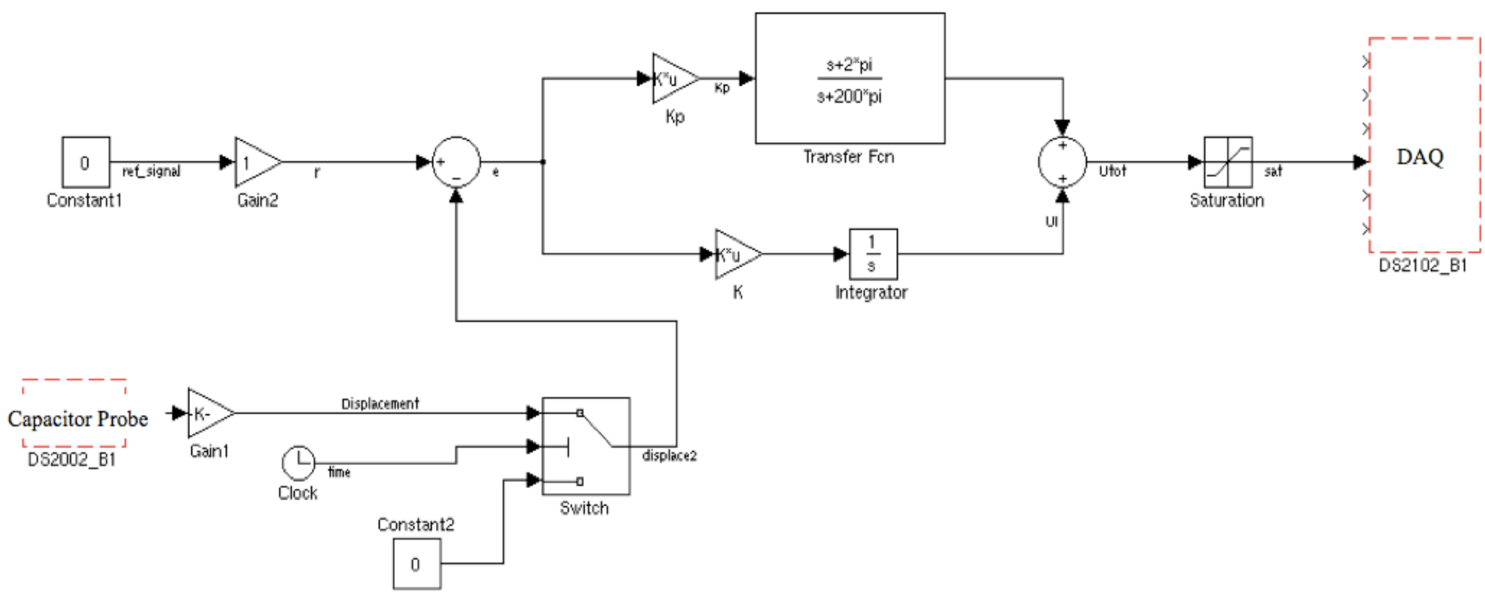

Figure 7-8: Simulink Block Diagram of Lead Lag Controller

When used with the cantilever beam, the lead-lag controller worked very well. The controller was able to reduce the steady state disturbance of the shaker table and reduce the damping time of perturbations by almost 40 times; a 20 second damping time versus half a second with control. Figure 7-9 displays the damping response time of a perturbation with no control. The cantilever beam oscillates at the natural frequency until it returns to a stationary position. Figure 7-10 displays the response time a somewhat larger perturbation, the initial magnitude of the displacement is larger, using the lead lag controller that is tuned for the specific beam. During the half second perturbation time, the system oscillates at the natural frequency of the beam, 17 Hz. When the controller is on and no disturbances are present, the system oscillates at a much higher frequency, greater than 100 Hz. This occurrence is also present in other tests when the control is on with no disturbance input.

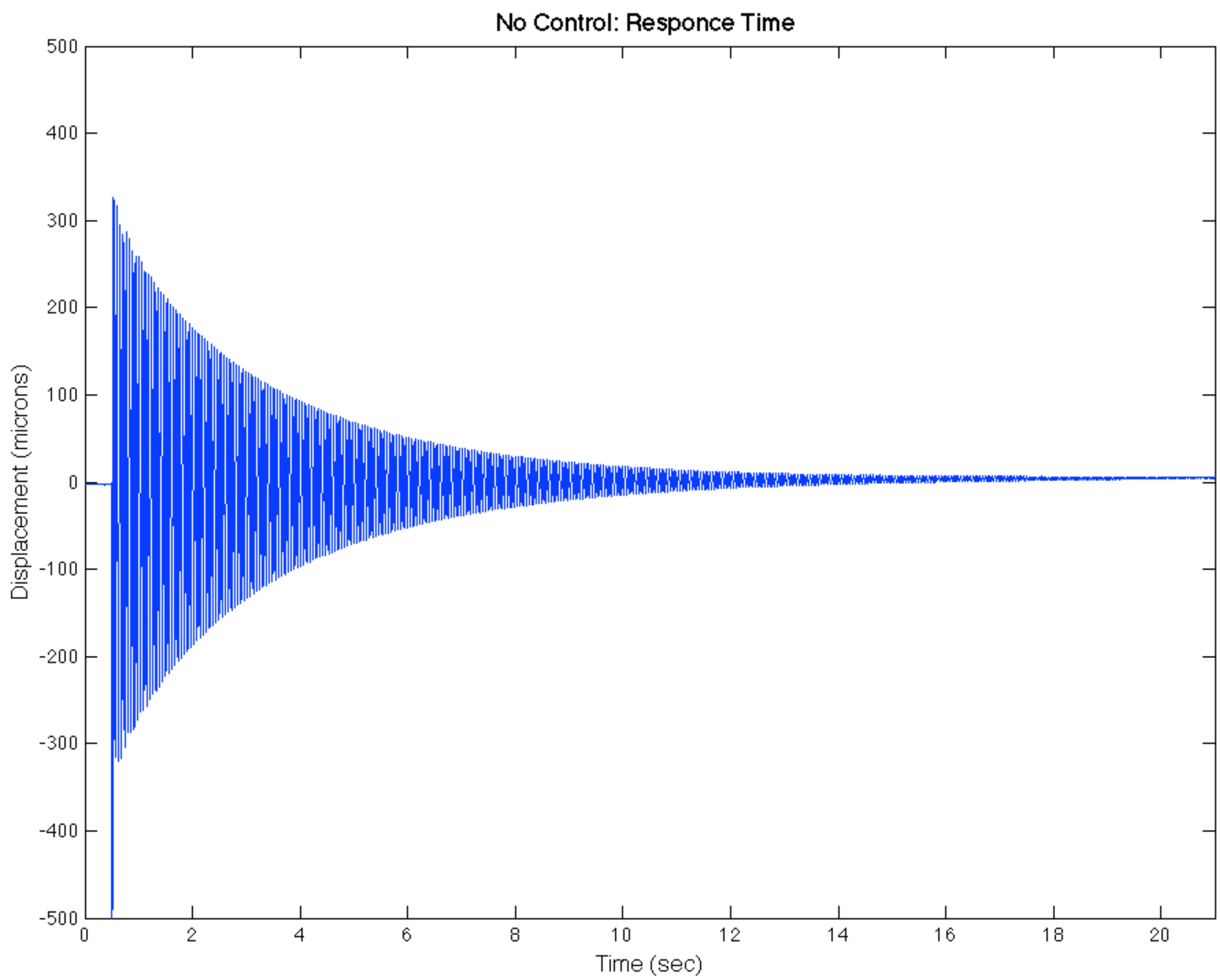

Figure 7-9: The Response of the Cantilever Beam to a Disturbance with No Control

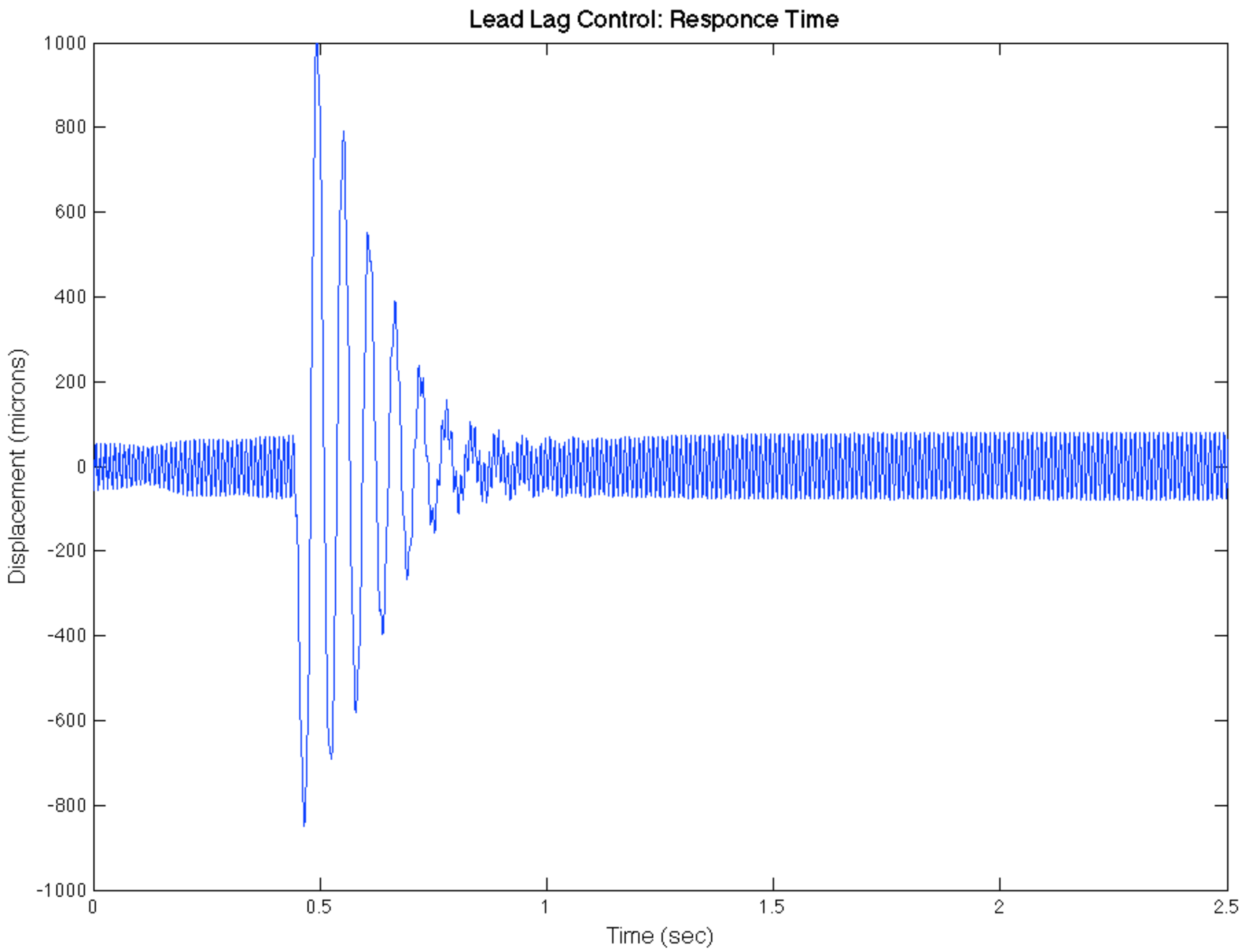

Figure 7-10: The Response of the Cantilever Beam to a Disturbance with Lead Lag Control

The prior experiments with the lead lag controller used single disturbances. The shaker table provides the ability to test the cantilever beam with the controller against constant steady state disturbances of varying magnitudes; this is also a much more accurate and quantifiable means of disturbing the system. Many tests were conducted using various bias voltages ranging from 100 volts to 500 volts and also low and high amplitude settings of the shaker. It was found that the higher the bias was set, the better the reduction of high magnitude disturbances. However, at lower magnitude disturbances, the bias did not need to be set very high to reduce the vibrations of the system. If the bias was set high, around 500 volts, during a lower magnitude disturbance test, the difference between the bias's steady state oscillation and the oscillations due to the steady state disturbance were difficult to distinguish between. With the shaker table set at 0.1g amplitude, comparable to 2.5g amplitude found to be comparable to the real diesel engine, the lead lag controller was able to reduce the magnitude of the vibrations by an order of magnitude. The shaker was set to a constant frequency dwell test with the frequency set to the largest resonant frequency of the beam, 17 Hz. Figure 7-11 displays the controller's effect. It is noted that the steady state oscillation of the controller prior to any disturbance is greater than 300 Hz and during the disturbance is equal to 17 Hz.

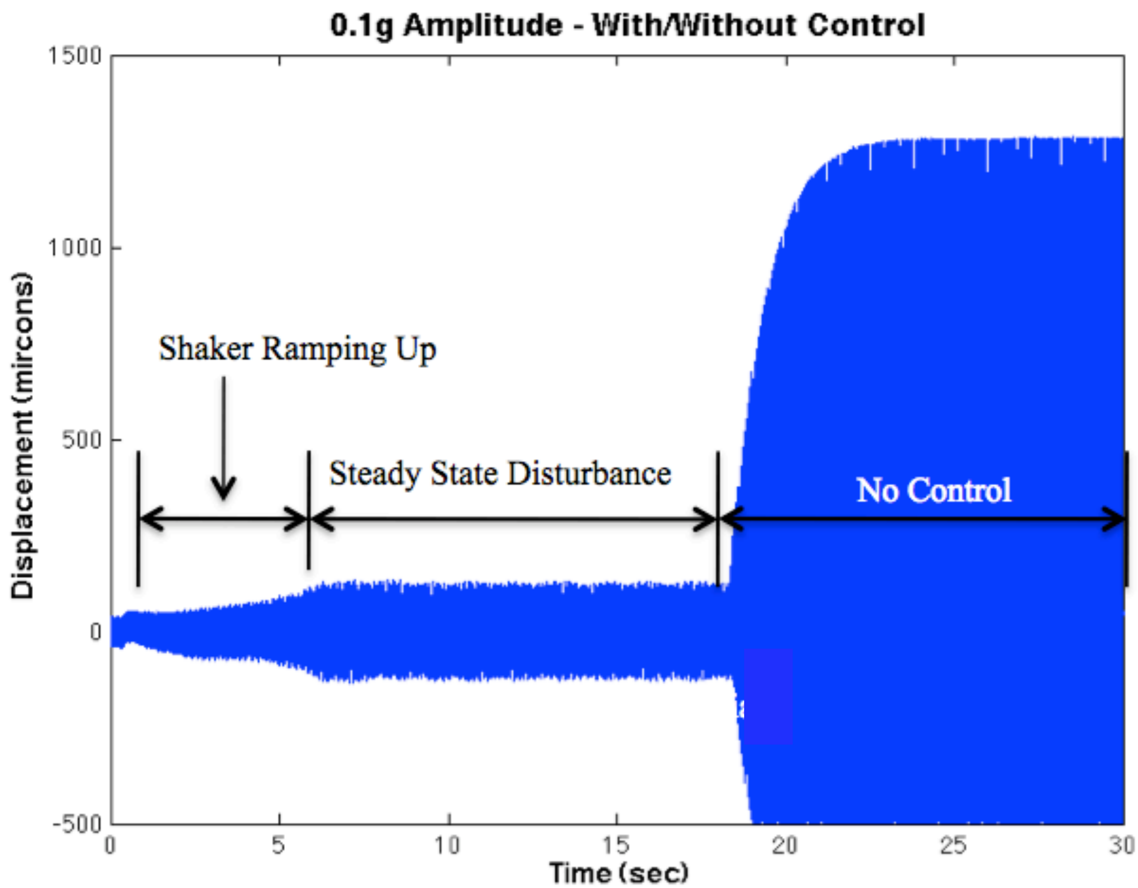

Figure 7-11: Steady State Disturbance at 0.1g With and Without Controller

With the shaker set at 2.5g amplitude, the lead lag controller was able to reduce the steady state disturbance from 1.6 mm peak to peak with the control on versus 35 mm peak to peak without the control. Due to the high magnitude amplitude of the shaker, the bias was set to 500 volts. This test can be seen in Figure 7-12. The 35 mm peak to peak displacement of the beam is not recording in this data due to the 2 mm range of the capacitor probe; the displacement was measured using calipers while the test was running and verified by viewing the frame-by-frame pictures of video captured during the test. It is noted that the steady state oscillation of the controller prior to any disturbance is about 100 Hz and during the disturbance is equal to 17 Hz.

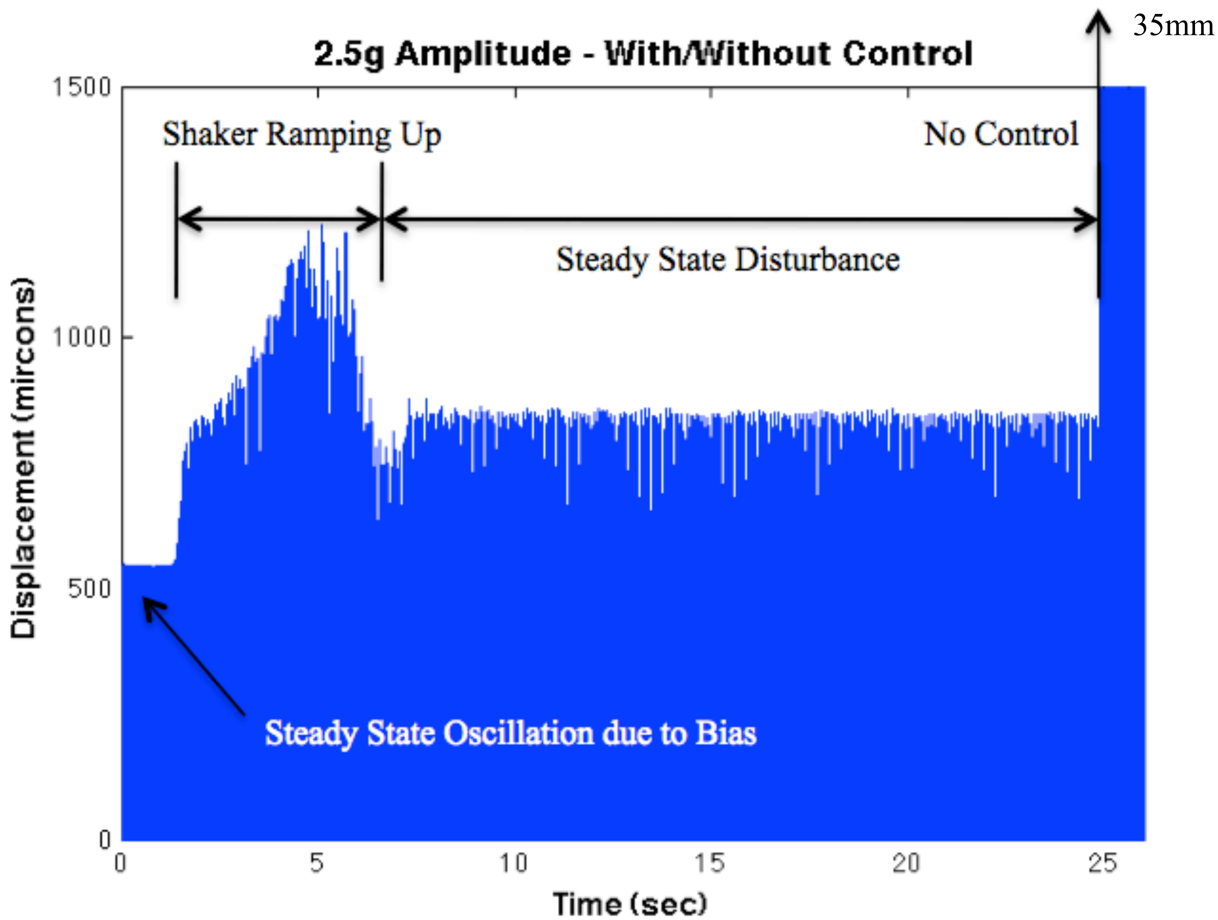

Figure 7-12: Steady State Disturbance at 2.5g With and Without Controller

The results using the cantilever beam proved the ability of the lead lag filter controller to reduce the vibrations of the system. However, when the controller was adjusted and tuned for the scale model gear cover, the controller's effect was not as prominent. The controller was adjusted to the natural and resonant frequencies of the scale model cover and then tuned. To tune the system, the filter's and integral's gains were increased until the system went unstable, and then slightly reduced allowing the controlling to remain in a stable region for testing. During all tests conducted with the cantilever beam and the scale model cover, the controller would drive the system to the zero reference. This did occur with the scale model cover meaning that the lead lag filter controller was influencing the system. Single disturbances were applied to the cover like the cantilever beam. However, the response time with the controller on and off could not be distinguished between due to a damping response time of less than tenth of a second; the scale model cover, when assembled with the gear housing, is a very stiff structure. The effectiveness of the controller on the scale model cover for small single perturbations could not be addressed. The scale model had to be tested with a steady state disturbance to determine if the controller could reduce the input vibrations on the system.

The scale model cover and housing were attached to the shaker table and multiple resonant frequencies were tested with and without the controller. The shaker was set at an amplitude of 2.5g, the corresponding amplitude of the actual diesel engine. The controller was tested and edited using a trial and error approach but could not get a reduction in the vibrations being input into the system. The bias voltage was also varied for each test; even at 500 volts, the controller could not reduce the steady- state disturbances. There were even cases for certain frequencies that the MFC actuators would increase the steady state disturbance. This leads to the conclusion that either the MFCs did not produce enough force to attenuate the vibrations or the lead lag controller was not tuned correctly for the scale model. The latter is the more probable conclusion due to the fact the lead lag controller was very effective with the cantilever beam since it was designed and modeled more using finite element analysis of the beam model.

7.3 Sound Data and Results

Sound data was collected for the addition of each component of the scale model design and also the original single layer and dual layer gear covers provided by Cummins. Most data collected pertained to frequency sweeps in the same range of the data provided by Cummins for comparison. Figure 7-13 is the graph of radiated sound power provided by

Cummins Inc. of the single layer gear cover tested on the actual engine. This was the only source of data provided as a reference. The original single layer gear cover was tested using the shaker equipment and sound level meter to determine if the shaker table would suffice as a similar system to substitute for the physical diesel engine. It is seen in Figure 7-14 that when compared to the reference graph of the original gear cover, the shaker table is able to replicate the effects of a physical engine without any major differences that would hinder later comparisons and effectiveness of the design. The shaker amplitude that provided the closest resemblance to the reference data was at the 2.5g setting. This is the amplitude that all tests were run at to maintain consistency and retain the ability to compare data.

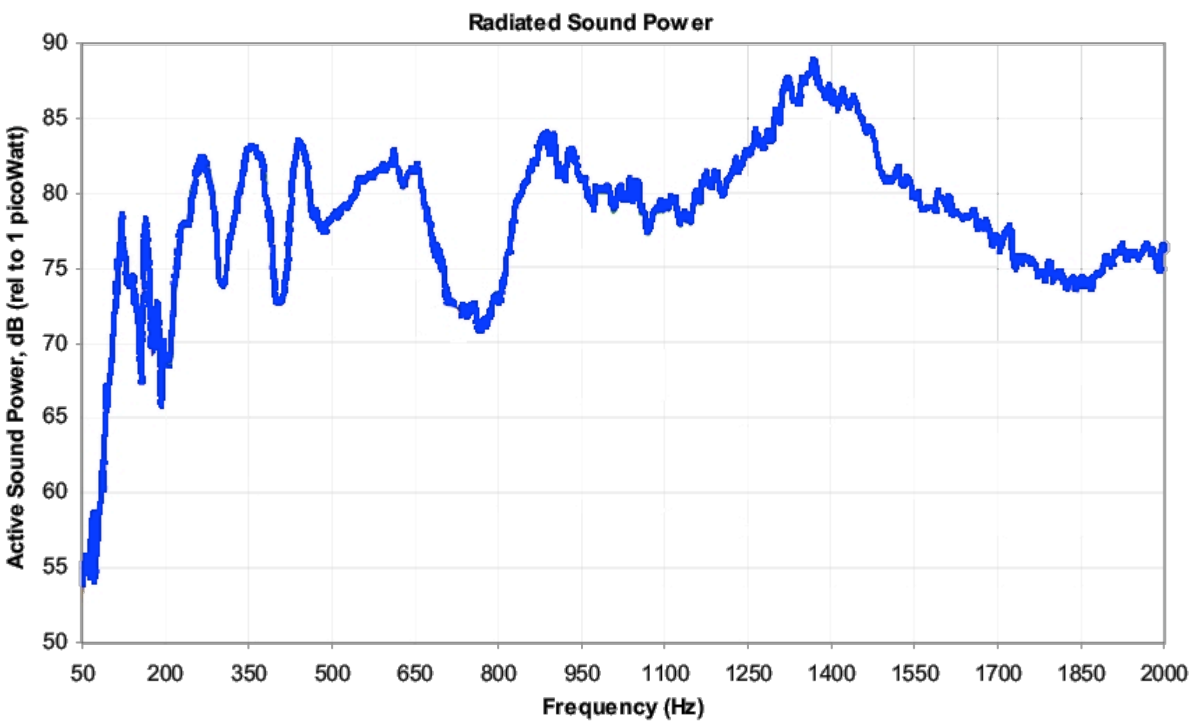

Figure 7-13: Reference Graph of Sound Power for Original Single Layer Gear Cover

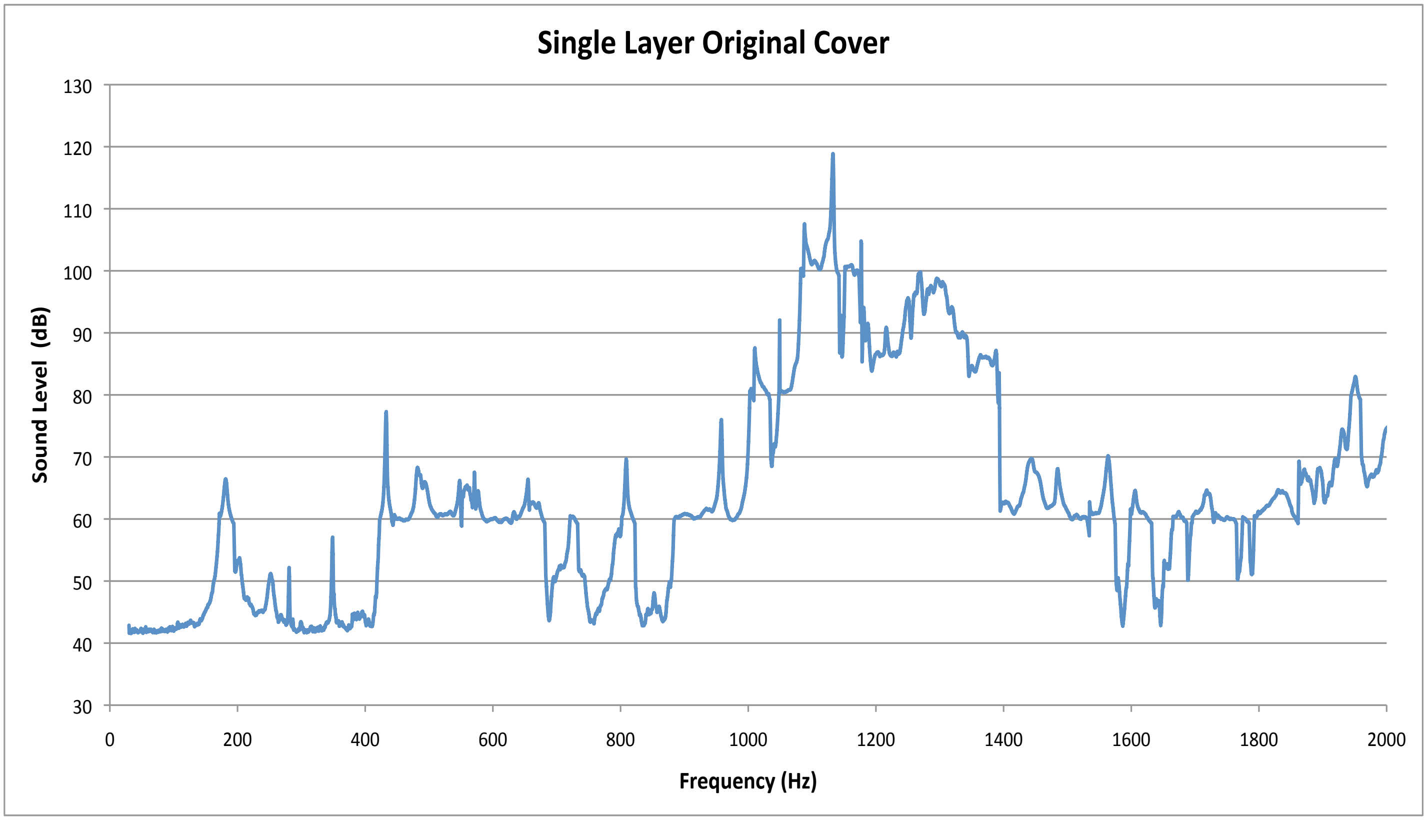

Figure 7-14: Sound Power of Original Single Layer Gear Cover

It is evident from Figure 7-14 that similar increases in decibels over the 1000 Hz to 1400 Hz range and 1800 Hz and above range are present in the data collected and the reference data. Figure 7-14 also demonstrates how the sound data was analyzed and presented for comparison. The difference each component makes is even clearer when charts are overlapped, like in Figure 7-15.

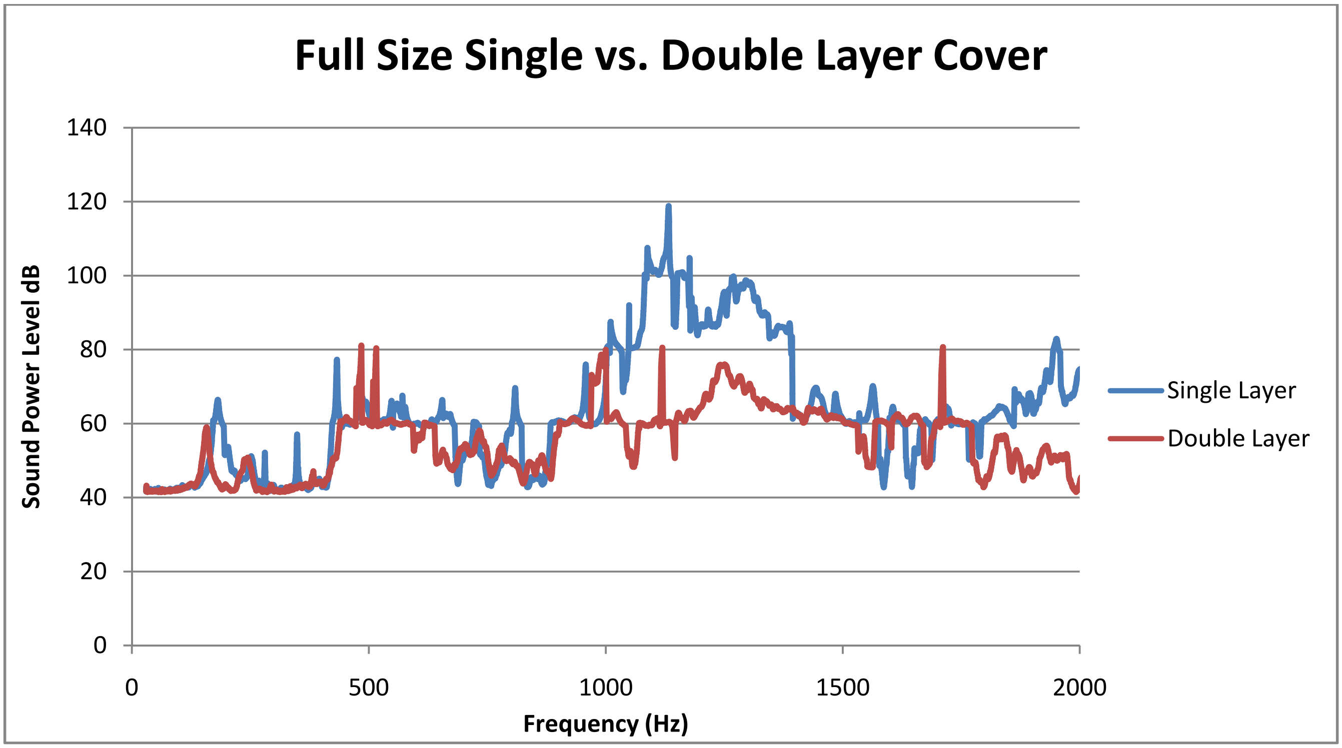

Figure 7-15: Sound Power of Original Single and Dual Layer Gear Covers

The testing data from Figure 7-14 and Figure 7-15 also provides credible evidence that using a multiple layering technique is effective at reducing the emitted noise of the gear cover. This data added to the usefulness of incorporating a sound barrier panel into the design. Each component of the scale model was tested when the scale model cover had no MFCs attached. The specific charts can be seen in Appendix C. Table 7-A summarizes the main effects each component had on the system as they were added.

Table 7-A: Summary of Scale Model (no MFCs)

Layering	Increase/Decrease	Sound Level	Frequency Range
Vibra Block Washer	Decrease	10 dB	1750-2000 Hz
Dual Layer with Vibra Block	Decrease	15 dB	200 Hz
	Decrease	10 dB	1800-200 Hz
Sound Barrier	Decrease	15 dB	500-700 Hz
	Decrease	10 dB	1600-1800 Hz
	Increase	10 dB	1800-2000 Hz
Sound Absorbing Foam	Decrease	15-20 dB	500-1000 Hz

The data from these tests and the summary of Table 7-A allows one to conclude that using the vibra block as a washer and the addition of a sound barrier combined with sound absorbing foam has a large positive effect on emitted noise of the gear cover. Figure 7-16 shows the scale gear cover unaltered versus the scale gear cover with the addition of all the components.

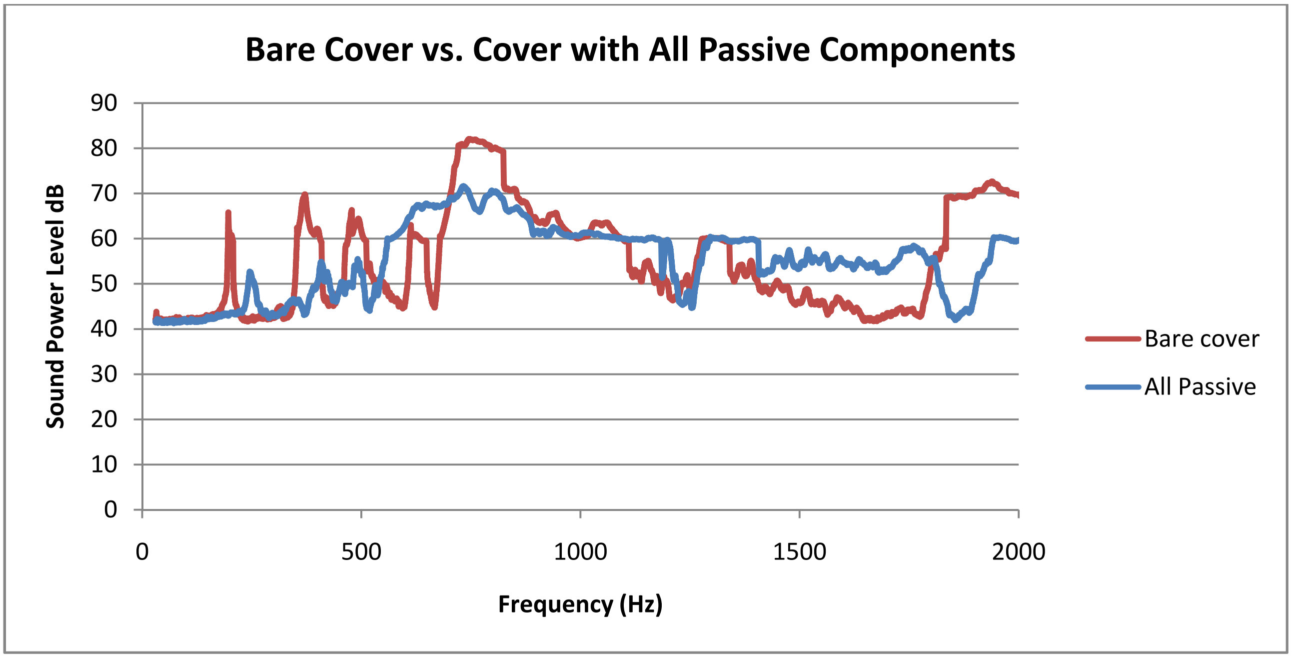

Figure 7-16: Sound Power of Scale Model Gear Cover vs. Scale Model Complete Assembly

In the tests previously mentioned, the sound barrier panel was attached using all 13 hole locations. As mentioned in Section 4, different arrangements of attachment locations were tested. C-clamps were used to attach the barrier panel to the scale model housing. The turning pins used to tighten the c-clamps were removed prior to each test to eliminate the rattling of the pins, which would add to the noise. It was found that attaching the five outer corners is the best means of retaining a quality level of sound attenuation. The specific charts concerning these tests can be seen in Appendix C.

Each component of the scale model was tested again but with a scale model cover with the MFCs attached. More tests could be conducted at this time due to the ability to use the lead lag filter control, shunt circuit method, or constant voltage on the MFC actuators.

The specific charts can be seen in Appendix C. Table 7-B summarizes the main effects each component had on the system as they were added.

Table 7-B: Summary of Scale Model (with MFCs)

Layering	**Increase/Decrease**	**Sound Level**	**Frequency Range**
MFCs (no voltage)	Decrease	20 dB	700-800 Hz
	Decrease	10-20 dB	1800-2000 Hz
	Decrease	Constant 5 dB	After 700 Hz
Control vs. No Control	Decrease	5 dB	@ 1150 & 1400
Sound Barrier	Decrease	10 dB	@ 300, 450, 750
	Decrease	10 dB	1250-1400 Hz
	Decrease	5 dB	1700-2000 Hz
Sound Absorbing Foam	Decrease	5 dB	Main Drop @ 500
	Decrease	5 dB	1400-2000 Hz

The data from these tests and the summary of Table 7-B allows one to conclude that just by adding the MFCs to the gear cover reduces the sound emitted from the gear cover. This is due to the increase in stiffness of the cover, just like the addition of ribs to the original single layer gear cover. Also, it is evident that the lead lag controller did not have any major effect on the system and only reduced two resonance peaks by approximately five decibels. As proven with previous testing, the addition of the sound barrier panel and sound absorbing foam reduces the noise emitted, especially in the higher frequency ranges. The barrier panel by itself did not produce a large decrease in decibels but it was effect at reducing the sharp resonance peaks. The foam, like the barrier panel, by itself did not produce a large decrease in decibels but it did have an overall downward shift in the frequency range that was very evident to the human ear during testing. Figure 7-17 shows the scale gear cover with MFCs versus the scale gear cover with the addition of all the components and maximum voltage applied to the MFCs. It is interesting to note that comparing the data collected of the improvement to noise reduction that Cummins was able to achieve, the original single layer gear cover versus the addition of two layers, to the scale model designed, the scale model was able to decrease the noise emitted over a larger frequency range. The main difference seen in sound power between the single and dual layer gear covers is a decrease over the 1100 Hz to 1400 Hz range and the 1800 Hz and above range. The scale model was able to decrease the emitted noise over a lower 700 to 850 Hz range as well as the 1250 Hz to 1450 Hz range and 1800 Hz and above range.

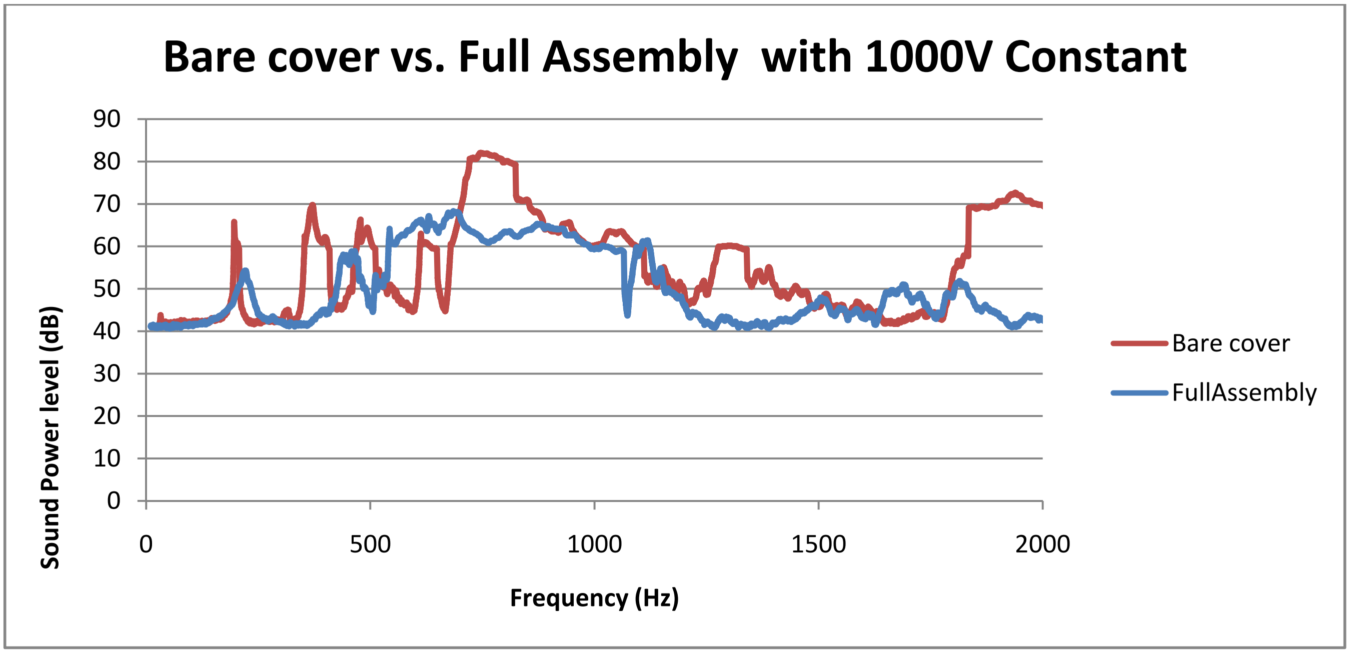

Figure 7-17: Sound Power of Scale Model Gear Cover vs. Scale Model Complete Assembly with MFCs at Maximum Voltage

Overall, the scale model design was a success at reducing the noise emitted from the gear cover but was unable to harness the abilities of the MFC actuators to make a further reduction.

8 Final Cost Analysis

8.1 Budget Analysis

Table 8-A: Budget Analysis

Component	***Quantity***	***Unit Price ($)***	***Total Price ($)***
Fiberglass sheet: 1/32” x 12” x 24”	1	7.43	7.43
85mm x 28mm PZT Macro Fiber	5	116.10	570.50
Vibra Block .040 x 6 x 48 inches	1	37.85	37.85
SSP Foam 1/8" thick by 48" wide	3	5.45	16.35
Delta dB Coating Gel (1 Gallon Bucket)	1	**	0.00
6061 Aluminum: 3/4" Thick x 6" Width x 12" Length	1	37.86	37.86
Steel Sheet Metal: .036" Thick, 24" x 48"	1	34.14	34.14
3M DP460 Epoxy Cartridge	1	14.29	14.29
3M DP460 Epoxy Applicator Gun	1	42.43	42.43
3M DP460 Epoxy Mixing Nozzles (A package of 12)	1	14.09	14.09
1/4-20 by 3/4" length Socket Cap Screw	13	10.46	10.46
M6 by 12mm length Socket Cap Screw	4	7.31	7.31
1/4-20 Threaded Rod	1	2.51	2.51
1/4-20 Hex Nut	10	4.07	4.07
1/4 ID Rubber Washer	10	0.46	4.60
2.5” C-Clamp	9	2.26	20.34
Carbon Fiber Sheet: 1/32” x 12” x 24”	1	62.43	62.43
1-Axis Precision Strain Gauges, 10 mm Grid, 350 ohms	10	7.50	75.00
Strain Gauge Instant Adhesive	1	10.00	10.00
Extech Sound Level Meter 407730	1	95.08	95.08
2.5mm SGA to BNC Adapter	1	2.63	2.63
6061 Aluminum: 1/2" Thick x 12” Width x 12” Length	1	38.01	38.01
Total *			1107.38
Budget			1500.00
Remaining Budget			392.62

* The total amount does not include shipping costs, tax, or miscellaneous items bought personally such as fasteners or tools.

** The Delta dB Coating Gel was acquired as a sample, free of charge by the manufacture.

8.2 Effectiveness and Cost Analysis

One of the main aspects of the design project is to determine how effect each component is at reducing the radiated noise over the frequency range of the engine. When comparing the cost of each component versus the decrease in radiated noise, it is quite evident that using active control of the gear cover is not very effective. However, adding the MFCs did have a large decrease in the noise level, but this is due to the passive stiffening effect the MFCs had on the gear cover. At almost $400 per model, the MFCs are not a cost efficient means of stiffening the gear cover. Adding ribs to the cover is a much more cost effective mean of increasing the stiffness. Using the MFCs at maximum voltage is also a passive means of using the patch actuators and using ribs would have the same effect. Overall, it was most cost efficient to use the sound absorbing foam and the sound barrier addition to the design to reduce the radiated noise. The sound barrier panel was a success at producing a nearly broadband reduction in sound power for little added material cost. The manufacturing and assembly cost of using adding a sound barrier panel to the system was not investigated due to unknown machining costs and time constraints of the project.

One visually appealing method to grasp the overall effects of each component when considering the cost of the component and the amount of noise reduction is using a pie chart to display results. Figure 8-1 consists of two pie charts; one comparing the cost of each component for one scale model and the other is the percentage decrease in decibels for each component. It is noted that the percentage decrease for each component was calculated by estimating the area between corresponding curves of sound data; an example would be the area between the scale model cover with MFC actuators versus the scale model utilizing the sound barrier panel. This area estimation was calculated using Simpson’s rule for numerical integration. Figure 8-2 essentially splits the pie chart for sound decibel drop into two halves; one pie chart is the percentage decrease in decibels for the lower frequencies, 0 to 1000 Hz, and the other pie chart is for the higher frequencies, 1000 Hz to 2000 Hz.

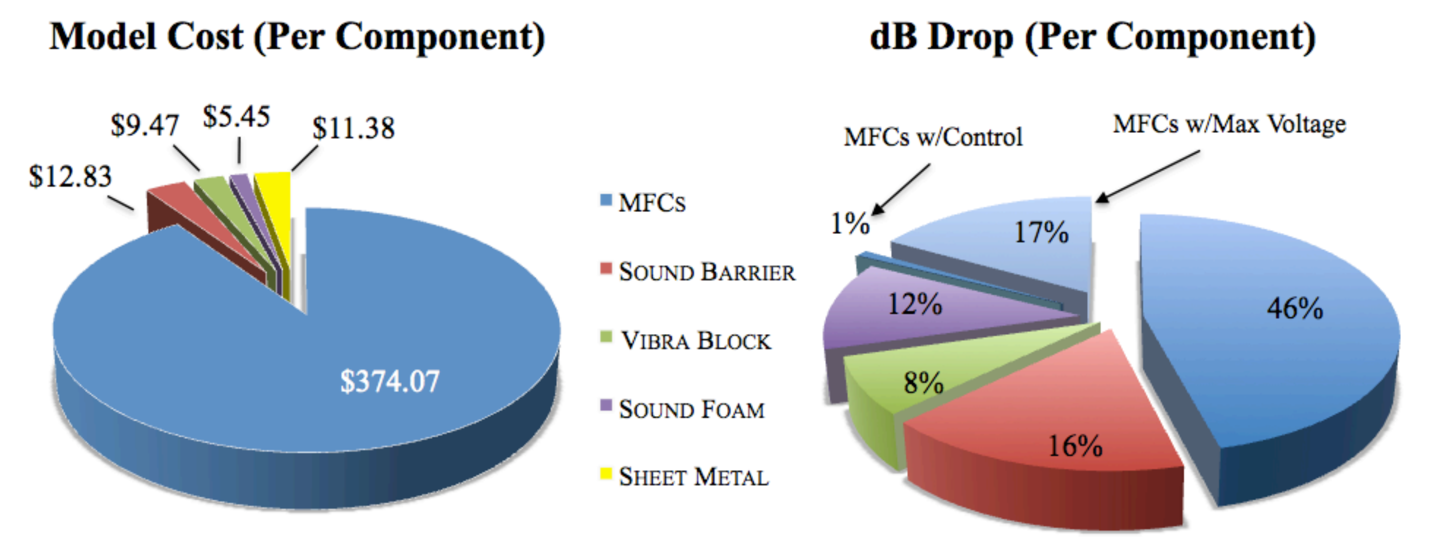

A) B)

Figure 8-1: Pie Charts Displaying A) Model Cost for Each Component for One Scale Model and B) Decibel Drop for Each Component

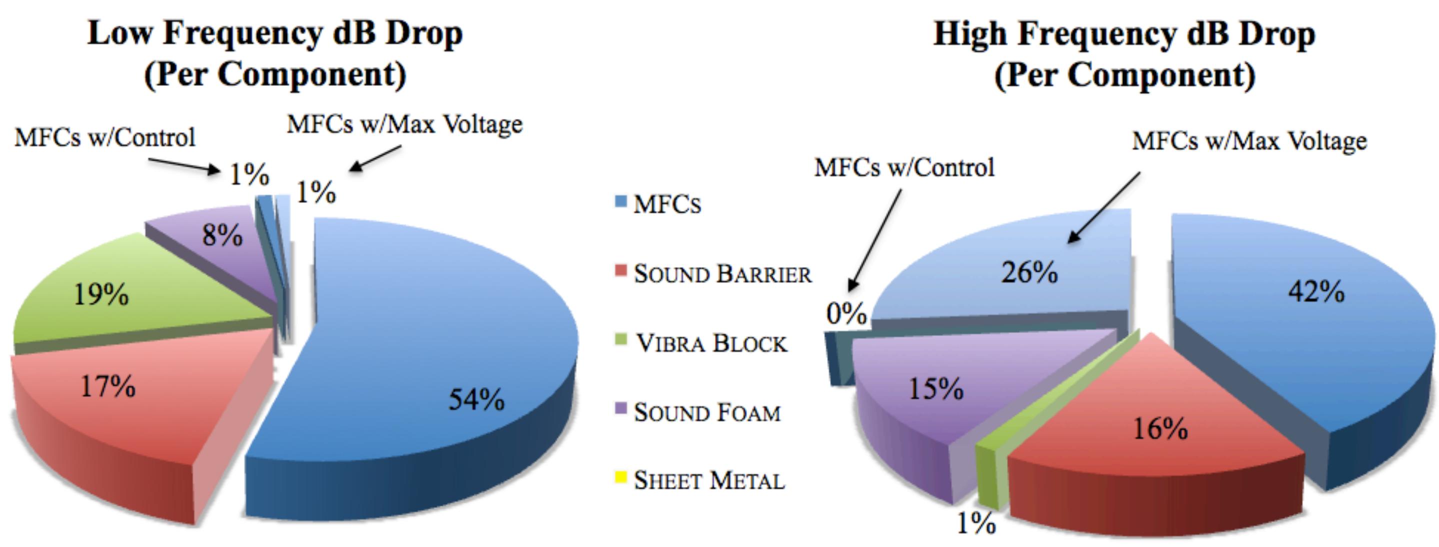

A) B)

Figure 8-2: Pie Charts Displaying A) Decibel Drop for Low Frequencies and B) Decibel Drop for High Frequencies

9 Summary

Cummins is a leading provider in the design and manufacture of a wide range of engines and their related components. The processes that take place within these engines include the rotation of shafts and the firing of individual cylinders that result in overall engine vibrations. These vibrations are transmitted throughout the engine to locations such as engine gear covers, which, due to their size and location, act much like a speaker cone resulting in an increase in total engine noise. Reducing the noise from the gear cover can result in a significant reduction in overall engine noise. Passive and active attenuation techniques can be utilized to achieve this reduction and in combination can optimize the maximum amount of sound reduction. However, active attenuation is a new focus of the research conducted on structure born vibrations and the ability of these active materials in the automotive world is quite unknown.

The active portion of the design project implemented piezoelectric Macro Fiber Composite actuators. This type of actuator proved ideal for this application due to the fact they are flexible, environmentally sealed, and very thin. Computer aided simulations were performed to verify the actuators ability to manipulate the system. In order to determine the location and orientation of these actuators as well as devise a simplified control scheme, it was first necessary to characterize their behavior under the specified conditions. A simplified cantilever beam was used for this characterization. Using the cantilever experiments a control scheme was developed using the specific dynamic characteristics of the beam, which resulted in a proof of concept for the lead lag filter controller. The actuator was able to reduce overall vibrations of the cantilever significantly even in resonance. Small to large perturbations were tested with the cantilever beam and the controller successfully attenuated the disturbances; a 35mm peak-to-peak disturbance was reduced to 1.6mm. It became evident upon application to our scale gear cover that a more complex control scheme would be necessary in the future in order to duplicate the results seen with the cantilever beam. Due to the complexity of the scale model gear cover, the actuators were much less effective, resulting in a less than one percent reduction in sound power level. However, with a similar implementation and an ever progressing control scheme, a higher level of attenuation can be achieved. Regardless of the control scheme, it is likely that this attenuation method may prove to not be cost effective in comparison to other methods.

In combination with the piezoelectric actuators, a sound barrier was also implemented into the design utilizing several passive vibration damping materials. The sound barrier itself was composed of a fiberglass panel cut in a shape identical to that of the scale cover. On the interior of this panel, hybrid sound absorbing foam was used in order to prevent the sound from being reflected off of the interior side of the barrier. In order to prevent system vibrations from reaching the sound barrier, a compliant seal was utilized along the periphery of the cover to prevent surface to surface vibration transmission. Each individual material was tested to determine its damping characteristics and then be combined to optimize sound reduction.

The overall sound reduction utilizing both the active and passive systems resulted in attenuation over nearly the entire range of frequencies; a 0 to 2000 Hz frequency range replicating that of an actual design engine. The passive materials behaved very similarly to the Cummins dual layer cover especially in combination and proved to be a very cost effective method of sound attenuation. It is important to note when considering the active portion of the system that using the current control scheme the Macro Fiber Composite actuators demonstrated better sound attenuation when being used to add stiffness with constant voltage as opposed to using the simplified control scheme devised for the cantilever beam.

If more time were permitted for this project, testing could continue on the scale model cover to determine which characteristics of the MFC actuators and controller needs improvement for better vibration attenuation. During testing, only the 2.5g magnitude for the shaker table was used for testing the active control for the scale model cover. By reducing the magnitude of the shaker, it would have been more evident if the actuators needed more force to improve vibration reduction or if it was in fact the controller that needed better tuning. It is clear that the MFCs were able to reduce vibrations, but it is unclear why the MFC actuators where unable to reduce the vibrations with any major effect on the scale model cover. It is the group's consensus that with more time allotted to this project, the scale model cover with active control would reduce the radiated noise emitted but would still remain quite costly.

10 Acknowledgements

Thanks to the following for their help throughout the progress of the design project:

Richard Varo – Cummins Representative

David Moenssen – Cummins Representative

Dr. Daudi Waryoba – Course Instructor

Dr. Chiang Shih – Course Instructor

Dr. William Oates – Faculty Advisor

Dr. Emmanuel Collins – Mechanical Shaker Lab

Boby Avant – AAPL Machinist

Dr. Clark – Stride Lab

Chris Kulinka – Stride Lab Assistant

Figure 10-1: Cummins Active Noise Control Group

11 References

About Cummins. 12 July 2007. Cummins Inc. 21 Sept. 2008 <http://www.cummins.com/cmi/content.jsp?siteId=1&langId=1033&menuId=1&overviewId=0&menuIndex=none>.

Aoki, Y, P Gardonio, S J Elliot. "Modeling of a peizoceramic patch actuator for velocity feedback control." Smart Material and Structure Vol. 17. 2008.

Composite Products, LLC – Uncompromising Carbon Fiber Performance. 2007. Composite Products, LLC. 29 Nov. 2008 <http://www.composite.com/technology.htm>.

Cunefare, Kenneth A. "Negative capacitance shunts for vibration suppression: wave based tuning and reactive input power." Active 2006 18-20 Sept. 2006.

Goransson, Peter. "Tailored acoustic and vibrational damping in porous solids – Engineering performance in aerospace applications." Aerospace Science and Technology 12 (2008): 26-41.

Damping Products For Reducing Vibrations – Structureborne Noise Problems. 2008. American Micro Industries Inc. 2 Dec. 2008 <http://www.soundprooffoam.com/vibra-block.html>.

EMCO, High Voltage Power Supply Manufacturer. 1996-2008. EMCO High Voltage Corporation. 2 Dec. 2008 <http://emcohighvoltage.com/>.

ETREMA Products, Inc. 2003. ETREMA Products, Inc. 28 Sept. 2008 <http://www.etrema-usa.com/core/galfenol/>.

FrostyTech – Best Heat Sinks & PC Cooling Reviews. 1999-2008. www.frostytech.com. 28 Sept. 2008 <frostytech.com/soundmat1.cfm>.

Green, Edward Ray. “A Examination of “smart” Foams for Active Noise Control.” Purdue University. Dissertation Abstracts International 56 (1995): 4372.

Mascoat Products – Worldwide Leaders in Insulation Coatings. 2008. Mascoat Products. 1 Dec. 2008 <http://www.mascoat.com>.

Melamine Fire Resistant Foam For Soundproofing and Sound Control. 2008. American Micro Industries Inc. 28 Sept. 2008 <http://www.soundprooffoam.com/melamine_foam.html>.

Moheimani, S. O. Reza. “A Survey of Recent Innovations in Vibration Damping and Control Using Shunted Piezoeletric Transducers.” IEEE Transactions on Control Systems Technology 11, No. 4 (July 2008): 482-494.

Oates, William S., Evans, Phillip G., Smith, Ralph C., Dapino, Marcelo J. “Experimental Implementation of a Hybrid Nonlinear Control Design for Magnetostrictive Actuators.”

Peizoelectric actuator. DirectIndustry. 28 Sept. 2008 <http://www.directindustry.com/industrial-manufacturer/piezoelectric-actuator-79919.html>.

PI Ceramic. 2008. PI Ceramic GmbH. 28 Sept. 2008 <http://www.piceramic.de/site/pica.html>.

Smart Material. 2003 through 2008. Smart Material. 28 Nov. 2008 <http://www.smart-material.com>.

Song, G., V. Sethi, H.-H. Li. “Vibration control of civil structures using piezoceramic smart materials: A review.” Engineering Structures 28 (2006): 1513-1524.

TRS Technologies, Inc. 2007. TRS Technologies, Inc. 28 Sept. 2008 <http://www.trstechnologies.com>.

SSP Foam Mat – Super Soundproofing, Co. 2005. Dydacomp. 28 Sept. 2008 <https://shop3.mailordercentral.com/supersoundproofing/prodinfo.asp?number=09-42719>.

Vibration damping materials. X-site Media. 28 Sept. 2008 <http://www.desibelprodukter.no/vibra.damp.htm#Visco>.

Vibration Damping – Self Adhesive Viscoelastic Sheets/Tapes. 2005. Jupiter Infomedia Pvt. Ltd. 28 Sept. 2008 <http://suppliers.jimtrade.com/75/74210/44836.htm>.

Wu, Shu-yau, Travis L. Turner. "Piezoelectric shunt vibration damping of F-15 panel under high acoustic excitation". SPIE Proceedings Vol. 3989. March 2008.

APPENDIX A: Calculations

Cantilevered Beam (One End fixed and the other Free)

Statics equations for beam.

$$w = L$$

$$I = \frac{1}{3} \cdot m \cdot \left(L^2 + w^2\right)$$

$$\theta = \frac{F \cdot L^2}{8 \cdot E \cdot I}$$

$$\theta_{dot} = \frac{d}{dt}\theta$$

$$\theta_{doubleDot} = \frac{d}{dt}\theta_{dot}$$

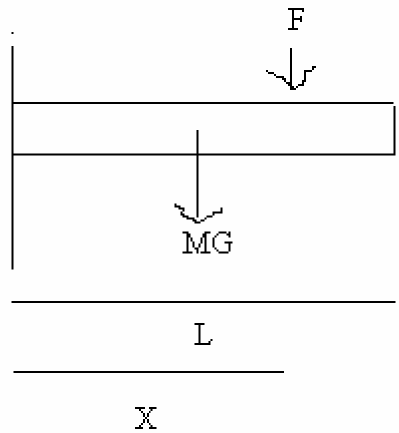

By observing the value of θdot we can determine the frequency of the vibration feedba given a certain input force (F). If it's a high value of θdot, we can call that a high freque vibration. And if we have a low value for theta dot that would be considered a low frequency vibration. We can get a rough idea of the feedback we will get and the behav can be a little more predictable given the use of these equations

Approach Using Dynamic Equations

$$\alpha = -\theta_{doubleDot}$$

$$\Sigma M = I \cdot \alpha$$

$$F_r = m \cdot g + F$$

$$-F_r\left(\frac{L}{2}\right) - F(L - x) = -I \cdot \alpha$$

$$\theta_{doubleDot} = \frac{(-m \cdot g - F) \cdot \left(\frac{L}{2}\right) - F(L - x)}{I}$$

$$\theta_{dot} = \int \theta_{doubleDot}\, d\theta = \int \frac{(-m \cdot g - F) \cdot \left(\frac{L}{2}\right) - F(L - x)}{I}\, d\theta$$

APPENDIX A: Calculations Cont.

Two Fixed Ends Beam

Statics Equations for Two Fixed Ends Beam.

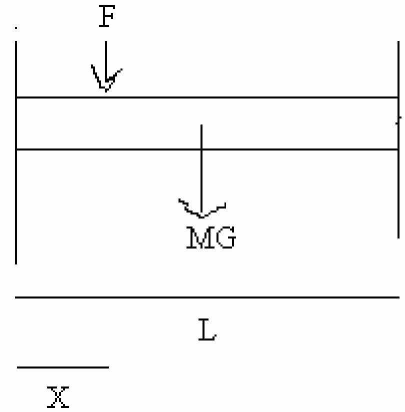

$$\theta = \frac{F \cdot L^2}{16 \cdot E \cdot I}$$

$$\theta_{dot} = \frac{d}{dt}\theta$$

$$\theta_{doubleDot} = \frac{d}{dt}\theta_{dot}$$

Approach Using Dynamic Equations of Motion

$$\Sigma M = I \cdot \alpha$$

$$F_{RLeft} + F_{RRight} - (m \cdot g) - F = 0$$

$$F_{RLeft} = F_{RRight}$$

$$F_{RRight} = \frac{m \cdot g + F}{2}$$

$$F_{RRight} \cdot L - \left(m \cdot g \cdot \frac{L}{2}\right) - F \cdot x = -I \cdot \theta_{doubleDot}$$

$$\theta_{doubleDot} = \frac{F_{RRight} \cdot L - m \cdot g \cdot \frac{L}{2} - F \cdot x}{-I}$$

$$\theta_{dot} = \int \theta_{doubleDot}\, d\theta = \int \frac{(-m \cdot g) \cdot \left(\frac{L}{2}\right) - F(x) + F_{RRight}}{-I}\, d\theta$$

APPENDIX A: COMSOL Equations

From Section 3.4.2:

$\sigma := E \cdot \varepsilon$

$\sigma = E \cdot \varepsilon - e_p \cdot E_v$

$\varepsilon = du / dx + d_p \cdot E_v$

$\sigma_x = C_{11} \cdot \varepsilon_x + C_{12} \cdot \varepsilon_y - e_{31} \cdot E_y$

$\sigma_y = C_{12} \cdot \varepsilon_x + C_{22} \cdot \varepsilon_y - e_{33} \cdot E_y$

$\sigma_{xy} = G \cdot \varepsilon_{xy} - G \cdot e_{16} \cdot E_x$

$\varepsilon_x = \sigma_x / E_1 - \upsilon_{12} \cdot \sigma_y / E_1 + d_{31} \cdot E_y$

$\varepsilon_y = \sigma_y / E_2 - \upsilon_{21} \cdot \sigma_y / E_2 + d_{33} \cdot E_y$

$\varepsilon_{xy} = \sigma_{xy} / G + d_{16} \cdot E_x$

APPENDIX B: Graphs

Scale Modal Nodal Analysis Computed in COMSOL:

The finite element data of the actual gear cover was provided by Cummins Incorporated. Both modal analysis of gear cover and scale model design are provided for comparison of nodal locations and relative deformation strength. As one can see, there are slight differences in exact nodal locations. However, once conclusions from the cantilever beam characterization next semester have been completed, this data can be used to make a concise approximation of where to orient the piezoceramic patches in relation to the nodal locations.

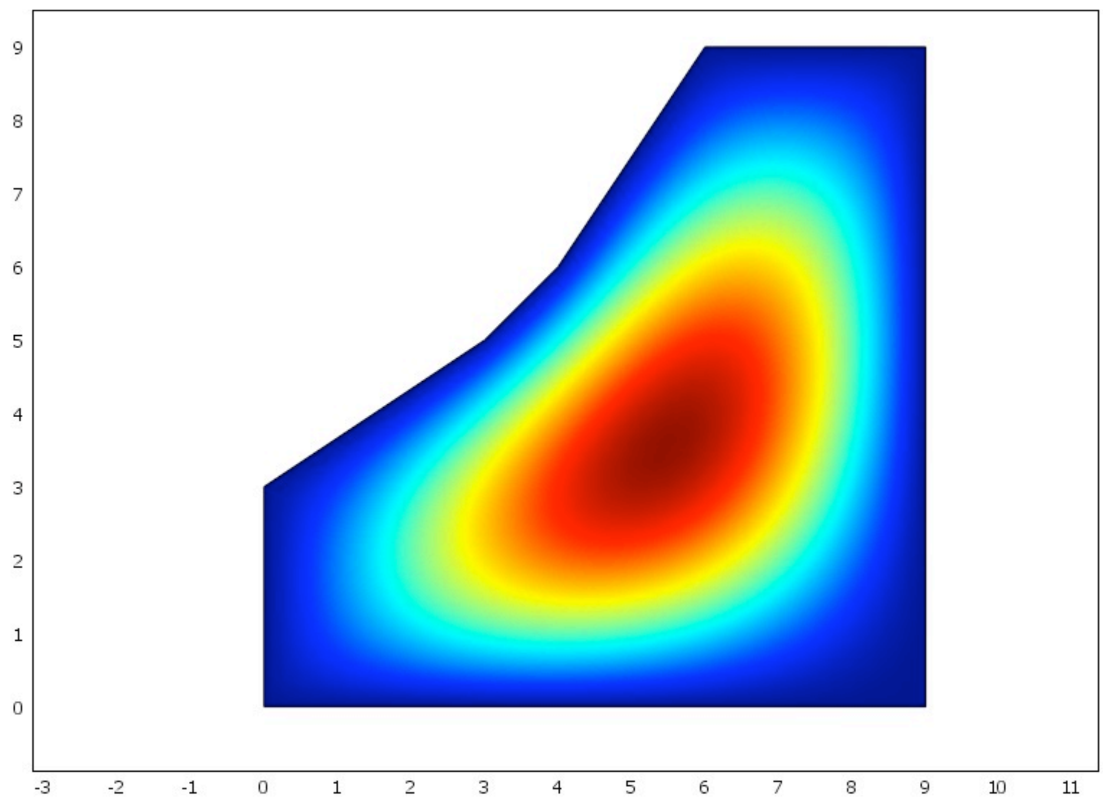

Figure B1: First Mode

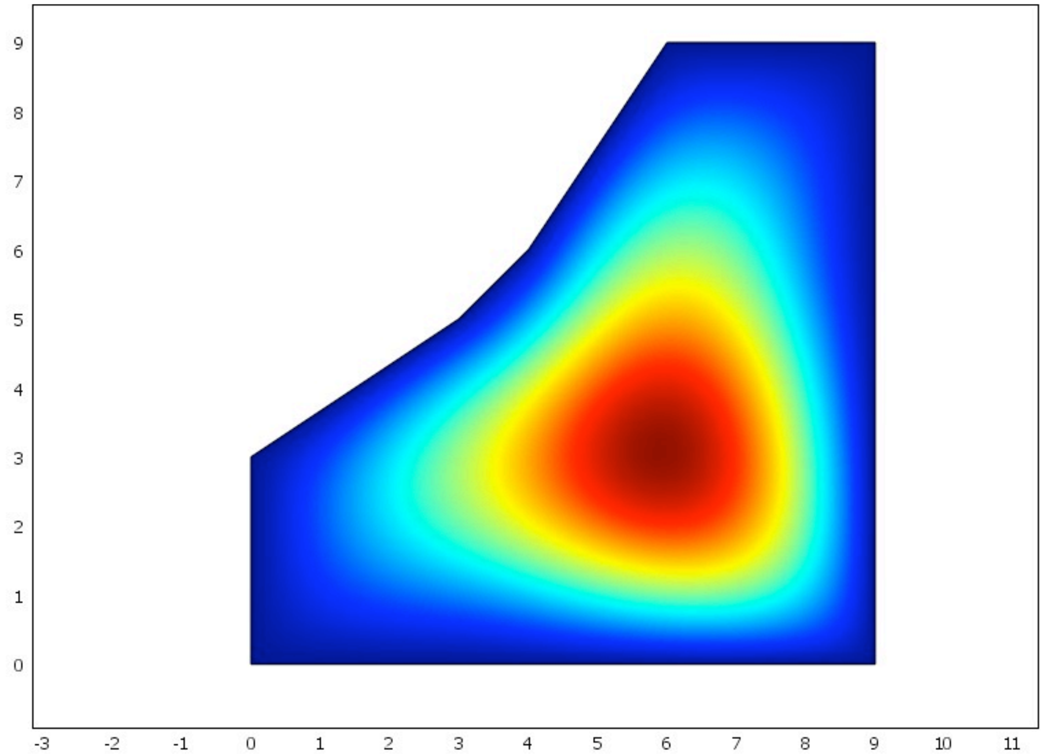

Figure B2: Second Mode

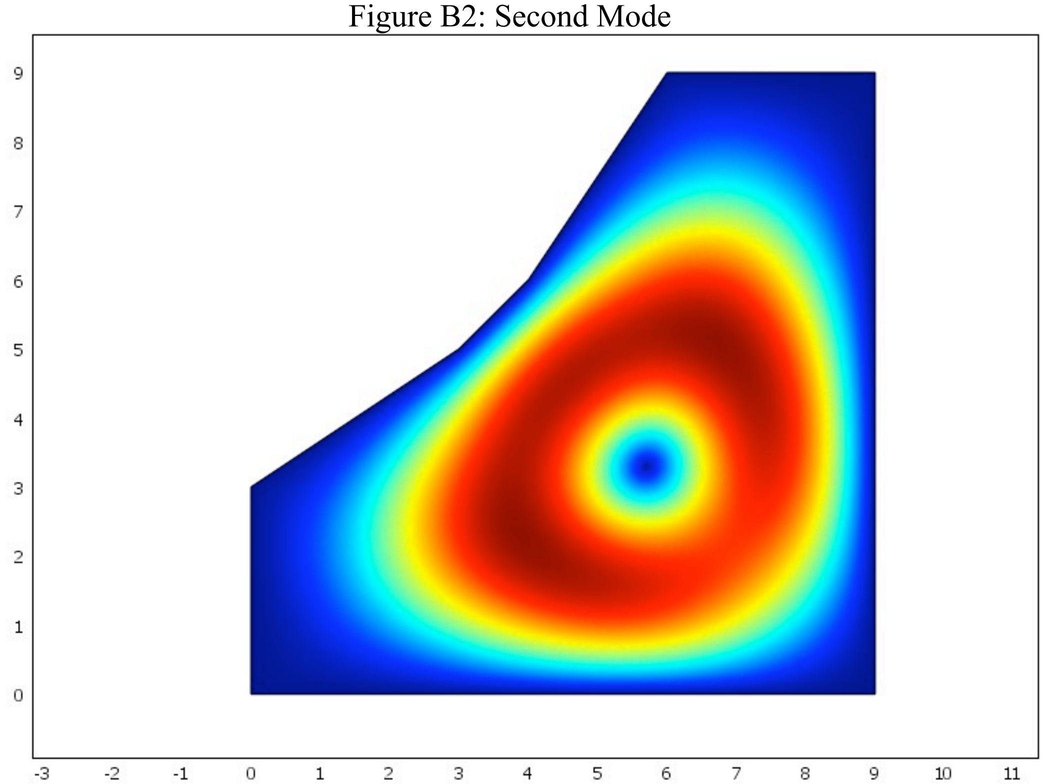

Figure B3: Third Mode

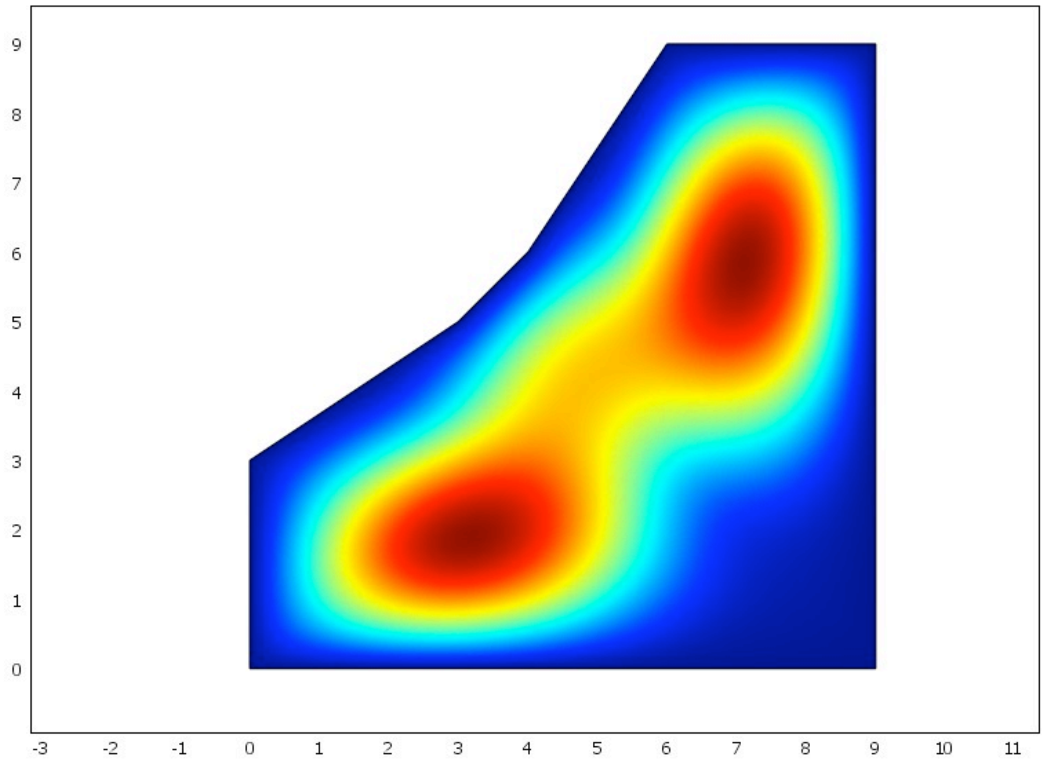

Figure B4: Fourth Mode

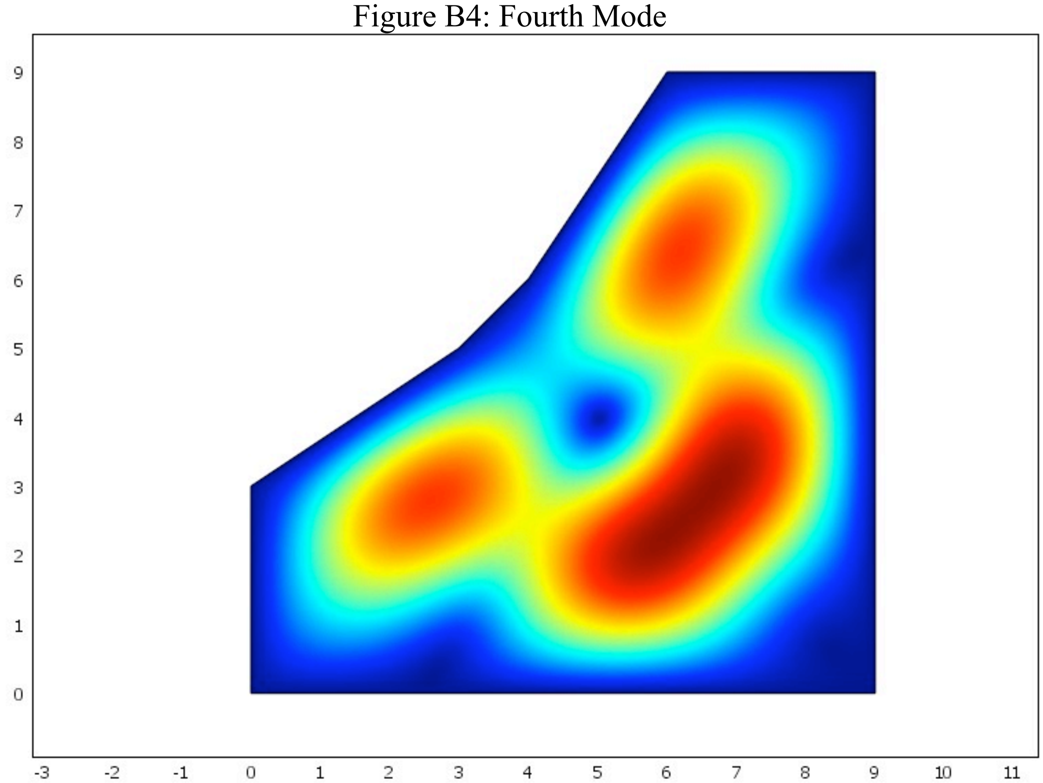

Figure B5: Fifth Mode

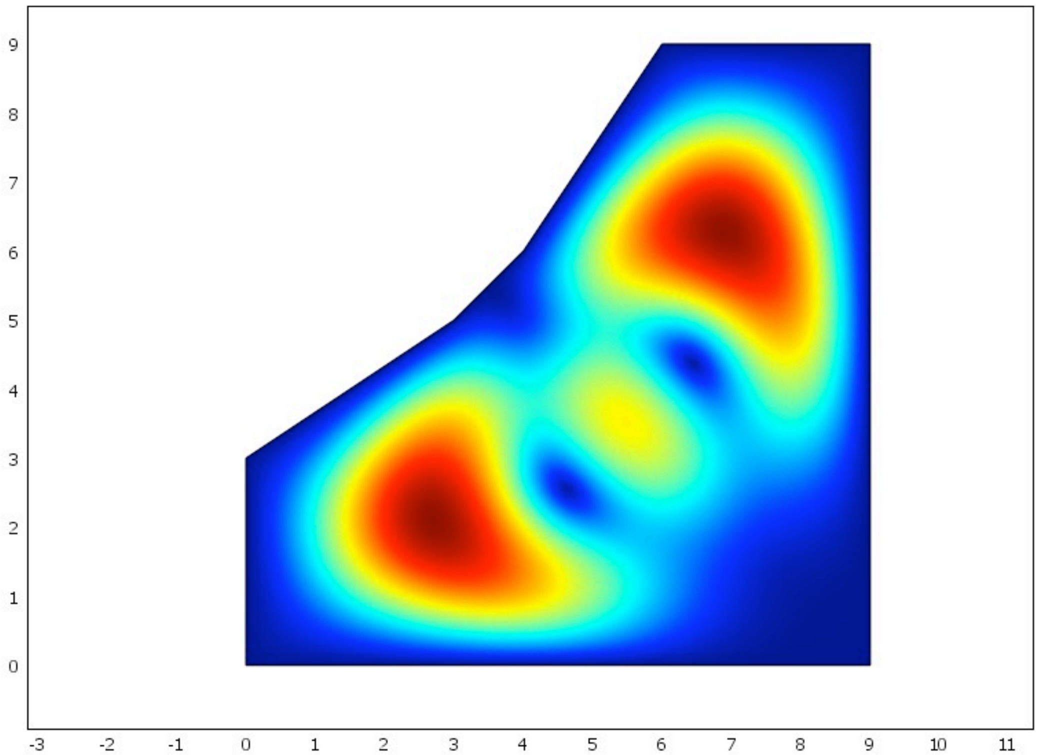

Figure B6: Sixth Mode

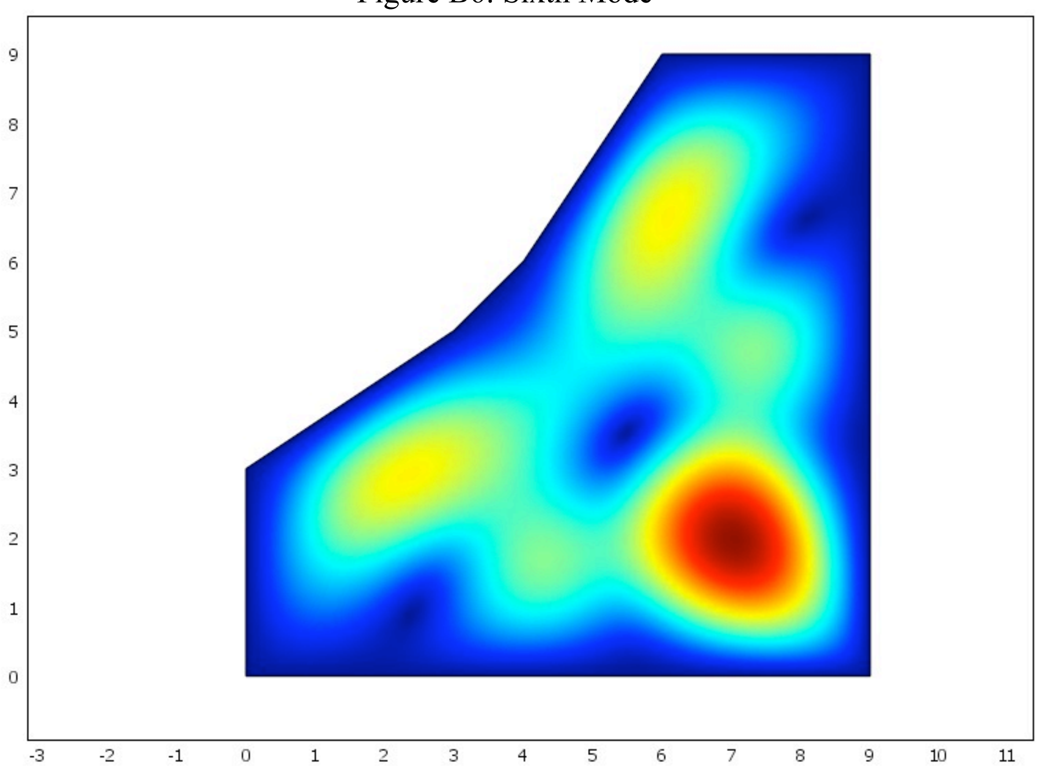

Figure B7: Seventh Mode

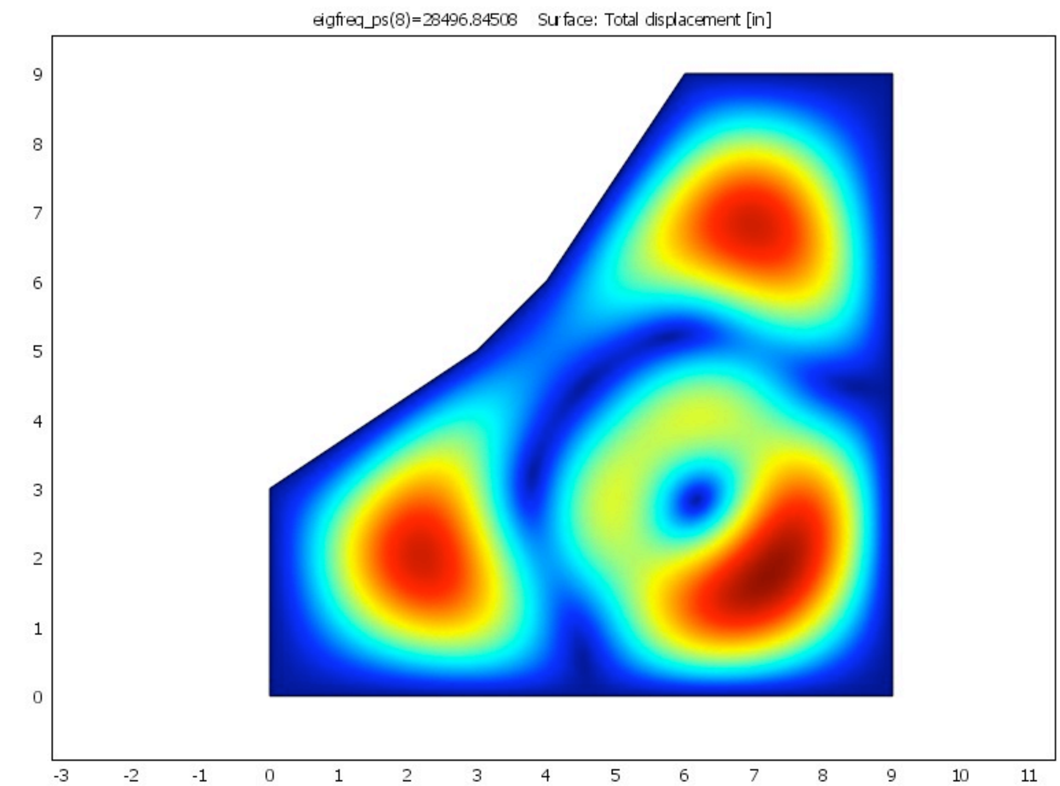

Figure B8: Eighth Mode

Actual Gear Cover Modal Analysis Provided by Cummins Incorporated:

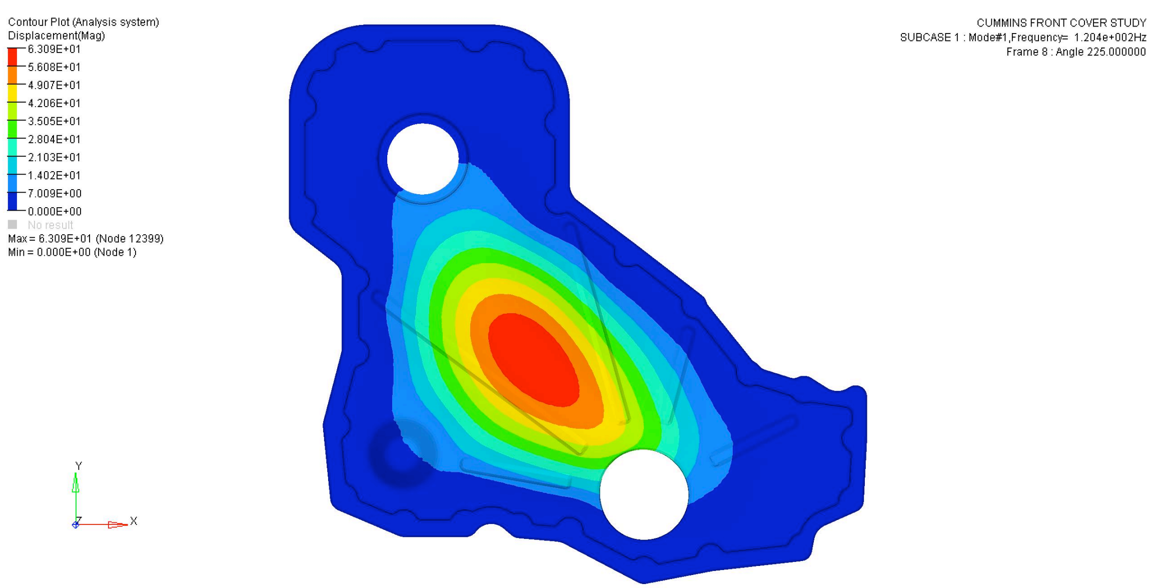

Figure B9: First Mode

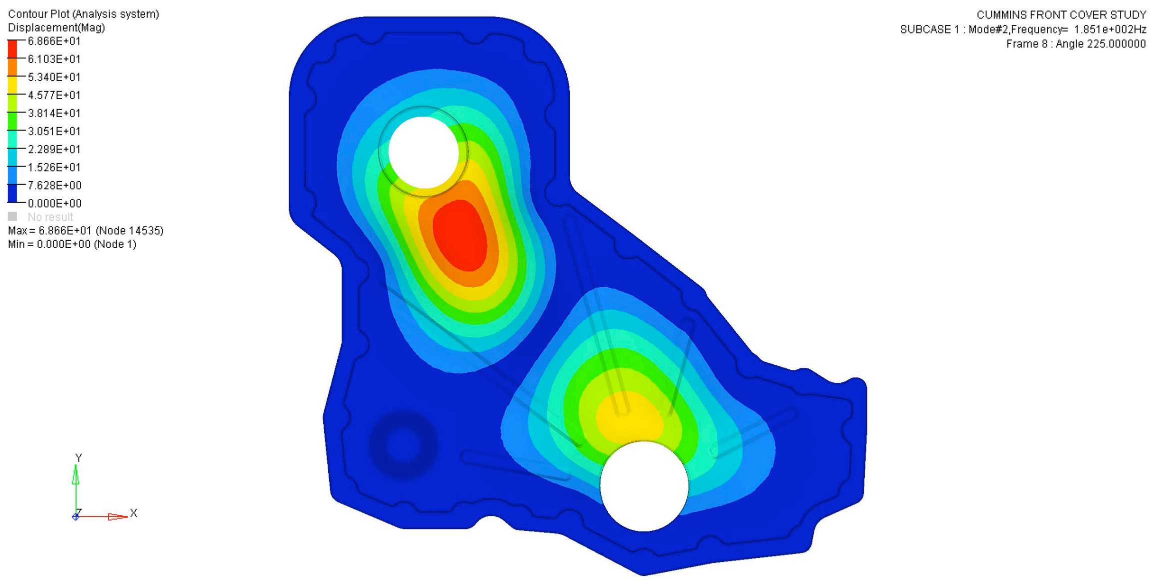

Figure B10: Second Mode

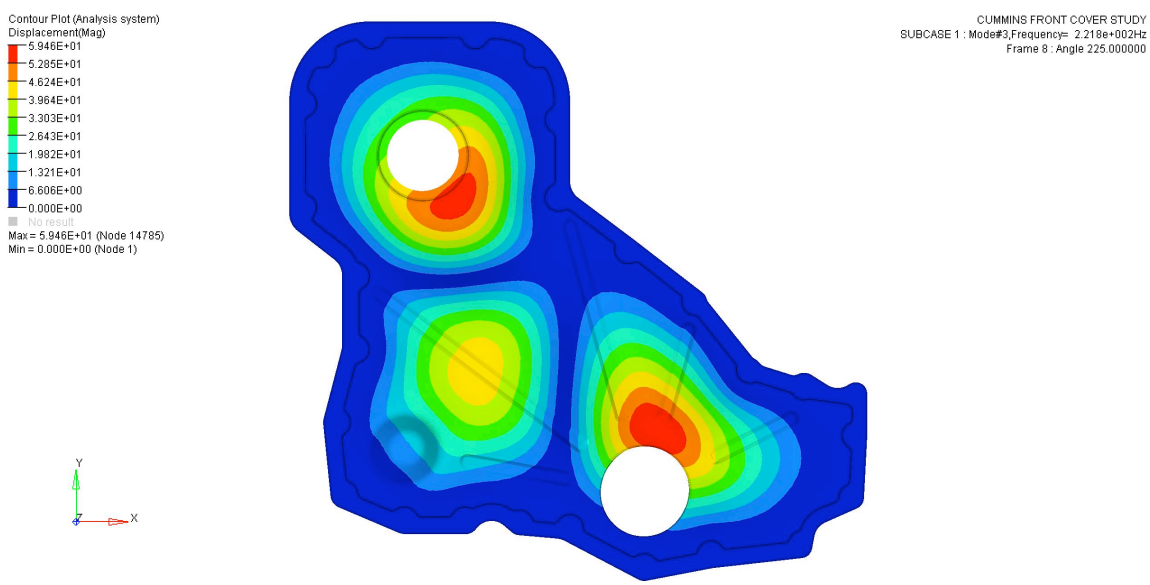

Figure B11: Third Mode

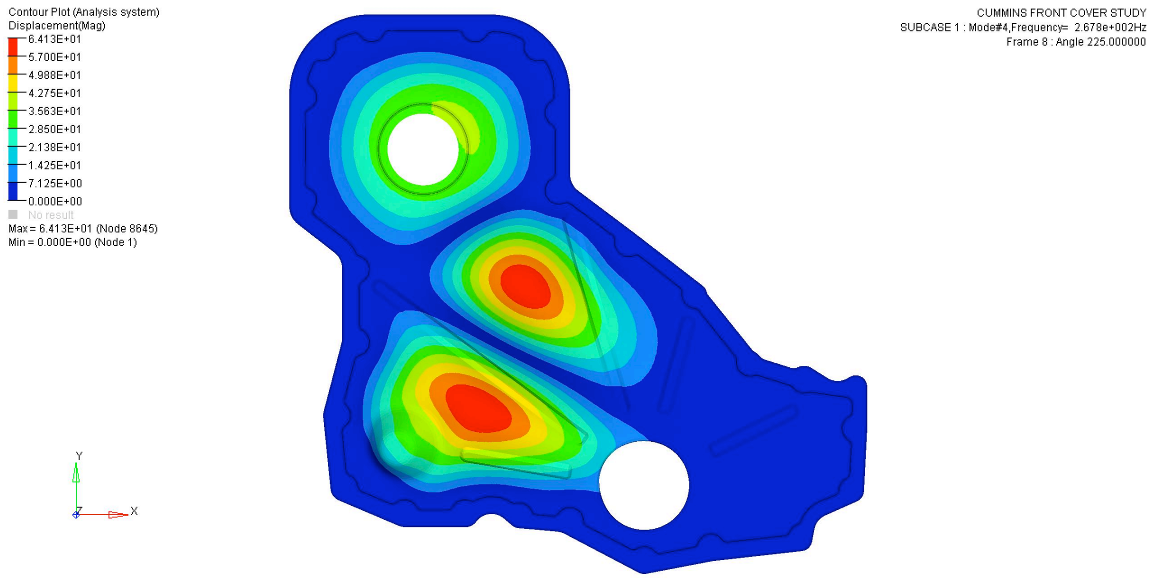

Figure B12: Fourth Mode

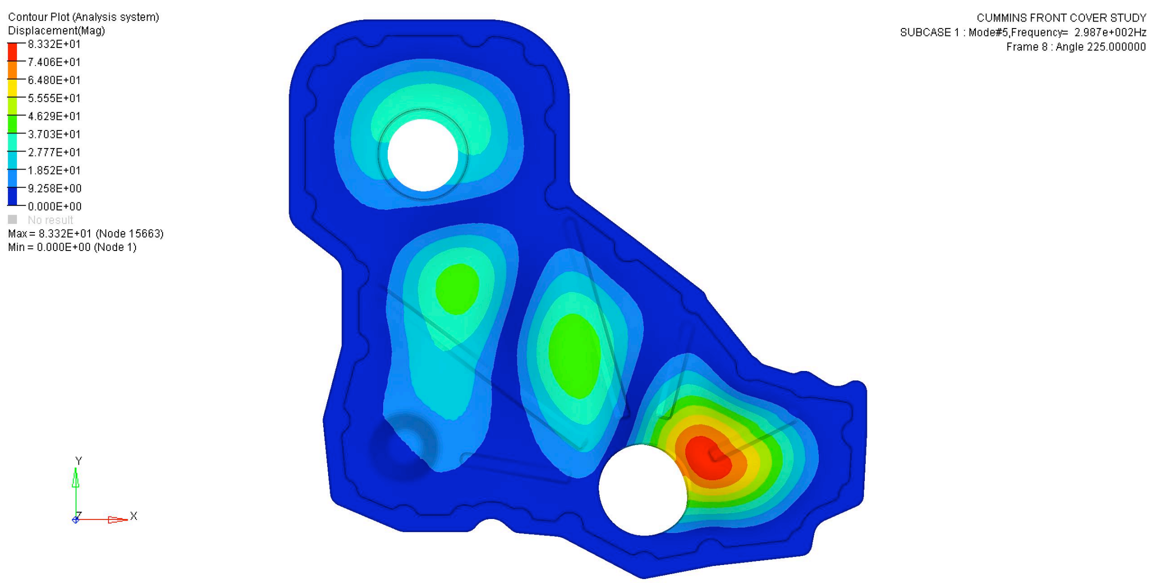

Figure B13: Fifth Mode

COMSOL Deformation Graphs for Clarification:

The following solutions where obtained in COMSOL multi-physics for each given condition mentioned in Section 3.2.

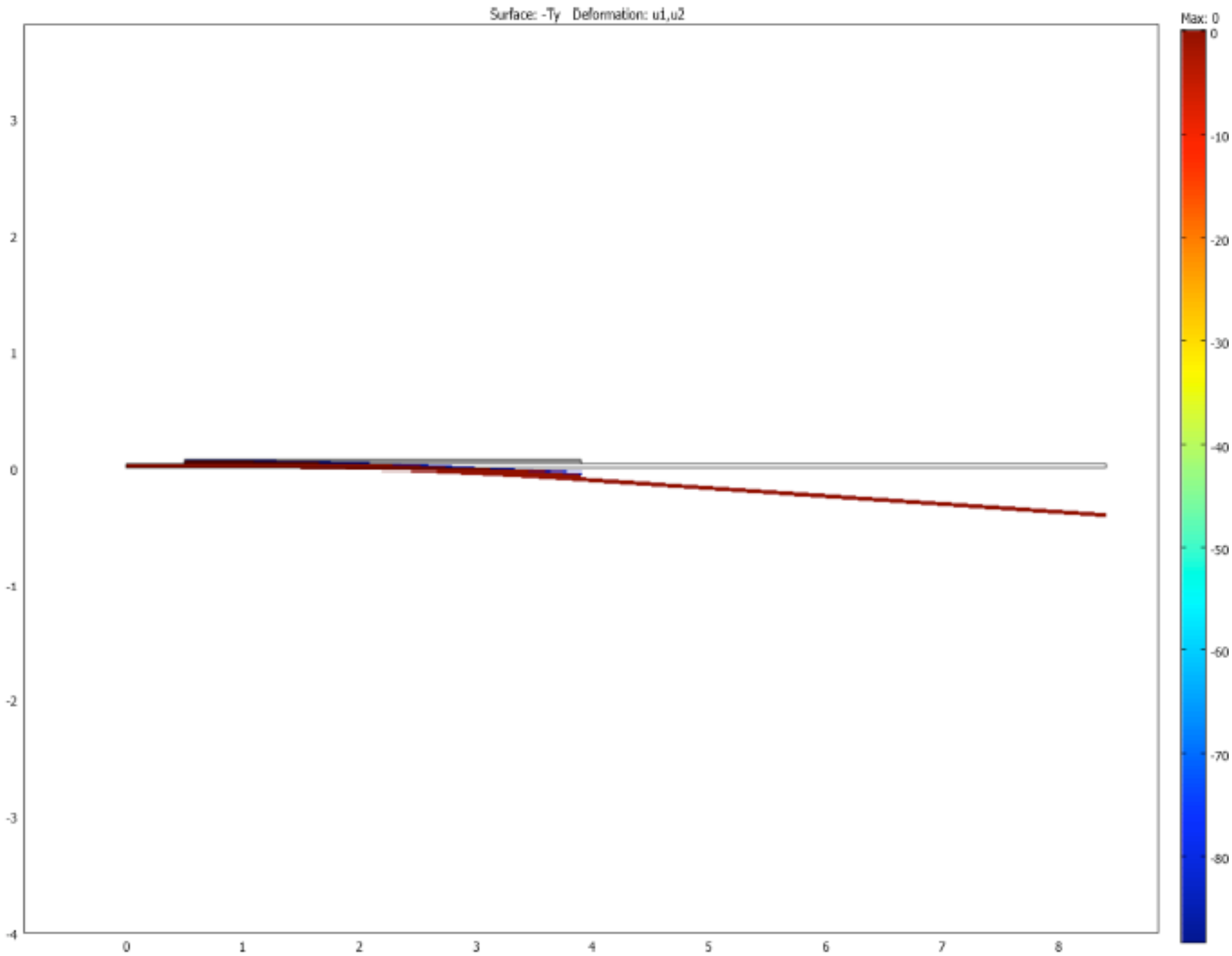

Figure B-14: One Fixed End With Positive Potential Difference

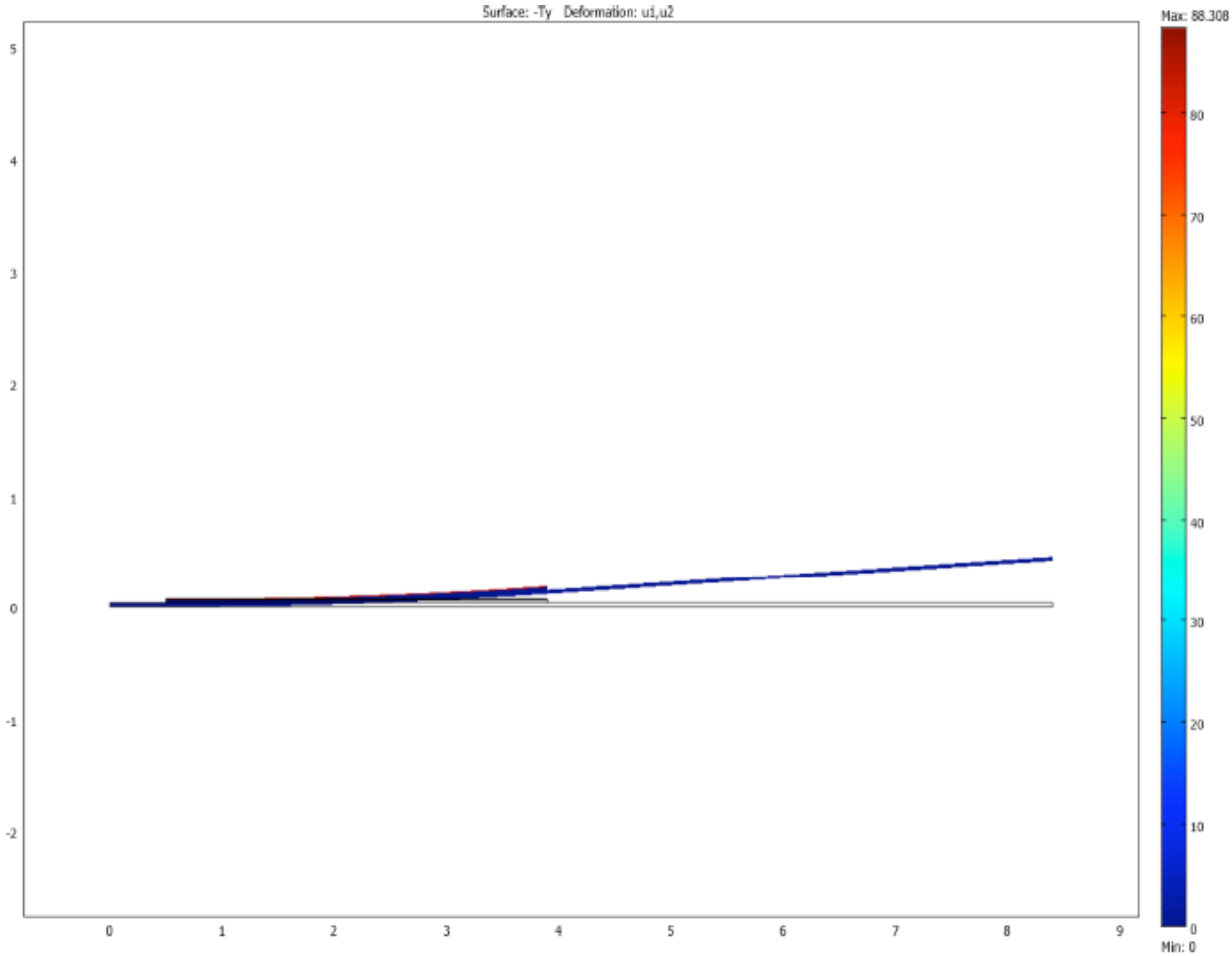

Figure B-15: One Fixed End With Negative Potential Difference

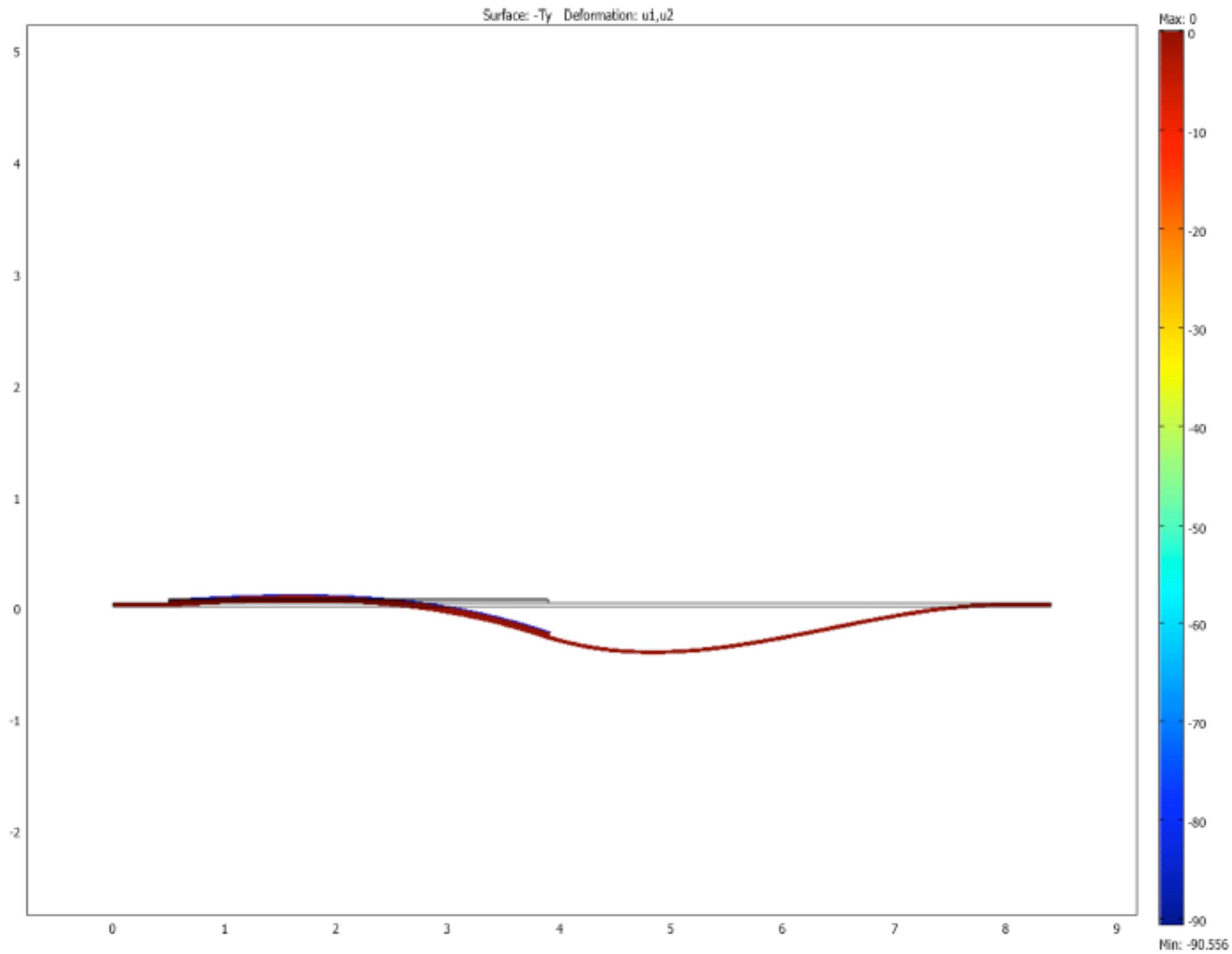

Figure B-16: Two fixed ends and positive potential difference.

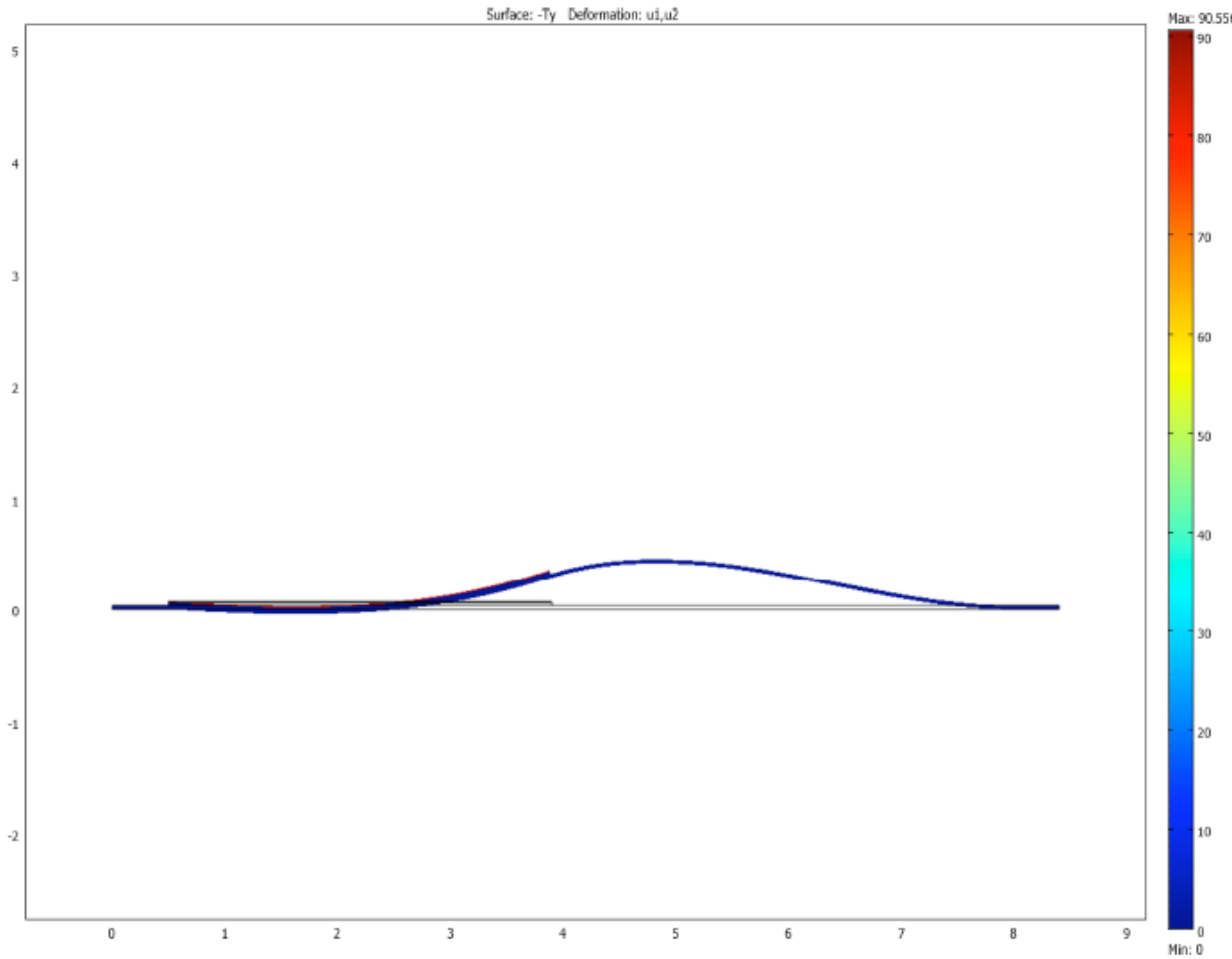

Figure B-17: Two Fixed Ends and Negative Potential Difference.

It is evident from Figures B-14 through 17 that the COMSOL model qualitatively agrees with the theoretical predictions in terms of how the actuator affects the system. The overall displacement will depend directly on the applied voltage, shown as 100V. Referring back to equations 4 and 5 it can be determined that the displacement is linearly related to the applied voltage by the piezoelectric constants. However, the scale at which these movements are taking place is very small; in the range of about 1E-6 meters.

Given that the system's intended use is vibration attenuation, the first three resonance modes have also been examined to find what if any effect the actuator has on the system during resonance. Figures B-18 through B-20 show the first three modes of the one fixed end model.

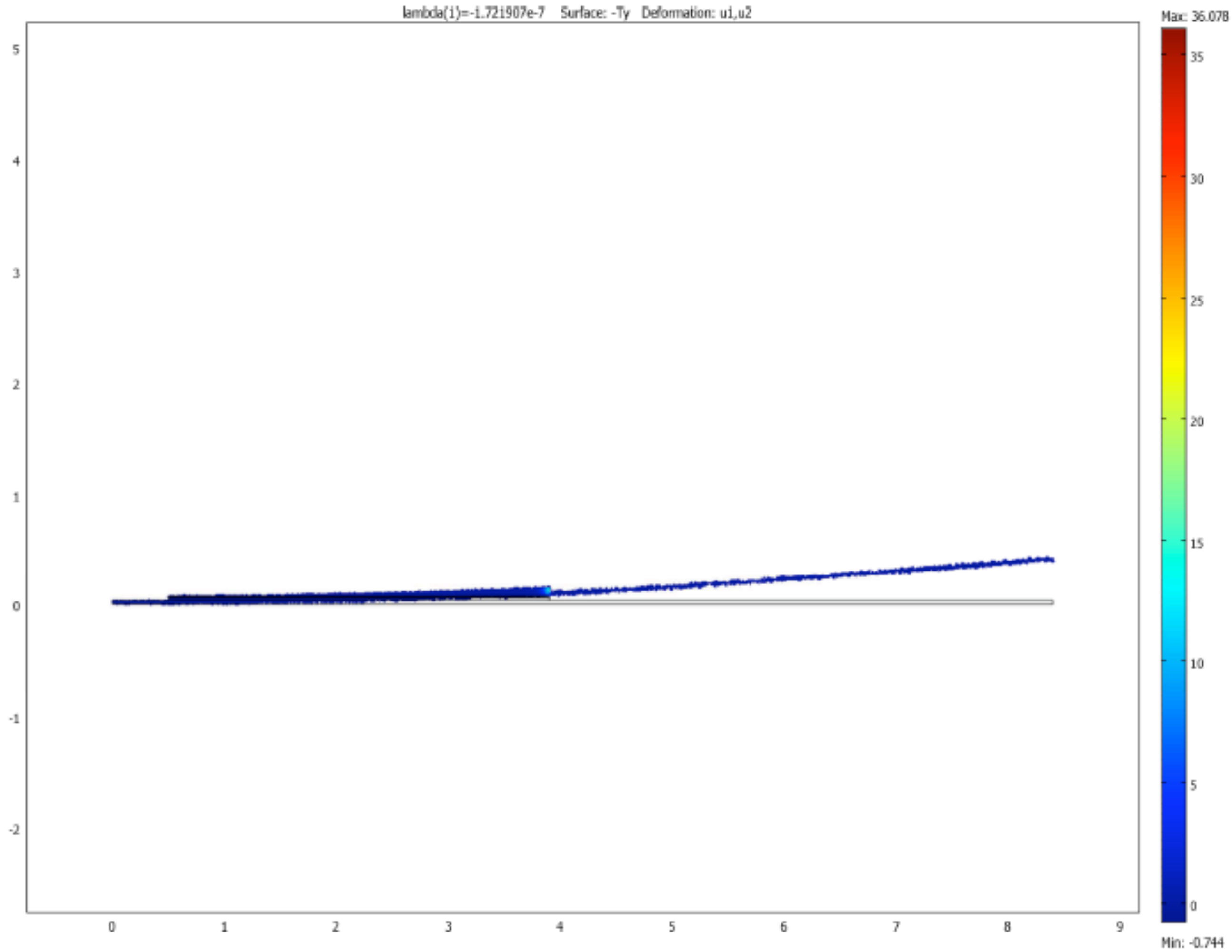

lambda(1)=-1.721907e-7 Surface: -Ty Deformation: u1,u2
Max: 36.078
Min: -0.744

(a)

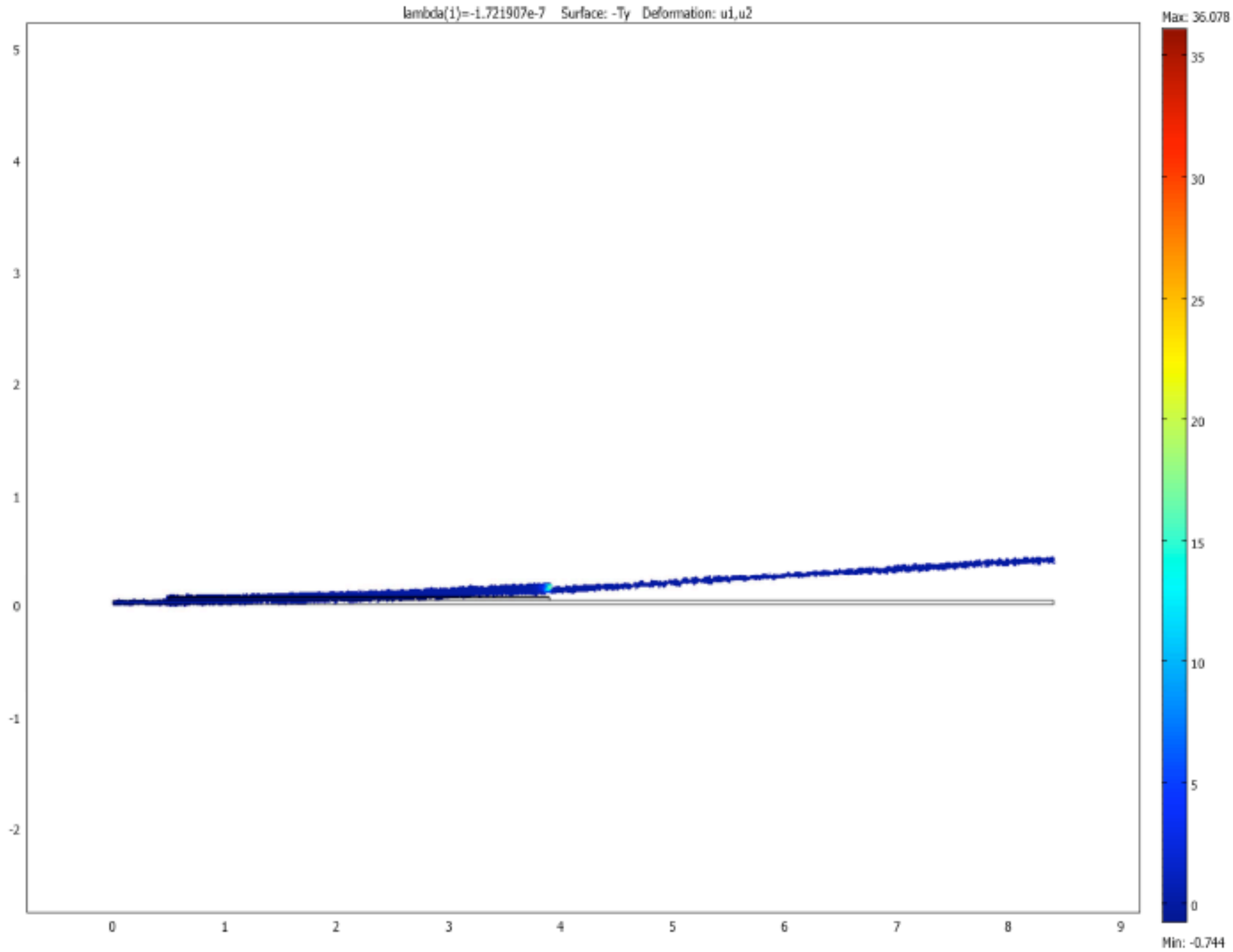
lambda(1)=-1.721907e-7 Surface: -Ty Deformation: u1,u2
Max: 36.078
Min: -0.744
35
30
25
20
15
10
5
0
5
4
3
2
1
0
-1
-2
0
1
2
3
4
5
6
7
8
9

(b)

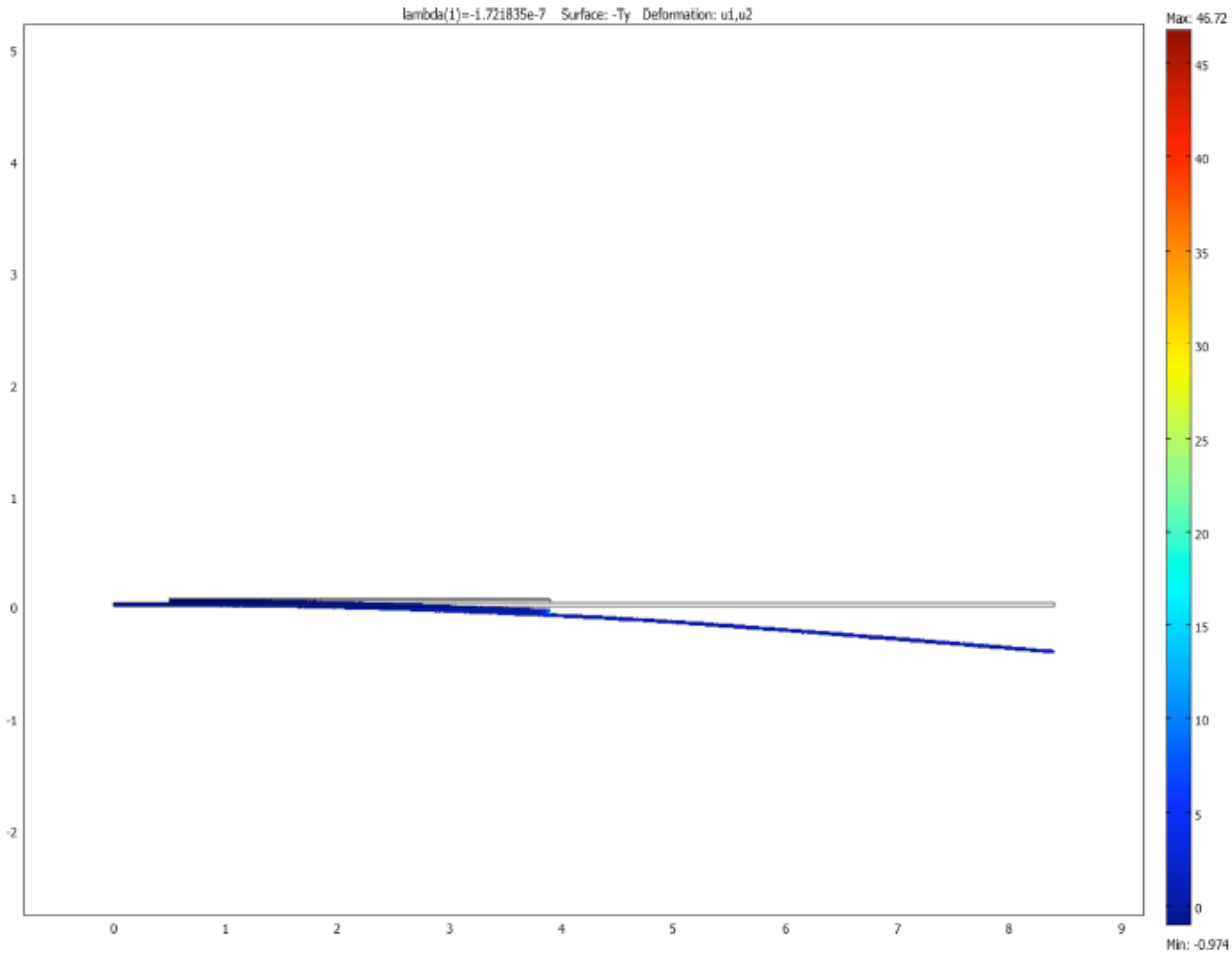

(c)

Figure B-18: Resonance Mode 1 with (a) No Voltage (b) Negative Potential Difference (c) Positive Potential Difference

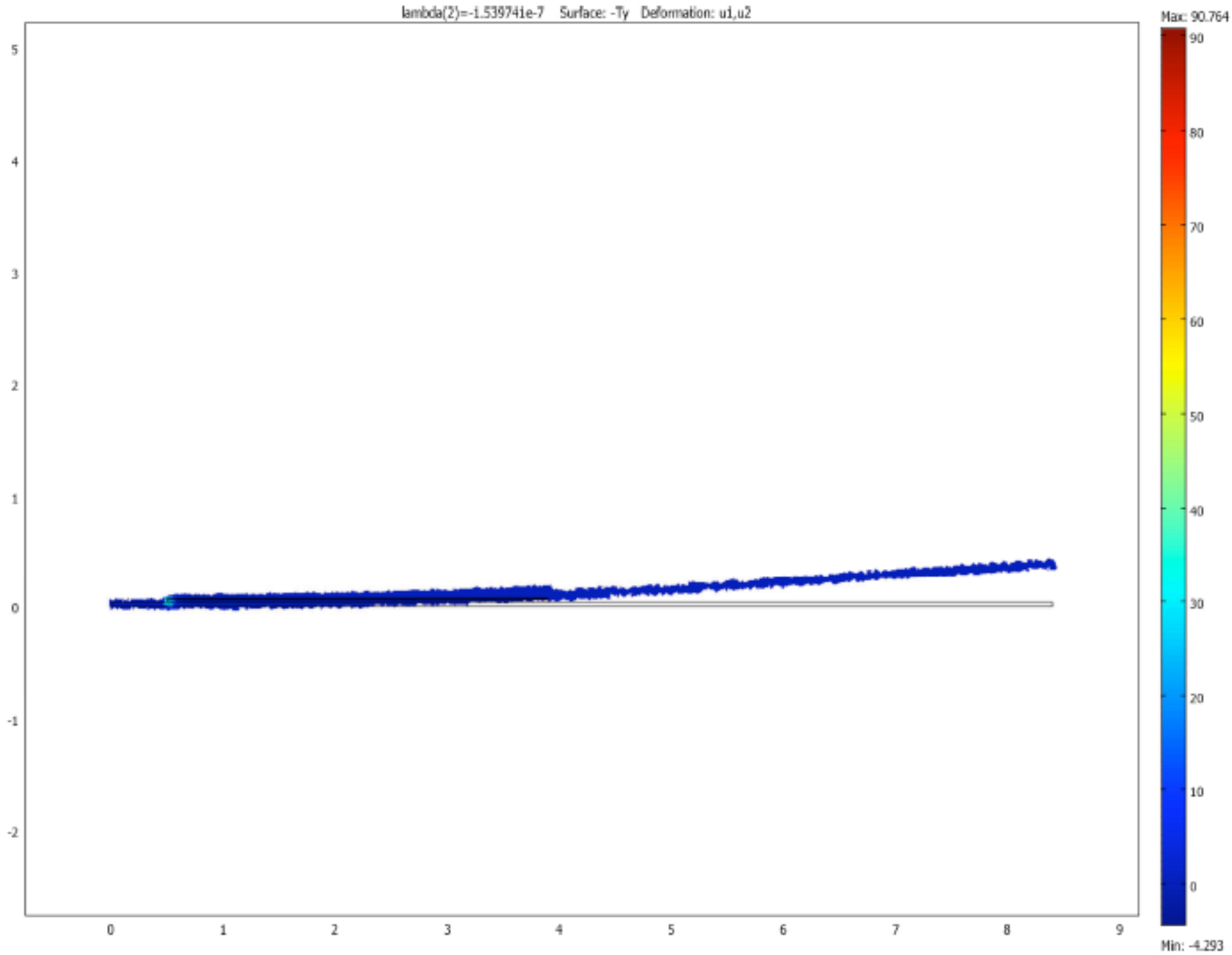
lambda(2)=-1.53974ie-7 Surface: -Ty Deformation: u1,u2
Max: 90.764
Min: -4.293

(a)

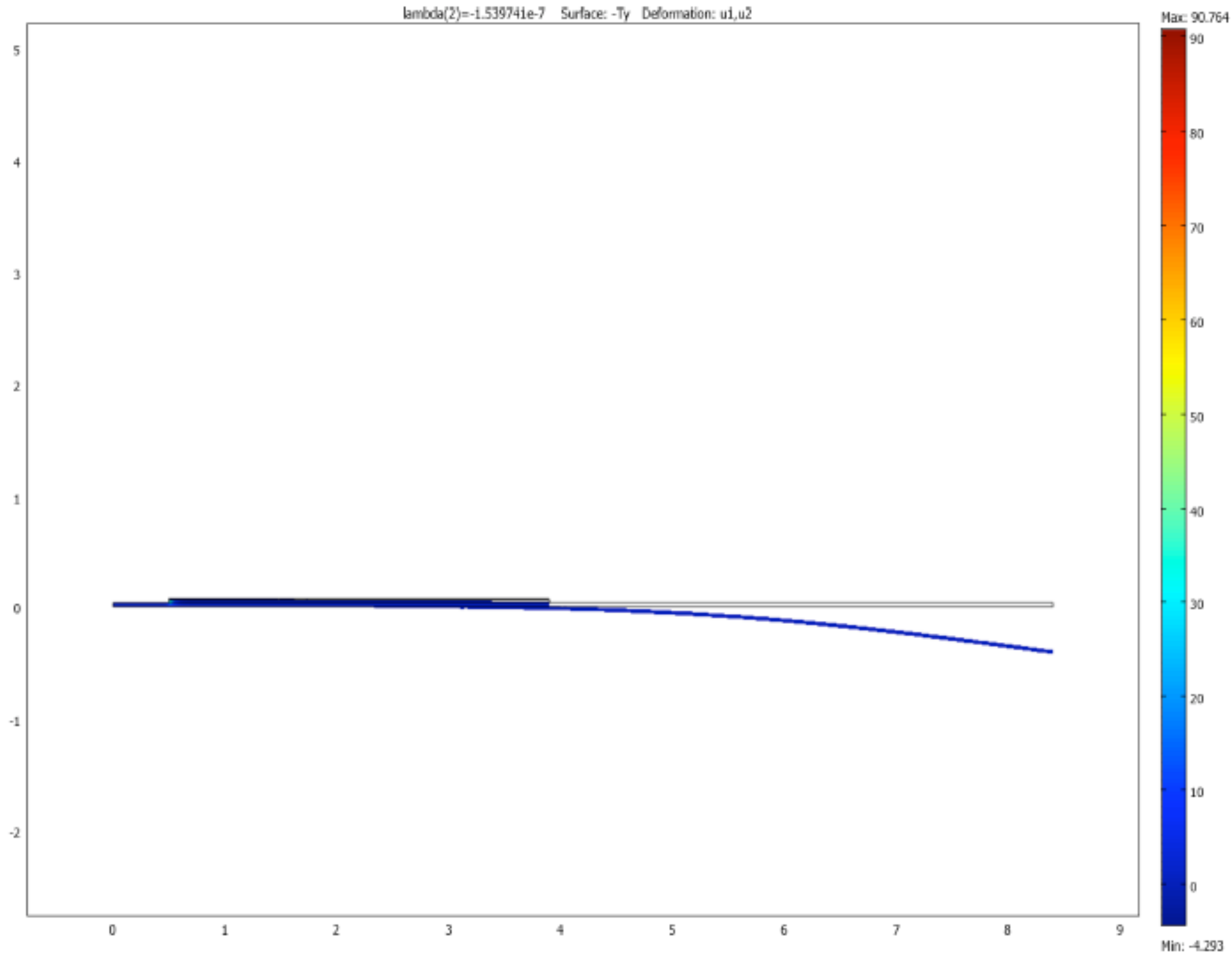
lambda(2)=-1.539741e-7 Surface: -Ty Deformation: u1,u2
Max: 90.764
Min: -4.293
90
80
70
60
50
40
30
20
10
0
5
4
3
2
1
0
-1
-2
0
1
2
3
4
5
6
7
8
9

(b)

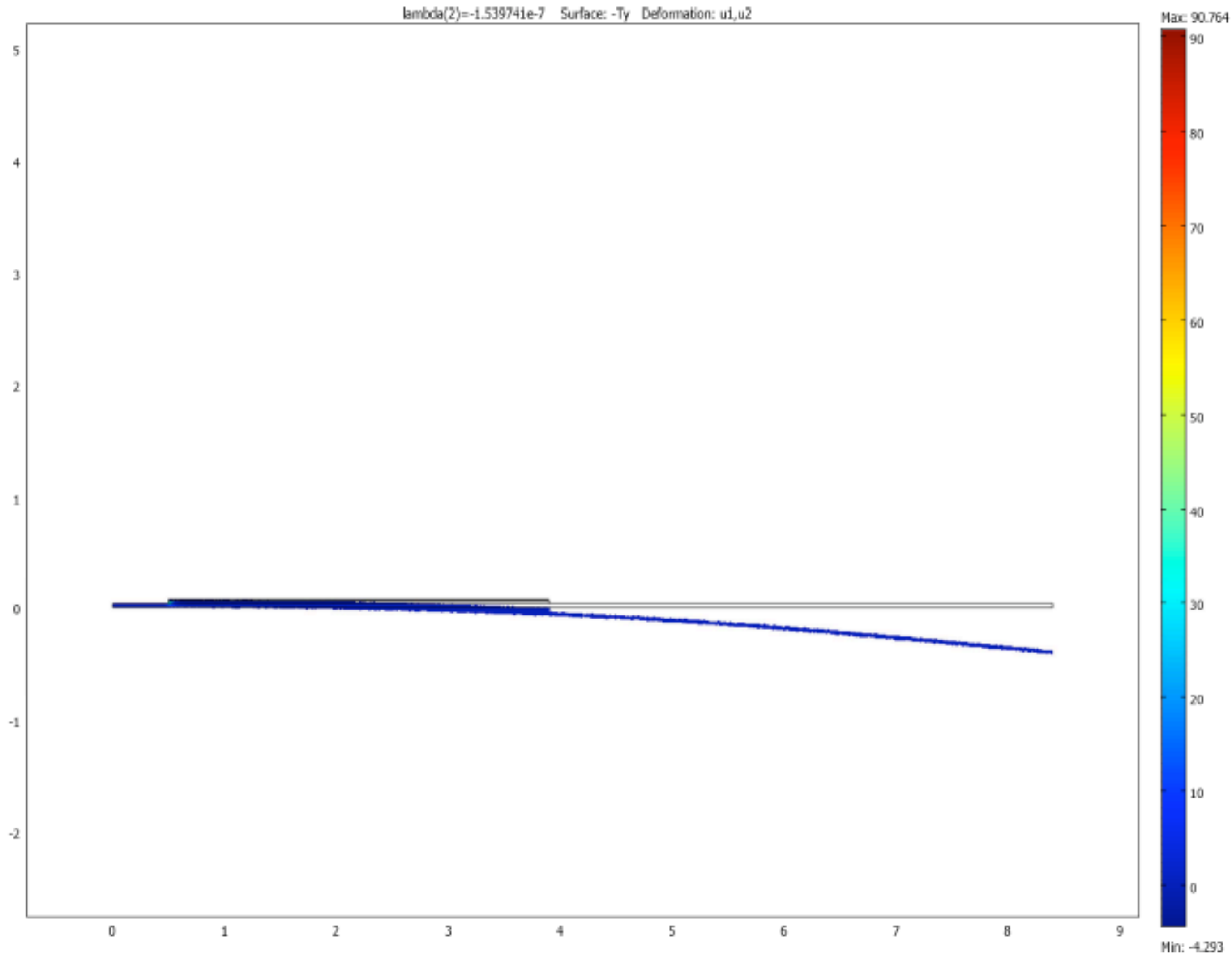

(c)

Figure B-19: Resonance Mode 2 With (a) No Voltage (b) Negative Potential Difference (c) Positive Potential Difference

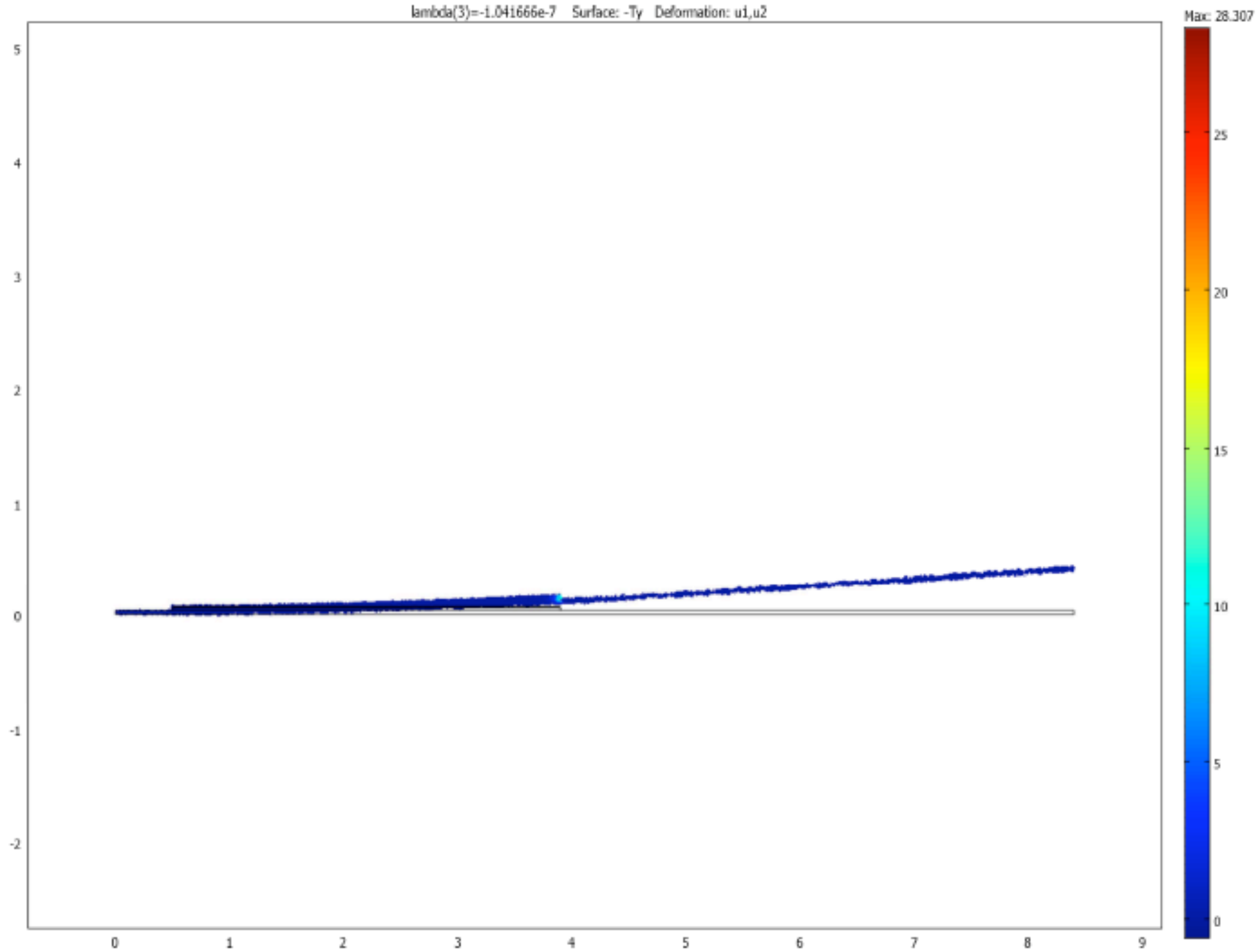
lambda(3)=-1.041666e-7 Surface: -Ty Deformation: u1,u2
Max: 28.307
Min: -0.583

(a)

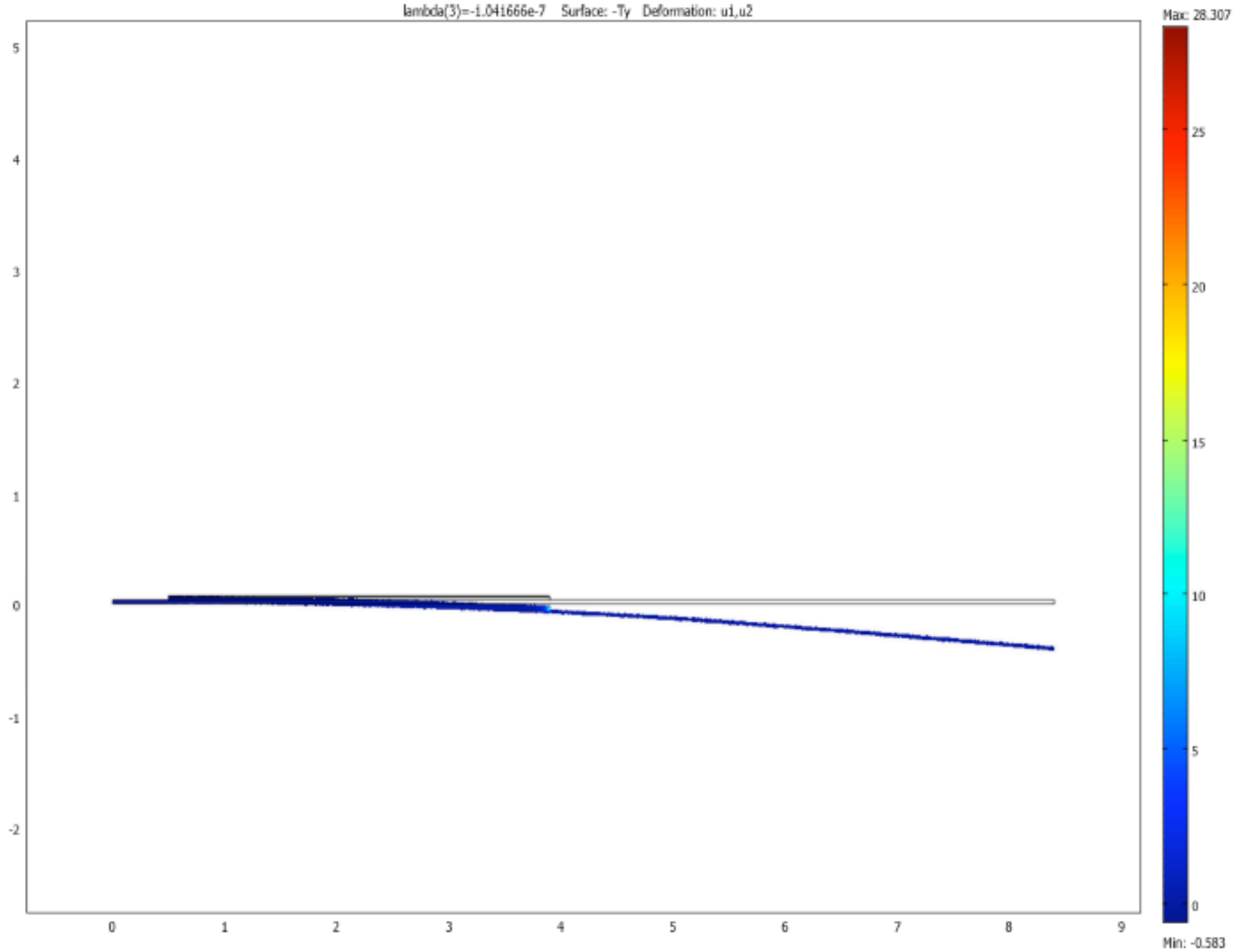
lambda(3)=-1.041666e-7 Surface: -Ty Deformation: u1,u2
Max: 28.307
Min: -0.583

(b)

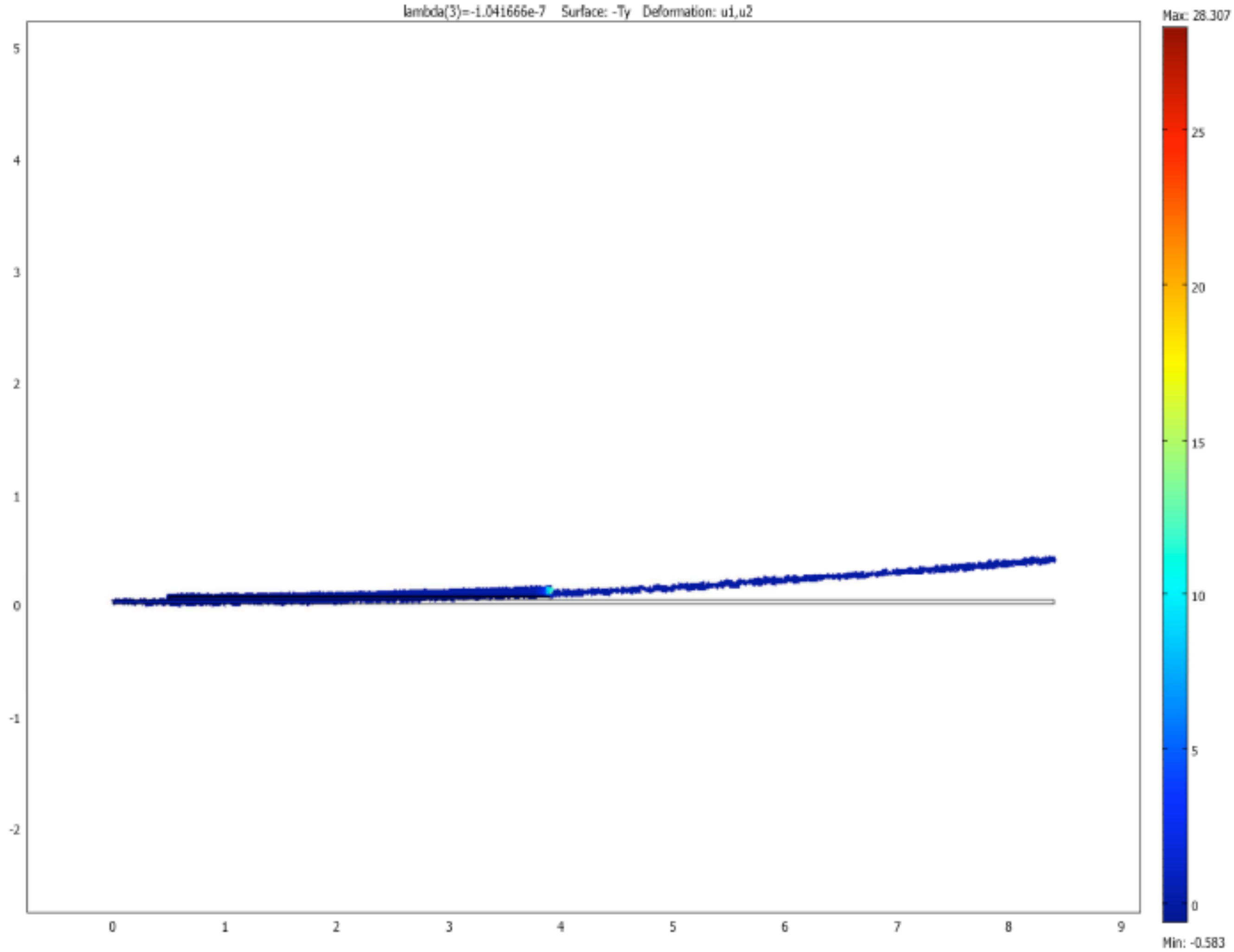

(c)

Figure B-20: Resonance Mode 3 With (a) No Voltage (b) Negative Potential Difference (c) Positive Potential Difference

The above figures show that the actuator will have an effect on the vibration properties. There is an observable difference in the stress concentrations at the locations near the actuator when the actuator is in closed circuit, ie. a positive or negative potential difference. The location and magnitude of the stress concentrations move depending on the voltage and resonance mode.

COMSOL Deformation Graphs:

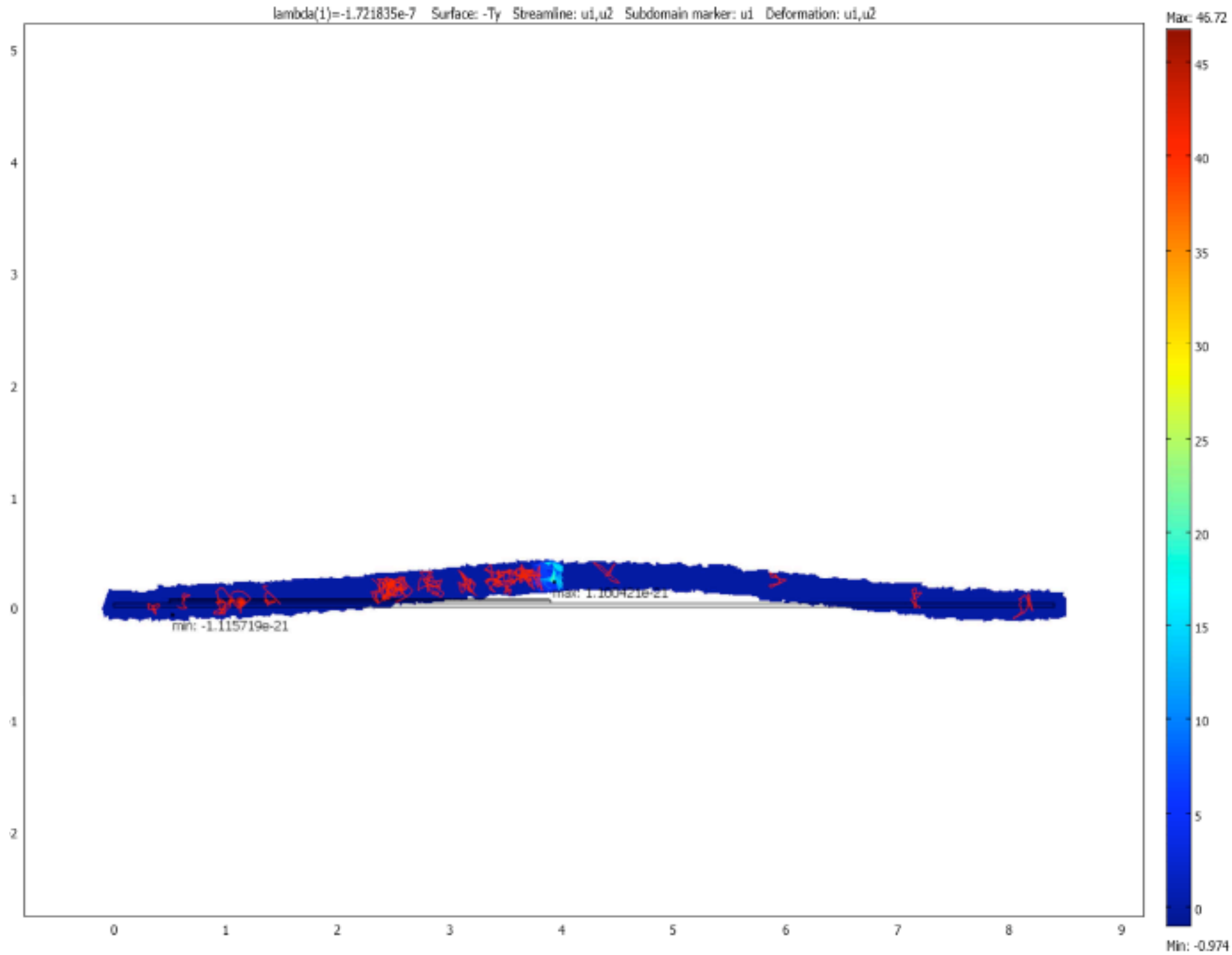

(a)

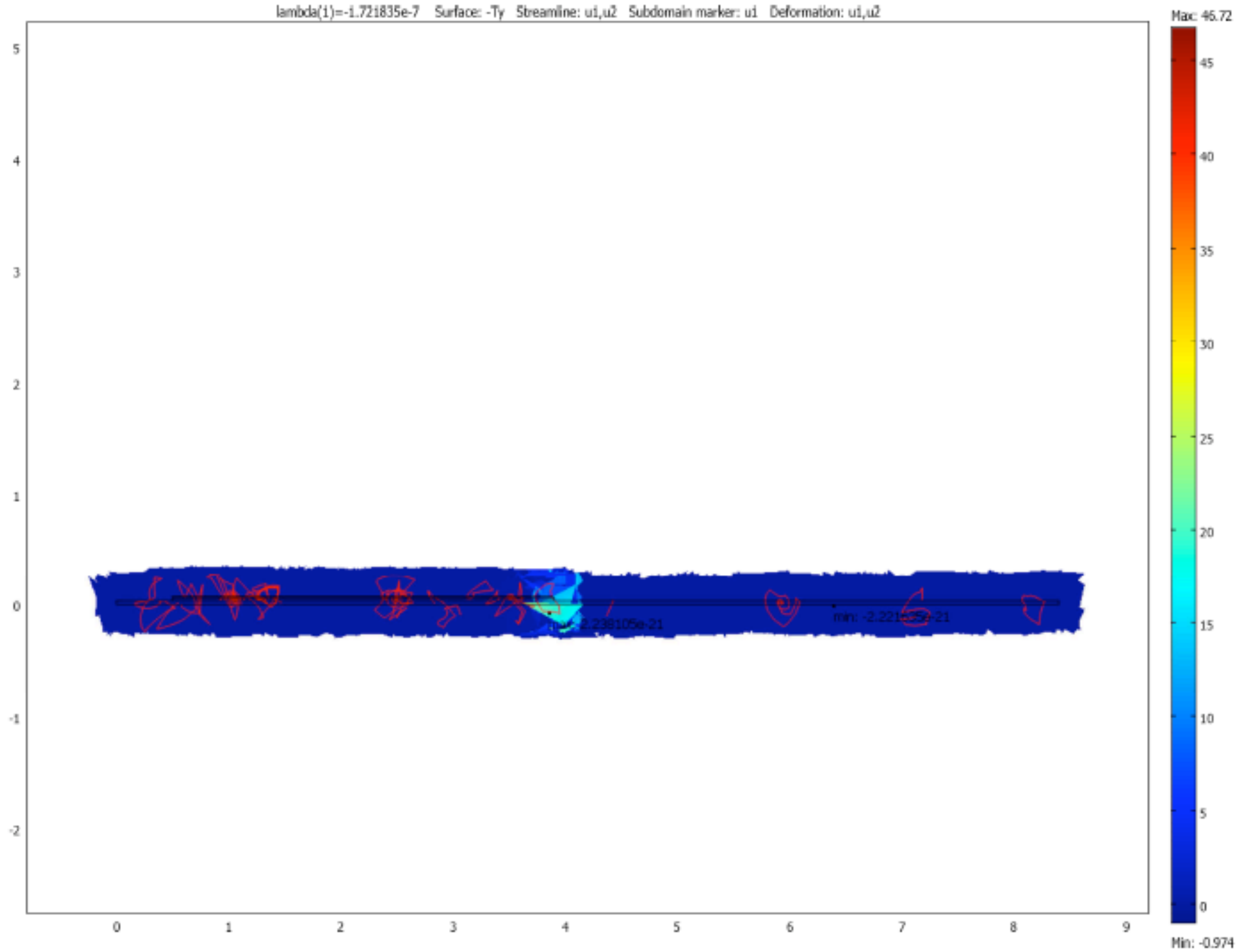
lambda(1)=-1.721835e-7 Surface: -Ty Streamline: u1,u2 Subdomain marker: u1 Deformation: u1,u2
Max: 46.72
Min: -0.974
45
40
35
30
25
20
15
10
5
0
5
4
3
2
1
0
-1
-2
0
1
2
3
4
5
6
7
8
9

(b)

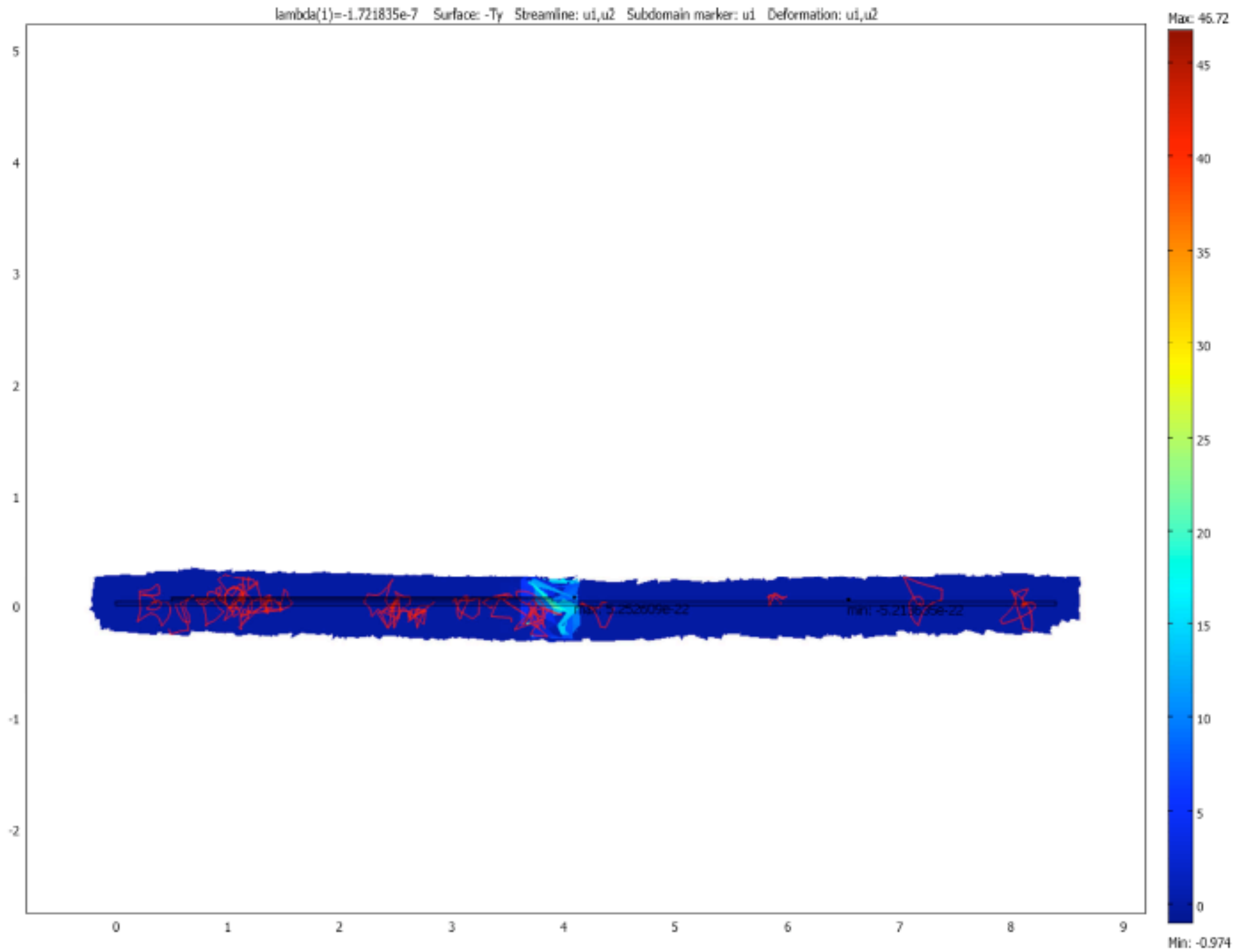

(c)

Figure B-21: double fixed end Mode 1 (a) no voltage (b) negative potential difference (c) positive potential difference

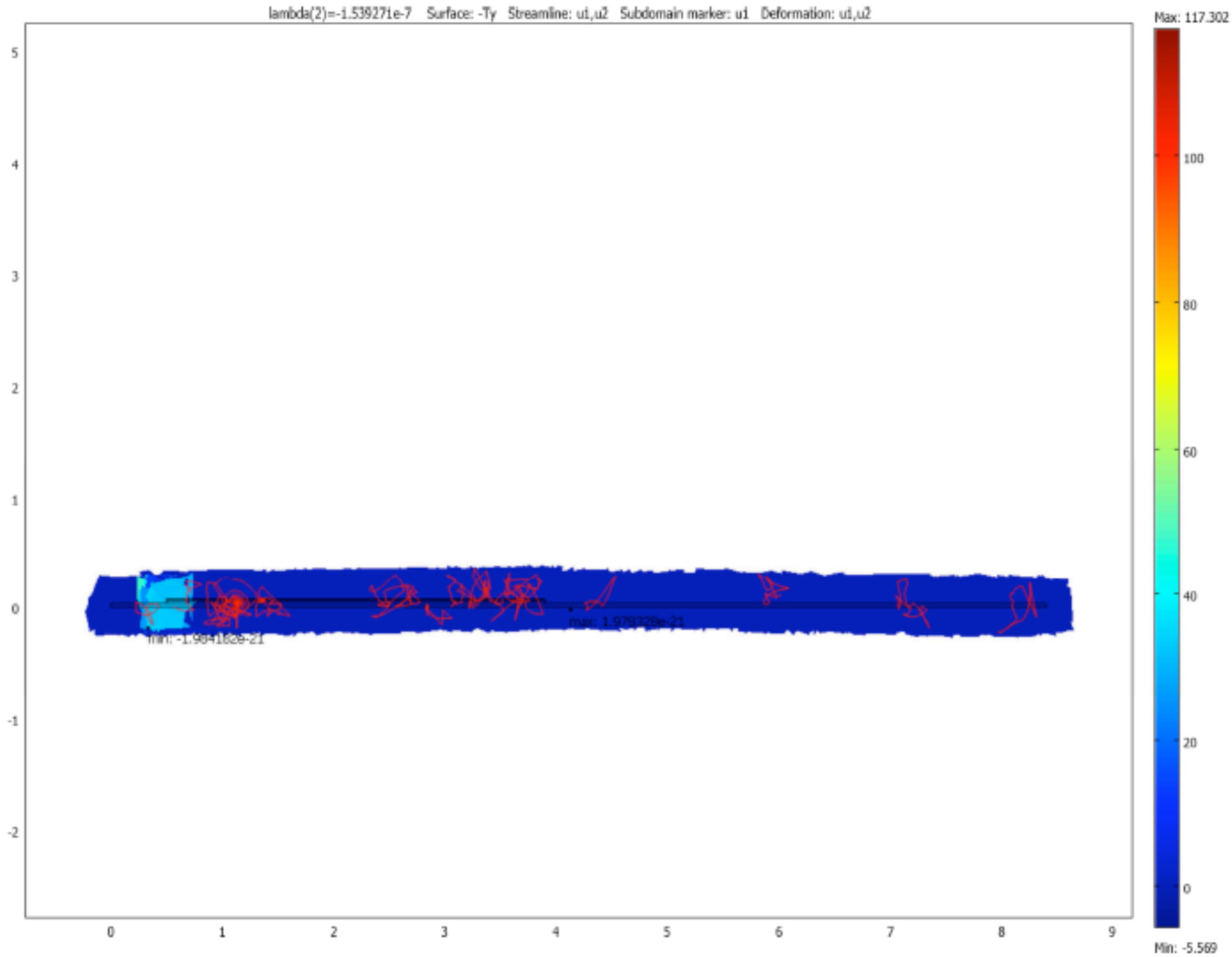
lambda(2)=-1.539271e-7 Surface: -Ty Streamline: u1,u2 Subdomain marker: u1 Deformation: u1,u2
Max: 117.302
Min: -5.569
100
80
60
40
20
0
5
4
3
2
1
0
-1
-2
0
1
2
3
4
5
6
7
8
9

(a)

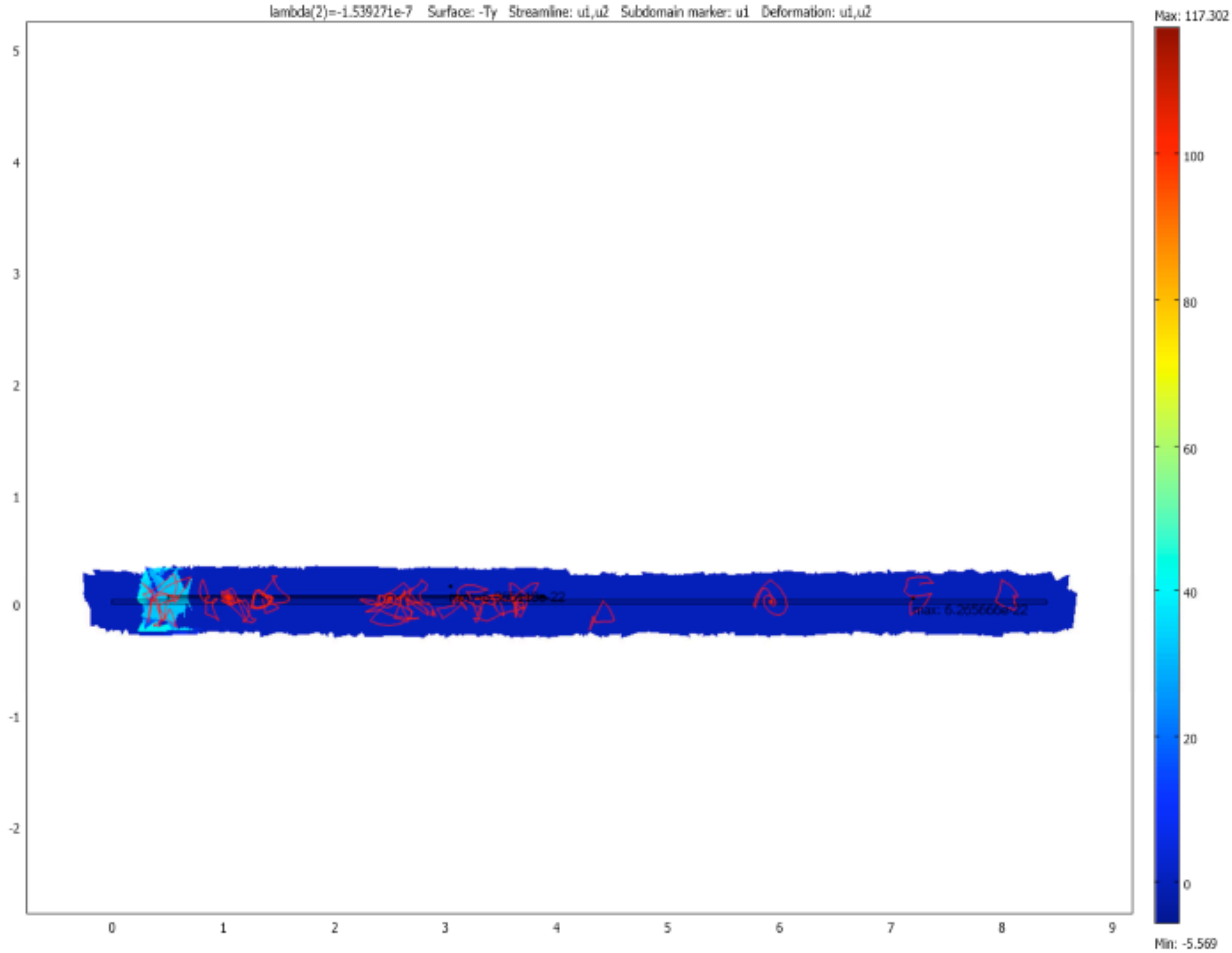

lambda(2)=-1.539271e-7 Surface: -Ty Streamline: u1,u2 Subdomain marker: u1 Deformation: u1,u2
Max: 117.302
Min: -5.569

(b)

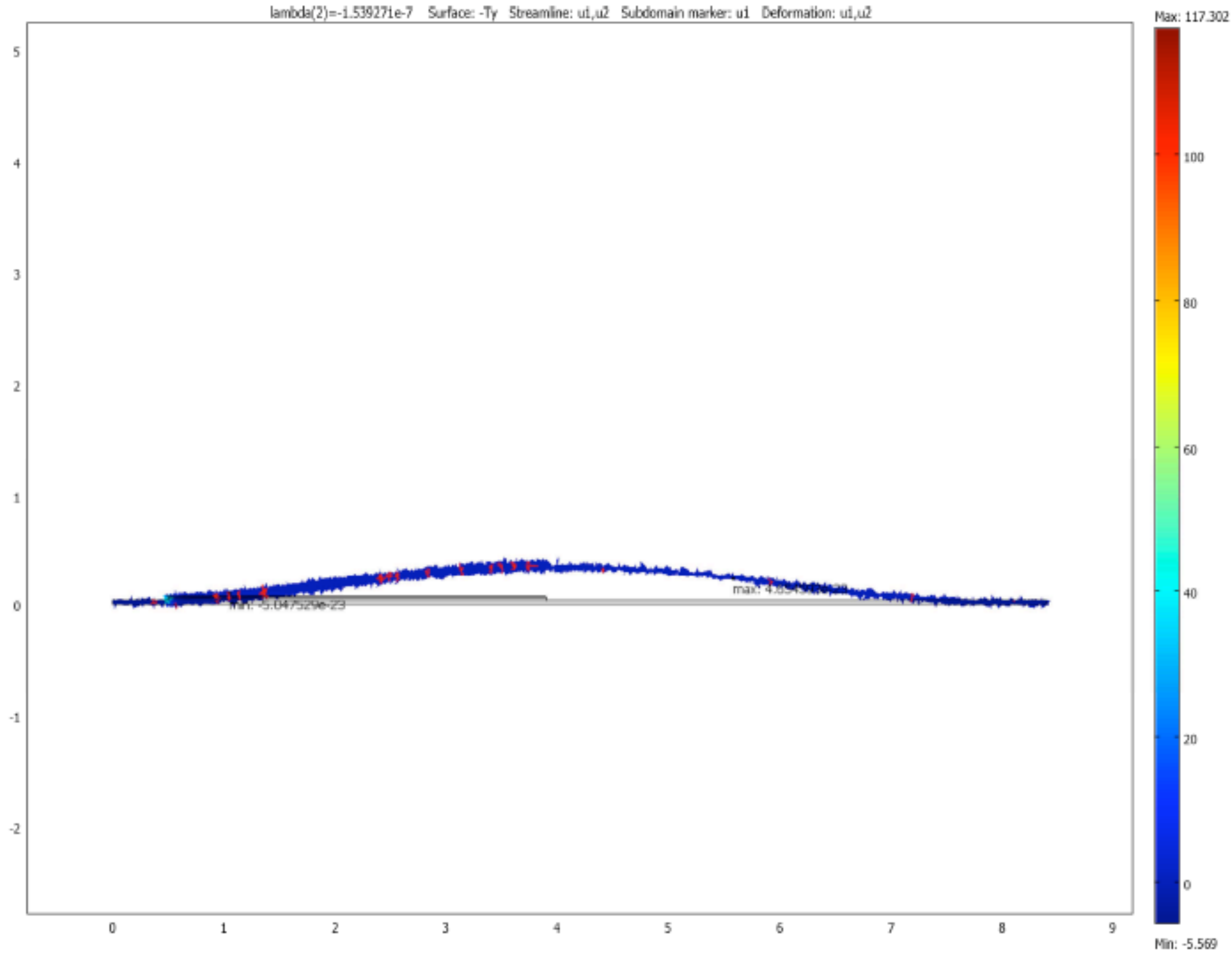

(c)

Figure B-22: double fixed end Mode 2 (a) no voltage (b) negative potential difference (c) positive potential difference

APPENDIX C: Sound Data

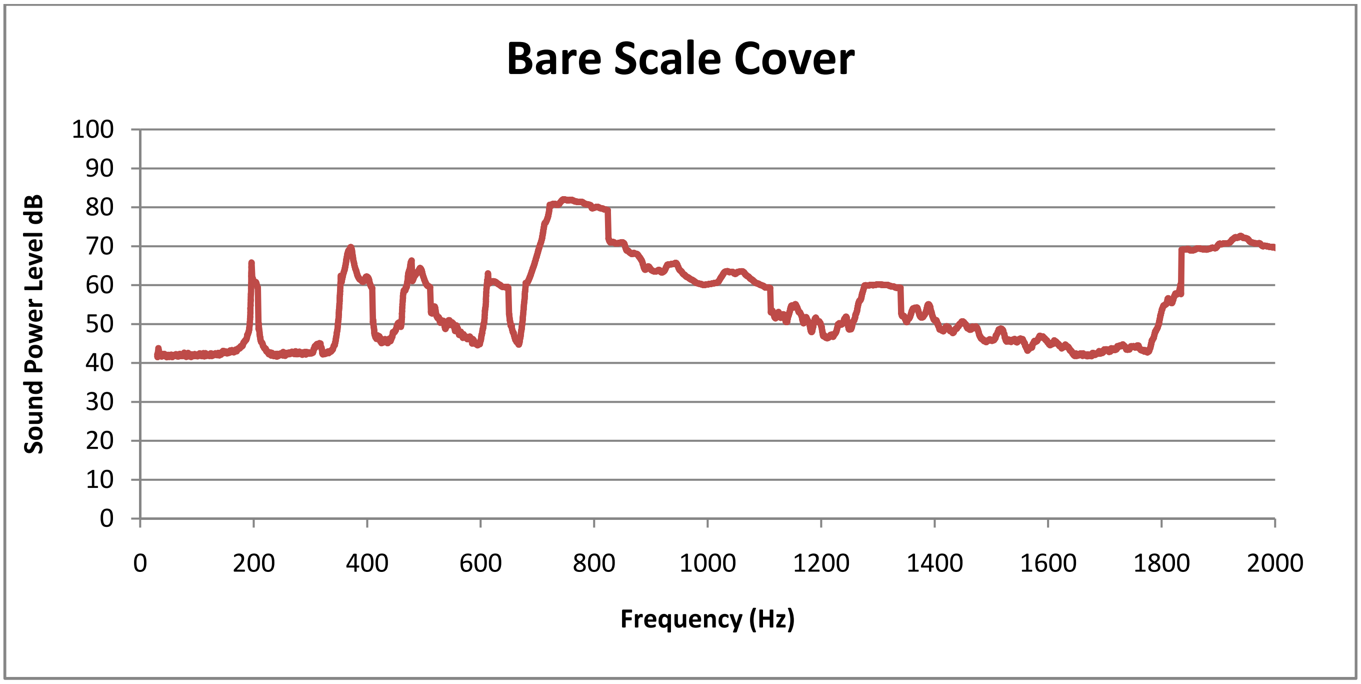

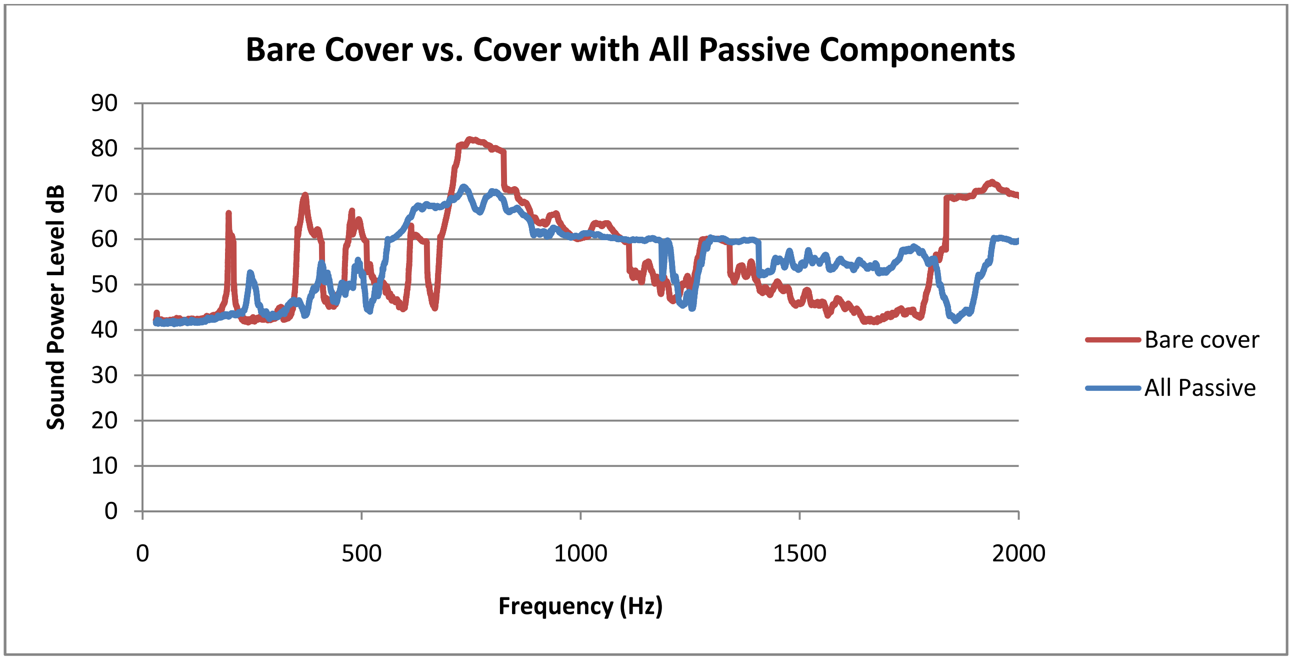

Bare Cover vs. Cover with All Passive Components
Sound Power Level dB
90
80
70
60
50
40
30
20
10
0
0
500
1000
1500
2000
Frequency (Hz)
Bare cover
All Passive

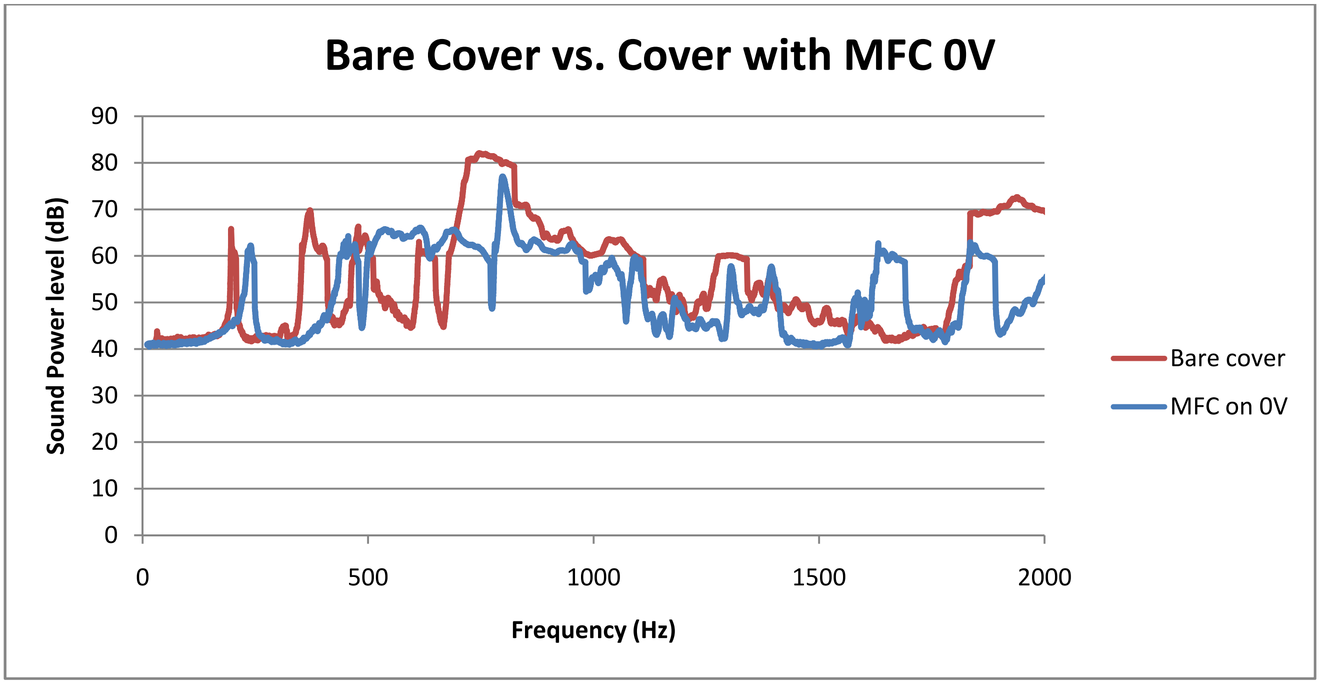

Bare Cover vs. Cover with MFC 0V
Sound Power level (dB)
90
80
70
60
50
40
30
20
10
0
0
500
1000
1500
2000
Frequency (Hz)
Bare cover
MFC on 0V

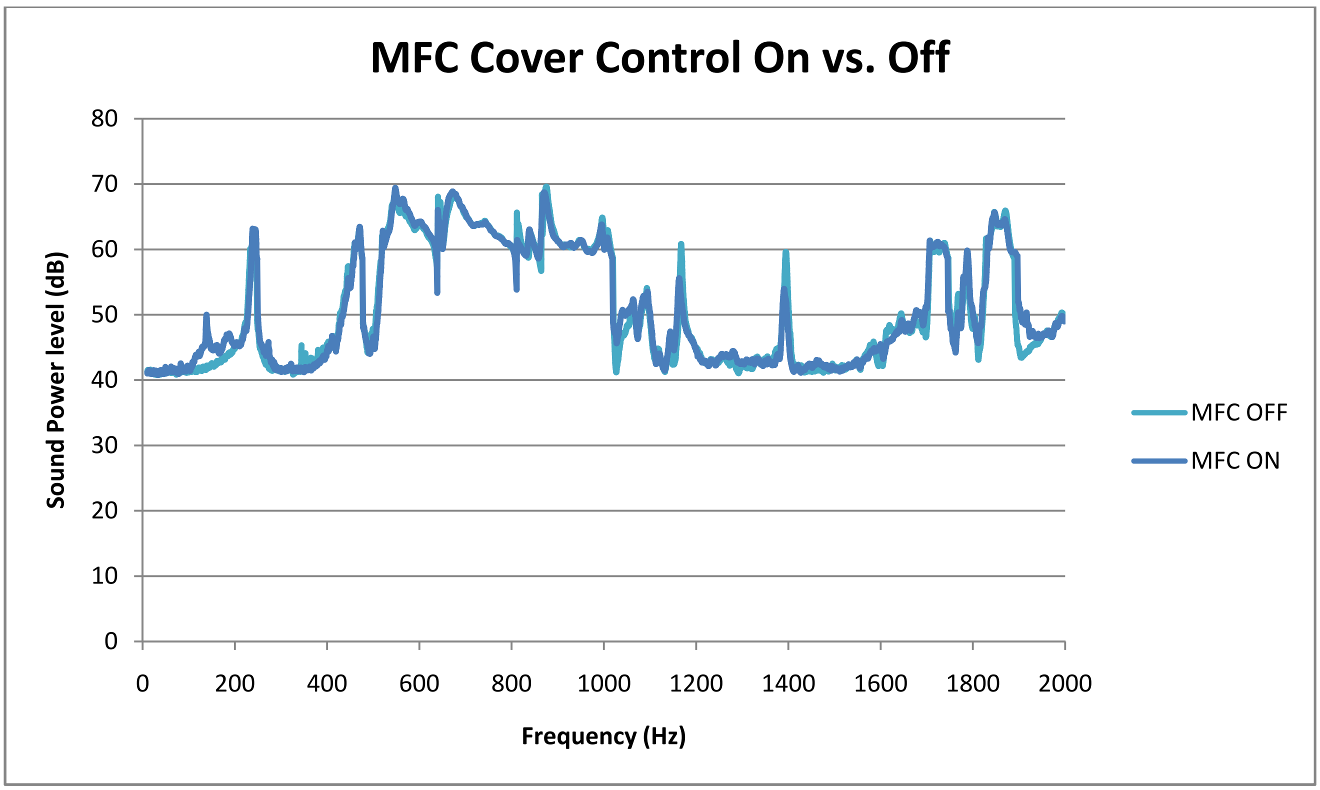

MFC Cover Control On vs. Off
Sound Power level (dB)
80
70
60
50
40
30
20
10
0
0
200
400
600
800
1000
1200
1400
1600
1800
2000
Frequency (Hz)
MFC OFF
MFC ON

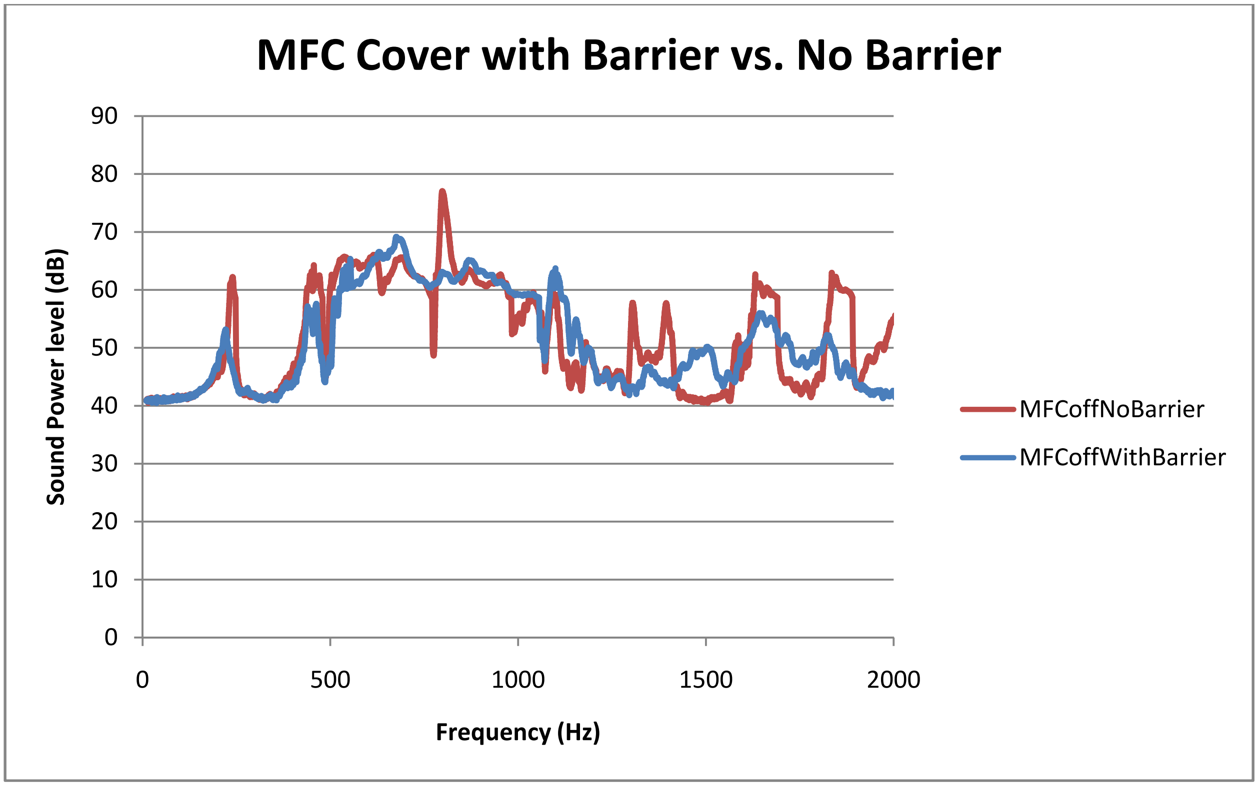
MFC Cover with Barrier vs. No Barrier
Sound Power level (dB)
90
80
70
60
50
40
30
20
10
0
0
500
1000
1500
2000
Frequency (Hz)
MFCoffNoBarrier
MFCoffWithBarrier

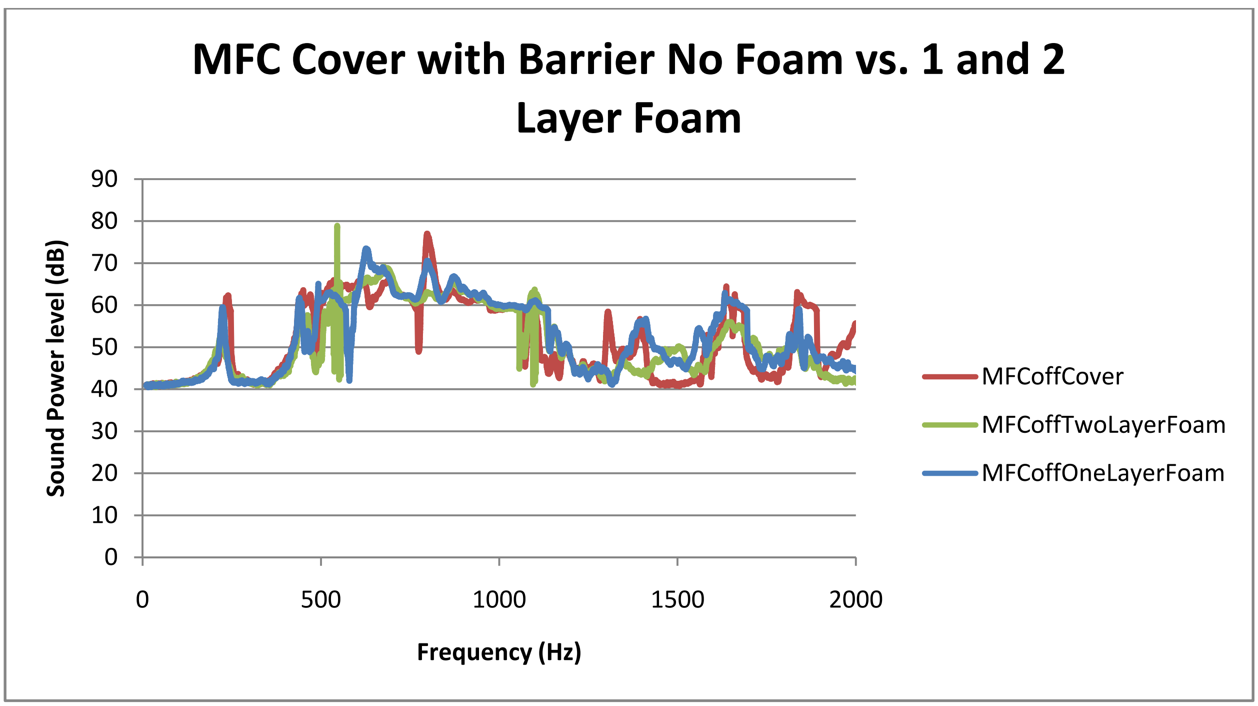
MFC Cover with Barrier No Foam vs. 1 and 2 Layer Foam
Sound Power level (dB)
90
80
70
60
50
40
30
20
10
0
0
500
1000
1500
2000
Frequency (Hz)
MFCoffCover
MFCoffTwoLayerFoam
MFCoffOneLayerFoam

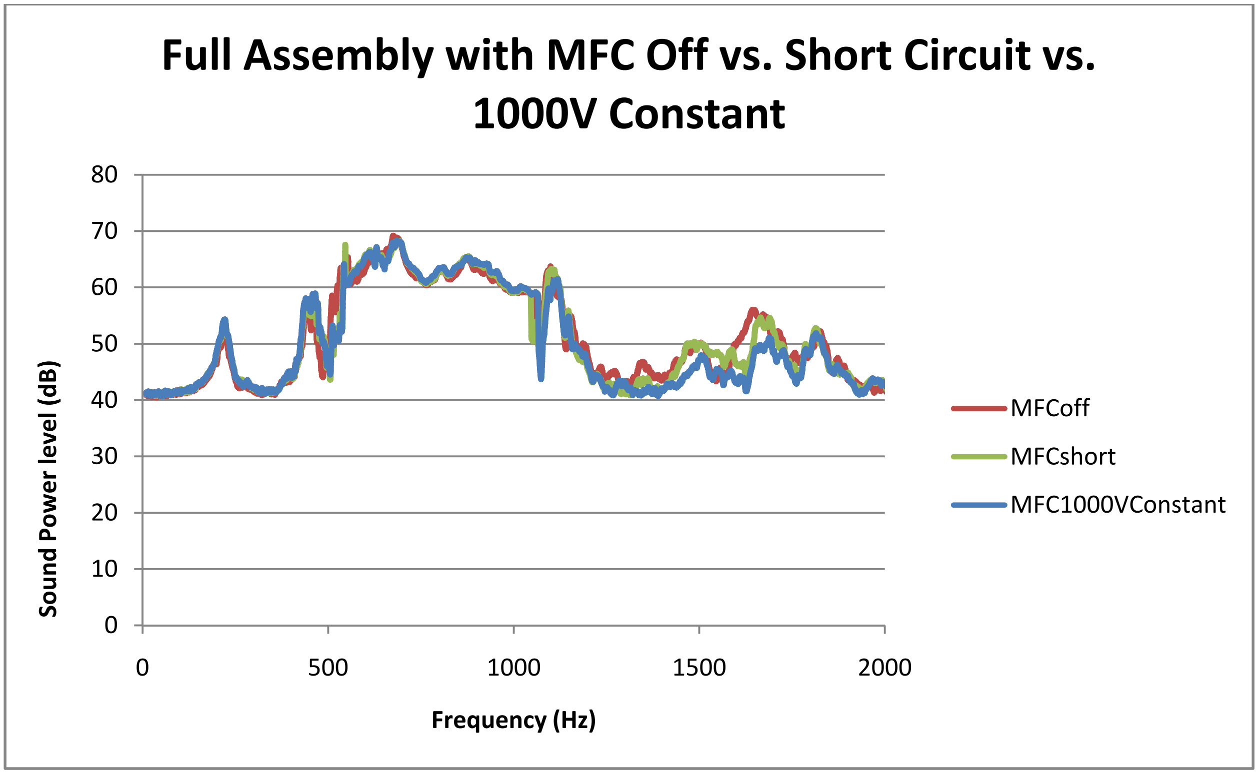

Full Assembly with MFC Off vs. Short Circuit vs. 1000V Constant
Sound Power level (dB)
80
70
60
50
40
30
20
10
0
0
500
1000
1500
2000
Frequency (Hz)
MFCoff
MFCshort
MFC1000VConstant

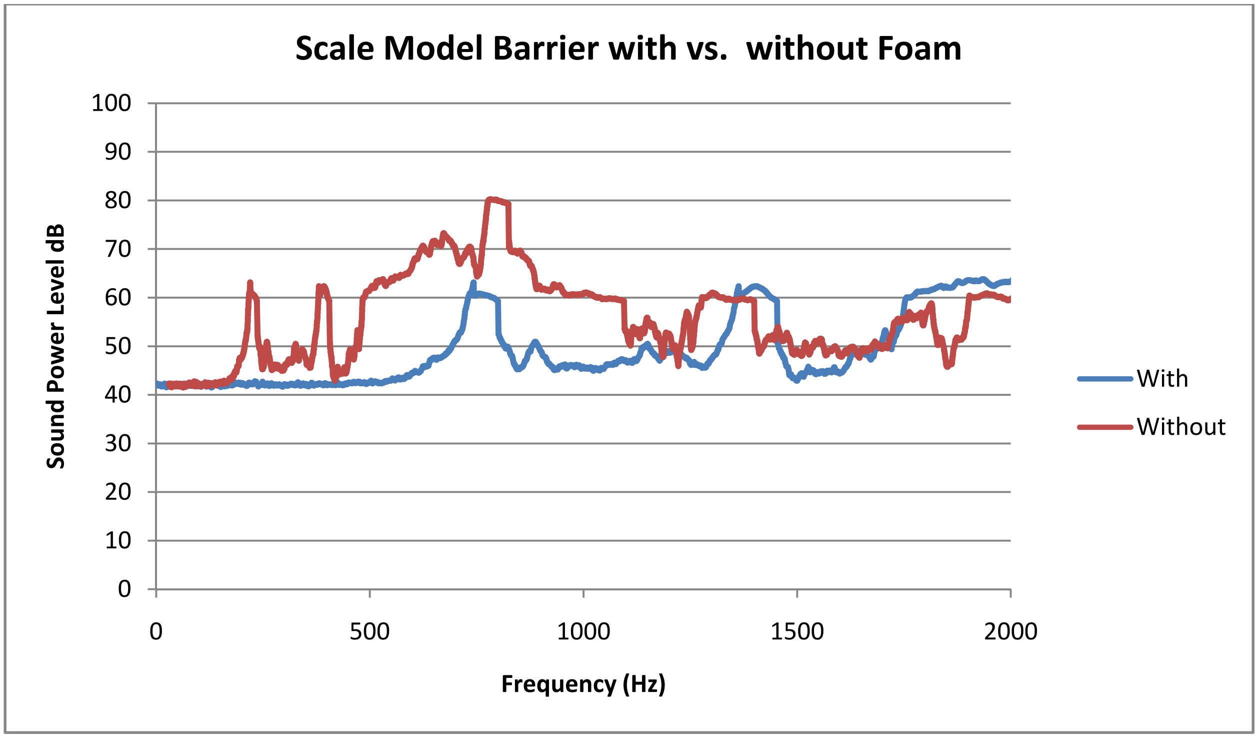
Scale Model Barrier with vs. without Foam
100
90
80
70
60
50
40
30
20
10
0
0
500
1000
1500
2000
Sound Power Level dB
Frequency (Hz)
With
Without

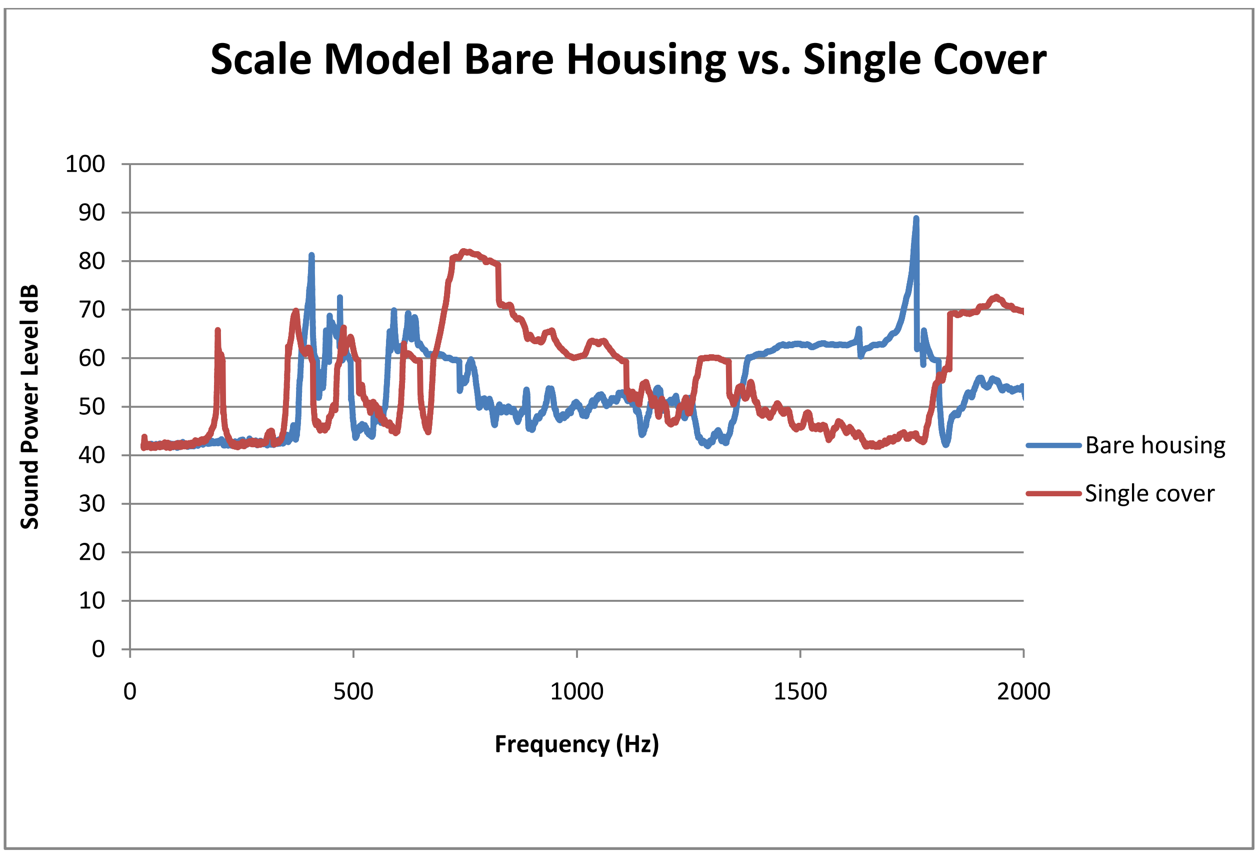
Scale Model Bare Housing vs. Single Cover
100
90
80
70
60
50
40
30
20
10
0
0
500
1000
1500
2000
Sound Power Level dB
Frequency (Hz)
Bare housing
Single cover

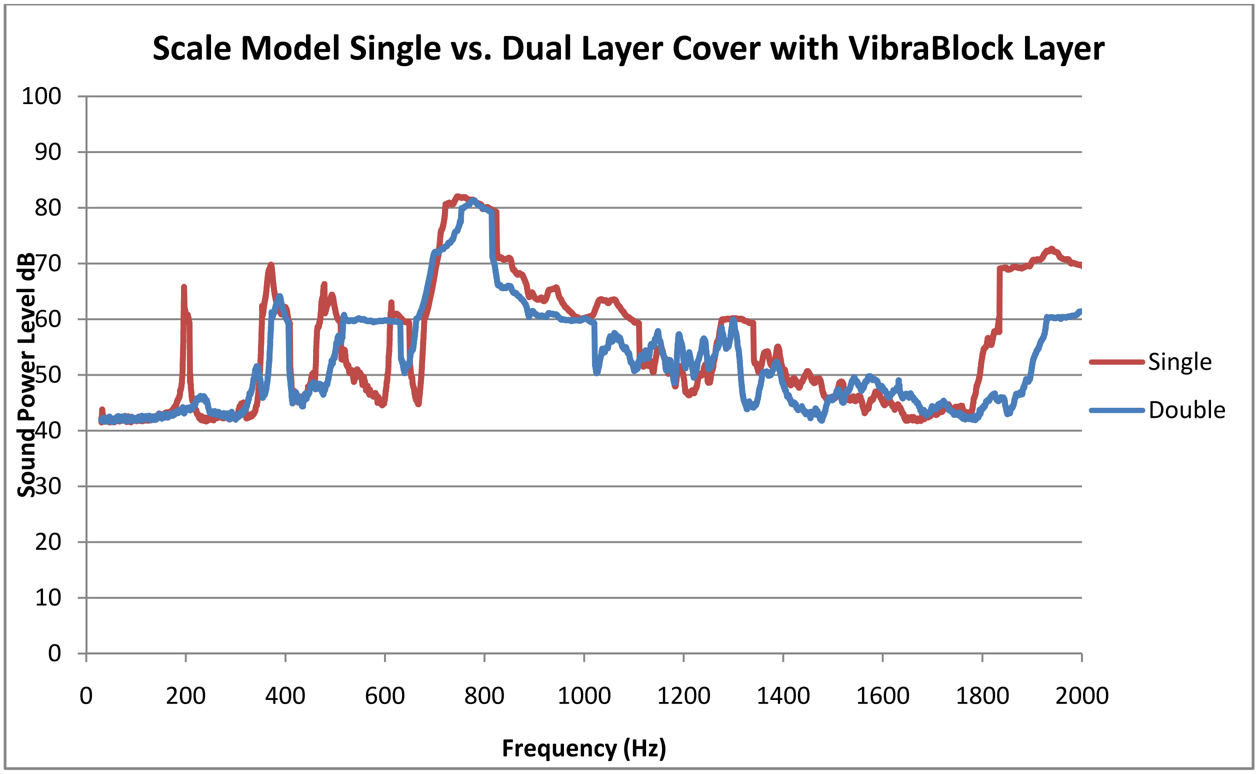

Scale Model Single vs. Dual Layer Cover with VibraBlock Layer
Sound Power Level dB
Frequency (Hz)
Single
Double
0
10
20
30
40
50
60
70
80
90
100
0
200
400
600
800
1000
1200
1400
1600
1800
2000

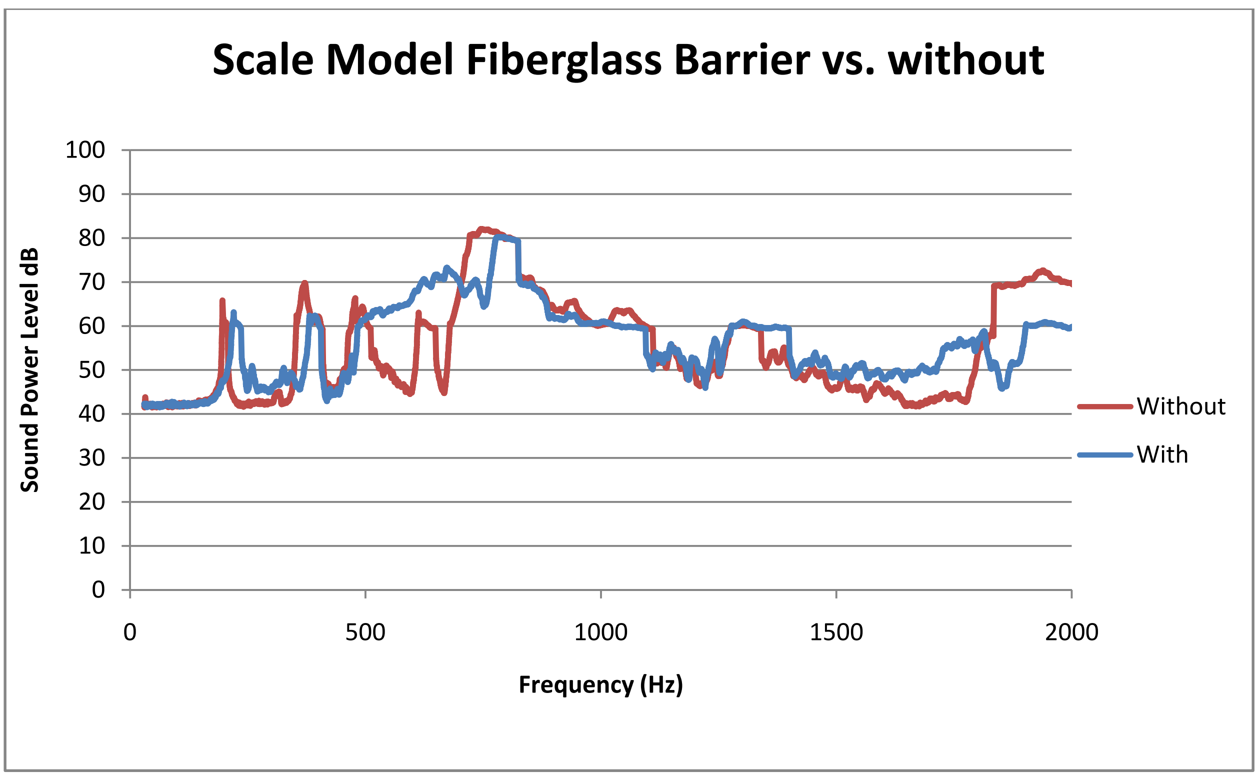

Scale Model Fiberglass Barrier vs. without
Sound Power Level dB
Frequency (Hz)
Without
With
0
10
20
30
40
50
60
70
80
90
100
0
500
1000
1500
2000

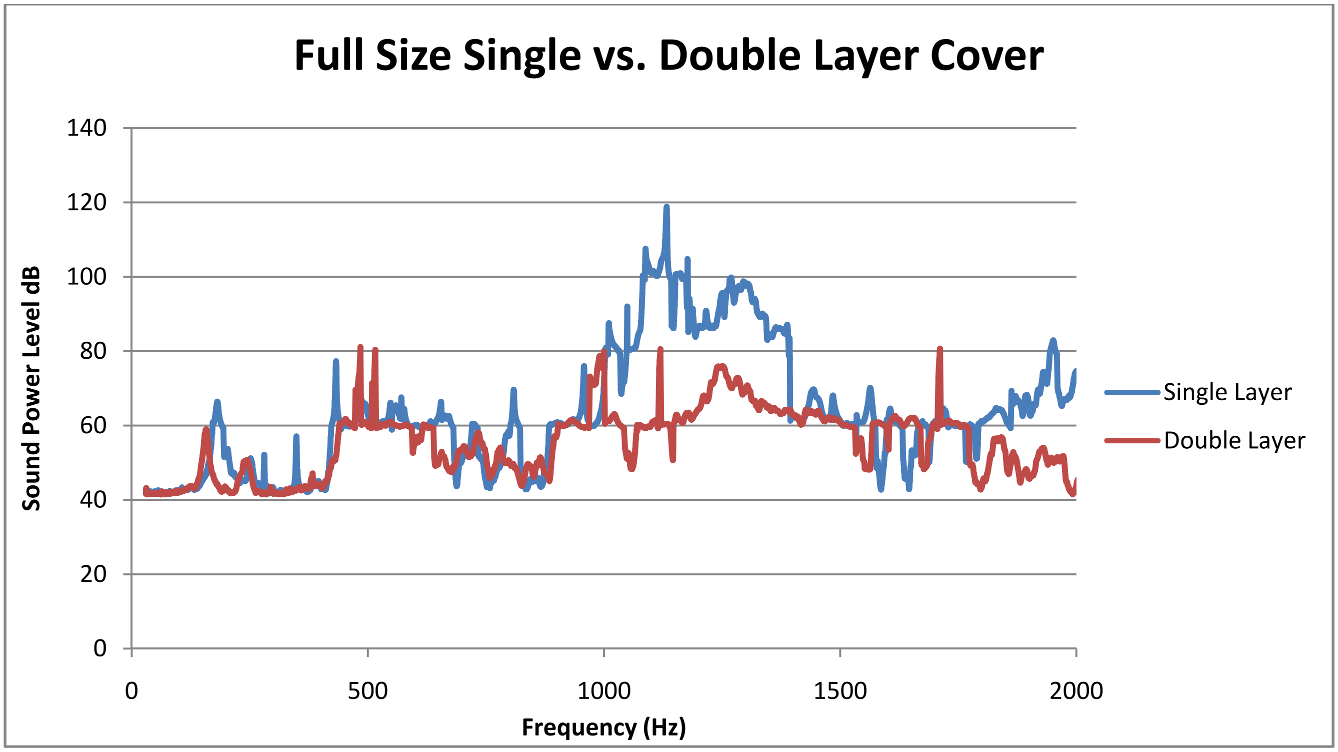

Full Size Single vs. Double Layer Cover
Sound Power Level dB
140
120
100
80
60
40
20
0
0
500
1000
1500
2000
Frequency (Hz)
Single Layer
Double Layer

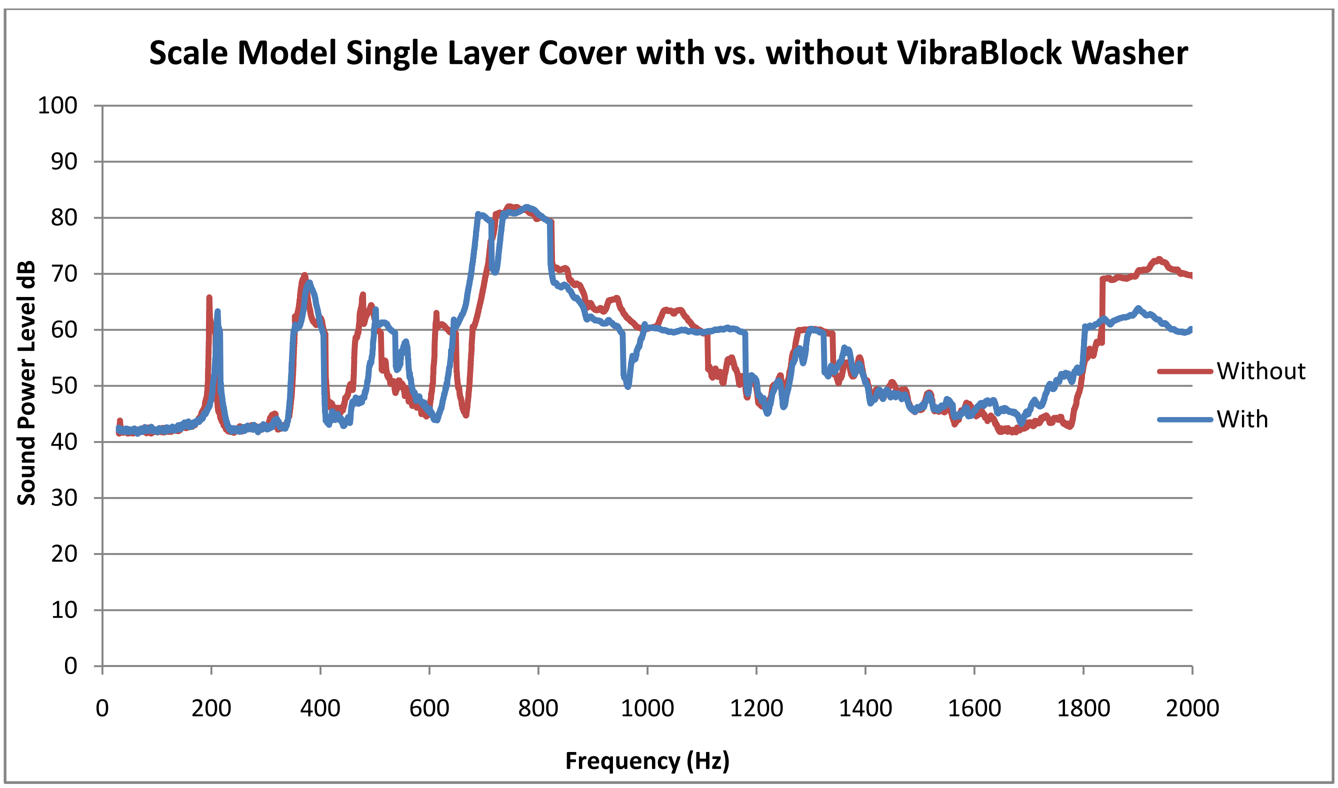

Scale Model Single Layer Cover with vs. without VibraBlock Washer
Sound Power Level dB
100
90
80
70
60
50
40
30
20
10
0
0
200
400
600
800
1000
1200
1400
1600
1800
2000
Frequency (Hz)
Without
With

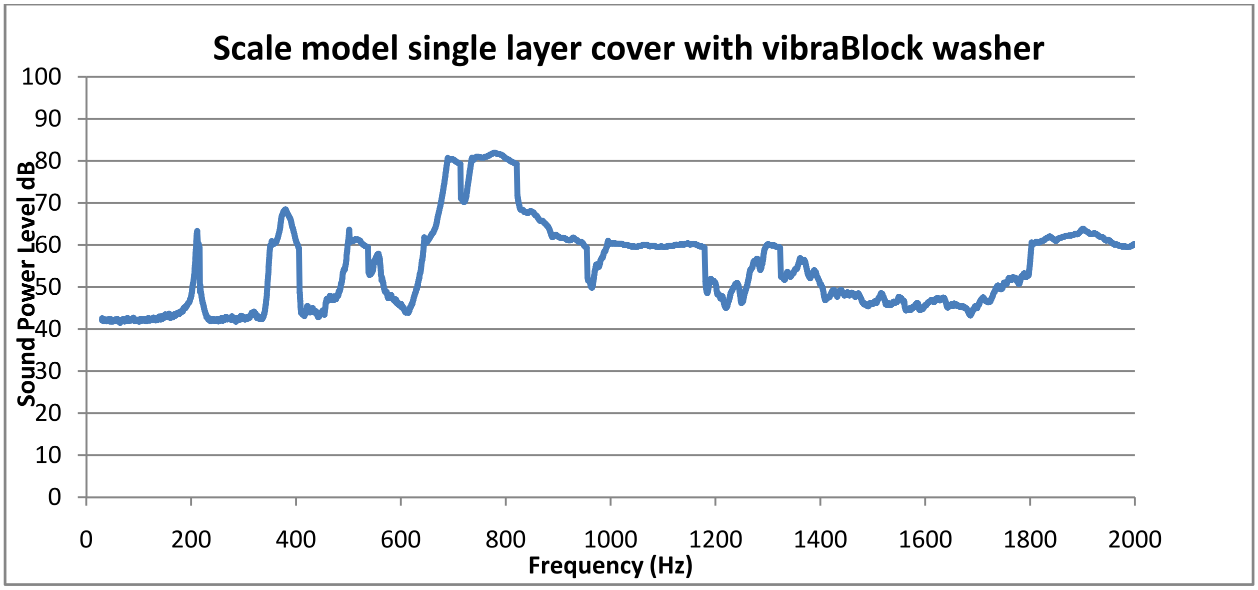
Scale model single layer cover with vibraBlock washer
Sound Power Level dB
Frequency (Hz)
0
10
20
30
40
50
60
70
80
90
100
0
200
400
600
800
1000
1200
1400
1600
1800
2000

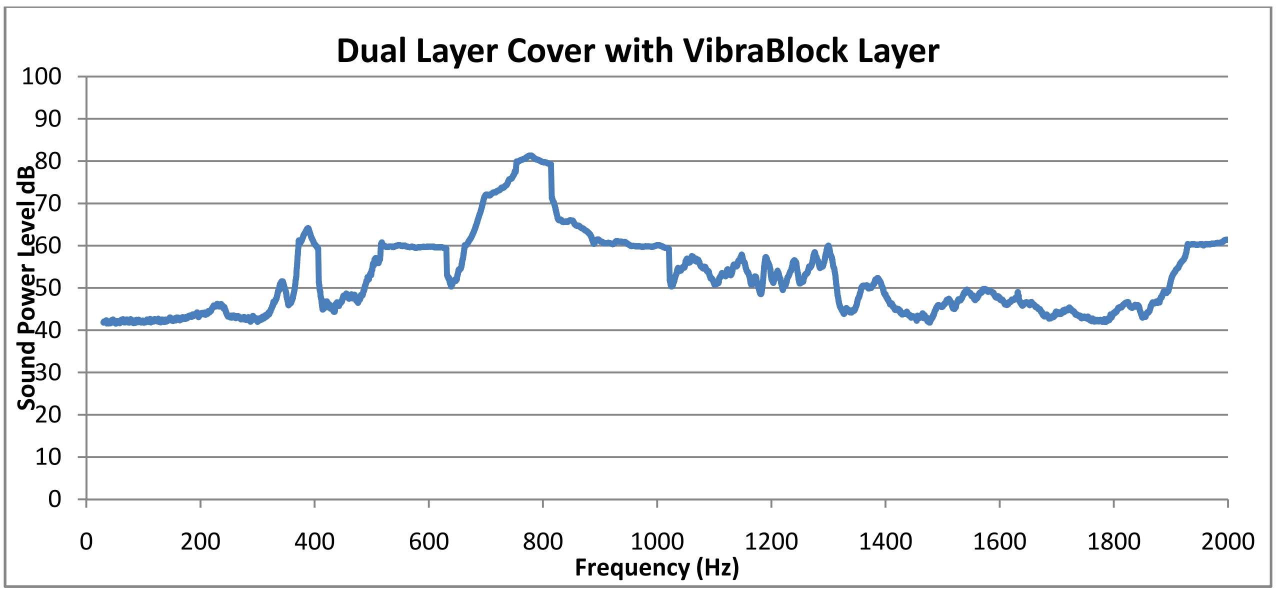
Dual Layer Cover with VibraBlock Layer
Sound Power Level dB
Frequency (Hz)
0
10
20
30
40
50
60
70
80
90
100
0
200
400
600
800
1000
1200
1400
1600
1800
2000

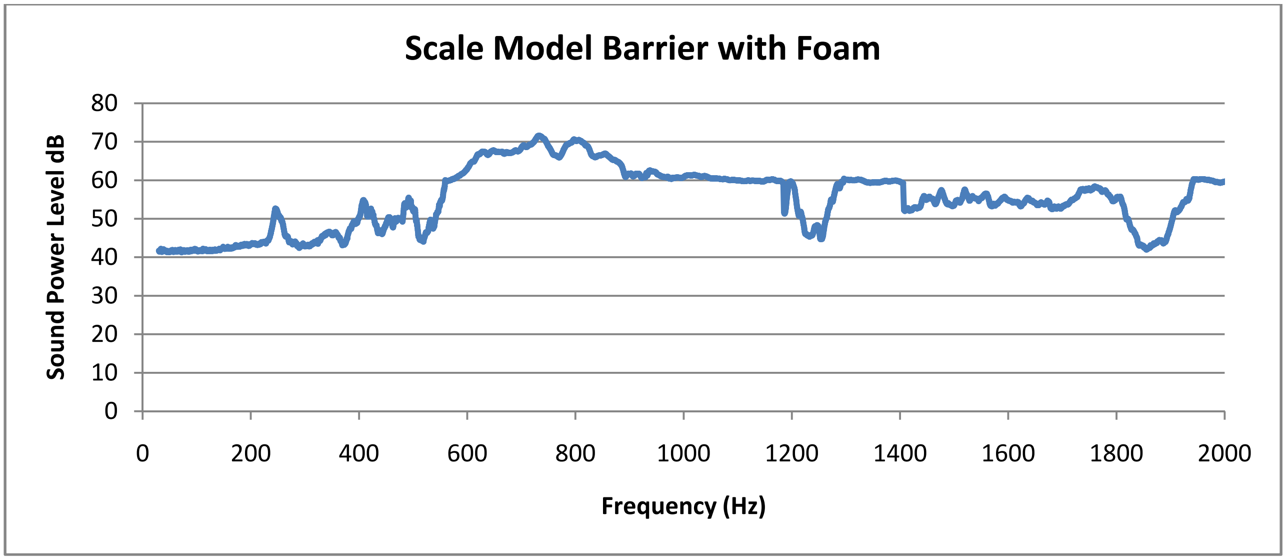

Scale Model Barrier with Foam
Sound Power Level dB
80
70
60
50
40
30
20
10
0
0
200
400
600
800
1000
1200
1400
1600
1800
2000
Frequency (Hz)

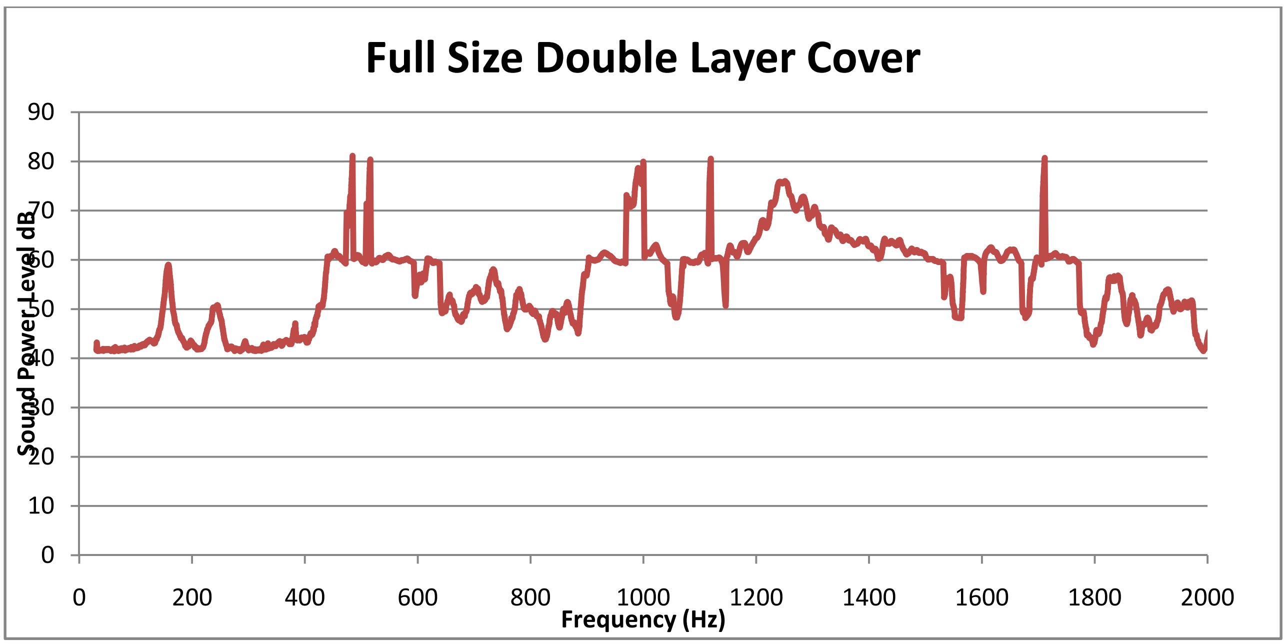

Full Size Double Layer Cover
Sound Power Level dB
90
80
70
60
50
40
30
20
10
0
0
200
400
600
800
1000
1200
1400
1600
1800
2000
Frequency (Hz)

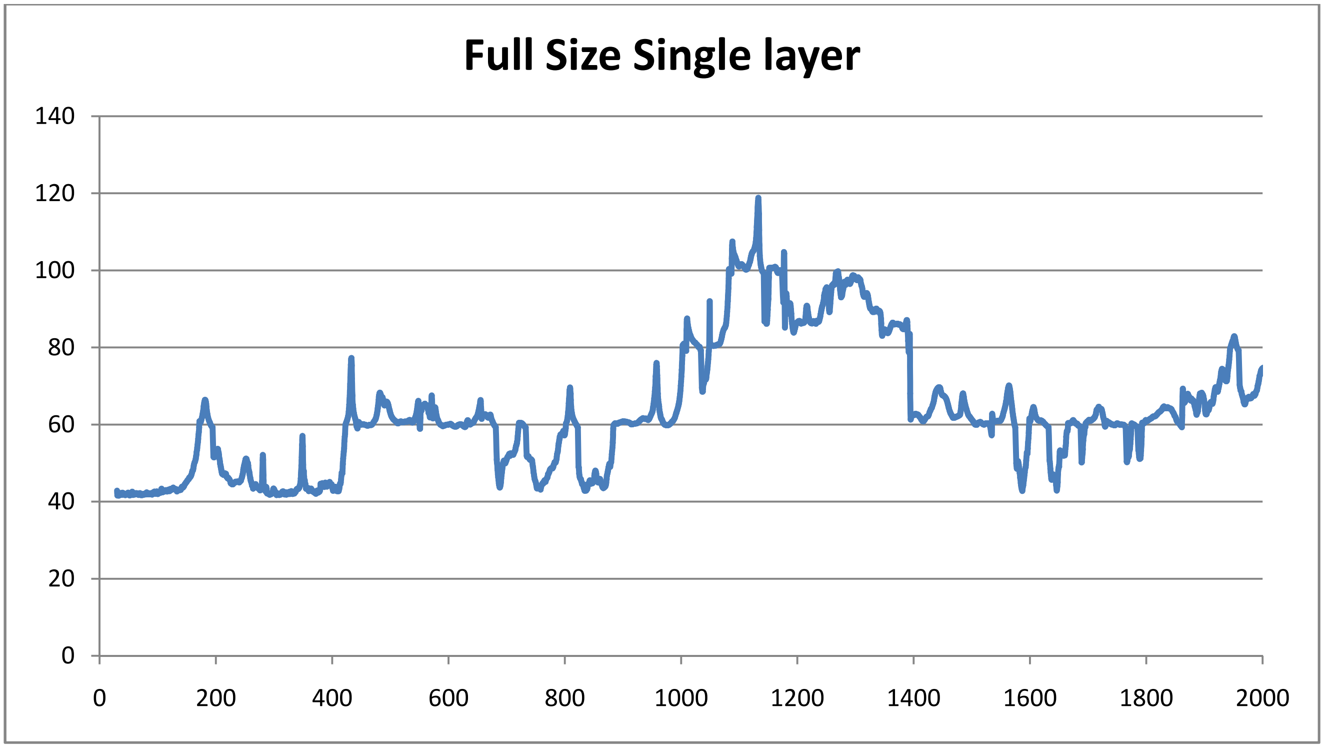

Full Size Single layer
140
120
100
80
60
40
20
0
0
200
400
600
800
1000
1200
1400
1600
1800
2000

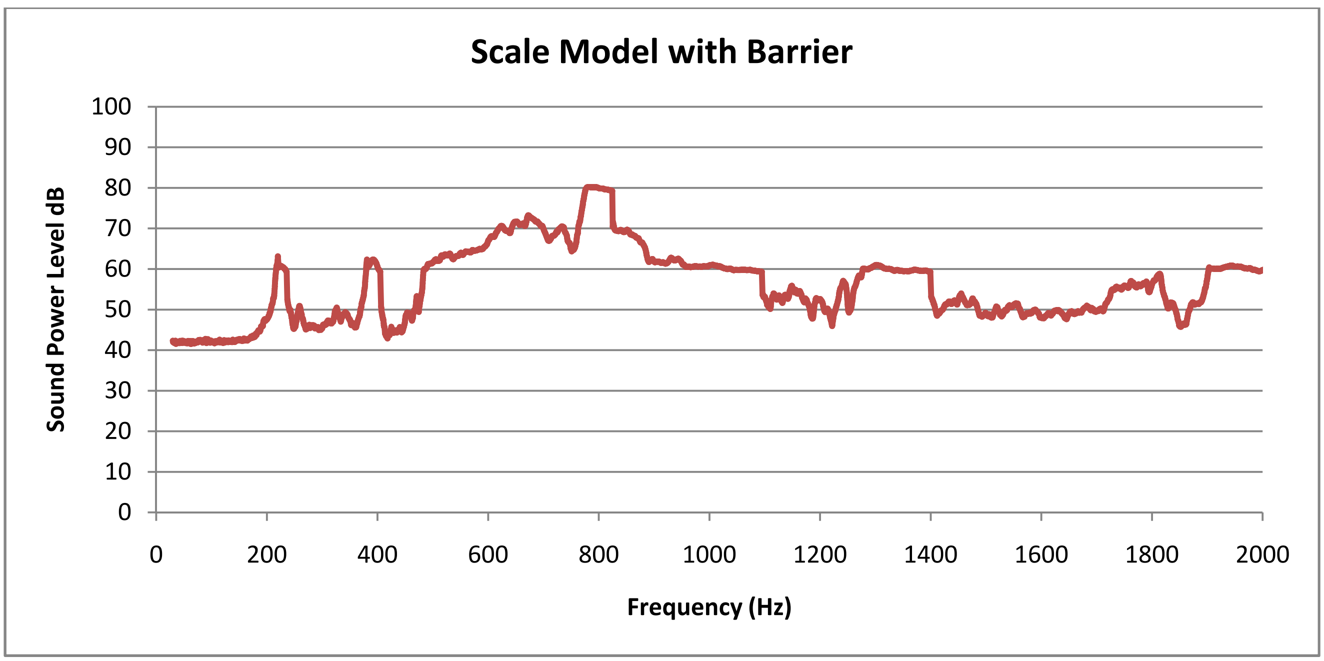

Scale Model with Barrier
Sound Power Level dB
100
90
80
70
60
50
40
30
20
10
0
0
200
400
600
800
1000
1200
1400
1600
1800
2000
Frequency (Hz)

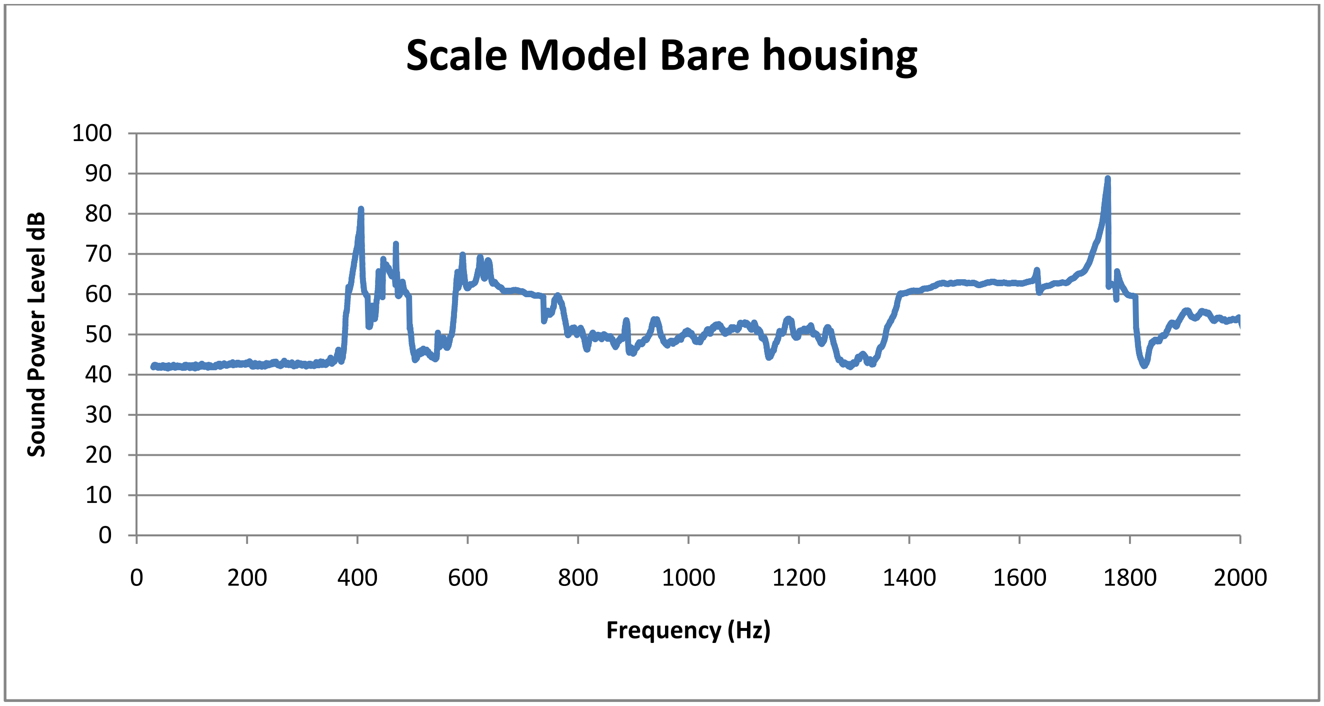
Scale Model Bare housing
Sound Power Level dB
Frequency (Hz)
100
90
80
70
60
50
40
30
20
10
0
0
200
400
600
800
1000
1200
1400
1600
1800
2000

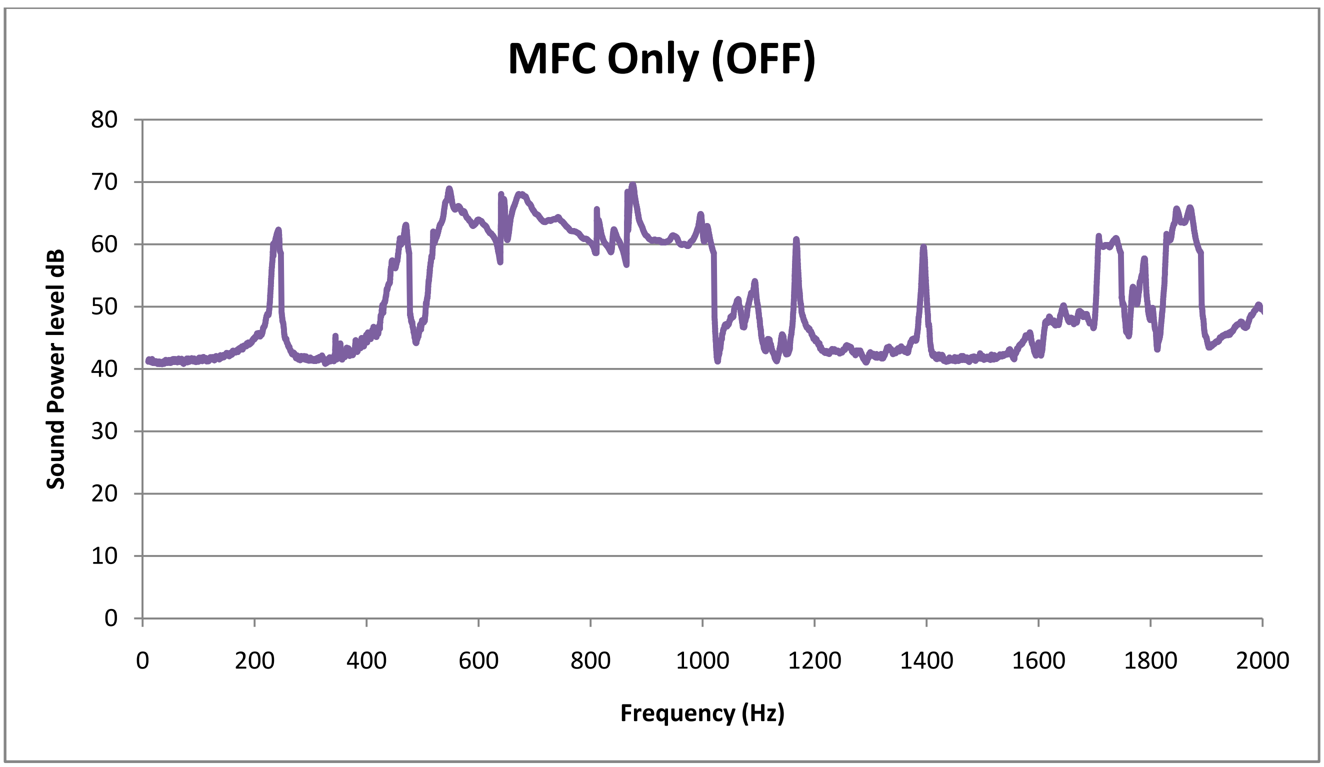
MFC Only (OFF)
Sound Power level dB
Frequency (Hz)
80
70
60
50
40
30
20
10
0
0
200
400
600
800
1000
1200
1400
1600
1800
2000

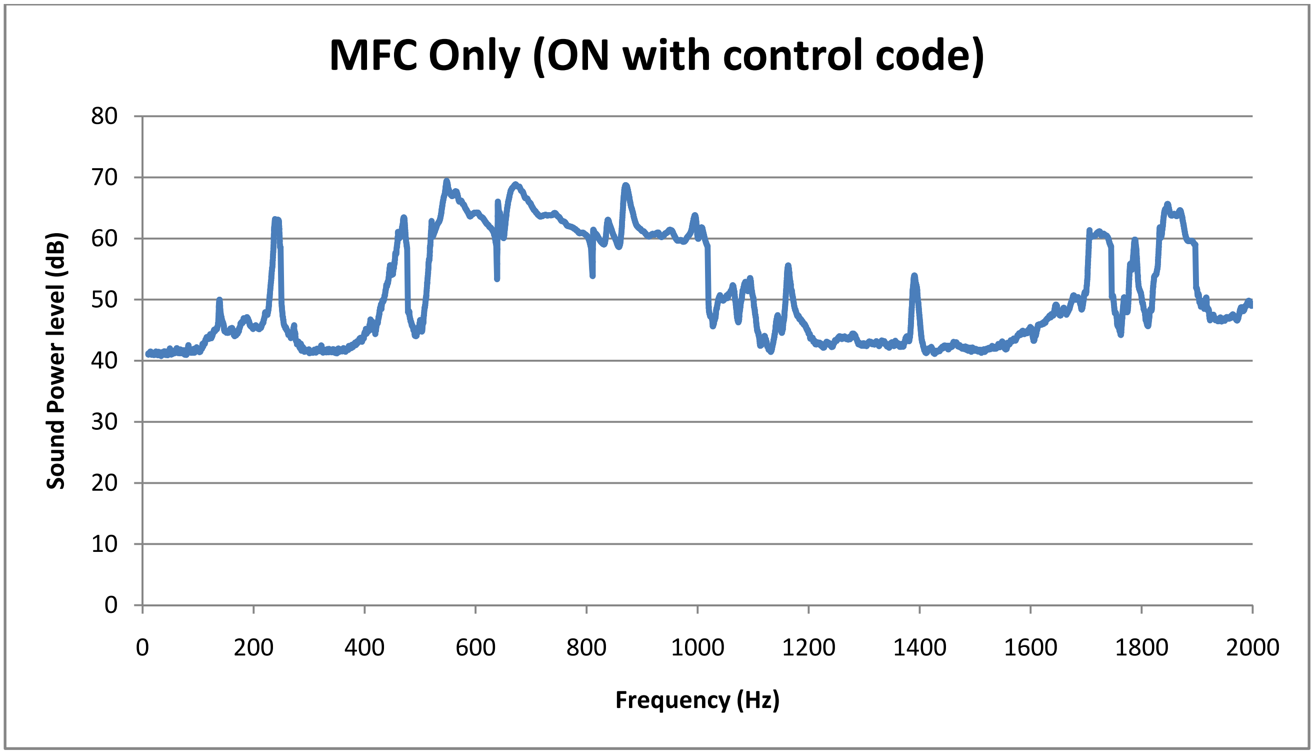

MFC Only (ON with control code)
Sound Power level (dB)
Frequency (Hz)
0
10
20
30
40
50
60
70
80
0
200
400
600
800
1000
1200
1400
1600
1800
2000

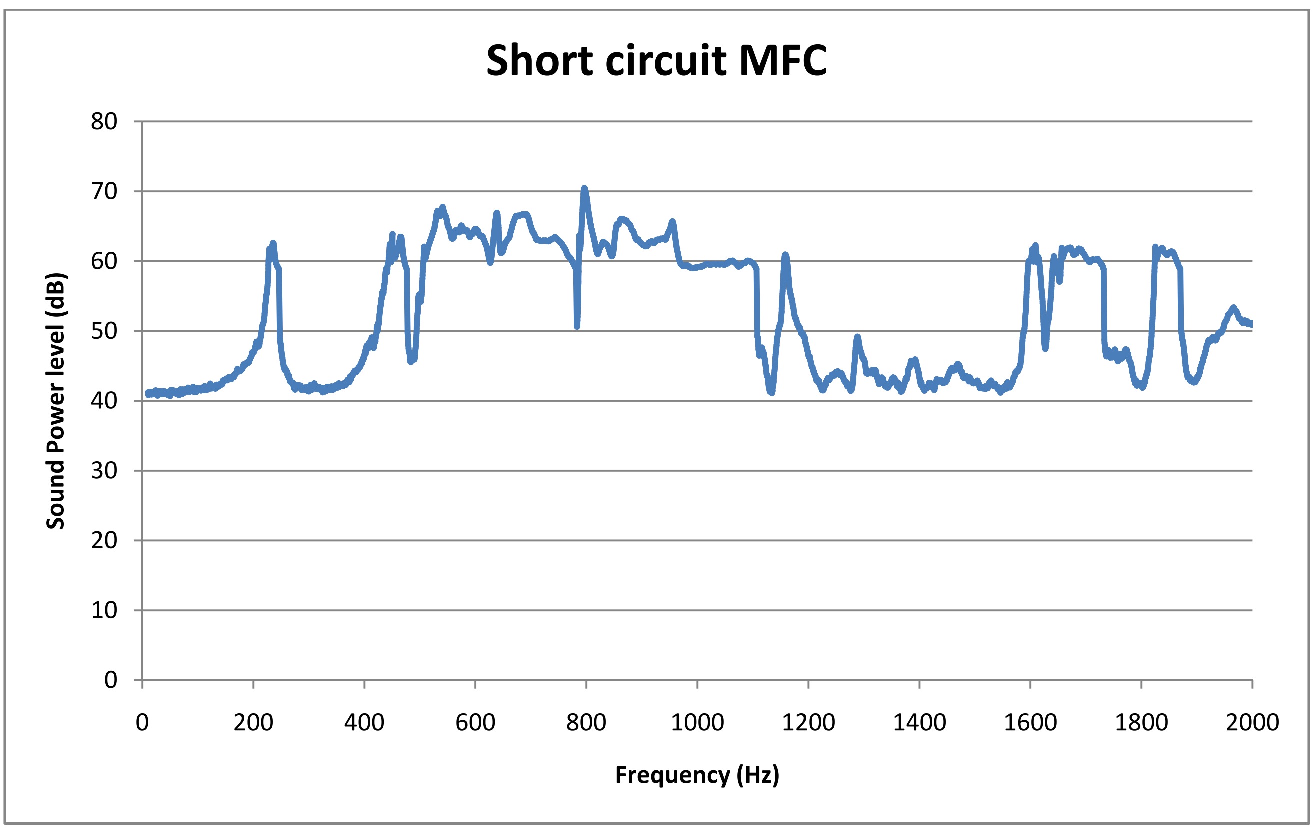

Short circuit MFC
Sound Power level (dB)
Frequency (Hz)
0
10
20
30
40
50
60
70
80
0
200
400
600
800
1000
1200
1400
1600
1800
2000

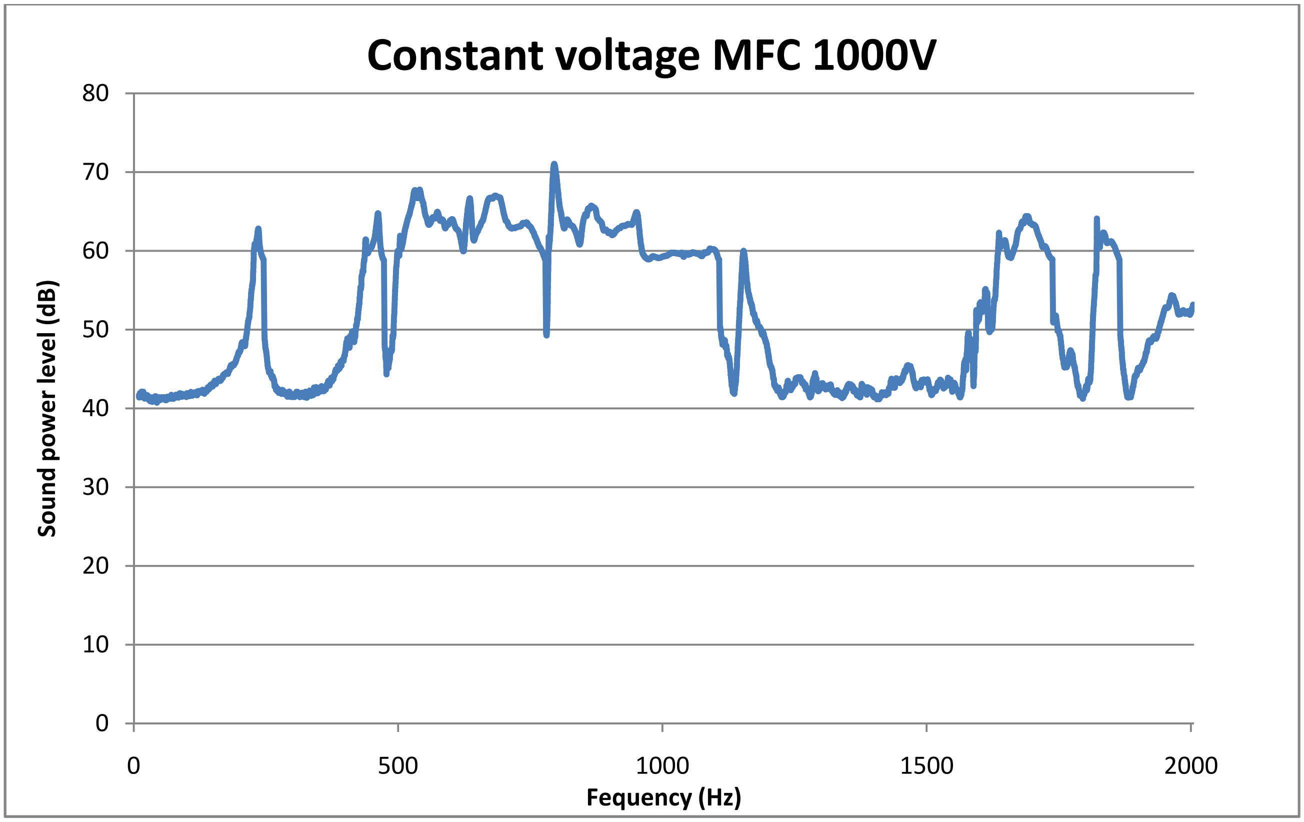
Constant voltage MFC 1000V
Sound power level (dB)
0
10
20
30
40
50
60
70
80
0
500
1000
1500
2000
Fequency (Hz)

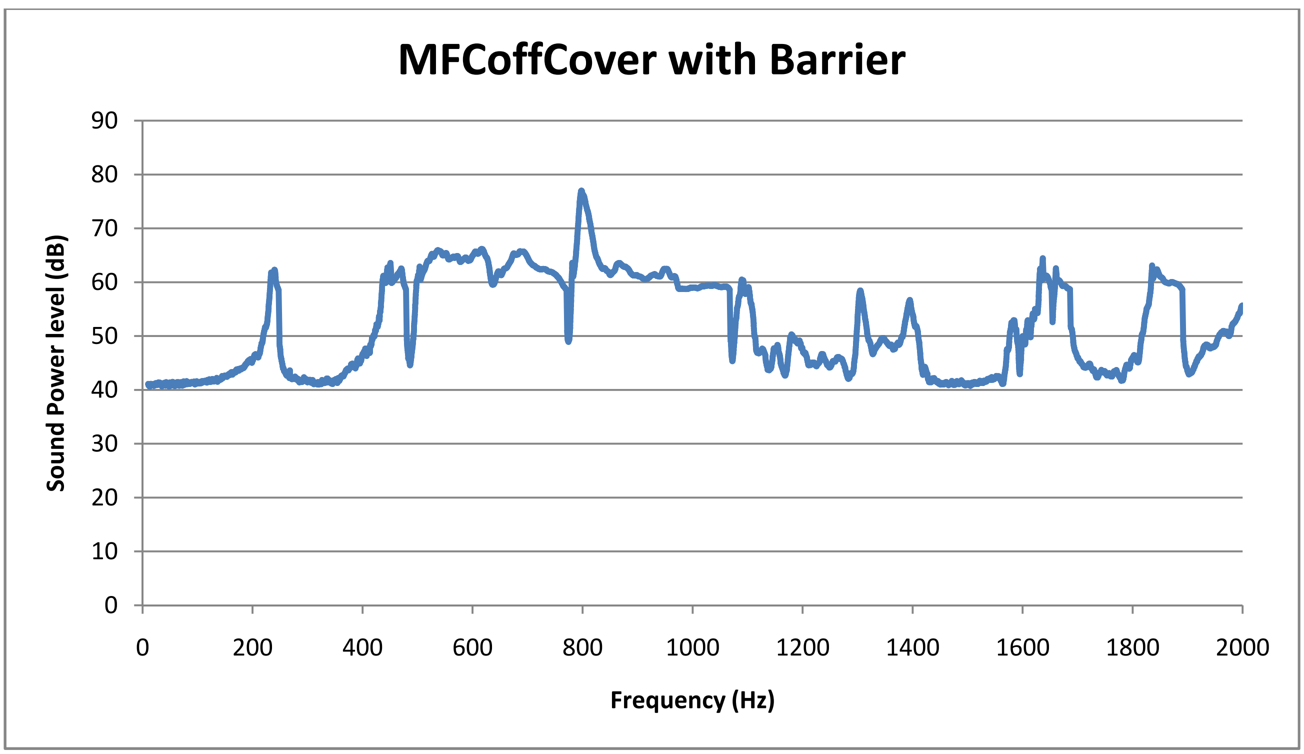
MFCoffCover with Barrier
Sound Power level (dB)
0
10
20
30
40
50
60
70
80
90
0
200
400
600
800
1000
1200
1400
1600
1800
2000
Frequency (Hz)

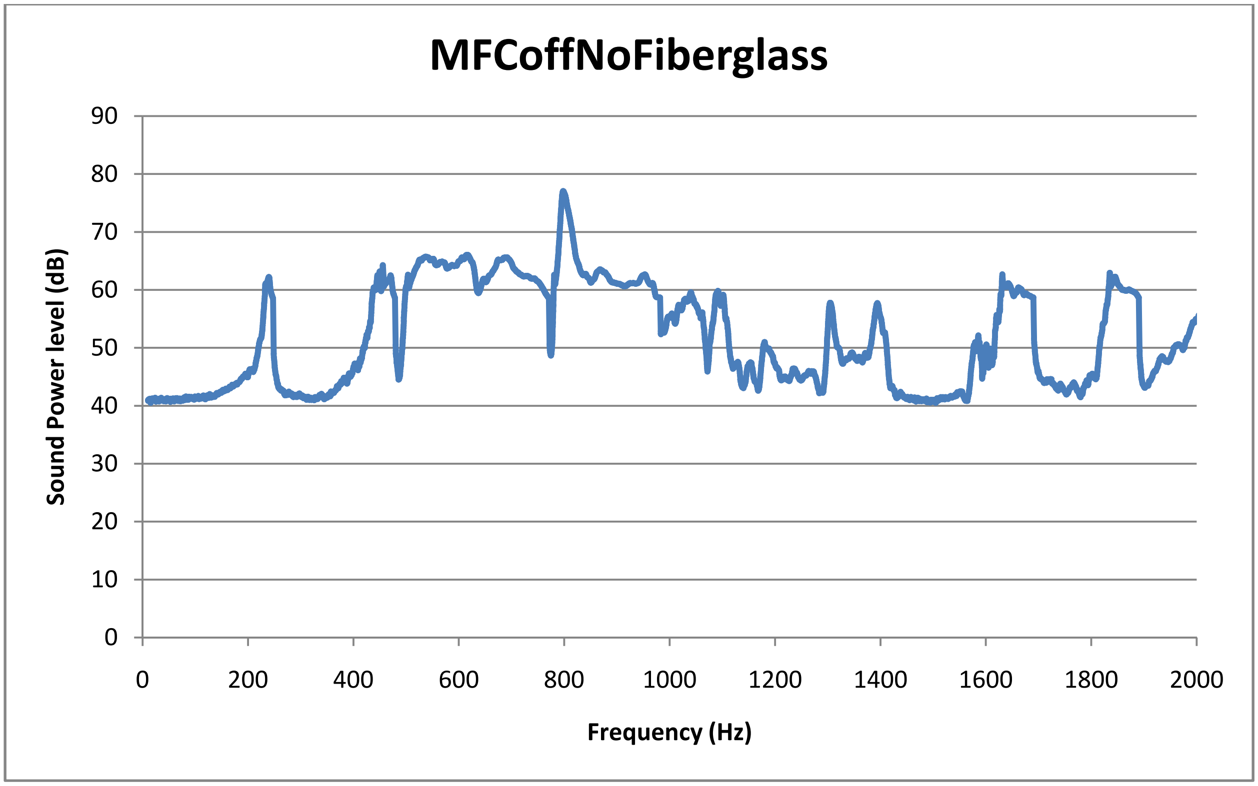
MFCoffNoFiberglass
Sound Power level (dB)
0
10
20
30
40
50
60
70
80
90
0
200
400
600
800
1000
1200
1400
1600
1800
2000
Frequency (Hz)

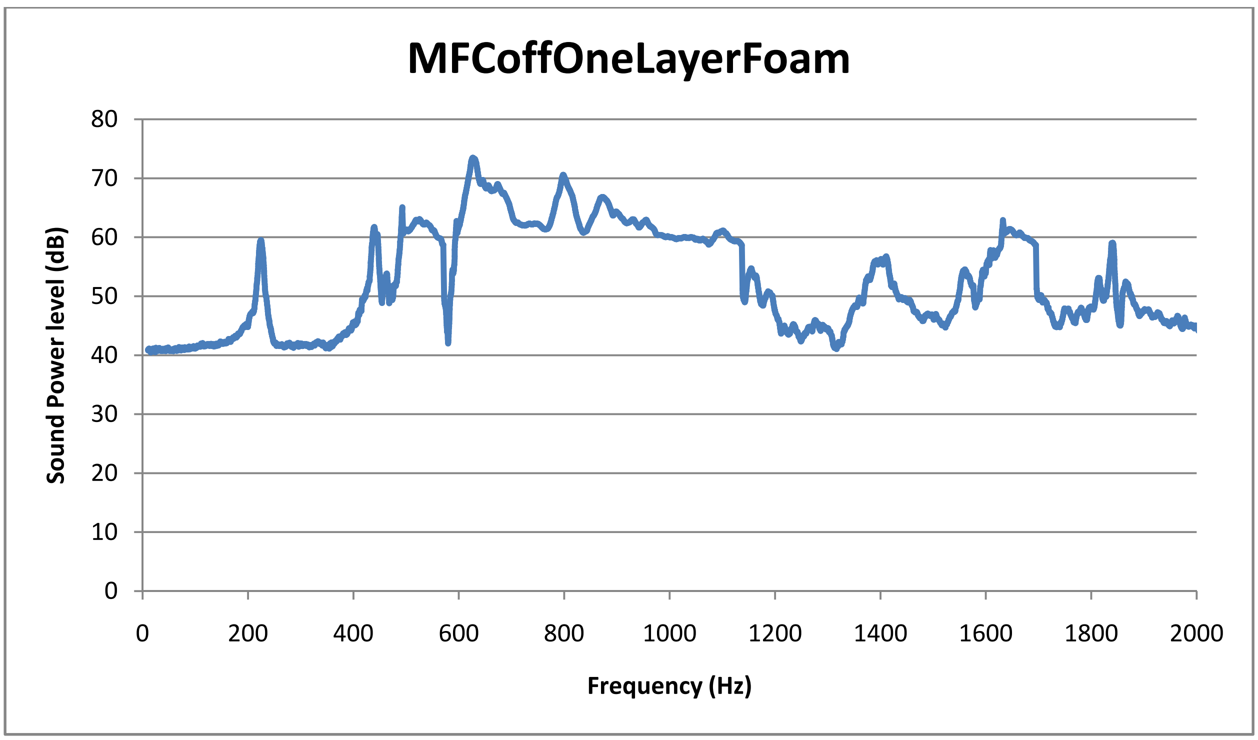
MFCoffOneLayerFoam
Sound Power level (dB)
0
10
20
30
40
50
60
70
80
0
200
400
600
800
1000
1200
1400
1600
1800
2000
Frequency (Hz)

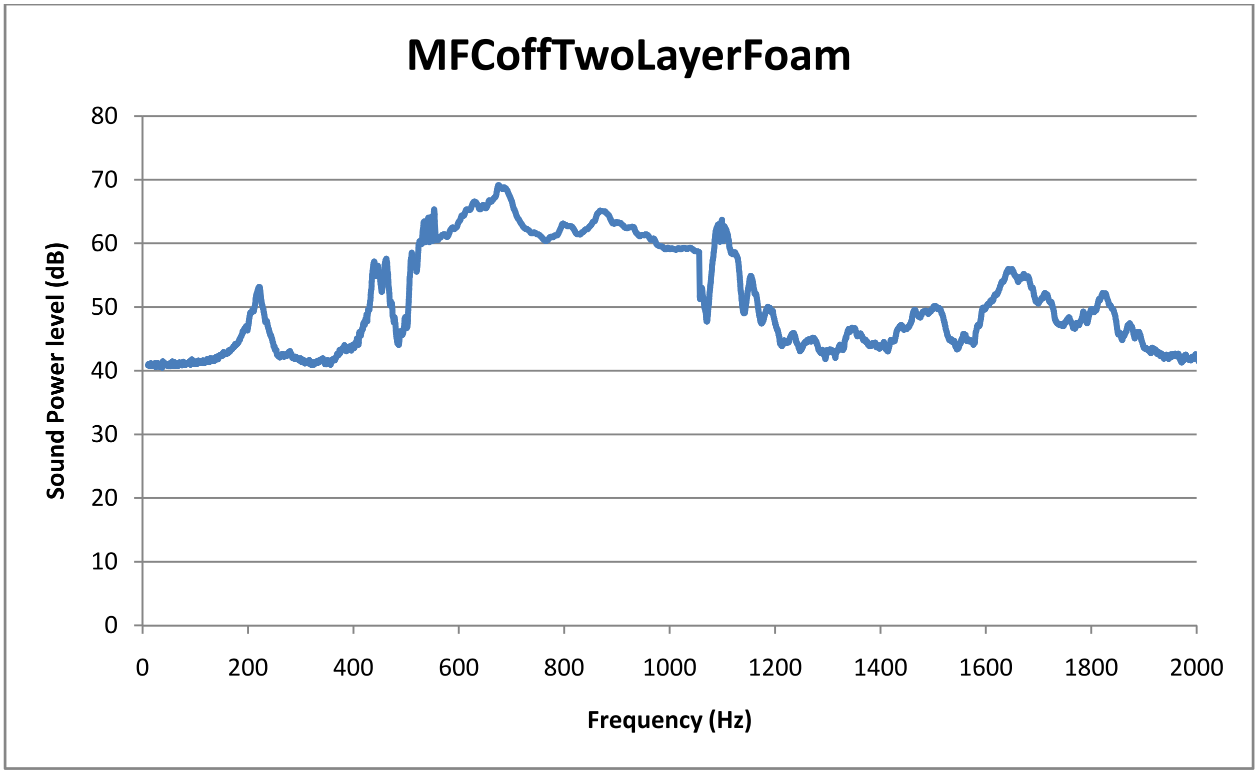
MFCoffTwoLayerFoam
Sound Power level (dB)
Frequency (Hz)
0
10
20
30
40
50
60
70
80
0
200
400
600
800
1000
1200
1400
1600
1800
2000

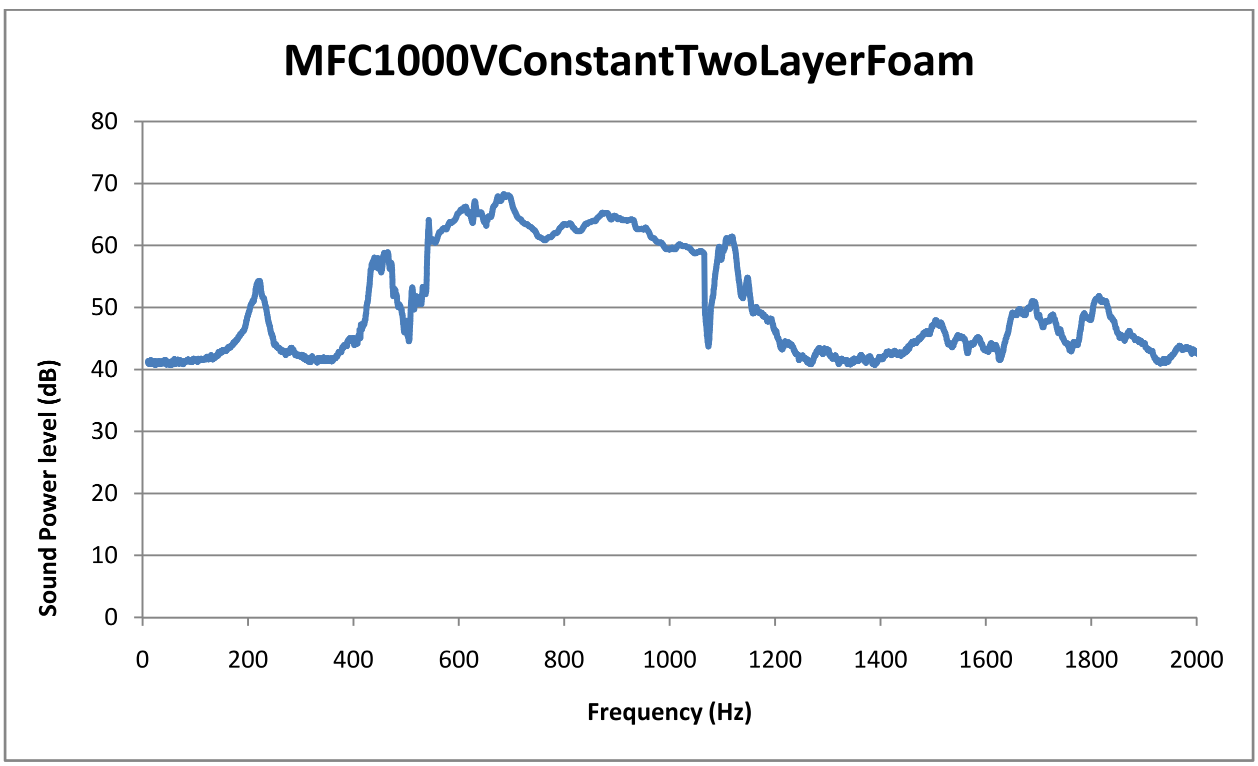
MFC1000VConstantTwoLayerFoam
Sound Power level (dB)
Frequency (Hz)
0
10
20
30
40
50
60
70
80
0
200
400
600
800
1000
1200
1400
1600
1800
2000

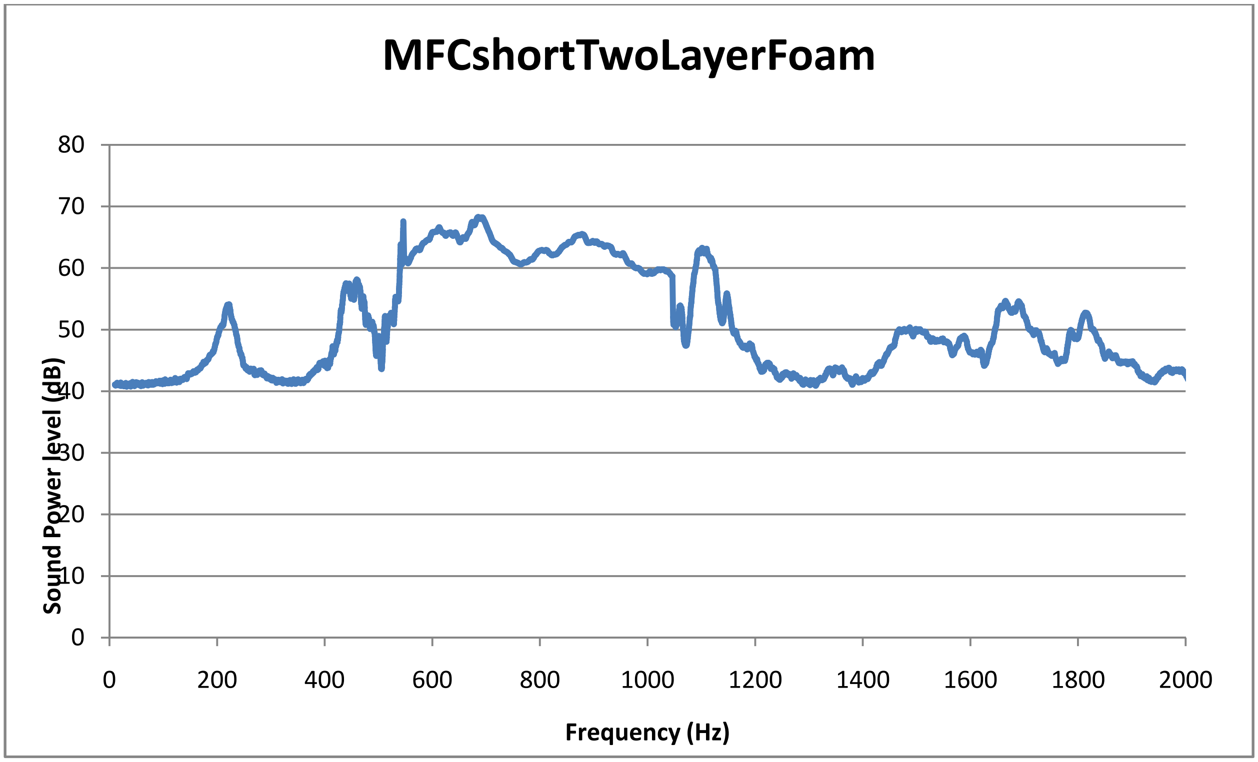
MFCshortTwoLayerFoam
Sound Power level (dB)
Frequency (Hz)
0
10
20
30
40
50
60
70
80
0
200
400
600
800
1000
1200
1400
1600
1800
2000

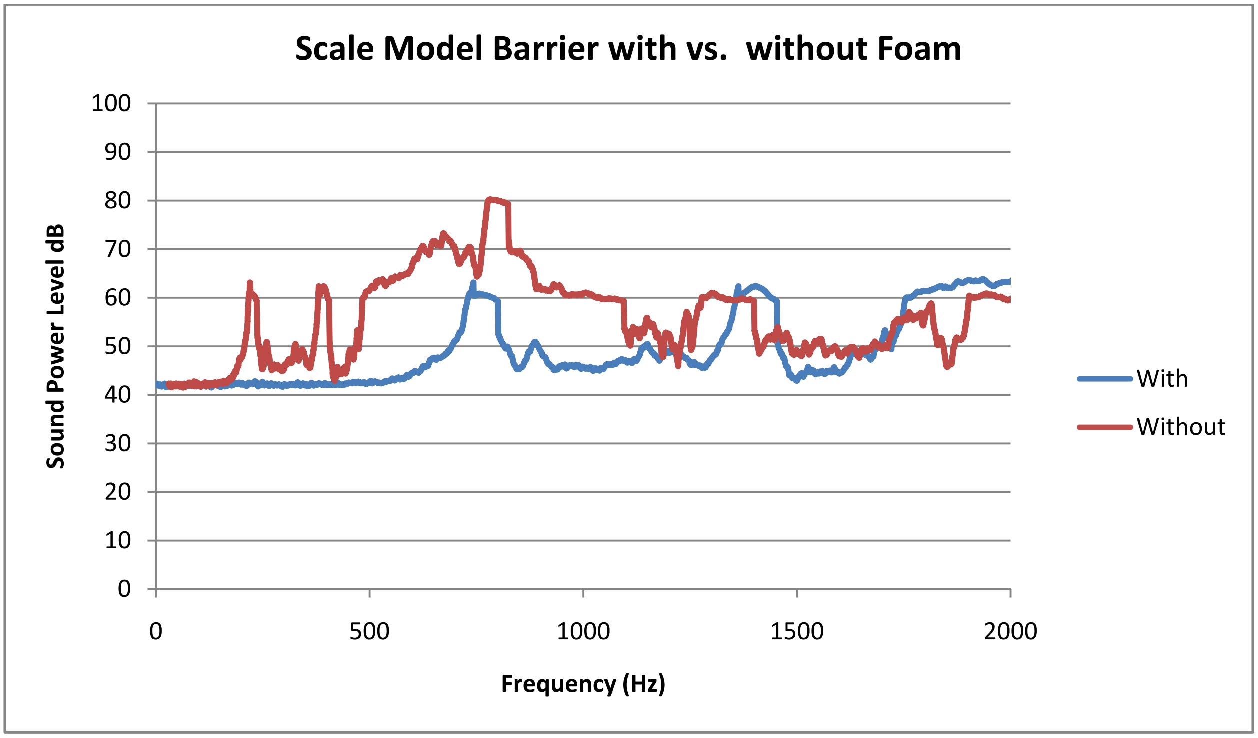

Scale Model Barrier with vs. without Foam
Sound Power Level dB
100
90
80
70
60
50
40
30
20
10
0
0
500
1000
1500
2000
Frequency (Hz)
With
Without

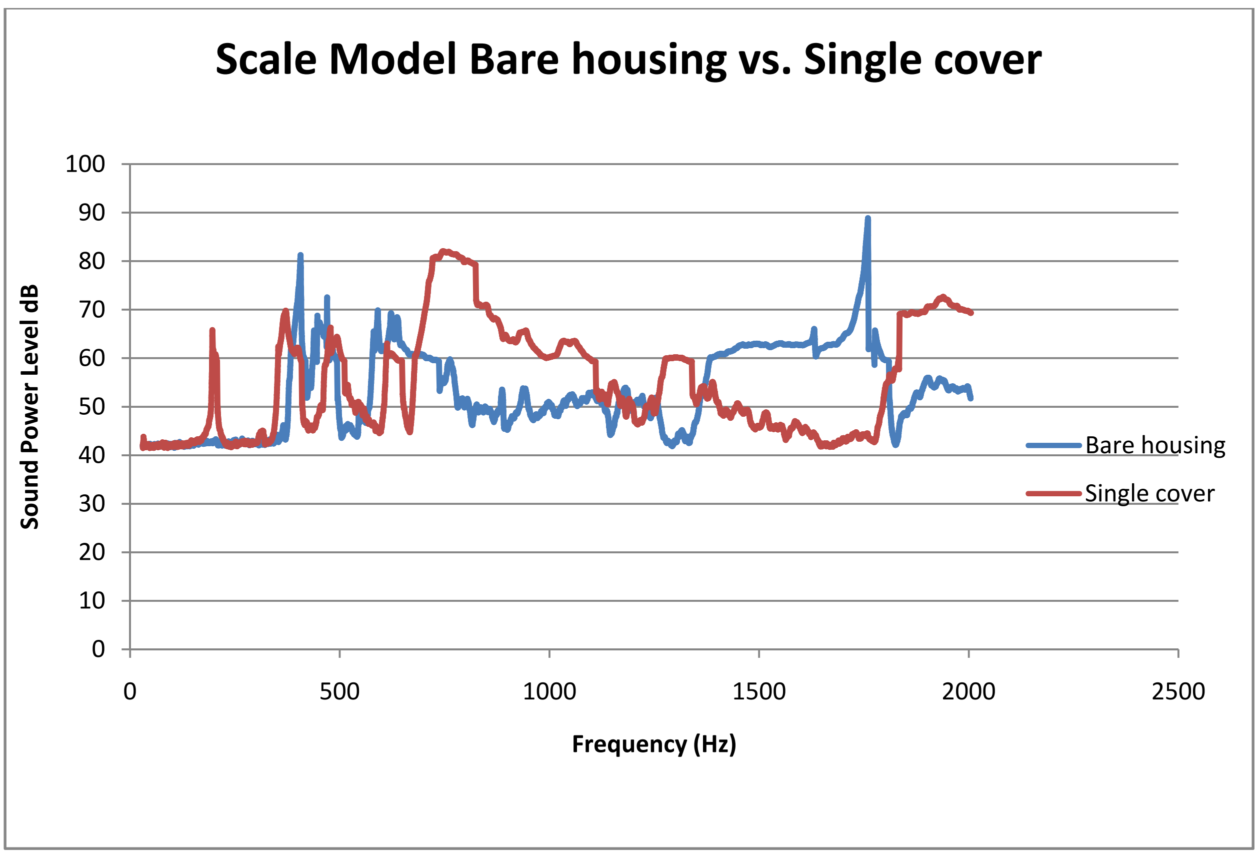

Scale Model Bare housing vs. Single cover
Sound Power Level dB
100
90
80
70
60
50
40
30
20
10
0
0
500
1000
1500
2000
2500
Frequency (Hz)
Bare housing
Single cover

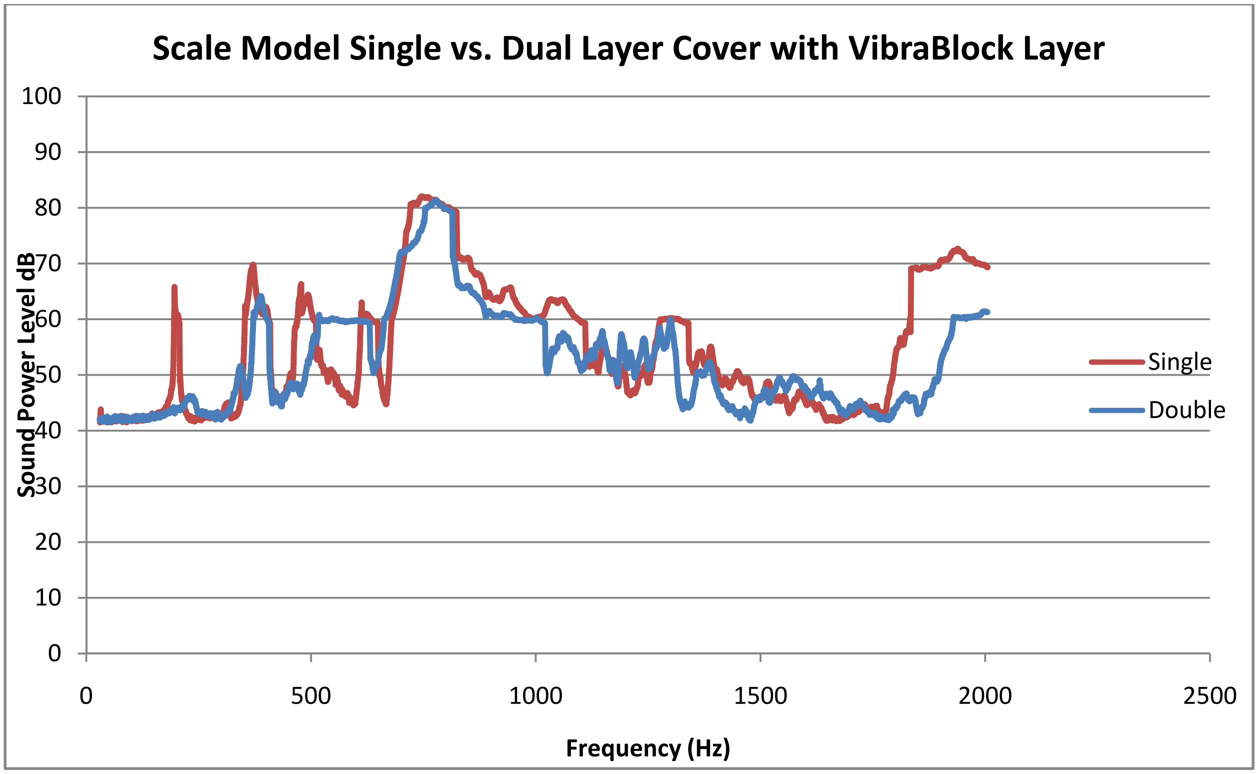
Scale Model Single vs. Dual Layer Cover with VibraBlock Layer
Sound Power Level dB
Frequency (Hz)
Single
Double
0
10
20
30
40
50
60
70
80
90
100
0
500
1000
1500
2000
2500

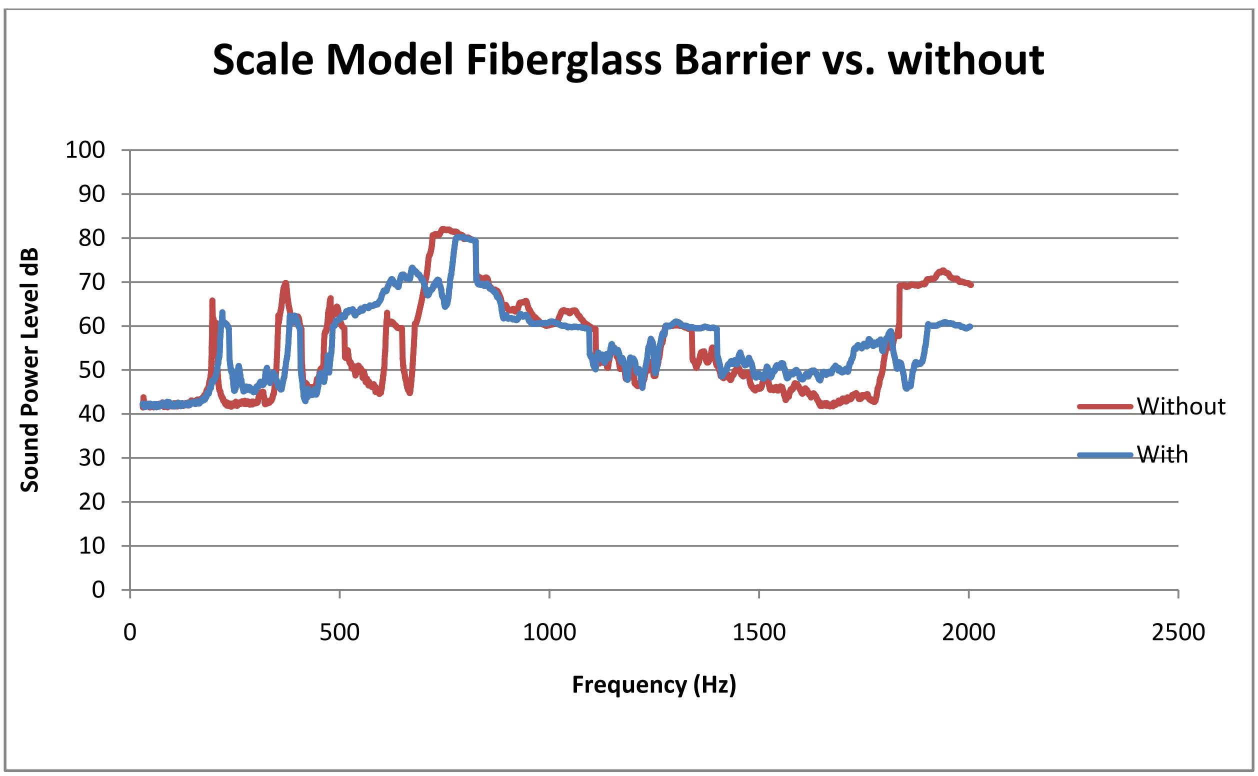
Scale Model Fiberglass Barrier vs. without
Sound Power Level dB
Frequency (Hz)
Without
With
0
10
20
30
40
50
60
70
80
90
100
0
500
1000
1500
2000
2500

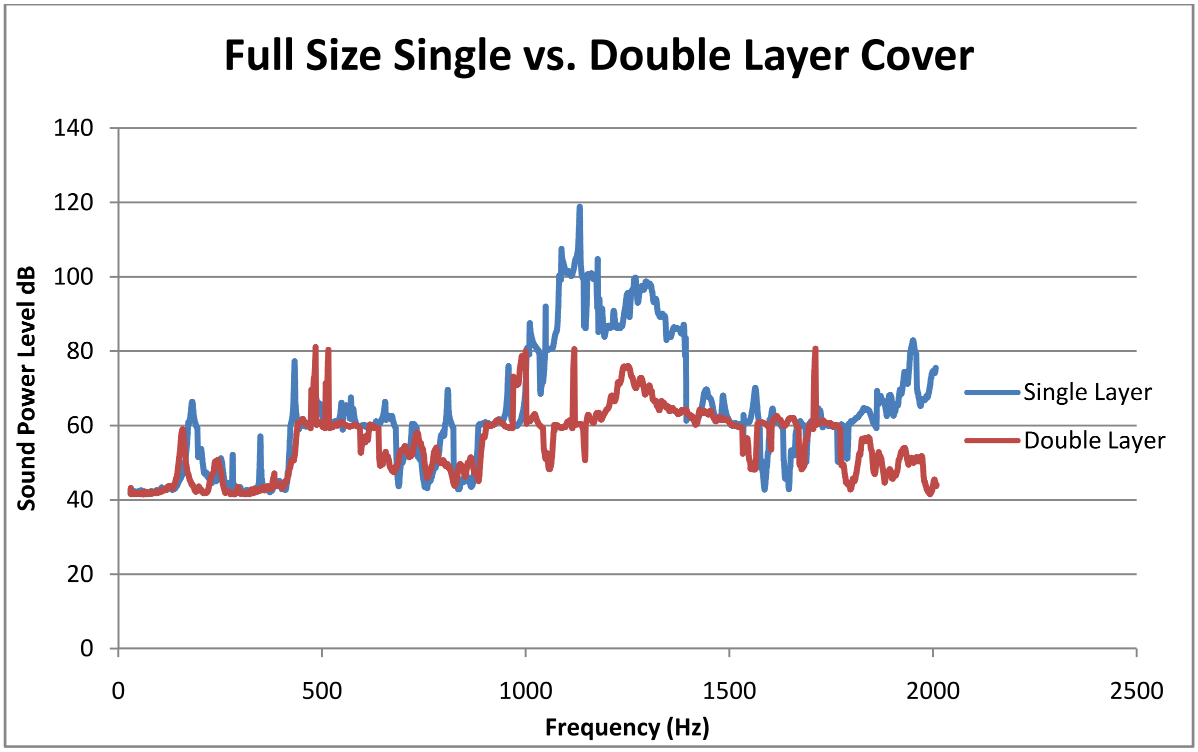

Full Size Single vs. Double Layer Cover
Sound Power Level dB
140
120
100
80
60
40
20
0
0
500
1000
1500
2000
2500
Frequency (Hz)
Single Layer
Double Layer

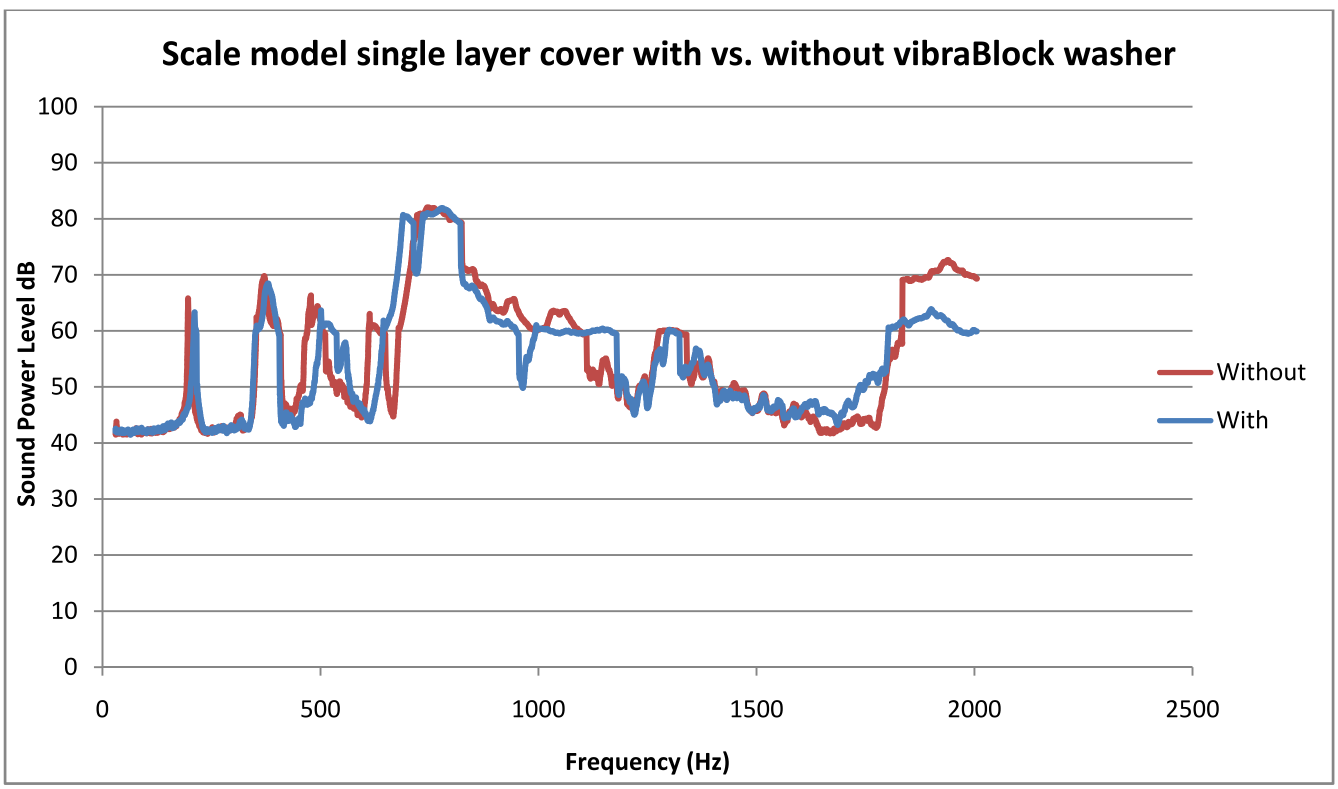

Scale model single layer cover with vs. without vibraBlock washer
Sound Power Level dB
100
90
80
70
60
50
40
30
20
10
0
0
500
1000
1500
2000
2500
Frequency (Hz)
Without
With

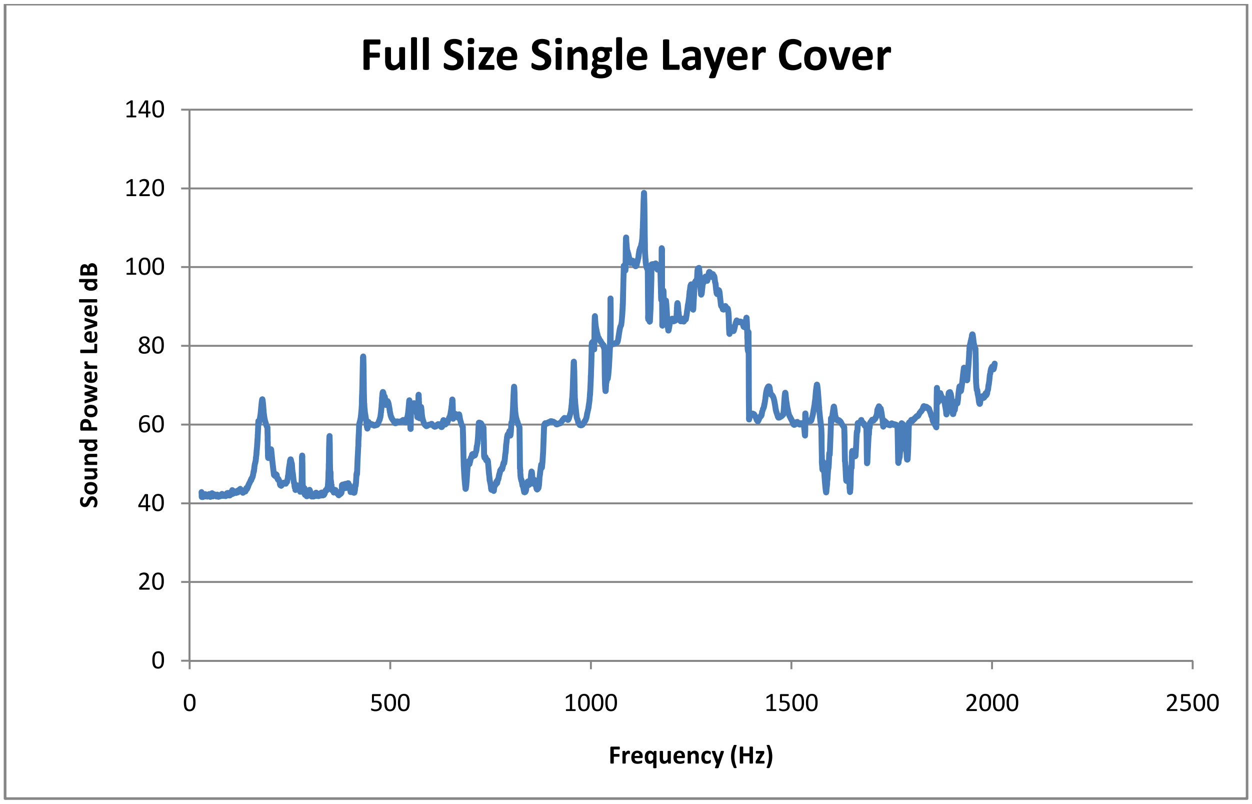
Full Size Single Layer Cover
Sound Power Level dB
140
120
100
80
60
40
20
0
0
500
1000
1500
2000
2500
Frequency (Hz)

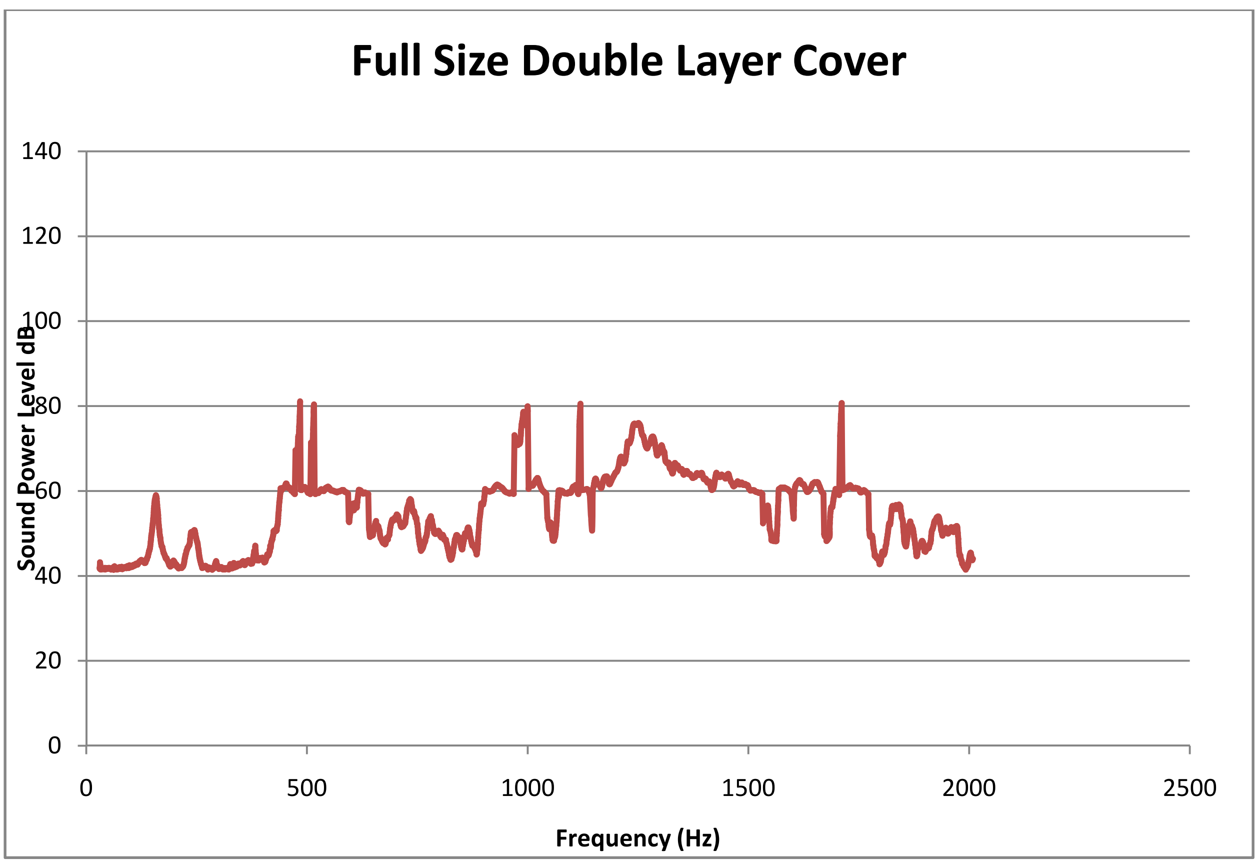
Full Size Double Layer Cover
Sound Power Level dB
140
120
100
80
60
40
20
0
0
500
1000
1500
2000
2500
Frequency (Hz)

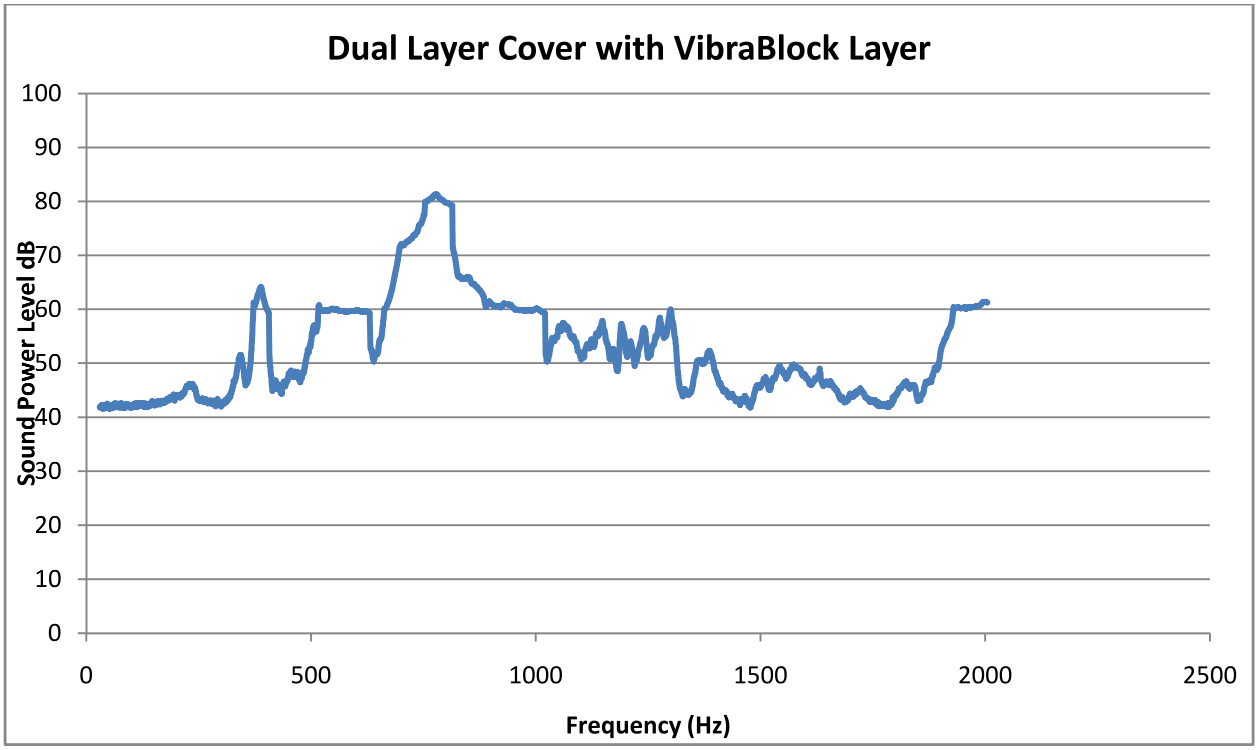
Dual Layer Cover with VibraBlock Layer
Sound Power Level dB
Frequency (Hz)
0
10
20
30
40
50
60
70
80
90
100
0
500
1000
1500
2000
2500

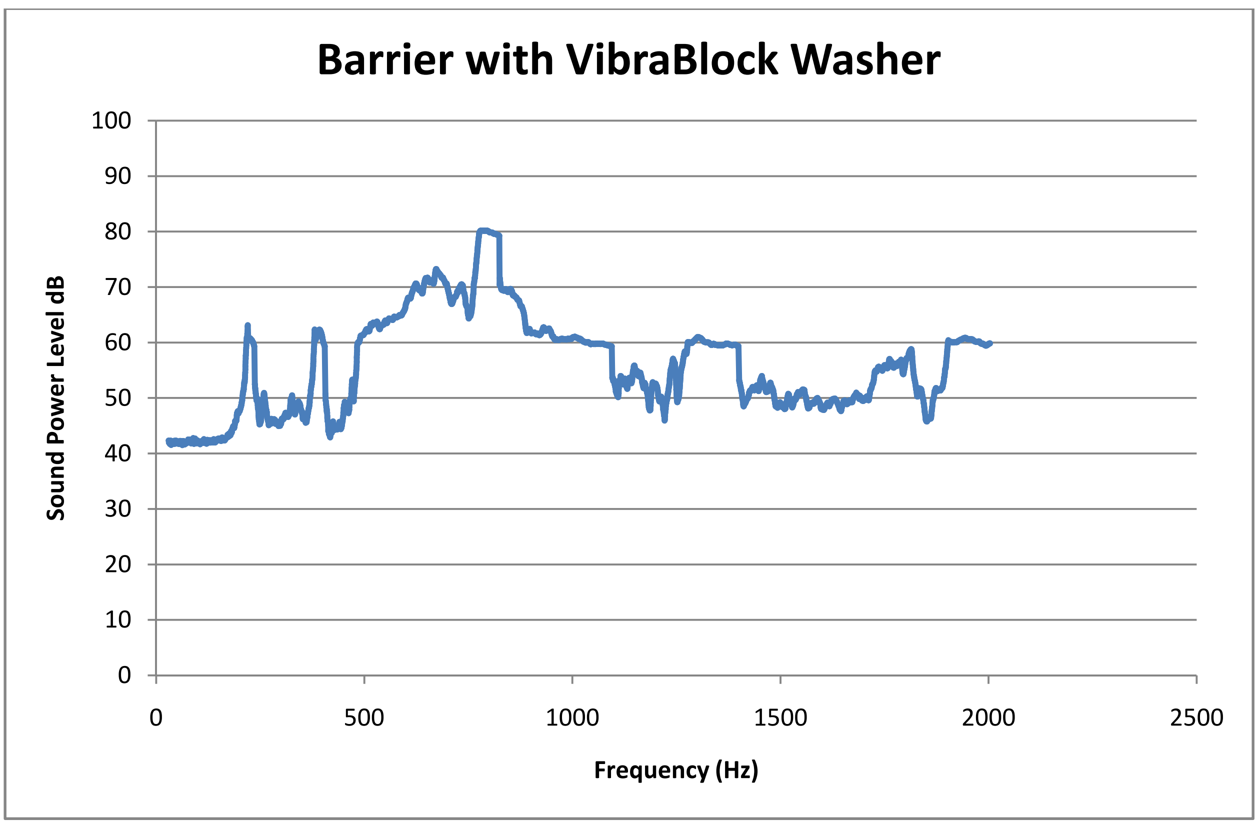
Barrier with VibraBlock Washer
Sound Power Level dB
Frequency (Hz)
0
10
20
30
40
50
60
70
80
90
100
0
500
1000
1500
2000
2500

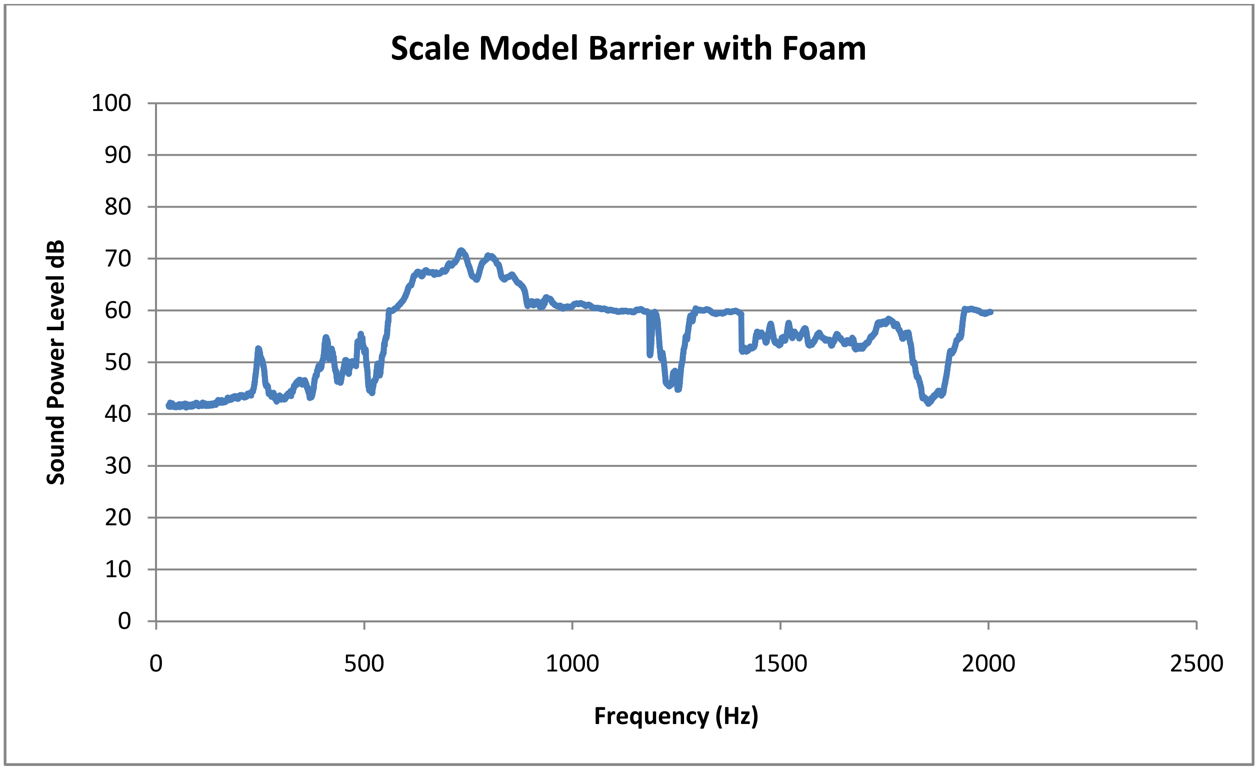

Scale Model Barrier with Foam
Sound Power Level dB
Frequency (Hz)
100
90
80
70
60
50
40
30
20
10
0
0
500
1000
1500
2000
2500

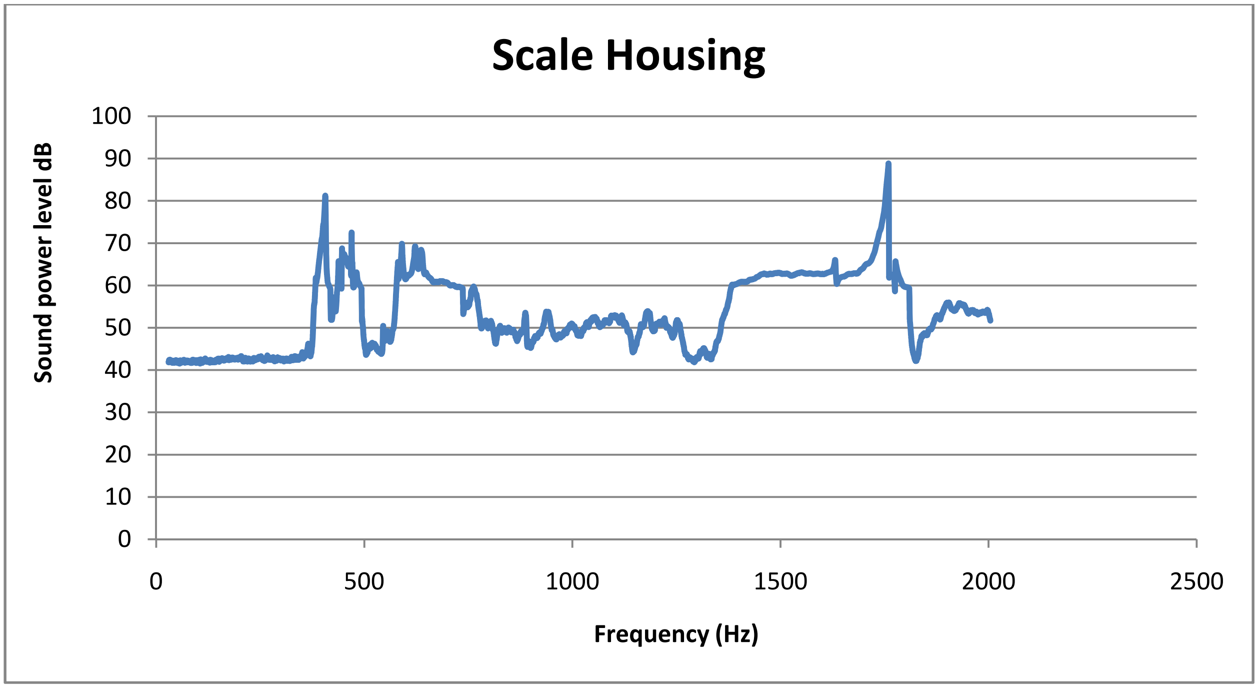

Scale Housing
Sound power level dB
100
90
80
70
60
50
40
30
20
10
0
0
500
1000
1500
2000
2500
Frequency (Hz)

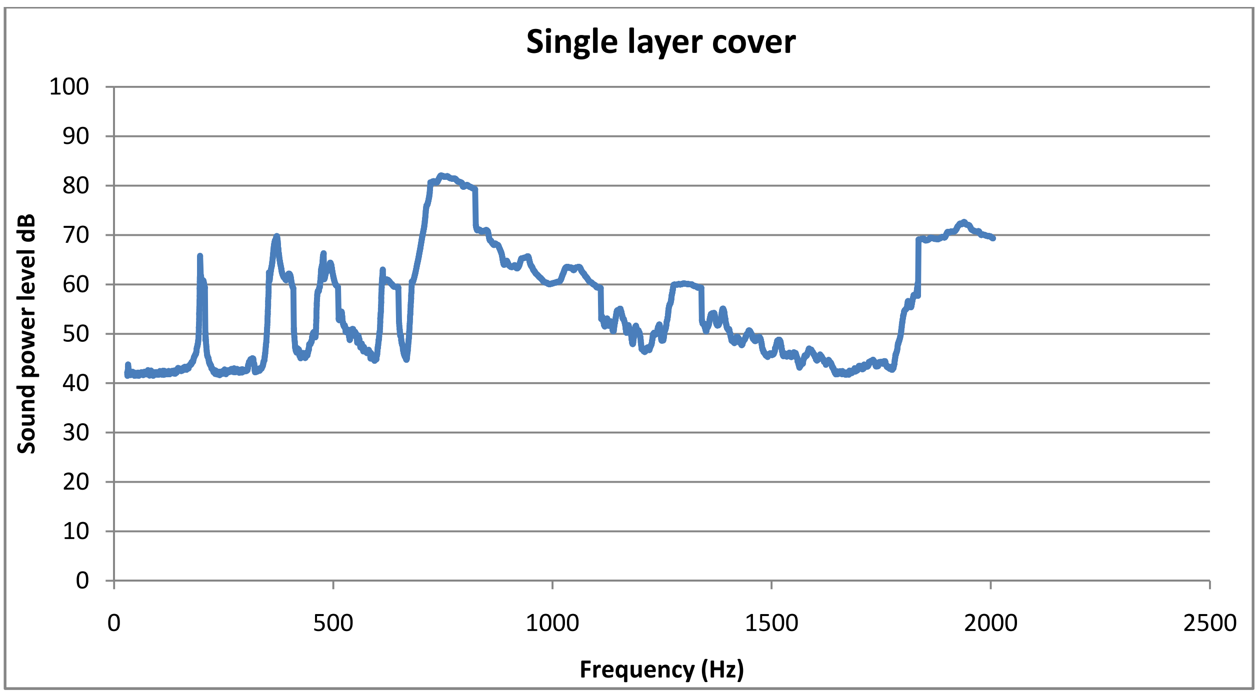

Single layer cover
Sound power level dB
100
90
80
70
60
50
40
30
20
10
0
0
500
1000
1500
2000
2500
Frequency (Hz)

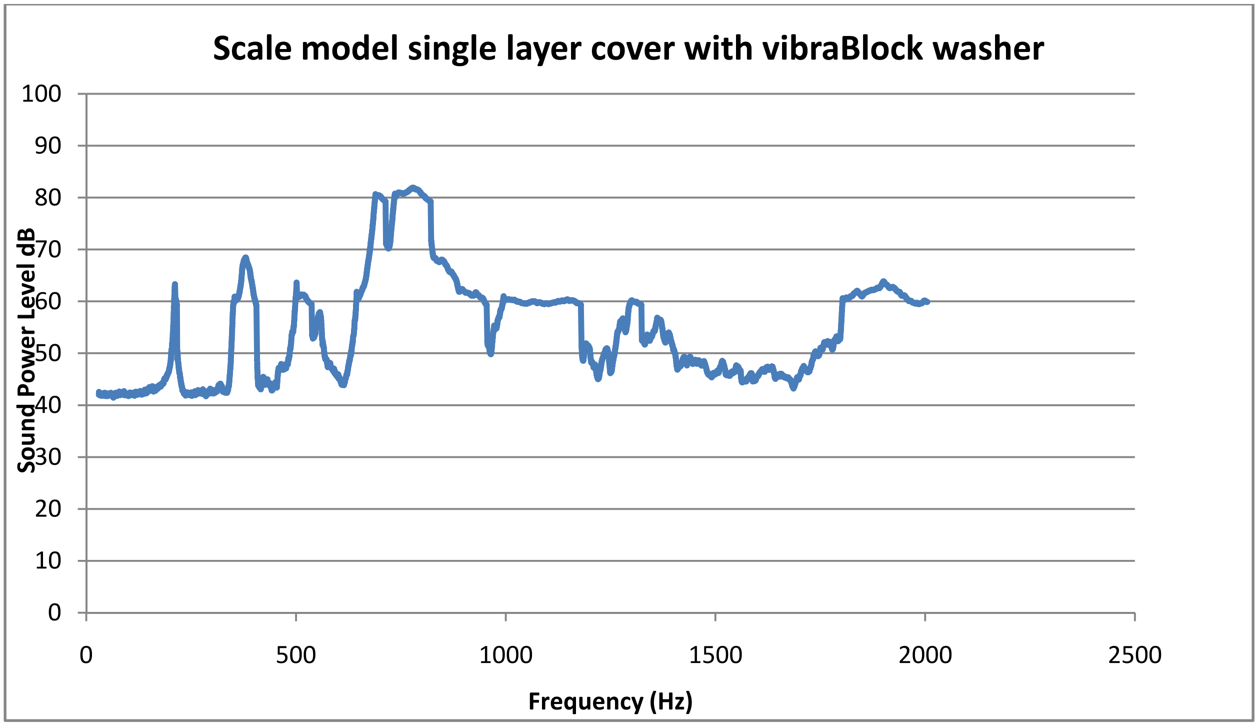
Scale model single layer cover with vibraBlock washer
Sound Power Level dB
Frequency (Hz)
0
10
20
30
40
50
60
70
80
90
100
0
500
1000
1500
2000
2500

APPENDIX D: Attribute Tables

Decision Matrix and Attribute Charts:

Active Materials:

The following tables were constructed in a deliverable for material comparison.

Table D1: Active Materials Attribute Tables

		Materials				
		High Temperature Piezo	*Single Crystal Piezo*	*Macro Fiber Composite*	*Galfenol*	*Terfenol*
Attribute	*Temperature Range*	*****	**	**	*****	****
	Frequency Range	****	**	***	*****	***
	Force	****	****	**		*****
	Displacement	**	**	****	**	**
	Ease of Attachment	***	***	****		
	Ease of use	****	****	*****	***	***
	Cost	***	***	****	*	*

		Attributes					
		Curie Temp (°C)	*Density (g/cm^3)*	*Displacement (pm/V)*	*Force*	*Frequency*	*Dielectric Constant*
Material	*High Temperature Piezo*	450	7.7	401	1000 N	MHz	1578
	Single Crystal Piezo	160	8	2700	1000 N		4000-8500
	GaFeNol	500		1200		MHz	
	Terfenol	380	9.25	1200	1330-1370 N	0-30 KHz	
	Macro Fiber Composite	140	N/A	460	650 N	10 kHz	

Active Materials:

The following table was constructed in a deliverable for material comparison.

		Design Concept 1		**Design Concept 2**		**Design Concept 3**	
		MFC Strip	*Peizo Stack*	*MFC Strip*	*Peizo Stack*	*PZT Gasket*	*PZT Washers*
Criteria	***Weighting***						
Cost	*11*	11	4	11	4	0	3
Size	*15*	15	6	15	5	15	15
Weight	*3*	3	1	3	1	1	3
Durability	*8*	0	5	0	5	2	3
Width of Frequency Range	*4*	4	4	4	4	4	4
Application/Incorporation	*7*	4	3	4	3	3	7
Power Demands	*6*	2	3	2	3	4	8
Aesthetics/Clutter	*5*	5	2	5	2	5	3
Availability of Parts/Materials	*6*	3	4	3	4	0	2
Safety	*10*	10	10	10	10	10	10
Longevity	*10*	5	8	5	8	3	8
Force	*15*	2	15	0	15	15	15
Total	*100*	64	65	62	64	62	81

Table D2: Active Materials Decision Matrix

Passive Materials:

The following table was constructed in a deliverable for material comparison.

		Attributes						
		Frequency Range	*Temperature Range*	*Cost*	*Ease of Adaptation*	*Attenuation*	*Durability*	*Size*
Materials	*Viscoelastic Sheets*	max attenuation in 3000-8000hz	up to 347 °F		***	max of 35-45 db's (high freq.)	****	**
	Damped Sheet Metal PVP	max attenuation in 3000-8000hz			***	max of 35-45 db's (high freq.)	****	
	Melamine Foam	max attenuation from 1000-4000hz	up to 300 °F	*****	***	82-99% reduction from 1-4 kHz	*****	***
	Damper Layer SWEDAC	*****				****		
	Damping Glue SWEDAC			****	*****			*****
	Delta dB	***	***	***	*****	***	****	*****
	Carbon Fiber	***	*****	***	***	***	***	***
	SSP Foam	****	***	*****	****	****	**	***
	Vibra-Block	****	****	*****	***	****	****	****

Table D3: Passive Material Attribute Chart

The following decision matrix was performed for the passive materials in regards to the active material chosen from the active materials.

		Passive Materials							
		Melamine Foam	**Viscoelastic Sheets**	**Viscoelastic Glue**	**Damping Layer Swedac**	**Delta dB**	**Carbon Fiber**	**SSP foam**	**Vibra-Block**
Criteria	***Weighting***								
Cost	11	11	1	2	0	*11*	*8*	*11*	*11*
Size	15	15	15	15	15	*15*	*13*	*8*	*15*
Weight	3	3	0	3	3	3	3	3	3
Durability	8	0	8	0	8	8	5	5	5
Frequency Range	9	5	4	2	4	7	5	9	6
Application	7	7	2	7	7	6	6	4	5
Power Demands	6	6	6	6	6	6	6	6	6
Aesthetics/Clutter	5	5	5	5	0	5	4	5	4
Availability of Materials	6	6	6	6	0	5	3	6	6
Safety	15	10	10	10	10	15	14	13	15
Longevity	15	8	11	4	11	10	12	10	8
Total	*100*	***78***	*68*	*60*	*64*	91	79	80	84

Table D4: Passive Material Decision Matrix

APPENDIX E: Pro-E Drawings

SCALE 0.400
Tolerance +/-0.005

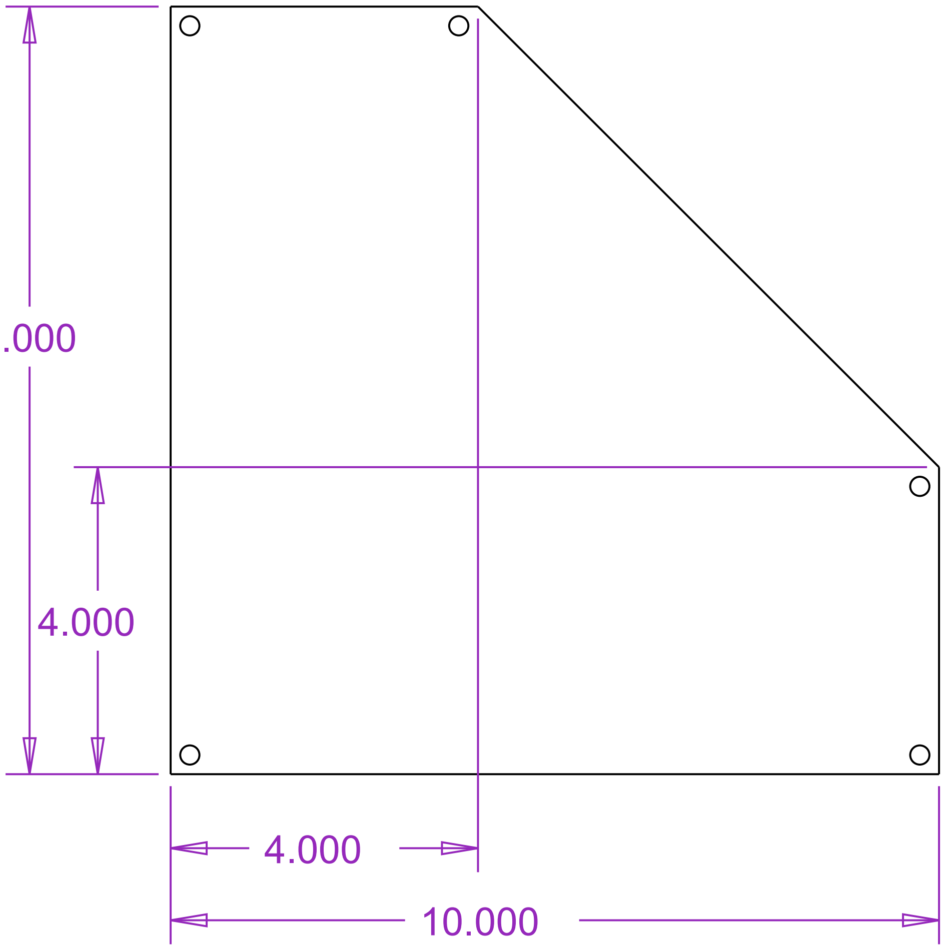

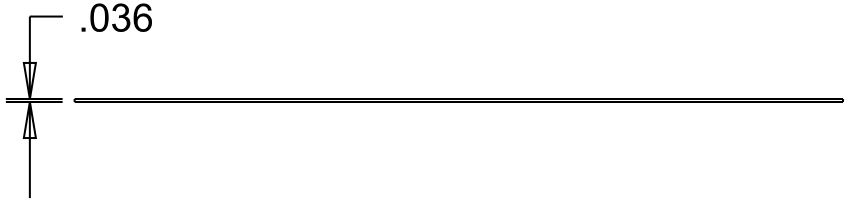

Gear Cover Assm	
Cummins Group 7	

	Barrier
SHEET #	001
LAST REVISION	04/07/09
REVISION #	001
DRAWING #	SD-P-001

SCALE 0.400
Tolerance +/-0.005

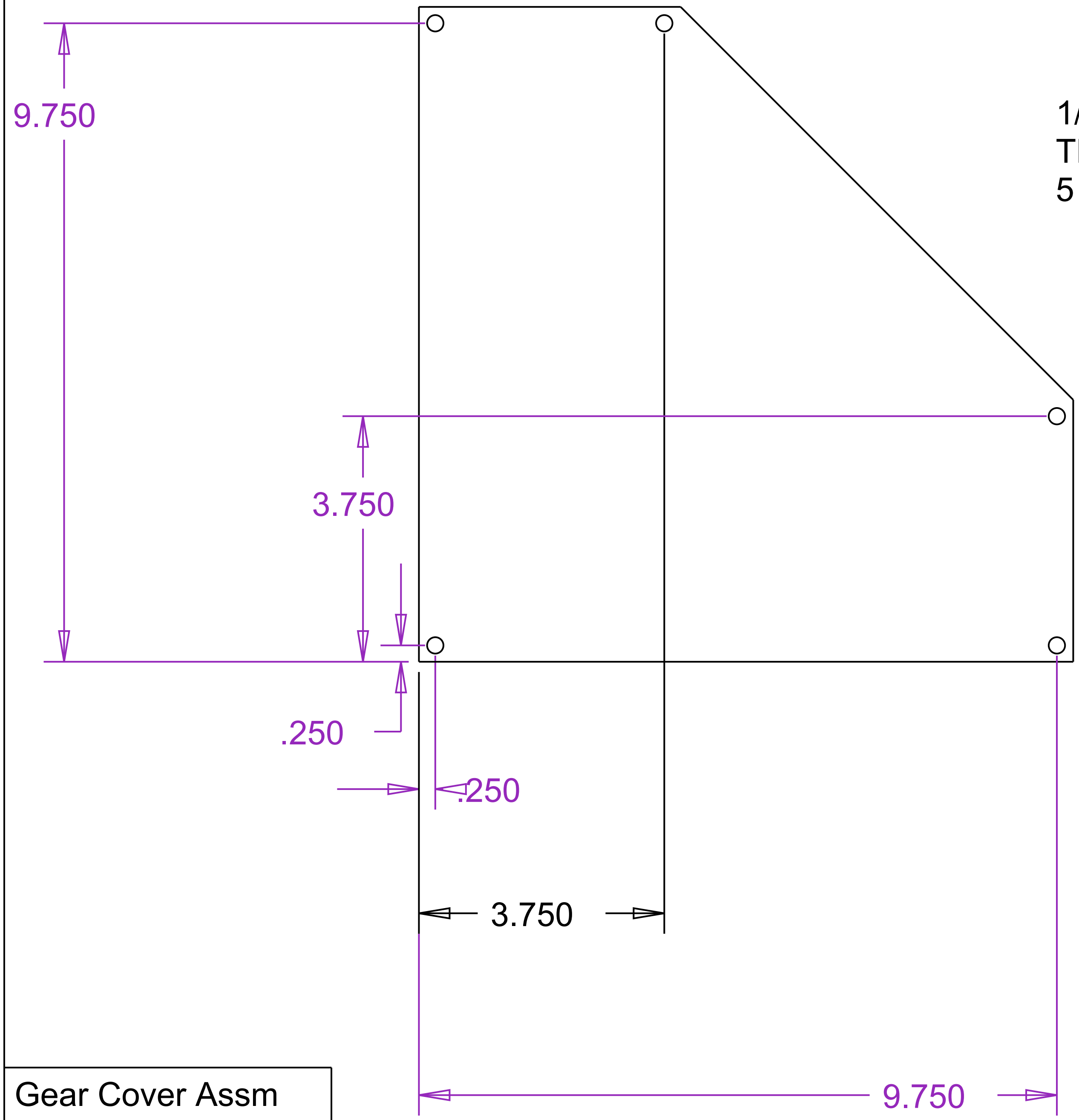

1/4 - 20
THRU ALL
5 PLACES

Gear Cover Assm	
Cummins Group 7	

	Barrier
SHEET #	002
LAST REVISION	04/07/09
REVISION #	001
DRAWING #	SD-P-001

Scale 0.400
Tolerance +/-0.005

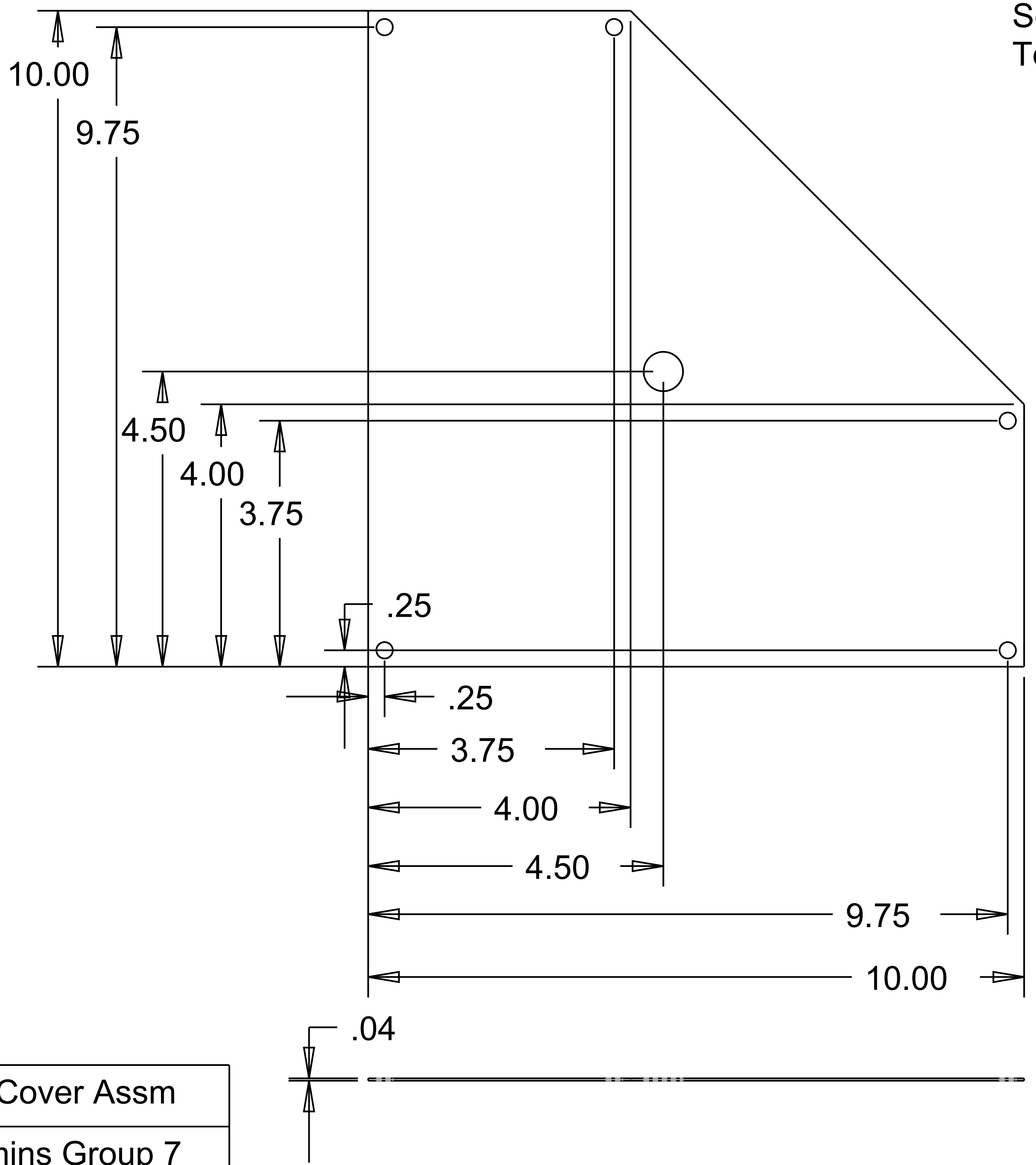

Gear Cover Assm	
Cummins Group 7	

Sound Barrier Modified	
SHEET #	001
LAST REVISION	04/07/09
REVISION #	001
DRAWING #	SD-P-019

SCALE 0.350
Tolerance +/-0.005

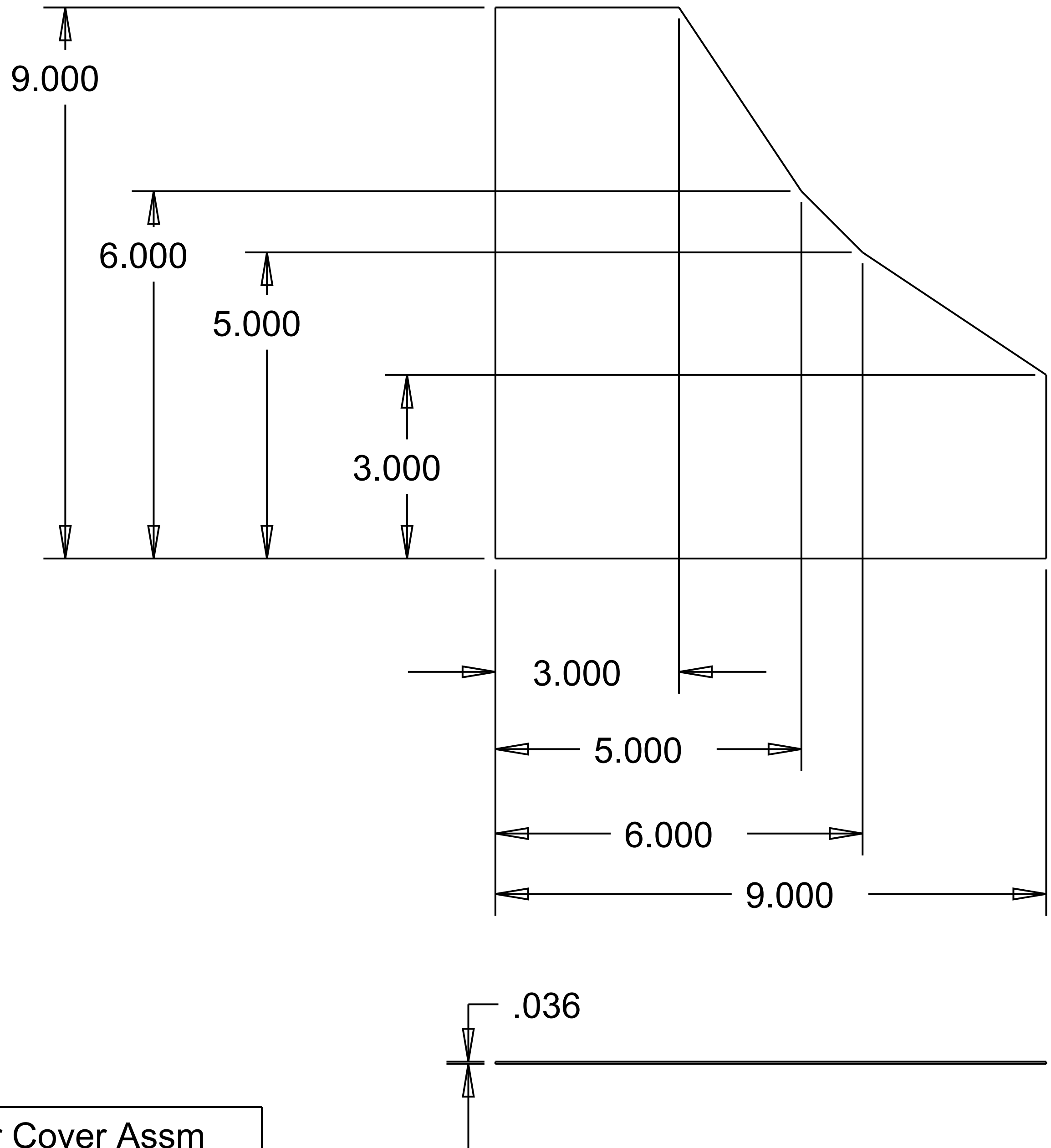

	Foam
SHEET #	001
LAST REVISION	11/21/08
REVISION #	001
DRAWING #	SD-P-002

Gear Cover Assm

Cummins Group 7

SCALE 0.350
Tolerance +/-0.005

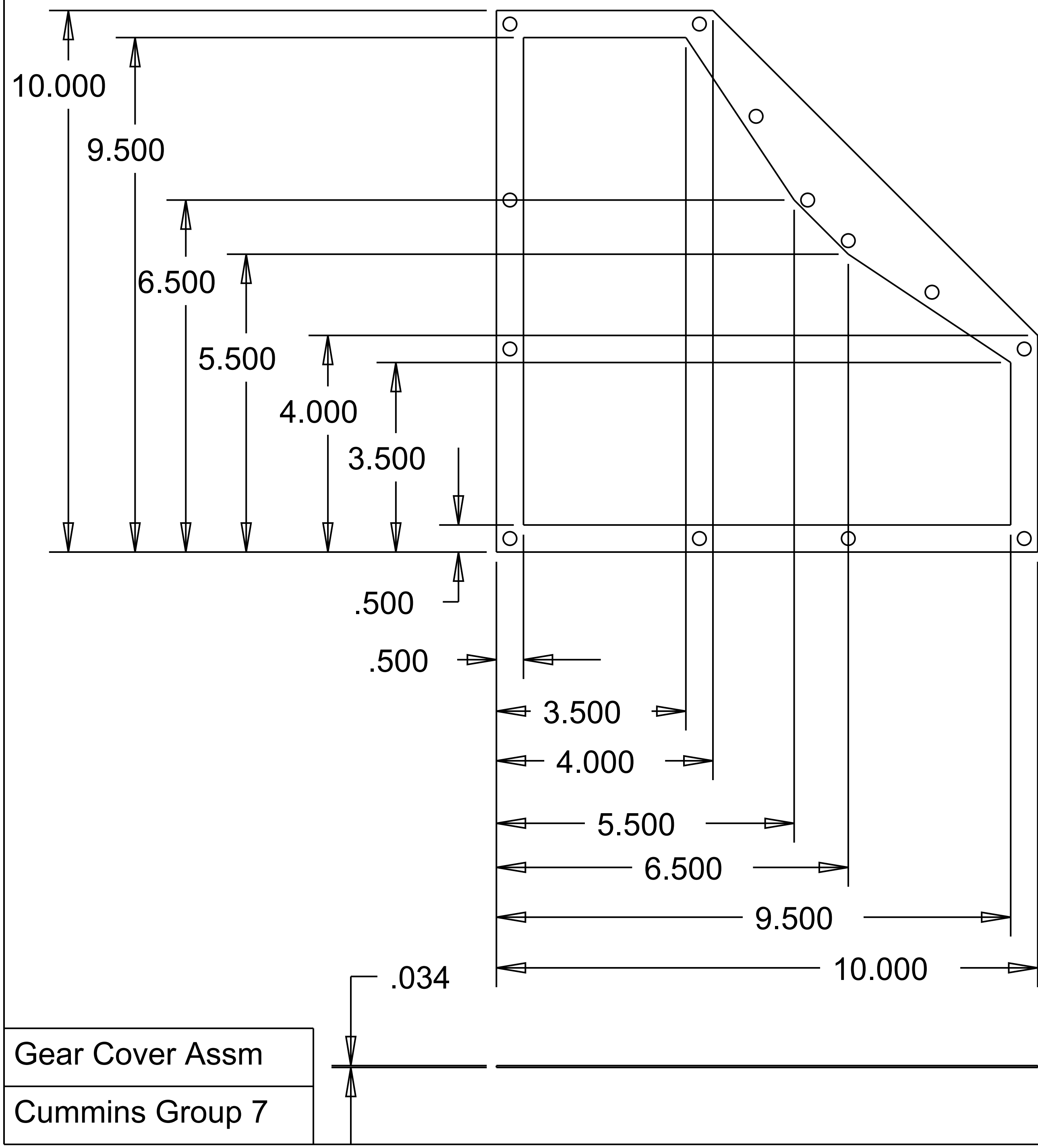

Gear Cover Assm	
Cummins Group 7	

	Seal
SHEET #	001
LAST REVISION	11/21/08
REVISION #	001
DRAWING #	SD-P-005

SCALE 0.350
Tolerance +/-0.005

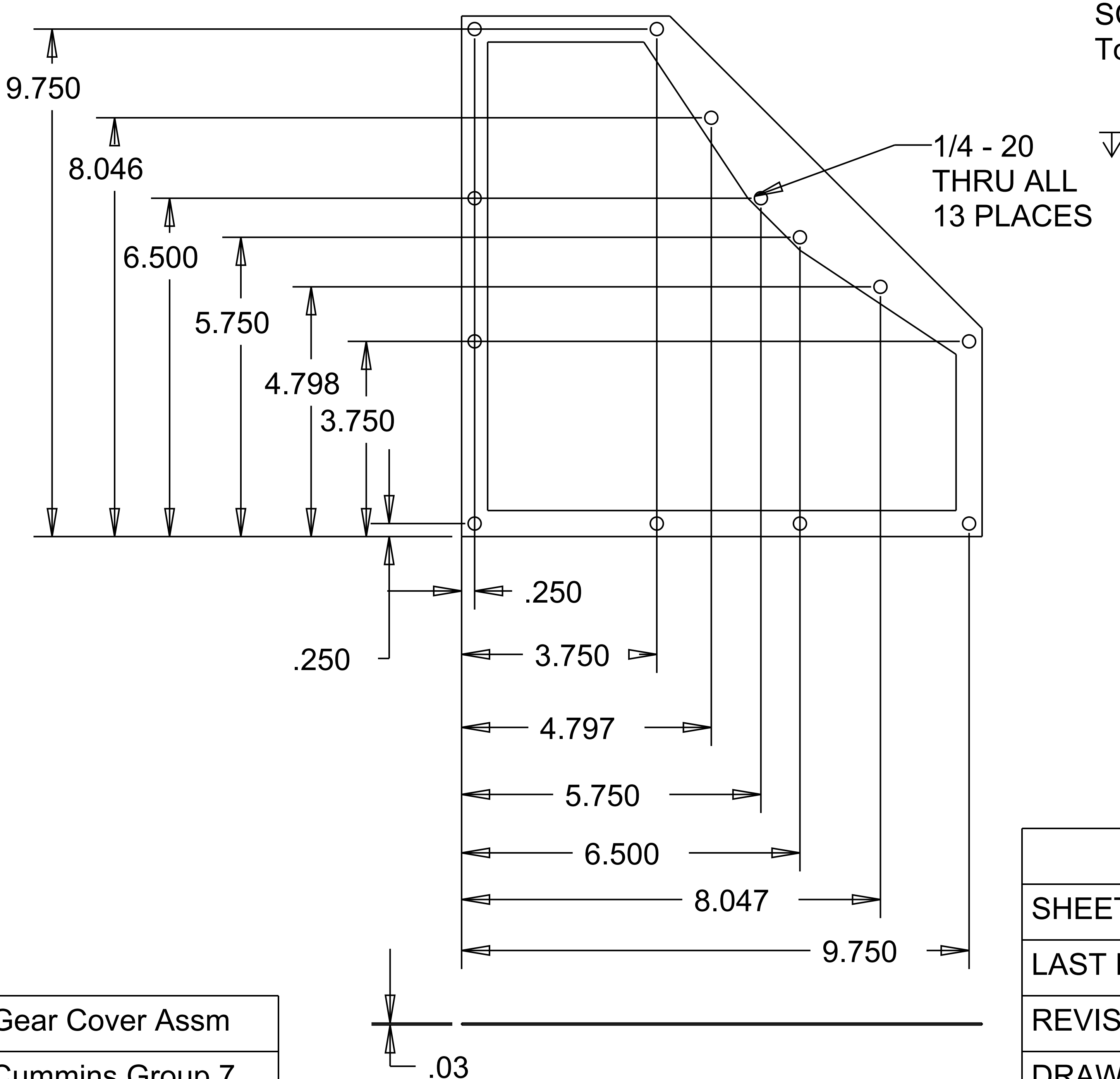

Gear Cover Assm	
Cummins Group 7	

	Seal
SHEET #	002
LAST REVISION	11/21/08
REVISION #	001
DRAWING #	SD-P-0015

SCALE 0.350
Tolerance 0.005

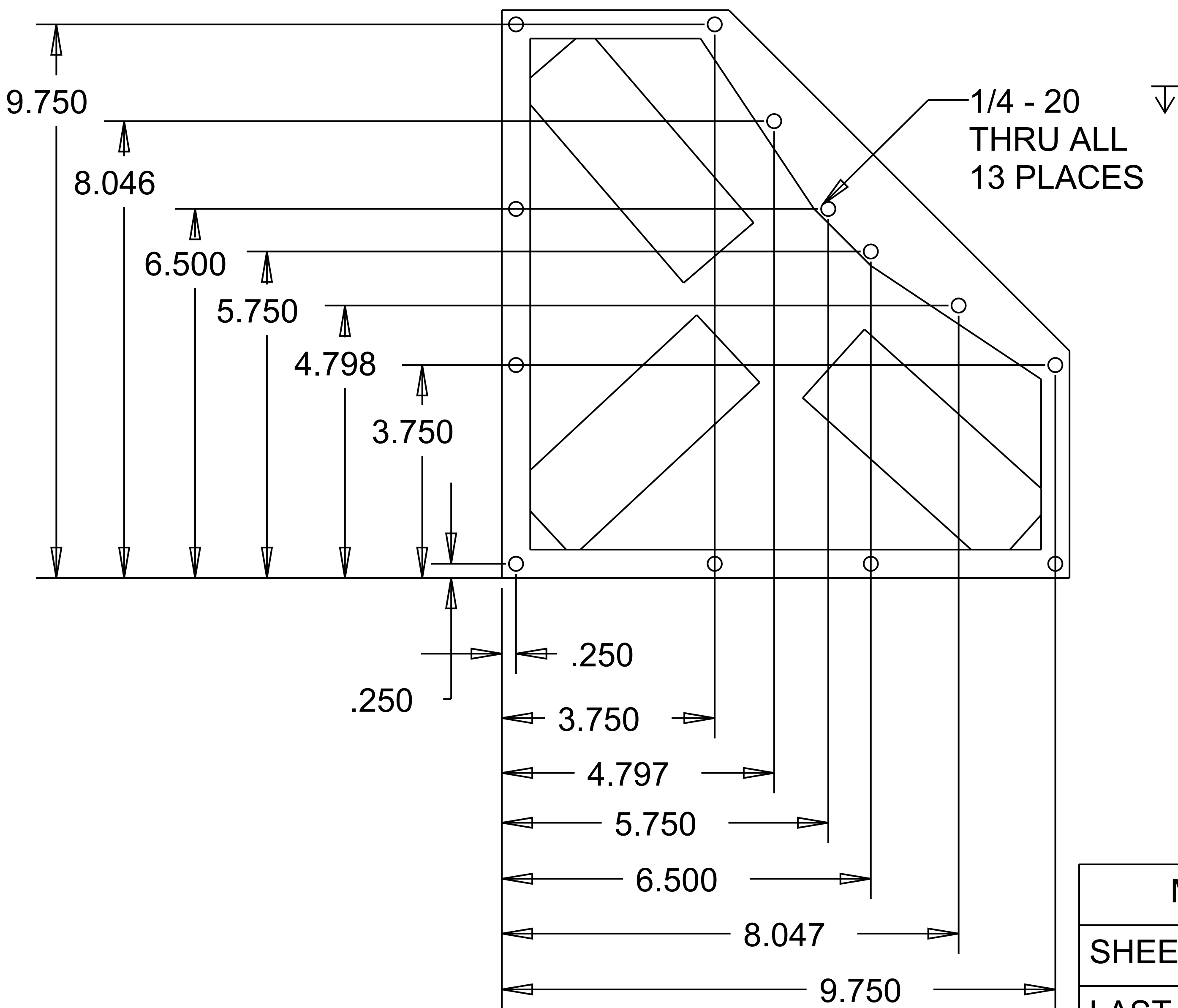

Model Cover with VB	
SHEET #	002
LAST REVISION	11/21/08
REVISION #	001
DRAWING #	SD-P-003

Gear Cover Assm

Cumins Group 7

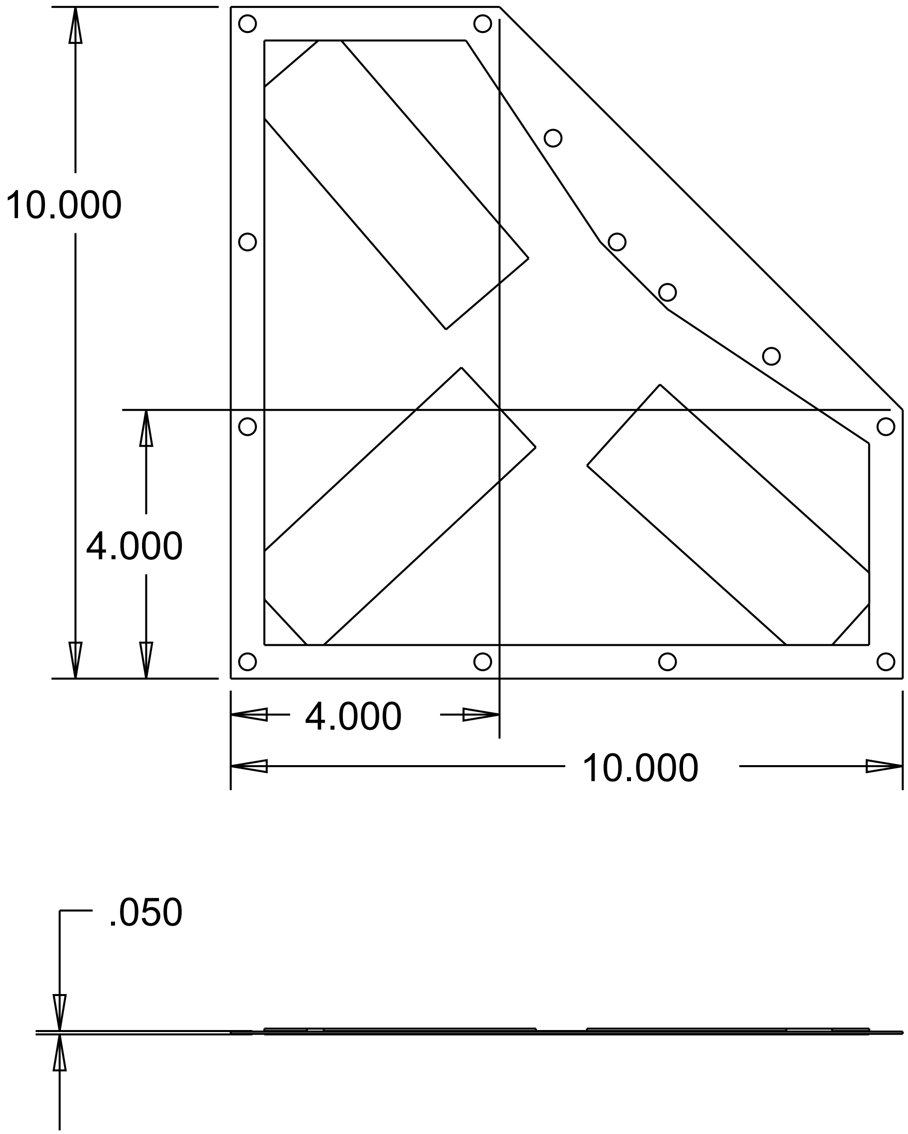

SCALE 0.350
Tolerance +/-0.005

Model Cover	
SHEET #	001
LAST REVISION	04/07/09
REVISION #	002
DRAWING #	SD-P-003

Gear Cover Assm

Cummins Group 7

SCALE 0.350
Tolerance +/-0.005

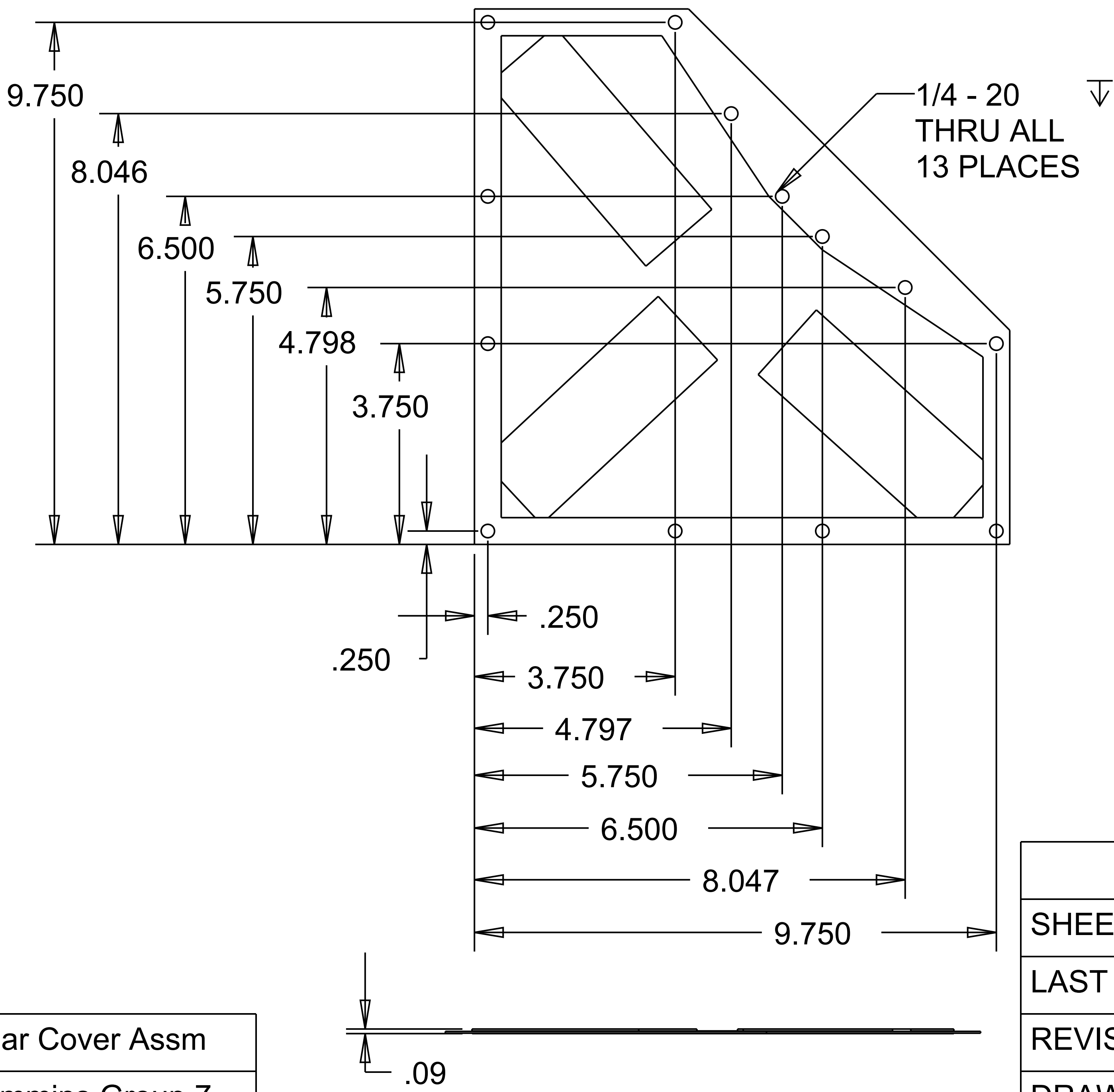

Gear Cover Assm	
Cummins Group 7	

Model Cover	
SHEET #	002
LAST REVISION	04/07/09
REVISION #	001
DRAWING #	SD-P-003

SCALE 0.350
Tolerance +/-0.005

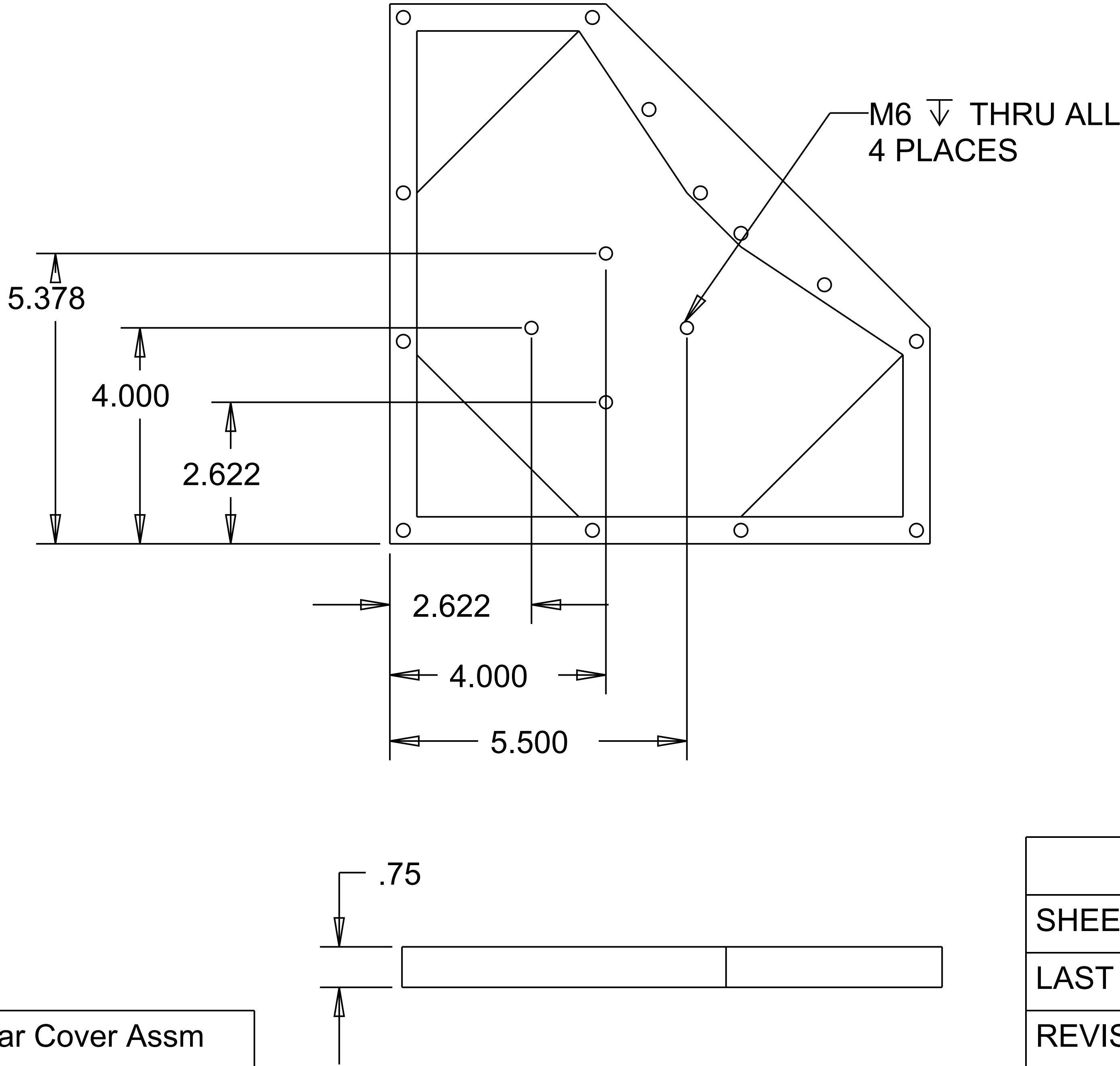

Model Housing	
SHEET #	003
LAST REVISION	04/07/09
REVISION #	001
DRAWING #	SD-P-004

Gear Cover Assm
Cumins Group 7

SCALE 0.350
Tolerance +/-0.005

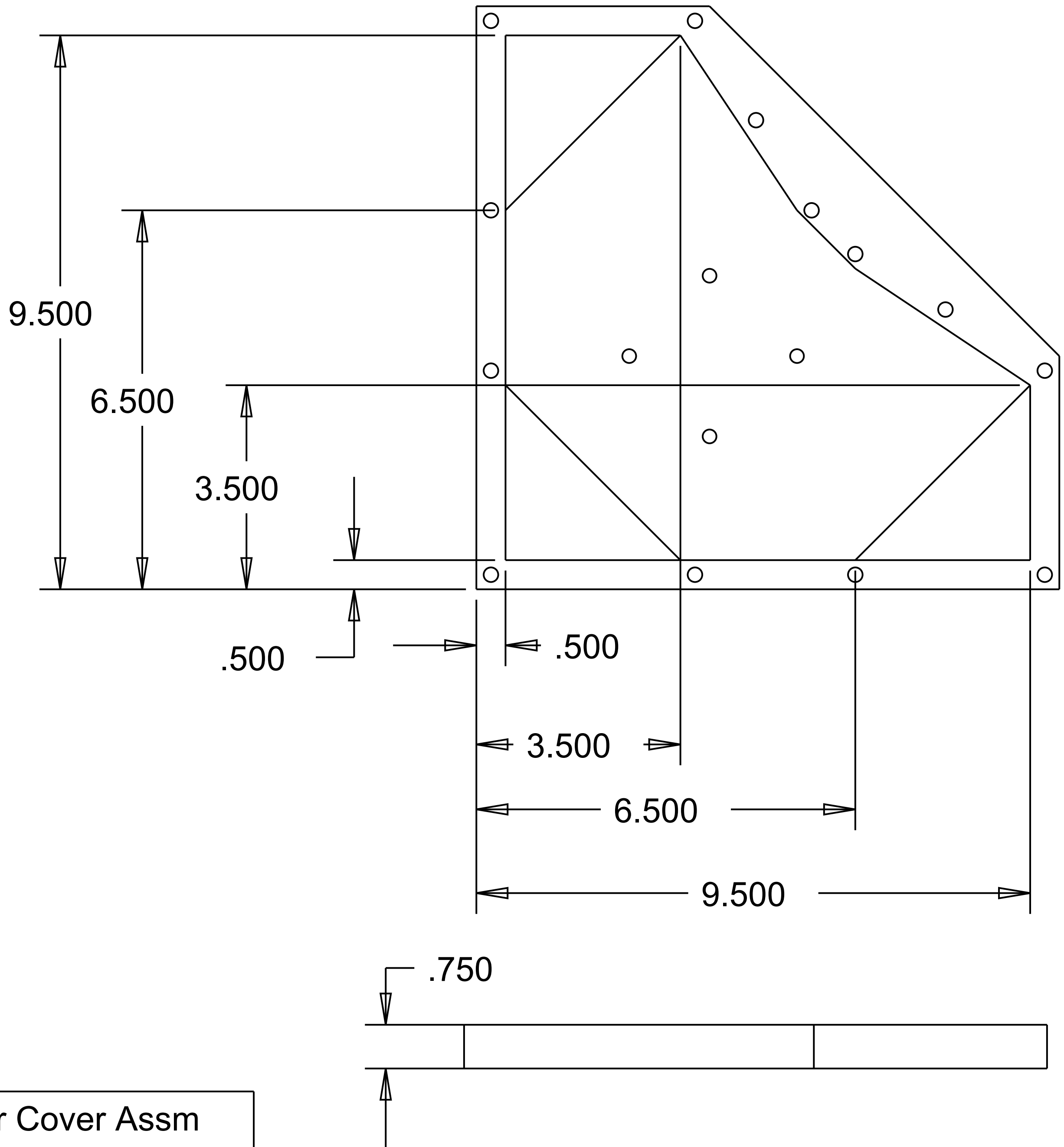

Model Housing	
SHEET #	004
LAST REVISION	04/07/09
REVISION #	001
DRAWING #	SD-P-0020

Gear Cover Assm

Cummins Team 7

SCALE 0.500
Tolerance +/-0.005

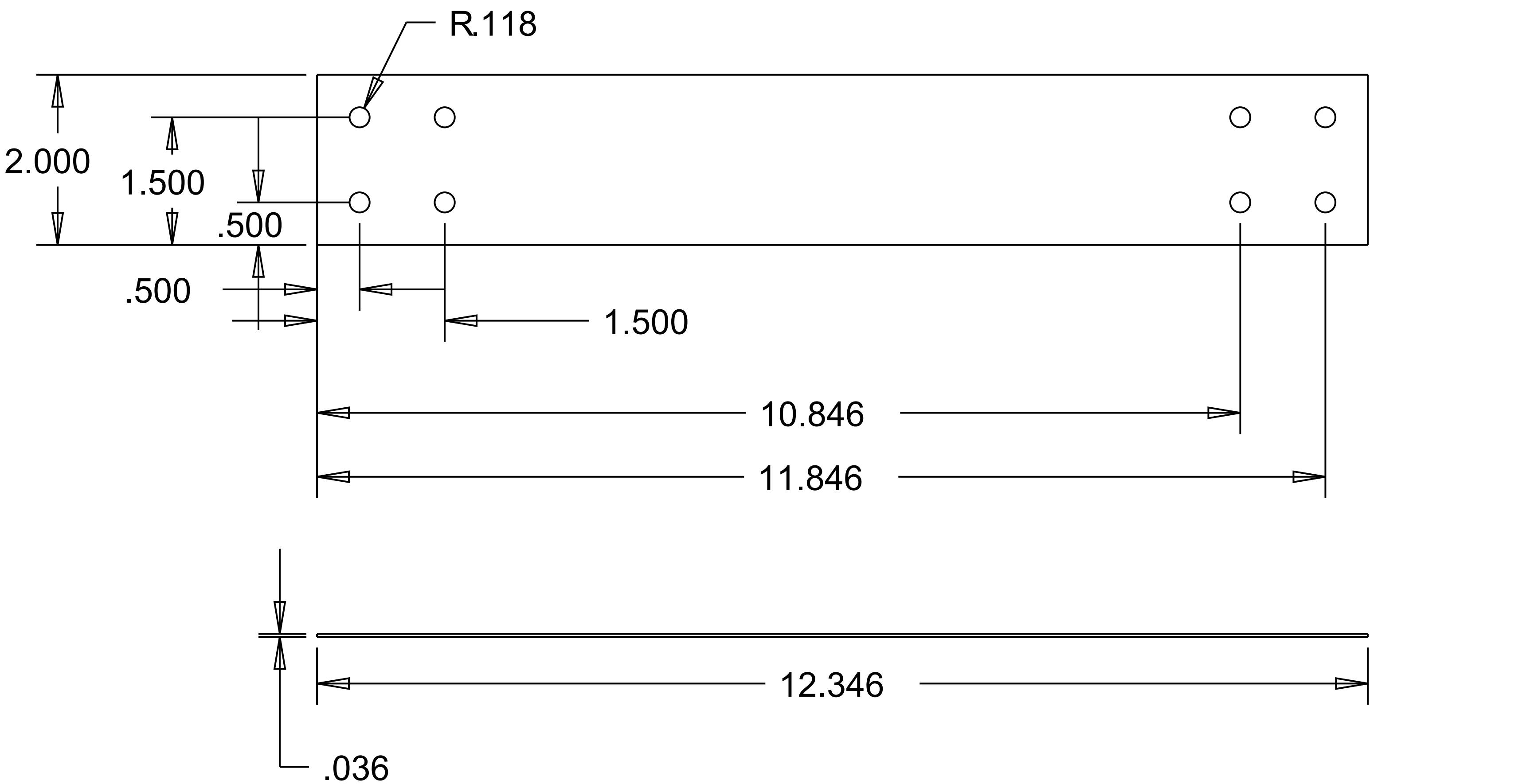

Long Cantilever	
SHEET #	001
LAST REVISION	11/21/08
REVISION #	001
DRAWING #	SD-M-001

Gear Cover Assm
Cummins Group 7

SCALE	0.600
Tolerance	+/-0.005

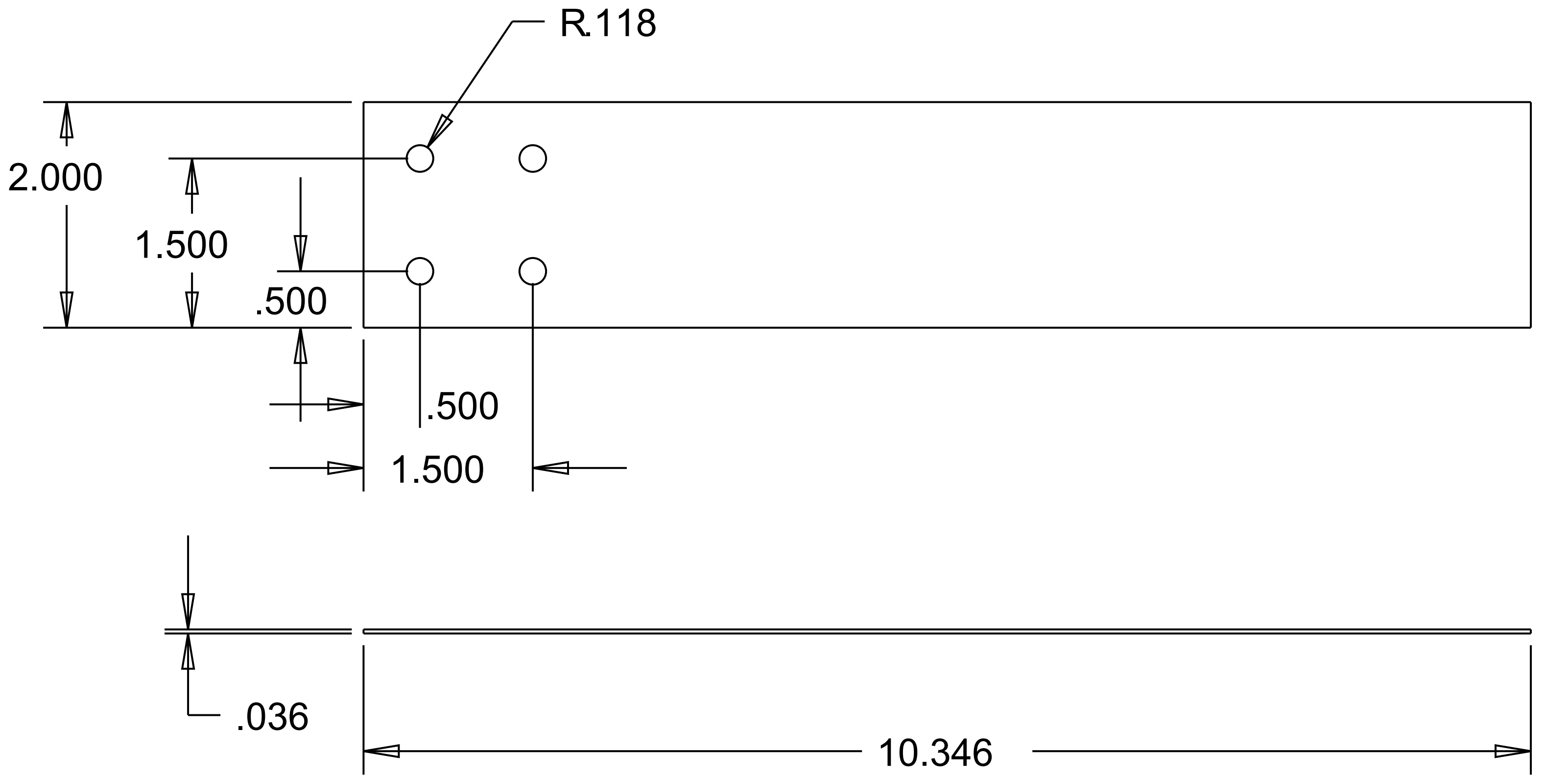

Gear Cover Assm	
Cummins Group 7	

Short Cantilever	
SHEET #	001
LAST REVISION	11/21/08
REVISION #	001
DRAWING #	SD-M-002

SCALE 1.000
Tolerance +/-0.005

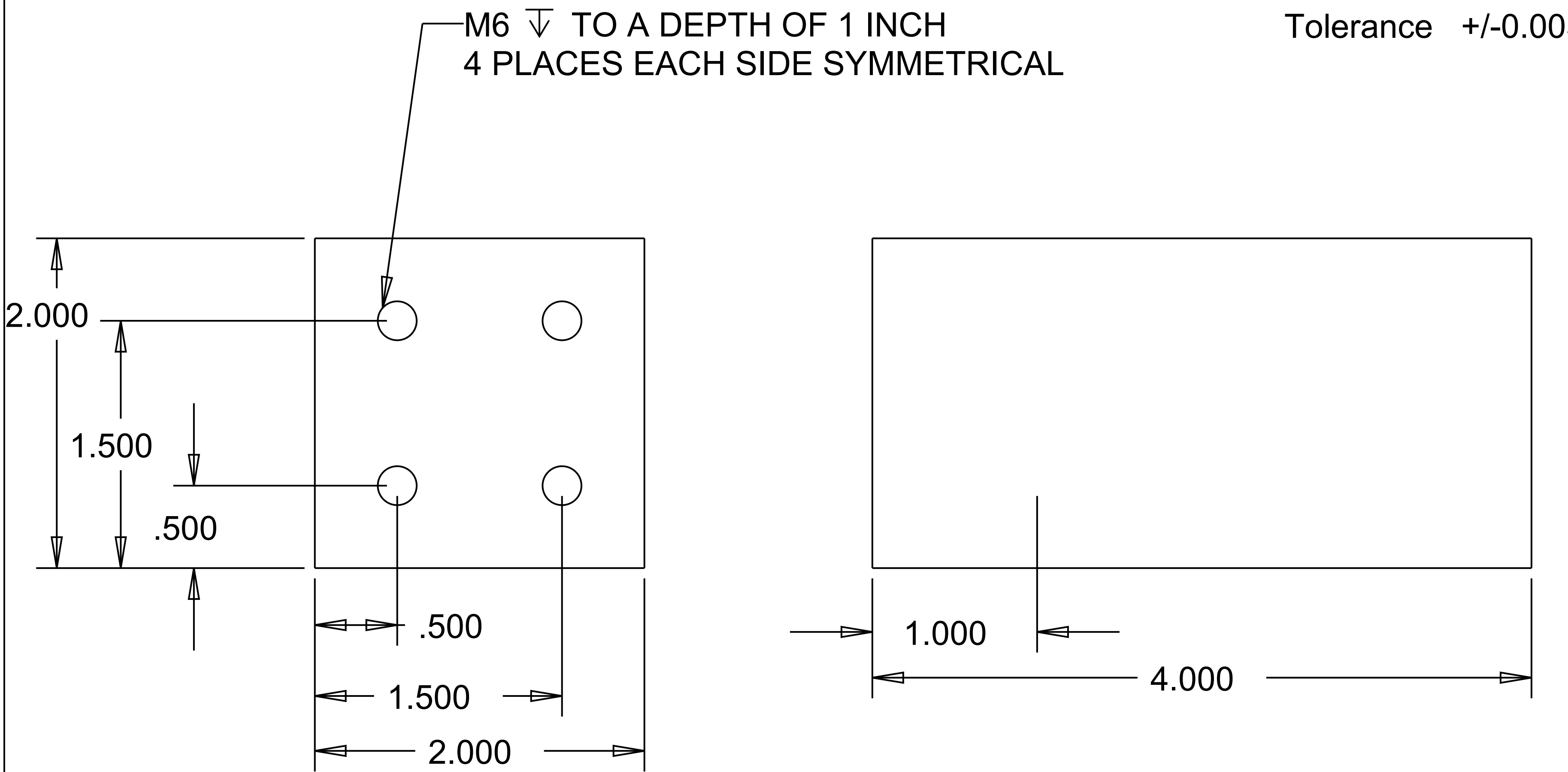

PZT TEST APP.	
CUMMINS GROUP 7	

	SUPPORT
SHEET #	002
LAST REVISION	12/2/08
REVISION #	001
DRAWING #	SD-P-018

SCALE 0.400
Tolerance +/-0.005

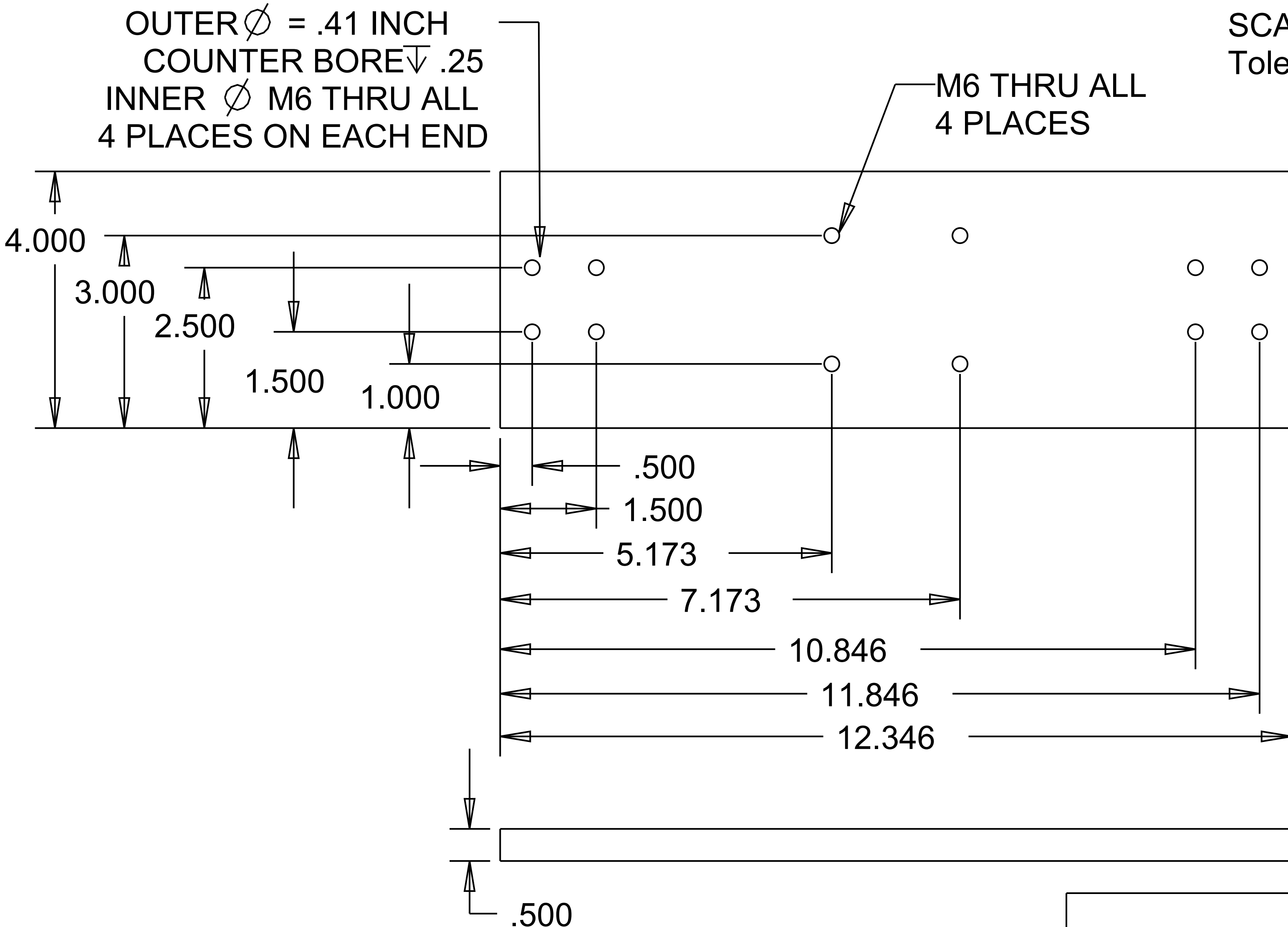

Baseplate	
SHEET #	001
LAST REVISION	04/07/09
REVISION #	001
DRAWING #	SD-P-019

PZT TEST APP.

CUMMINS GROUP 7